Cyclotron Harmonic Wave Propagation and Instabilities

by

J. A. Tataronis

December 1967 ~~1968~~

SU-IPR Report No. 205

NASA Grant NGR 05-020-077

and

AEC Contract AT(04-3)-326

(Project Agreement No. 1)

INSTITUTE FOR PLASMA RESEARCH

STANFORD UNIVERSITY, STANFORD, CALIFORNIA

LEGAL NOTICES

This report was prepared as an account of Government sponsored work. Neither the United States, nor the Commission, nor any person acting on behalf of the Commission:

A. Makes any warranty or representation, expressed or implied, with respect to the accuracy, completeness, or usefulness of the information contained in this report, or that the use of any information, apparatus, method, or process disclosed in this reportmay not infringe privately owned rights; or

B. Assumes that any liabilities with respect to the use of, or for damages resulting from the use of any information, apparatus, method or process disclosed in this report.

As used in the above, "person acting on behalf of the Commission" includes any employee or contractor of the Commission, or employee of such contractor, to the extent that such employee or contractor of the Commission, or employee of such contractor prepares, disseminates, or provides access to, any information pursuant to his employment or contract with the Commission, or his employment with such contractor.

CYCLOTRON HARMONIC WAVE PROPAGATION AND INSTABILITIES

by

J. A. Tataronis

NASA Research Grant NGR 05-020-077

and

AEC Contract AT(04-3)326
(Project Agreement No. 1)

SU-IPR Report No. 205

December 1967

Institute for Plasma Research
Stanford University
Stanford, California

ABSTRACT

This work is a theoretical study of the electrostatic space-charge waves which propagate in a hot plasma immersed in a constant and uniform magnetic field. It is based on the self-consistent solution of the collisionless Boltzmann equation with Poisson's equation in infinite planar geometry and is restricted to interactions which involve only electrons. By considering a series of velocity distributions $f_o(\underset{\sim}{v})$, a clear and comprehensive picture of the propagation characteristics and stability properties of these waves has been obtained.

The frequency and wave number of the normal modes are connected through a dispersion relation which has been solved here, and the results are displayed in both graphical and analytical forms. For perpendicular propagation a mode is found near each harmonic of the electron cyclotron frequency. If $(\partial f_o/\partial v_\perp) > 0$ for some range of the velocity component perpendicular to the magnetic field, $v_\perp$, it is shown that these modes can couple to form regions in the dispersion diagram where complex frequencies exist with negative imaginary part and real wave number, indicating that the plasma supports space-charge waves which grow with time. The exact threshold conditions for these instabilities are derived for several distributions, and the growth rates are computed as a function of the electron density. However, if $(\partial f_o/\partial v_\perp) < 0$ for all $v_\perp > 0$ or if the electron density is sufficiently low, the propagation in this direction can occur without growth or collisionless damping; this suggests that, experimentally, excitation and detection of these waves should be readily attainable. When electron/neutral collisions are taken into account, the results show that for collision frequencies much less than the electron cyclotron frequency, damping is significant only at points on the dispersion curves where the group velocity vanishes.

The results of the investigation of oblique propagation reveal two classes of normal modes, one of which has no counterpart in the case of purely perpendicular propagation. This leads to a new set of instabilities

that are characterized by (1) onset conditions that are much less stringent than that of perpendicular propagation, and (2) growth rates that are strongly dependent on T, the ratio of the electron temperature perpendicular and parallel to the magnetic field. In the limit of an isotropic Maxwellian velocity distribution, $T = 1$ and all obliquely propagating modes decay with time as a result of Landau and cyclotron damping.

Finally, a study has been made on the analyticity of the Laplace transform of the electrostatic Green's function. This leads to (1) a classification of the space-charge instabilities as either absolute or convective, and (2) a prediction of resonances at harmonics of the electron cyclotron frequency, at the cold-plasma upper hybrid frequency, and at intermediate frequencies between succeeding harmonics. The results show that instabilities associated with perpendicular propagation are absolute, while oblique propagation can support either absolute or convective instabilities, depending on the electron density and the distribution in electron velocity.

Contents

Contents (Cont)

Tables

Illustrations

Illustrations (Cont)

Illustrations (Cont)

SYMBOLS

$a_n(k_\perp)$	function defined by Eq. (3.2)
$\underset{\sim}{a}_{\alpha n}(\underset{\sim}{r},\underset{\sim}{v},t)$	particle acceleration (q_α/m_α) $(\underset{\sim}{E}_n + \underset{\sim}{v} \times \underset{\sim}{B}_n)$
b_n	coefficient defined by Eq. (4.48b)
c_n	coefficient defined by Eq. (3.13); also coefficient defined by Eq. (4.48c)
d_n	coefficient defined by Eq. (3.19); also coefficient defined by Eq. (4.48d)
$f_\alpha(\underset{\sim}{n},\underset{\sim}{v},t)$	velocity distribution of particle species α
$f_{\alpha n}(\underset{\sim}{r},\underset{\sim}{v},t)$, $f_n(\underset{\sim}{r},\underset{\sim}{v},t)$	n^{th} term in perturbation expansion of $f_\alpha(\underset{\sim}{n},\underset{\sim}{v},t)$
$f_\perp(v_\perp)$	distribution in the transverse speed $v_\perp$
$f_{\|}(v_{\|})$	distribution in the parallel speed $v_{\|}$
$f(t)$	temporal part of external charge density, $\rho_s(x,t) = g(x)f(t)$
$f(\omega)$	Laplace transform of $f(t)$
$g(x)$	spatial part of external charge density, $\rho_s(x,t) = g(x)f(t)$
$g(k_\perp)$	Fourier transform of $g(x)$
h_n	Fourier coefficient defined by Eq. (5.60)
i	$\sqrt{-1}$
j	integer index
$\underset{\sim}{k}$	wave vector
k	$\lvert\underset{\sim}{k}\rvert = (k_\perp^2 + k_{\|}^2)^{1/2}$; also used as an integer summation index

$k_i(\omega)$	i^{th} root of dispersion relation for perpendicular propagation
(k_x, k_y, k_z)	Cartesian coordinates of wave vector $\underset{\sim}{k}$
$k_\perp, k_\parallel$	components of $\underset{\sim}{k}$ perpendicular and parallel, respectively, to the applied magnetic field $\underset{\sim}{B}_o$
$k_{\perp r}, k_{\perp i}$	real and imaginary parts of $k_\perp$, respectively
$k_{\parallel r}, k_{\parallel i}$	real and imaginary parts of $k_\parallel$, respectively
$k_{\perp 1}$	$(2\pi/L)$
m_α, m	particle mass of species α
n	integer index
$n_\alpha(\underset{\sim}{r}, t)$	particle density of species α
$n_{\alpha o}, n_o$	average particle density of species α
p_n	coefficient defined by Eq. (2.78)
q_α, q	electric charge of particle species α
q_n	coefficient defined by Eq. (2.79)
$\underset{\sim}{r}$	position vector
$\underset{\sim}{r}_{\alpha o}(t), \underset{\sim}{r}_o(t)$	position of charged particle in the presence of zero order fields
$s_{-1,\nu}(z)$	Lommel's function
t	time
t'	integration variable
$\underset{\sim}{v}$	velocity vector
v	$\lvert\underset{\sim}{v}\rvert = (v_\perp^2 + v_\parallel^2)^{1/2}$

v_o	electron speed for spherical shell velocity distribution
$v_{o\perp}$	electron speed for ring velocity distribution
$v_{o\parallel}$	constant electron drift speed along the magnetic field
(v_x, v_y, v_z)	Cartesian coordinates of velocity vector $\underset{\sim}{v}$
v_t	thermal electron speed
$v_{t\perp}$	thermal electron speed perpendicular to the magnetic field
$v_{t\parallel}$	thermal electron speed parallel to the magnetic field
$\underset{\sim}{v}_{\alpha o}(t), \underset{\sim}{v}_o(t)$	velocity of charged particle in the presence of zero order fields: $v_{\alpha o}(t) = d\underset{\sim}{r}_{\alpha o}(t)/dt$
$v_\perp, v_\parallel$	components of $\underset{\sim}{v}$ perpendicular and parallel to the magnetic field respectively
$(\hat{v}_\perp, \hat{v}_\psi, \hat{z})$	unit base vectors in velocity space
w_n	$(\omega - n\omega_c)/k_\parallel$
w_{nr}, w_{ni}	real and imaginary parts of w_n respectively
x	displacement along x axis
$\hat{x}$	unit vector along x axis
z	displacement along z axis; also dummy variable
$\underset{\sim}{B}(\underset{\sim}{r}, t)$	magnetic field
$\underset{\sim}{B}_n(\underset{\sim}{r}, t)$	n^{th} term in perturbation expansion of $\underset{\sim}{B}(\underset{\sim}{r}, t)$
$\underset{\sim}{B}_o(\underset{\sim}{r}, t), \underset{\sim}{B}_o$	applied zero order magnetic field
$D(\omega, k_\perp)$	function defined by Eq. (4.17b)

$\underset{\sim}{E}(r,t)$	electric field
$\underset{\sim}{E}_n(\underset{\sim}{r},t)$	n^{th} term in perturbation expansion of $\underset{\sim}{E}(\underset{\sim}{r},t)$
$\underset{\sim}{E}_1(\underset{\sim}{k},\omega)$	Fourier and Laplace transforms of $\underset{\sim}{E}_1(\underset{\sim}{r},t)$
$F_o(\tau)$	function defined by Eq. (3.5)
$F(\omega,x)$	function defined by Eq. (3.76)
$G(\omega,x)$	plasma Green's function, Eq. (5.4)
$H_n(v_{\|})$	function defined by Eq. (2.69)
H_n^+, H_n^-	positive and negative "frequency" parts of H_n respectively
$H_n^{(m)}(v_{\|})$	$\partial^m H_n(v_{\|})/\partial v_{\|}^m$
$I_n(z)$	Bessel function with imaginary argument
$\underset{\sim}{J}(\underset{\sim}{r},t)$	total particle current density of plasma
$\underset{\sim}{J}_s(\underset{\sim}{r},t)$	current density due to external sources
$J_n(z)$	Bessel function
$K(\omega,\underset{\sim}{k})$	effective plasma dielectric constant, Eq. (2.50)
$K_c(\omega)$	cold-plasma dielectric constant perpendicular to $\underset{\sim}{B}_o$, Eq. (3.10)
K^+, K^-	positive and negative "frequency" parts of K respectively
L	period of spatially periodic source (Chapter V)
$N(\omega,k_{\perp})$	function defined by Eq. (4.17a)
P	principal value of singular integral
$\underset{\approx}{R}(t-t')$	rotation matrix, Eq. (2.42)
$\mathcal{R}_j$	residue

$\underset{\approx}{T}(t-t')$	matrix defined by Eq. (2.43)
T	$(v_{t\parallel}/v_{t\perp})$
$Z(z)$	plasma dispersion function, Eq. (4.36)
α	index for particle species; also the proportion of the total electron density that is Maxwellian in a plasma with a mixture of ring and Maxwellian velocity distributions
α_{nm}	m^{th} zero of the Bessel function of the first kind of order n
β	$(v_{o\perp}/v_t)$
β_1,β_2,β_3	coefficients defined by Eq. (5.20)
γ_1,γ_2	coefficients defined by Eq. (5.29)
δ	small expansion parameter
$\delta(z)$	Dirac delta function
ϵ	sign of electric charge
ϵ_o	permittivity of free space = 8.854×10^{-12} F/m
η	(ω_p^2/ω_c^2)
θ	angle between $\underset{\sim}{k}$ and z axis; also polar angle in complex frequency plane (Chapter V)
κ	Boltzmann's constant = 1.38×10^{-23} J/°K
λ	$(k_\perp v_t/\omega_c)^2$ and $(k_\perp v_{t\perp}/\omega_c)^2$
λ_l	$(k_{\perp l} v_t/\omega_c)^2$
μ	$(kv_{o\perp}/\omega_c)$
μ_o	permeability of free space = $4\pi \times 10^{-7}$ H/m

$\mu_\perp$	$(k_\perp v_{o\perp}/\omega_c)$
ν	electron-neutral collision frequency
$\xi_\perp$	$(k_\perp v_o/\omega_c)$
$\rho(\underset{\sim}{r},t)$	total charge density of plasma
$\rho_s(\underset{\sim}{r},t)$	charge density of external sources
$\rho_s(\underset{\sim}{k},\omega)$	Fourier and Laplace transforms of $\rho_s(\underset{\sim}{r},t)$
τ	$\omega_c t$
φ	$\omega_c(t-t')$; also dummy variable (Chapter V)
ψ	cylindrical coordinate of velocity vector, $\underset{\sim}{v} = (v_\perp,\psi,v_\parallel)$
ω	frequency (rad/s)
ω_r,ω_i	real and imaginary parts of ω respectively
$\omega_j(\underset{\sim}{k})$	j^{th} root of dispersion relation
ω_m	root of Eq. (5.64)
$\omega_{p\alpha},\omega_p$	plasma frequency = $(n_o q/\epsilon_o m)^{1/2}$
ω_c	cyclotron frequency = $\lvert q\rvert\beta_o/m$
ω_H	cold-plasma upper hybrid frequency
$\Gamma(z)$	gamma function
Θ	spherical coordinate of velocity vector, $\underset{\sim}{v} = (v,\psi,\Theta)$
$\Phi(\underset{\sim}{r},t)$	electric potential
Ω	(ω/ω_c)

ACKNOWLEDGMENT

I wish to express my appreciation to Professor F. W. Crawford, my thesis supervisor, for his advice and encouragement during the course of this research, and for his constructive criticisms during the preparation of this manuscript. Thanks are also due to Dr. T. J. Fessenden and Professor J. L. Moll for their reading of the dissertation.

I am grateful to Dr. T. D. Mantei and R. Bruce for their assistance with some of the computations, to Drs. H. Derfler and T. C. Simonen for use of their computer program that generates the plasma dispersion function, Eq. (4.36), and to Miss Mary McGrath for her assistance in the preparation of the manuscript.

I am also indebted to the staff of the publications department of the Stanford Electronics Laboratories for their many favors.

I. INTRODUCTION

A plasma is a collection of positive and negative charges of suitably high density that is characterized by a tendency to remain electrically neutral. Any displacement of oppositely charged particles in this medium creates a strong electric field that resists the displacement, and leads to collective oscillations of the charges about their equilibrium position. These oscillations have been studied extensively in various plasma models over a long period of time [1] - [5], and a number of conclusions can be drawn: (1) in the cold-plasma approximation where the random thermal motion of the charged particles is neglected, oscillations of an infinite plasma are nondispersive; (2) if thermal energy is taken into consideration, space-charge oscillations are transported through the plasma in the form of propagating longitudinal waves; and (3) the amplitude of these waves may decay or grow in time, depending on the distribution of the particle velocities.

In recent years there has been considerable interest in wave motion of this type that occurs in hot plasmas immersed in a magnetic field. These waves are termed "cyclotron harmonic waves" since a mode of propagation is found near each harmonic of the electron and ion cyclotron frequencies; they are predicted when the collisionless Boltzmann equation is solved self-consistently with Maxwell's equations in the quasi-static approximation. This interest has been stimulated largely by numerous observations of strong cyclotron harmonic effects in magnetoplasmas. Examples of this are the emission [6] - [10] and absorption [8] of radiation at the electron cyclotron harmonics, and the excitation of resonances in the ionosphere at these frequencies [11]. In the latter experiments, the Canadian satellite Alouette I, using a pulsed transmitter of variable frequency, received a signal at the harmonics for several periods after transmitting a pulse. A more complete review of these phenomena is given in a paper by Crawford [12].

At first it might appear that the radiation emitted by an electron gyrating in a magnetic field would explain some of these observations. However, computations show that relativistic energies are required to

account for the measured intensities, whereas the experiments were carried out in low temperature plasma. This suggests that strong collective effects were playing an important role. Tanaka et al [13], [14], and Canobbio and Croci [15] proposed that electrostatic cyclotron harmonic waves are excited and radiate by coupling to an electromagnetic field. It has also been suggested that cyclotron harmonic wave instabilities of the type investigated by Harris [4], [5] may explain some of the experimental results. Harris [4], [5], [16], and Ozawa, Kaji, and Kito [17] have obtained approximate threshold conditions for these instabilities near the electron cyclotron frequency, while Kammash and Heckrotte [18], and Hall, Heckrotte, and Kammash [19] consider unstable electrostatic oscillations that occur near the ion cyclotron frequency.

Full appreciation of the detailed behavior of cyclotron harmonic waves in these studies is difficult since the dispersion relation which describes the propagation is formidable. Simplifying assumptions are usually made to facilitate the analysis, and consequently some effects may have escaped notice. In this work the solutions to the dispersion relation describing cyclotron harmonic wave propagation in a hot magnetoplasma are examined in detail. Computations are presented which show for the first time the dispersion characteristics of these waves, how instability arises from coupling of the individual modes of propagation, and the exact threshold conditions for these instabilities. The numerical results are compared with analytic solutions of the dispersion relation that are obtainable in certain limiting cases, and a detailed analysis is made of the steady state conditions of the plasma in cases where instability is absent. Based on this research, a clear and comprehensive picture of cyclotron harmonic wave propagation is constructed.

The basic plasma model that is investigated consists of an equal number of electrons and ions immersed in a uniform magnetic field and free of any electric field. The theory which predicts electrostatic space-charge oscillations in this medium is considered in Chapter II. Matrix notation is used wherever possible in the analysis to keep the equations tractable. It has been found that the dispersion relation can acquire a relatively simple form for certain classes of particle velocity distributions, and this leads to important conclusions regarding the behavior of the waves.

Chapter III is devoted to a detailed study of the solutions of the dispersion relation for propagation that is perpendicular to the applied magnetic field, and Chapter IV treats oblique propagation. The dispersion relation is first solved for complex frequency in terms of a real propagation vector, and the results are displayed in both graphical and analytical forms for several important velocity distributions. This leads to an accurate prediction of the threshold conditions for instability and the expected growth rates of the excited waves. These instabilities are classified as either absolute (corresponding to growth in time) or convective (corresponding to spatial amplification at a real frequency). The steady state conditions of the plasma, characterized by the complex wave number solutions of the dispersion relation for real frequency, are also examined in the cases where the plasma is stable. In Chapter V a study is made of the electrostatic resonances that occur in a hot magnetoplasma. This problem has possible applications to plasma ringing that has recently been detected in ionospheric [11] and laboratory [20], [21] plasmas. Finally, a general discussion of the results is given in Chapter VI.

II. WAVE PROPAGATION IN A HOT MAGNETOPLASMA

The dispersion relation that describes the propagation of plane, electrostatic, space-charge waves in a hot, collisionless magnetoplasma is derived in this chapter. Several forms of this derivation are available in the literature [3], [5], [22]. The one developed here follows in principle the works of Stix [22] and Crawford [23], but as a result of improved notation through the use of matrices, the presentation given in this chapter is much more tractable and general. We also consider as special cases two classes of velocity distributions which simplify the form of the dispersion relation.

The basic equations and their perturbation expansion are presented in Section A. After specifying the unperturbed state of the plasma in Section B, we derive in Section C the expression for the electric field associated with the propagating plasma wave and obtain the dispersion relation that describes those waves. In Section D the dispersion relation is reduced to a form that is convenient for numerical and analytical solution, and the chapter ends in Section E with a discussion of the results.

A. Basic Equations and Their Perturbation Expansion

The behavior of a collisionless plasma under the influence of applied and self-consistent electric and magnetic fields is determined by Vlasov's equation [24],

$$\frac{\partial f_\alpha}{\partial t} + \underset{\sim}{v} \cdot \nabla f_\alpha + \frac{q_\alpha}{m_\alpha} (\underset{\sim}{E} + \underset{\sim}{v} \times \underset{\sim}{B}) \cdot \frac{\partial f_\alpha}{\partial \underset{\sim}{v}} = 0 \ , \tag{2.1}$$

and by Maxwell's equations,

$$\nabla \times \underset{\sim}{E} = - \frac{\partial \underset{\sim}{B}}{\partial t} \ , \tag{2.2}$$

$$\nabla \times \underset{\sim}{H} = \underset{\sim}{J} + \underset{\sim}{J}_s + \epsilon_o \frac{\partial \underset{\sim}{E}}{\partial t} \ , \tag{2.3}$$

$$\nabla \cdot \underset{\sim}{E} = \frac{1}{\epsilon_o} (\rho + \rho_s) \ , \tag{2.4}$$

$$\nabla \cdot \underset{\sim}{B} = 0 \ , \tag{2.5}$$

where rationalized MKS units are assumed. In these expressions $f_\alpha(\underset{\sim}{r},\underset{\sim}{v},t)$ is the single-particle velocity distribution for species α; q_α and m_α are respectively the charge and mass of the species; $\underset{\sim}{E}(\underset{\sim}{r},t)$ is the electric field; $\underset{\sim}{B}(\underset{\sim}{r},t) = \mu_o \underset{\sim}{H}(\underset{\sim}{r},t)$ is the magnetic field; and ϵ_o and μ_o are respectively the permittivity and permeability of free space. Vlasov's and Maxwell's equations are coupled through the total charge density of the plasma

$$\rho(\underset{\sim}{r},t) = \sum_\alpha q_\alpha n_{\alpha o} \int d\underset{\sim}{v} \ f_\alpha(\underset{\sim}{r},\underset{\sim}{v},t) \ , \tag{2.6}$$

and the corresponding current density

$$\underset{\sim}{J}(\underset{\sim}{r},t) = \sum_\alpha q_\alpha n_{\alpha o} \int d\underset{\sim}{v} \ f_\alpha(\underset{\sim}{r},\underset{\sim}{v},t)\underset{\sim}{v} \ , \tag{2.7}$$

while $\rho_s(\underset{\sim}{r},t)$ and $\underset{\sim}{J}_s(\underset{\sim}{r},t)$ represent the charge density and current density due to particles that are distinct from the plasma and are looked upon as external sources. In Eqs. (2.6) and (2.7), $f_\alpha(\underset{\sim}{r},\underset{\sim}{v},t)$ has been normalized such that the particle density of the species is

$$n_\alpha(\underset{\sim}{r},t) = n_{\alpha o} \int d\underset{\sim}{v} \ f_\alpha(\underset{\sim}{r},\underset{\sim}{v},t) \ , \tag{2.8}$$

where $n_{\alpha o}$ is the average density. If the plasma is homogeneous, we then have the normalization

$$\int d\underset{\sim}{v} \ f_\alpha = 1 \ . \tag{2.9}$$

Equations (2.1) - (2.5) define a closed mathematical system which completely describes the behavior of the plasma. Because the electric and magnetic fields are functions of $\rho(\underset{\sim}{v},t)$ and $\underset{\sim}{J}(\underset{\sim}{r},t)$, and hence the

velocity distribution $f_\alpha(\underset{\sim}{r},\underset{\sim}{v},t)$, the system is nonlinear and recourse must be made to perturbation-theoretic techniques to obtain a solution. We expand all variables about a macroscopic state of the plasma for which the velocity distribution $f_{\alpha o}(\underset{\sim}{r},\underset{\sim}{v},t)$, the electric and magnetic fields $\underset{\sim}{E}_o(\underset{\sim}{r},t)$ and $\underset{\sim}{B}_o(\underset{\sim}{r},t)$, and the trajectory of the charged particles $\underset{\sim}{r}_{\alpha o}(t)$ are either known or can be solved for. In terms of a small expansion parameter δ we then write

$$f_\alpha(\underset{\sim}{r},\underset{\sim}{v},t) = \sum_{n=0}^{\infty} \delta^n f_{\alpha n}(\underset{\sim}{r},\underset{\sim}{v},t) \quad , \tag{2.10}$$

$$\underset{\sim}{E}(\underset{\sim}{r},t) = \sum_{n=0}^{\infty} \delta^n \underset{\sim}{E}_n(\underset{\sim}{r},t) \quad , \tag{2.11}$$

$$\underset{\sim}{B}(\underset{\sim}{r},t) = \sum_{n=0}^{\infty} \delta^n \underset{\sim}{B}_n(\underset{\sim}{r},t) \quad . \tag{2.12}$$

After substituting the series in Eq. (2.1), we find that the zero-order velocity distribution must satisfy the equation

$$\frac{\partial f_{\alpha o}}{\partial t} + \underset{\sim}{v} \cdot \nabla f_{\alpha o} + \underset{\sim}{a}_{\alpha o} \cdot \frac{\partial f_{\alpha o}}{\partial \underset{\sim}{v}} = 0 \quad , \tag{2.13}$$

while the higher order corrections, $f_{\alpha n}(\underset{\sim}{r},\underset{\sim}{v},t)$, are determined by

$$\frac{\partial f_{\alpha n}}{\partial t} + \underset{\sim}{v} \cdot \nabla f_{\alpha n} + \underset{\sim}{a}_{\alpha o} \cdot \frac{\partial f_{\alpha n}}{\partial \underset{\sim}{v}} = - \sum_{k=1}^{n} \underset{\sim}{a}_{\alpha k} \cdot \frac{\partial f_{\alpha(n-k)}}{\partial \underset{\sim}{v}} \quad , \qquad n \neq 0 \tag{2.14}$$

where

$$\underset{\sim}{a}_{\alpha n}(\underset{\sim}{r},\underset{\sim}{v},t) = \frac{q_\alpha}{m_\alpha}\left[\underset{\sim}{E}_n(\underset{\sim}{r},t) + \underset{\sim}{v} \times \underset{\sim}{B}_n(\underset{\sim}{r},t)\right] , \tag{2.15}$$

is the component of the particle acceleration due to the fields $\underset{\sim}{E}_n(\underset{\sim}{r},t)$ and $\underset{\sim}{B}_n(\underset{\sim}{r},t)$.

Equation (2.14) can be integrated formally by transforming to coordinates $(\underset{\sim}{r}_{\alpha o}(t),\ \underset{\sim}{v}_{\alpha o}(t))$ that follow the motion of a charged particle in the zero-order fields and hence satisfy the equations

$$\frac{d\underset{\sim}{r}_{\alpha o}(t)}{dt} = \underset{\sim}{v}_{\alpha o}(t) , \tag{2.16}$$

$$\frac{d\underset{\sim}{v}_{\alpha o}(t)}{dt} = \underset{\sim}{a}_{\alpha o}\left(\underset{\sim}{r}_{\alpha o}(t),\ \underset{\sim}{v}_{\alpha o}(t),t\right) . \tag{2.17}$$

In this case the left-hand side of Eq. (2.14) can be written in the form

$$\frac{\partial f_{\alpha n}}{\partial t} + \frac{d\underset{\sim}{r}_{\alpha o}}{dt} \cdot \nabla_{\alpha o} f_{\alpha n} + \frac{d\underset{\sim}{v}_{\alpha o}}{dt} \cdot \frac{\partial f_{\alpha n}}{\partial \underset{\sim}{v}_{\alpha o}} , \tag{2.18}$$

which is readily identified as the total time derivative (d/dt) of $f_{\alpha n}\left(\underset{\sim}{r}_{\alpha o}(t),\underset{\sim}{v}_{\alpha o}(t),t\right)$. Here, $\nabla_{\alpha o}$ is the gradient operator with respect to $\underset{\sim}{r}_{\alpha o}(t)$. Therefore the rate of change of $f_{\alpha n}$ along the zero-order trajectory is

$$\frac{df_{\alpha n}}{dt} = -\sum_{k=1}^{n} \underset{\sim}{a}_{\alpha k}(\underset{\sim}{r}_{\alpha o},\underset{\sim}{v}_{\alpha o},t) \cdot \frac{\partial f_{\alpha(n-k)}(\underset{\sim}{r}_{\alpha o},\underset{\sim}{v}_{\alpha o},t)}{\partial \underset{\sim}{v}_{\alpha o}} . \tag{2.19}$$

This is to be integrated from $t = 0$ when the sources are turned on, to the present time t when the particle's position and velocity, $r_{\alpha o}(t)$ and $\underset{\sim}{v}_{\alpha o}(t)$, coincide respectively with the Eulerian coordinates $\underset{\sim}{r}$ and $\underset{\sim}{v}$. This gives us

$$f_{\alpha n}(\underset{\sim}{r},\underset{\sim}{v},t) = -\sum_{k=1}^{n}\int_{0}^{t} dt'\ \underset{\sim}{a}_{\alpha k}(\underset{\sim}{r}'_{\alpha o},\underset{\sim}{v}'_{\alpha o},t')\cdot\frac{\partial f_{\alpha(n-k)}(\underset{\sim}{r}'_{\alpha o},\underset{\sim}{v}'_{\alpha o},t')}{\partial \underset{\sim}{v}'_{\alpha o}}\ , \tag{2.20}$$

where $\underset{\sim}{r}'_{\alpha o} = \underset{\sim}{r}_{\alpha o}(t')$, $\underset{\sim}{v}'_{\alpha o} = \underset{\sim}{v}_{\alpha o}(t')$, and it has been assumed that all initial conditions are zero.

In this work we shall consider only equations that are linear in δ. Consequently, instabilities predicted by this approximate theory may not be found in a more exact analysis since the nonlinear terms which are excluded here may stabilize the plasma. This will limit the time interval over which our equations are valid. Since this work is concerned only with space-charge waves, we also will invoke the quasi-static approximation at the outset and assume that the electric field perturbation $\underset{\sim}{E}_1(\underset{\sim}{r},t)$ can be represented as the negative gradient of a scalar potential, $\Phi_1(\underset{\sim}{r},t)$, that is, we assume $\underset{\sim}{E}_1(\underset{\sim}{r},t) = -\nabla\Phi_1(\underset{\sim}{r},t)$ and hence $\nabla \times \underset{\sim}{E}_1(\underset{\sim}{r},t) = 0$. This is equivalent to neglecting interactions which involve the magnetic field perturbation $\underset{\sim}{B}_1(\underset{\sim}{r},t)$, and is valid when the phase velocity of the wave is much smaller than the speed of light. In this approximation the full set of Maxwell's equations is replaced by the linearized Poisson's equation,

$$\nabla\cdot\underset{\sim}{E}_1(\underset{\sim}{r},t) = \frac{1}{\epsilon_o}\left[\rho_s(\underset{\sim}{r},t) + \sum_{\alpha} q_\alpha\, n_{\alpha o}\int d\underset{\sim}{v}\, f_{\alpha 1}(\underset{\sim}{r},\underset{\sim}{v},t)\right]. \tag{2.21}$$

The function $f_{\alpha 1}$ is obtainable from Eqs. (2.15) and (2.20), where $\underset{\sim}{B}_1(\underset{\sim}{r},t)$ is to be neglected in (2.15). Hence, Eq. (2.21) reads

$$\nabla\cdot\underset{\sim}{E}_1(\underset{\sim}{r},t) + \sum_{\alpha}\omega_{p\alpha}^2\int d\underset{\sim}{v}\int_0^t dt'\ \underset{\sim}{E}_1(\underset{\sim}{r}'_{\alpha o},t')\cdot\frac{\partial f_{\alpha o}(\underset{\sim}{r}'_{\alpha o},\underset{\sim}{v}'_{\alpha o},t')}{\partial \underset{\sim}{v}'_{\alpha o}} = \frac{\rho_s(\underset{\sim}{r},t)}{\epsilon_o}\ , \tag{2.22}$$

where $\omega_{p\alpha} = \left(n_{\alpha o} q_\alpha^2 / \epsilon_o m_\alpha\right)^{1/2}$ is the plasma frequency of species α. In writing these equations it is assumed that the source ρ_s is a term of order δ. This integrodifferential equation can be solved for the electric field after specifying the zero-order state of the plasma.

B. Zero-Order State

1. Particle Velocity Distribution

The zero-order state is defined by the equations

$$\frac{\partial f_o}{\partial t} + \underset{\sim}{v} \cdot \nabla f_o + \frac{q}{m}\left(\underset{\sim o}{E} + \underset{\sim}{v} \times \underset{\sim o}{B}\right) \cdot \frac{\partial f_o}{\partial \underset{\sim}{v}} = 0 , \tag{2.23}$$

$$\nabla \times \underset{\sim o}{E} = - \frac{\partial \underset{\sim o}{B}}{\partial t} , \tag{2.24}$$

$$\nabla \times \underset{\sim o}{H} = \sum_\alpha q n_o \int d\underset{\sim}{v}\, f_o \underset{\sim}{v} + \epsilon_o \frac{\partial \underset{\sim o}{E}}{\partial t} , \tag{2.25}$$

$$\nabla \cdot \underset{\sim o}{E} = \frac{1}{\epsilon_o} \sum_\alpha q n_o \int d\underset{\sim}{v}\, f_o , \tag{2.26}$$

$$\nabla \cdot \underset{\sim o}{B} = 0 , \tag{2.27}$$

where we have dropped the subscript α and will assume that the summation runs over the particle species. This convention will be followed throughout the remainder of the chapter. If perturbation techniques are to be useful, the zero-order state must be chosen so that it is physically realizable and yet analytically tractable. With this in mind, we consider a homogeneous plasma immersed in a uniform magnetic field $\underset{\sim o}{B}$ with no electric field present. All spatial derivatives in Eqs. (2.23) - (2.27) then vanish, and the state of the plasma is described by the equations

$$\frac{\partial f_o}{\partial t} + \frac{q}{m} (\underset{\sim}{v} \times \underset{\sim o}{B}) \cdot \frac{\partial f_o}{\partial \underset{\sim}{v}} = 0 \quad , \tag{2.28}$$

$$\sum_{\alpha} q n_o \int d\underset{\sim}{v}\, f_o \underset{\sim}{v} = 0 \quad , \tag{2.29}$$

$$\sum_{\alpha} q n_o \int d\underset{\sim}{v}\, f_o = 0 \quad . \tag{2.30}$$

In order to solve Eq. (2.28), it is convenient to express the velocity in terms of cylindrical coordinates $(v_\perp, \psi, v_\parallel)$ as defined in Fig. 1. This gives us

$$\underset{\sim}{v} = v_\perp \hat{v}_\perp + v_\parallel \hat{z} \quad , \tag{2.31}$$

$$\frac{\partial f_o}{\partial \underset{\sim}{v}} = \frac{\partial f_o}{\partial v_\perp} \hat{v}_\perp + \frac{1}{v_\perp} \frac{\partial f_o}{\partial \psi} \hat{v}_\psi + \frac{\partial f_o}{\partial v_\parallel} \hat{z} \quad , \tag{2.32}$$

$$\underset{\sim o}{B} = B_o \hat{z} \quad , \tag{2.33}$$

where $\hat{v}_\perp$, $\hat{v}_\psi$ and $\hat{z}$ are orthogonal base vectors, and it has been assumed without loss of generality that the magnetic field is parallel to the z axis. Using Eqs. (2.31) - (2.33), it is readily established that

$$(\underset{\sim}{v} \times \underset{\sim o}{B}) \cdot \frac{\partial f_o}{\partial \underset{\sim}{v}} = - B_o \frac{\partial f_o}{\partial \psi} \quad , \tag{2.34}$$

and hence Eq. (2.28) can be written in the form

$$\frac{\partial f_o}{\partial t} - \epsilon \omega_c \frac{\partial f_o}{\partial \psi} = 0 \quad , \tag{2.35}$$

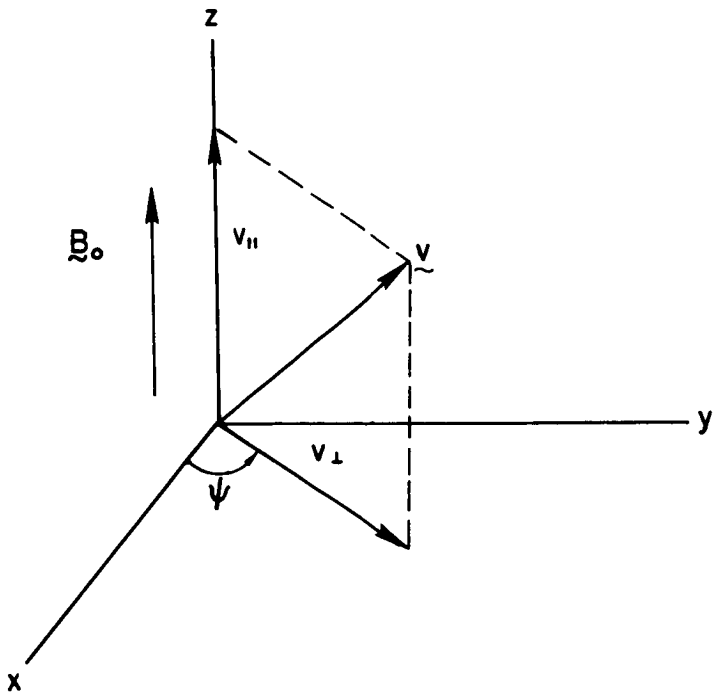

Fig. 1. CYLINDRICAL COORDINATES OF THE VELOCITY VECTOR $\underset{\sim}{v}$.

where $\epsilon = q/|q|$ is the sign of the charge and $\omega_c = |q|B_o/m$ is the cyclotron frequency.

The general solution of Eq. (2.35) is clearly

$$f_o = f_o(v_\perp, \psi + \epsilon\omega_c t, v_\parallel) \quad , \tag{2.36}$$

where f_o must be chosen such that the total current density and charge density of the plasma vanish in accordance with Eqs. (2.29) and (2.30). It is observed that the velocity distribution is a function of time only if it is also a function of the polar angle ψ. If there is no dependency on either t or ψ, the distribution must then be a member of the class of functions defined by

$$f_o = f_o(v_\perp, v_\parallel) \quad . \tag{2.37}$$

It is this class of velocity distributions that will be investigated in this work.

2. Particle Trajectory

The zero-order particle trajectory which is required in Eq. (2.22) is governed by the equations

$$\frac{d\underset{\sim}{r}_o(t')}{dt'} = \underset{\sim}{v}_o(t') \quad , \tag{2.38}$$

$$\frac{d\underset{\sim}{v}_o(t')}{dt'} = \frac{q}{m}\, \underset{\sim}{v}_o(t') \times \underset{\sim}{B}_o \quad , \tag{2.39}$$

since no electric field is present in this plasma model. The solution, which coincides with the Eulerian variables $(\underset{\sim}{r},\underset{\sim}{v})$ when $t' = t$, is readily obtained, and the result is conveniently expressed in matrix notation in the following manner:

$$\underset{\sim}{r}_o(t') = \underset{\sim}{r} - \frac{1}{\omega_c}\, \underset{\approx}{T}(t-t') \cdot \underset{\sim}{v} \quad , \tag{2.40}$$

$$\underset{\sim}{v}_o(t') = \underset{\approx}{R}(t-t') \cdot \underset{\sim}{v} \, , \tag{2.41}$$

where the elements of the matrices $\underset{\approx}{R}$ and $\underset{\approx}{T}$ in a cartesian coordinate system are

$$[R_{ij}] = \begin{bmatrix} \cos\varphi & -\epsilon \sin\varphi & 0 \\ \epsilon \sin\varphi & \cos\varphi & 0 \\ 0 & 0 & 1 \end{bmatrix} \quad , \tag{2.42}$$

$$[T_{ij}] = \begin{bmatrix} \sin\varphi & -\epsilon(1-\cos\varphi) & 0 \\ \epsilon(1-\cos\varphi) & \sin\varphi & 0 \\ 0 & 0 & \varphi \end{bmatrix} . \qquad (2.43)$$

Here, φ has been set equal to $\omega_c(t-t')$, and it has been assumed that $\underset{\sim}{B}_o$ is parallel to the z axis. It is readily established that the trajectory is a helical path parallel to the magnetic field. The radius of gyration in the transverse plane is $(v_\perp/\omega_c)$, and the frequency of rotation is ω_c. $\underset{\approx}{R}(t-t')$ will be recognized as a rotation operator in velocity space.

C. Dispersion Relation for Cyclotron Harmonic Waves

The spatial homogeneity and time invariance of the assumed plasma model permits us to solve Eq. (2.22) with transform techniques. We introduce a Fourier transform in space and a Laplace transform in time according to

$$\underset{\sim}{E}_1(\underset{\sim}{k},\omega) = \int d\underset{\sim}{r} \int_0^\infty dt\, \underset{\sim}{E}_1(\underset{\sim}{r},t) \exp\,[-i(\omega t - \underset{\sim}{k}\cdot\underset{\sim}{r})] , \qquad (2.44)$$

and the inverse formula

$$\underset{\sim}{E}_1(\underset{\sim}{r},t) = \int \frac{d\underset{\sim}{k}}{(2\pi)^3} \int_C \frac{d\omega}{2\pi}\, \underset{\sim}{E}_1(\underset{\sim}{k},\omega) \exp\,[i(\omega t - \underset{\sim}{k}\cdot\underset{\sim}{r})] , \qquad (2.45)$$

where $\underset{\sim}{k}$ is real and the contour C is a straight line parallel to the real axis in the lower-half complex ω plane, below all singularities of the integrand. This choice of C imposes the principle of causality in that the response of the plasma due to sources that are turned on at $t = 0$ is forced to be zero for $t < 0$.

Equation (2.22) is transformed first over $\underset{\sim}{r}$. The integral equation for the $\underset{\sim}{k}^{th}$ Fourier component of the electric field then reads

$$-i\underset{\sim}{k}\cdot \underset{\sim}{E}_1(\underset{\sim}{k},t) + \sum_{\alpha} \omega_p^2 \int d\underset{\sim}{v} \int_0^t dt' \; \underset{\sim}{E}_1(\underset{\sim}{k},t')$$

$$\cdot \frac{\partial f_o(v_\perp, v_\parallel)}{\partial \underset{\sim}{v}_o(t-t')} \exp\left[\frac{i}{\omega_c} \underset{\sim}{k}\cdot \underset{\approx}{T}(t-t')\cdot \underset{\sim}{v}\right] = \frac{1}{\epsilon_o} \rho_s(\underset{\sim}{k},t) \, , \tag{2.46}$$

where $\underset{\sim}{v}_o(t-t')$ is given by Eq. (2.41) and the time-invariant velocity distribution, Eq. (2.37), has been introduced. Since the left-hand side of this equation contains an integral of a function of t' multiplied by a function of $(t-t')$, we can invoke the convolution theorem

$$\int_0^\infty dt \exp(-i\omega t) \int_0^t dt' \, f_1(t') \, f_2(t-t') = f_1(\omega) \, f_2(\omega) \quad , \tag{2.47}$$

to find the Laplace transform of Eq. (2.46):

$$\left\{-ik + \sum_{\alpha} \omega_p^2 \int d\underset{\sim}{v} \int_0^\infty dt \, \frac{\partial f_o(v_\perp, v_\parallel)}{\partial \underset{\sim}{v}_o(t)} \exp\left[-i\omega t + \frac{i}{\omega_c} \underset{\sim}{k}\cdot \underset{\approx}{T}(t)\cdot \underset{\sim}{v}\right]\right\}$$

$$\cdot \underset{\sim}{E}_1(\underset{\sim}{k},\omega) = \frac{1}{\epsilon_o} \rho_s(\underset{\sim}{k},\omega) \, . \tag{2.48}$$

In the electrostatic approximation, $\underset{\sim}{E}(\underset{\sim}{k},\omega) = i\underset{\sim}{k}\Phi_1(\underset{\sim}{k},\omega)$, where $\Phi_1(\underset{\sim}{k},\omega)$ is the double transform of a scalar potential. Therefore, the solution to Eq. (2.48) is

$$\underset{\sim}{E}_1(\underset{\sim}{k},\omega) = \frac{i\underset{\sim}{k} \, \rho_s(\underset{\sim}{k},\omega)}{\epsilon_o k^2 K(\omega,\underset{\sim}{k})} \quad , \tag{2.49}$$

where the effective dielectric constant of the plasma is given by

$$K(\omega,\underset{\sim}{k}) = 1 + \sum_{\alpha} \frac{\omega_p^2}{k^2} \int d\underset{\sim}{v} \int_0^{\infty} dt\ i\underset{\sim}{k} \cdot \frac{\partial f_o(v_\perp, v_{||})}{\partial \underset{\sim}{v}_o(t)} \exp\left[-i\omega t + \frac{i}{\omega_c}\, \underset{\sim}{k} \cdot \underset{\approx}{T}(t) \cdot \underset{\sim}{v}\right] . \tag{2.50}$$

The stability of the assumed plasma - magnetic field configuration is determined by the $\underset{\sim}{k}^{th}$ Fourier component of the electric field, $\underset{\sim}{E}_1(\underset{\sim}{k},t)$, as $t \to \infty$. This limit is obtainable from the inverse Laplace transform of Eq. (2.49),

$$\underset{\sim}{E}_1(\underset{\sim}{k},t) = \int_C \frac{d\omega}{2\pi} \frac{i\underset{\sim}{k}\, \rho_s(\underset{\sim}{k},\omega) \exp(i\omega t)}{\epsilon_o k^2 K(\omega,\underset{\sim}{k})} , \tag{2.51}$$

with the procedure proposed by Landau [2]. In this procedure the ω integration is carried out along a contour C' that is formed by the continuous deformation of C around the singularities of the integrand into the upper half plane as shown in Fig. 2. As $t \to \infty$, the contribution from the horizontal portion of the contour vanishes exponentially, and, according to Cauchy's residue theorem, the limiting form of the electric field is determined by the encircled poles at $\omega = \omega_j(\underset{\sim}{k})$. It can consequently be written in the form

$$\lim_{t\to\infty} \underset{\sim}{E}_1(\underset{\sim}{k},t) = 2\pi i \sum_j \underset{\sim}{R}_j \exp[i\omega_j(\underset{\sim}{k})t] , \tag{2.52}$$

where $\underset{\sim}{R}_j = \lim_{\omega\to\omega_j} [(\omega-\omega_j)\underset{\sim}{E}_1(\underset{\sim}{k},\omega)]$ is the residue of the j^{th} pole, and $\omega_j(\underset{\sim}{k})$ satisfies the dispersion relation for electrostatic space-charge waves

$$K[\omega_j(\underset{\sim}{k}),\underset{\sim}{k}] = 0 . \tag{2.53}$$

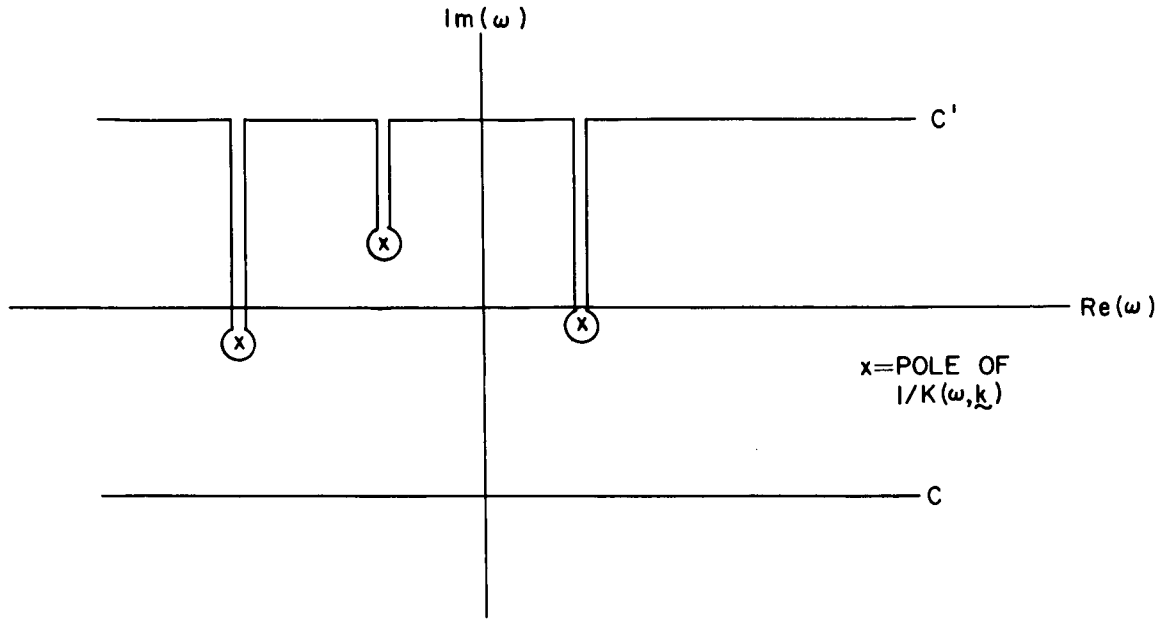

Fig. 2. ORIGINAL (C) AND DEFORMED (C') LAPLACE CONTOUR OF INTEGRATION.

The waves predicted by this equation are commonly referred to as cyclotron harmonic waves. It should be pointed out that this result is based on the assumption that the numerator and denominator in Eq. (2.51) are entire functions of ω and therefore the singularities are poles located at $\omega_j(\underset{\sim}{k})$. If this assumption is not satisfied, the appropriate contribution from any other singularities must be added to Eq. (2.52). It is now clear that the stability of the plasma is determined by the complex frequency solutions of the dispersion relation with $\underset{\sim}{k}$ real. If $\mathrm{Im}(\omega_j) < 0$, the electric field will grow in time, and the plasma is said to be unstable. Steady oscillations are excited if $\mathrm{Im}(\omega_j) = 0$, while the oscillations will decay in time if $\mathrm{Im}(\omega_j) > 0$.

It is our purpose to investigate next the solutions of Eq. (2.53) for several velocity distributions that are of general interest in plasma physics. The choice of distributions is guided largely by experiments that show evidence of instabilities and propagating waves in magneto-plasmas. The representation of the dielectric constant in Eq. (2.50) is in its present form inconvenient for this analysis and so, in the next section, a more useful form will be derived for that function.

D. Reduction of the Plasma Dielectric Constant

The purpose of this section is to obtain a form of the plasma dielectric constant that is convenient for the analytical and numerical solution of Eq. (2.53), the dispersion relation for cyclotron harmonic waves. Several representations of this term are available in the literature [3,4,5,19,49], but only those of immediate interest will be derived here.

The basic form of the dielectric constant is, from Eq. (2.50),

$$K(\omega,\underset{\sim}{k}) = 1 + \sum_{\alpha} \frac{\omega_p^2}{k^2} \int d\underset{\sim}{v} \int_0^\infty dt\ i\underset{\sim}{k} \cdot \frac{\partial f_o(v_\perp, v_{||})}{\partial \underset{\sim}{v}_o(t)} \exp\left[-i\omega t + \frac{i}{\omega_c} \underset{\sim}{k} \cdot \underset{\approx}{T}(t) \cdot \underset{\sim}{v}\right] . \tag{2.54}$$

Without loss of generality, it is assumed here that $\underset{\sim}{k}$ lies in the x-z plane at an angle θ to the magnetic field as shown in Fig. 3, permitting us to write for the cartesian components of the wave vector

$$(k_x, k_y, k_z) = (k_\perp, 0, k_{||}) , \tag{2.55}$$

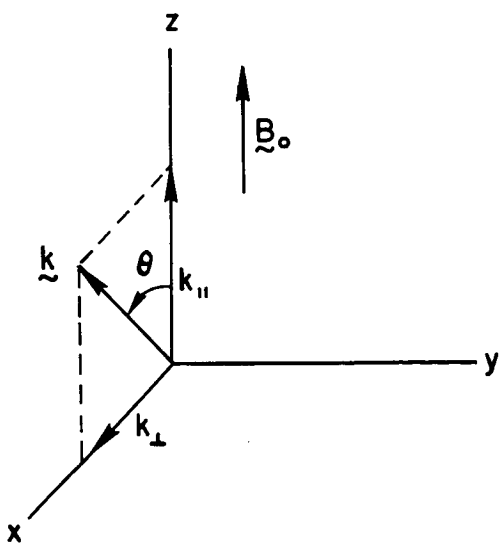

Fig. 3. COMPONENTS OF THE WAVE VECTOR $\underset{\sim}{k}$.

while the velocity space integration is most conveniently accomplished in terms of cylindrical variables $(v_\perp, \psi, v_\parallel)$ where

$$(v_x, v_y, v_z) = (v_\perp \cos\psi,\ v_\perp \sin\psi,\ v_\parallel) \ . \tag{2.56}$$

We now make use of Eqs. (2.43), (2.55), and (2.56) in order to obtain the expansion

$$\underset{\sim}{k} \cdot \underset{\approx}{T}(t) \cdot \underset{\sim}{v} = 2k_\perp v_\perp \sin\frac{\omega_c t}{2} \cos\left(\psi + \epsilon\frac{\omega_c t}{2}\right) + k_\parallel v_\parallel \omega_c t \ , \tag{2.57}$$

and similarly, with the aid of Eq. (2.41), it is readily established that

$$\underset{\sim}{k} \cdot \frac{\partial f_o(v_\perp, v_\parallel)}{\partial \underset{\sim}{v}_o(t)} = k_\perp \frac{\partial f_o}{\partial v_\perp} \cos(\psi + \epsilon\omega_c t) + k_\parallel \frac{\partial f_o}{\partial v_\parallel} \ . \tag{2.58}$$

Substitution of Eqs. (2.57) and (2.58) in Eq. (2.54) then yields the expression

$$K(\omega, \underset{\sim}{k}) = 1 + \sum_\alpha \frac{\omega_p^2}{k^2} \int_{-\infty}^{\infty} dv_\parallel \int_0^\infty v_\perp\, dv_\perp \int_0^{2\pi} d\psi \int_0^\infty dt\, i\left[k_\perp \frac{\partial f_o}{\partial v_\perp} \cos(\psi + \epsilon\omega_c t) + k_\parallel \frac{\partial f_o}{\partial v_\parallel}\right] G(\psi, t) \ , \tag{2.59}$$

where

$$G(\psi, t) = \exp\left[-i(\omega - k_\parallel v_\parallel)t + 2i\frac{k_\perp v_\perp}{\omega_c} \sin\frac{\omega_c t}{2} \cos\left(\psi + \epsilon\frac{\omega_c t}{2}\right)\right] \ . \tag{2.60}$$

We now make use of the Bessel function expansion [25]

$$\exp\ (iz\ \cos\ \alpha) = \sum_{n=-\infty}^{\infty} i^n\ J_n(z)\ \exp\ (in\alpha) \tag{2.61}$$

to evaluate the integrals with respect to ψ. This yields

$$\int_0^{2\pi} d\psi \begin{bmatrix} 1 \\ \cos\ (\psi + \epsilon\omega_c t) \end{bmatrix} G(\psi,t) = 2\pi \begin{bmatrix} J_o\left(2\ \frac{k_\perp v_\perp}{\omega_c}\ \sin\ \frac{\omega_c t}{2}\right) \\ i\ \cos\ \frac{\omega_c t}{2}\ J_1\left(2\ \frac{k_\perp v_\perp}{\omega_c}\ \sin\ \frac{\omega_c t}{2}\right) \end{bmatrix} \exp\left[-i(\omega - k_{\parallel} v_{\parallel})t\right] . \tag{2.62}$$

After introducing the identities [25]

$$J_o\left(2\ \frac{k_\perp v_\perp}{\omega_c}\ \sin\ \frac{\omega_c t}{2}\right) = \sum_{n=-\infty}^{\infty} J_n^2\left(\frac{k_\perp v_\perp}{\omega_c}\right) \exp\ (in\omega_c t)\ , \tag{2.63}$$

$$i\ \cos\ \frac{\omega_c t}{2}\ J_1\left(2\ \frac{k_\perp v_\perp}{\omega_c}\ \sin\ \frac{\omega_c t}{2}\right) = \sum_{n=-\infty}^{\infty} \frac{n\omega_c}{k_\perp v_\perp}\ J_n^2\left(\frac{k_\perp v_\perp}{\omega_c}\right) \exp\ (in\omega_c t)\ , \tag{2.64}$$

in Eq. (2.62) and substituting the result in Eq. (2.59), the dielectric constant can be written in the form

$$K(\omega,\underset{\sim}{k}) = 1 + \sum_{\alpha} \frac{\omega_p^2}{k^2} \sum_{n=-\infty}^{\infty} \int d\underset{\sim}{v} \left(\frac{n\omega_c}{v_\perp}\ \frac{\partial f_o}{\partial v_\perp} + k_{\parallel}\ \frac{\partial f_o}{\partial v_{\parallel}}\right) J_n^2\left(\frac{k_\perp v_\perp}{\omega_c}\right)$$

$$\cdot\ i \int_0^{\infty} dt\ \exp\ [-i(\omega - k_{\parallel} v_{\parallel} - n\omega_c)t]\ , \tag{2.65}$$

where the differential volume element in velocity space is $d\underset{\sim}{v} = 2\pi v_\perp dv_\perp dv_\parallel$ since the integrand is no longer a function of ψ.

The integration with respect to t will converge only if $\mathrm{Im}(\omega) < 0$. Under this restriction, it is clear that

$$i\int_0^\infty dt\, \exp\left[-i(\omega - k_\parallel v_\parallel - n\omega_c)t\right] = \frac{1}{\omega - k_\parallel v_\parallel - n\omega_c} \quad , \qquad (2.66)$$

and hence Eq. (2.65) reduces to

$$K(\omega,\underset{\sim}{k}) = 1 + \sum_\alpha \frac{\omega_p^2}{k^2} \sum_{n=-\infty}^{\infty} \int d\underset{\sim}{v} \left(\frac{n\omega_c}{v_\perp} \frac{\partial f_o}{\partial v_\perp} + k_\parallel \frac{\partial f_o}{\partial v_\parallel} \right) \frac{J_n^2\left(\frac{k_\perp v_\perp}{\omega_c}\right)}{\omega - k_\parallel v_\parallel - n\omega_c} \, ,$$

$$\mathrm{Im}(\omega) < 0 \, , \qquad (2.67)$$

which is equivalent to an expression derived by Harris [5]. It will be observed that if ω is located on the real axis, the integration with respect to $v_\parallel$ is no longer defined since a pole will be found on the contour of integration at $v_\parallel = (\omega - n\omega_c)/k_\parallel$. The correct definition of the dielectric constant for $\mathrm{Im}(\omega) \geq 0$ is the analytic continuation of Eq. (2.67) which can be obtained by using Landau's technique [2]; that is, as ω follows a continuous path across the real axis, into the upper half plane, the contour associated with the $v_\parallel$ integration is deformed into the complex plane ahead of the advancing pole at $v_\parallel = w_n [\equiv (\omega - n\omega_c/k_\parallel]$ as shown in Fig. 4 for $k_\parallel > 0$. This process leads to the following definition of $K(\omega,\underset{\sim}{k})$:

$$K(\omega,\underset{\sim}{k}) = \begin{cases} 1 + \sum_{\alpha} \frac{\omega_p^2}{k^2} \sum_{n=-\infty}^{\infty} \int_{-\infty}^{\infty} dv_{\parallel} \frac{H_n(v_{\parallel})}{\omega - k_{\parallel} v_{\parallel} - n\omega_c} , & \mathrm{Im}(\omega) < 0 , \\ 1 + \sum_{\alpha} \frac{\omega_p^2}{k^2} \sum_{n=-\infty}^{\infty} P \int_{-\infty}^{\infty} dv_{\parallel} \frac{H_n(v_{\parallel})}{\omega - k_{\parallel} v_{\parallel} - n\omega_c} + \pi i \sum_{\alpha} \frac{\omega_p^2}{|k_{\parallel}| k^2} \sum_{n=-\infty}^{\infty} H_n\left(\frac{\omega - n\omega_c}{k_{\parallel}}\right) , & \mathrm{Im}(\omega) = 0 , \\ 1 + \sum_{\alpha} \frac{\omega_p^2}{k^2} \sum_{n=-\infty}^{\infty} \int_{-\infty}^{\infty} dv_{\parallel} \frac{H_n(v_{\parallel})}{\omega - k_{\parallel} v_{\parallel} - n\omega_c} + 2\pi i \sum_{\alpha} \frac{\omega_p^2}{|k_{\parallel}| k^2} \sum_{n=-\infty}^{\infty} H_n\left(\frac{\omega - n\omega_c}{k_{\parallel}}\right) , & \mathrm{Im}(\omega) \geq 0 , \end{cases} \tag{2.68}$$

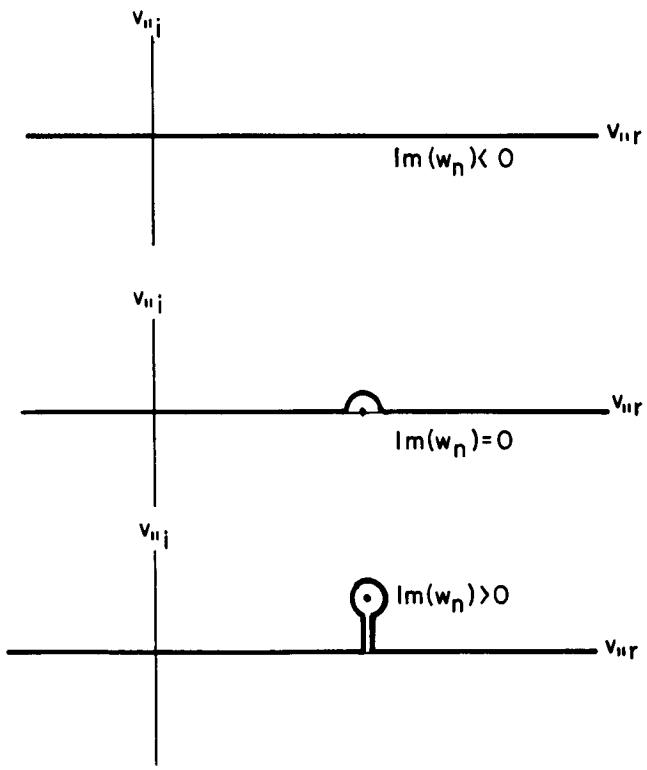

Fig. 4. ANALYTIC CONTINUATION OF PLASMA DIELECTRIC CONSTANT TO UPPER-HALF COMPLEX FREQUENCY PLANE BY DEFORMATION OF CONTOUR OF INTEGRATION IN COMPLEX $v_{\parallel}$ PLANE.

where P designates the principal value of the integral and

$$H_n(v_\parallel) = 2\pi \int_0^\infty dv_\perp \left(\frac{n\omega_c}{v_\perp} \frac{\partial f_o}{\partial v_\perp} + k_\parallel \frac{\partial f_o}{\partial v_\parallel} \right) J_n^2 \left(\frac{k_\perp v_\perp}{\omega_c} \right) v_\perp . \qquad (2.69)$$

Other representations of the dielectric constant are derivable from Eq. (2.59), and these will be presented in succeeding chapters as needed.

Further evaluation of the integral in Eq. (2.67) requires a specification of each particle velocity distribution. However, before doing this it is instructive to consider two classes of distribution functions that simplify the form of $K(\omega,\underset{\sim}{k})$ and lead to interesting conclusions.

1. Spherically Symmetric Velocity Distributions

This class is defined by

$$f_o \equiv f_o(v) , \qquad (2.70)$$

where $v[\equiv(v_\perp^2 + v_\parallel^2)^{1/2}]$ is the speed of the particle. For functions of this form, it is readily established that

$$\frac{1}{v_\perp} \frac{\partial f_o}{\partial v_\perp} = \frac{1}{v_\parallel} \frac{\partial f_o}{\partial v_\parallel} = \frac{1}{v} \frac{\partial f_o}{\partial v} , \qquad (2.71)$$

and hence, after this has been used in Eq. (2.67), together with the identity

$$\frac{n\omega_c + k_\parallel v_\parallel}{\omega - k_\parallel v_\parallel - n\omega_c} = -1 + \frac{\omega}{\omega - k_\parallel v_\parallel - n\omega_c} , \qquad (2.72)$$

the dielectric constant can be written in the form

$$K(\omega,\underset{\sim}{k}) = 1 - \sum_{\alpha} \frac{\omega_p^2}{k^2} \int d\underset{\sim}{v}\, \frac{1}{v} \frac{\partial f_o}{\partial v}$$

$$+ \sum_{\alpha} \frac{\omega_p^2}{k^2} \sum_{n=-\infty}^{\infty} \int d\underset{\sim}{v}\, \frac{\omega}{v} \frac{\partial f_o}{\partial v} \frac{J_n^2\left(\frac{k_\perp v_\perp}{\omega_c}\right)}{\omega - k_{\parallel} v_{\parallel} - n\omega_c} , \qquad \mathrm{Im}(\omega) < 0 , \tag{2.73}$$

where use has been made of the identity [26]

$$\sum_{n=-\infty}^{\infty} J_n^2\left(\frac{k_\perp v_\perp}{\omega_c}\right) = 1 . \tag{2.74}$$

It is shown in Appendix A that for $\underset{\sim}{k}$ real and $\mathrm{Im}(\omega) < 0$, the dielectric constant, Eq. (2.73), is nonzero if the velocity distribution of each particle species is a monotonically decreasing function of v. Since the dispersion relation is obtained by setting $K(\omega,\underset{\sim}{k})$ equal to zero, this result has the interpretation that the plasma cannot support space-charge waves which grow with time. Bernstein [3] proves this theorem for the case of an electron plasma with a neutralizing background of positive charge. The electron velocity distribution in that case is an isotropic Maxwellian. However, the proof in Appendix A has no restriction on the number of particle species or on the isotropic velocity distribution.

2. Distributions with the Form $f_o(v_\perp, v_{\parallel}) = f_\perp(v_\perp)\, \delta(v_{\parallel} - v_{o\parallel})$

Here, all particles of a given species drift parallel to the magnetic field with the same speed. It is pointed out that because of the unit normalization of f_o, that is, $\int d\underset{\sim}{v}\, f_o = 1$, the function $f_\perp(v_\perp)$ must satisfy the condition

$$2\pi \int_0^{\infty} dv_\perp\, f_\perp(v_\perp)\, v_\perp = 1 . \tag{2.75}$$

Substitution of the velocity distribution

$$f_o(v_\perp, v_\parallel) = f_\perp(v_\perp)\,\delta(v_\parallel - v_{o\parallel}) \quad , \tag{2.76}$$

in Eq. (2.67) yields after integrating with respect to $v_\parallel$

$$K(\omega,\underset{\sim}{k}) = 1 - \sum_\alpha \frac{\omega_p^2}{\omega_c^2}\left(\frac{k_\perp^2}{k^2}\sum_{n=-\infty}^{\infty} p_n \frac{n\omega_c}{\omega - k_\parallel v_{o\parallel} - n\omega_c} + \frac{k_\parallel^2}{k^2}\sum_{n=-\infty}^{\infty} q_n \frac{\omega_c^2}{(\omega - k_\parallel v_{o\parallel} - n\omega_c)^2}\right) , \tag{2.77}$$

where we define

$$p_n = -2\pi \frac{\omega_c^2}{k_\perp^2}\int_0^\infty dv_\perp \frac{df_\perp(v_\perp)}{dv_\perp} J_n^2\left(\frac{k_\perp v_\perp}{\omega_c}\right) \quad , \tag{2.78}$$

$$q_n = 2\pi \int_0^\infty dv_\perp f_\perp(v_\perp) J_n^2\left(\frac{k_\perp v_\perp}{\omega_c}\right) . \tag{2.79}$$

It is observed that the roots of $K(\omega,\underset{\sim}{k}) = 0$ must occur in complex conjugate pairs if $\underset{\sim}{k}$ is real, indicating that for every mode that grows with time, there is one that decays.

E. Discussion

The main purpose of this chapter has been to derive the dispersion relation for electrostatic space-charge waves propagating in a hot, collisionless plasma immersed in a uniform magnetic field. It has been shown that the plasma, in the quasi-static approximation, has an effective dielectric constant $K(\omega,\underset{\sim}{k})$ that is dependent on both frequency and wave

vector. The dispersion relation is obtained by setting K equal to zero. The form of K for special classes of velocity distributions was also considered. In the following chapters, the solution of the dispersion relation will be considered for several specific velocity distributions.

III. PERPENDICULAR PROPAGATION OF CYCLOTRON HARMONIC WAVES

The purpose of this chapter is to solve for the dispersion characteristics of cyclotron harmonic waves propagating perpendicular to the magnetic field. The plasma will consist of an equal number of electrons and ions, but the frequency of the waves will be high enough so that the motion of the ions can be neglected. By considering a series of electron velocity distributions, we shall demonstrate how instabilities set in through mode coupling, and derive threshold conditions for the onset of these instabilities.

The dispersion relation is presented in Section A, and some basic properties of the solutions are derived. In Section B the dispersion relation is solved for the ring, spherical shell and Maxwellian distributions, and the onset conditions are obtained for instability in a plasma consisting of a mixture of the ring and Maxwellian distributions. In Section C the instabilities are classified as either absolute or convective. A study is made in Section D of the steady state conditions of the plasma, with and without collisions, when cyclotron harmonic waves are excited by a source operating at a real frequency ω_o. The chapter ends with a discussion of the results.

A. Dispersion Relation

After setting $k_{\parallel}$ equal to zero in Eq. (2.67), the dispersion relation can be written in the form

$$K(\omega,k_\perp) = 1 - \frac{\omega_p^2}{\omega_c^2} \sum_{n=-\infty}^{\infty} a_n(k_\perp) \frac{n\omega_c}{\omega - n\omega_c} = 0 \ , \tag{3.1}$$

where

$$a_n(k_\perp) = - \frac{\omega_c^2}{k_\perp^2} \int d\underset{\sim}{v} \frac{1}{v_\perp} \frac{\partial f_o}{\partial v_\perp} J_n^2\left(\frac{k_\perp v_\perp}{\omega_c}\right) \ , \tag{3.2}$$

and the summation over particle species has been dropped since only electron motion is considered. For computational purposes, an integral representation of the dielectric constant $K(\omega,k_\perp)$ has been useful. This form may be derived from Eq. (2.59) by carrying out the integration over velocity space first. After setting $k_\parallel$ equal to zero and integrating with respect to ψ, with the aid of the second identity in Eq. (2.62), the dielectric constant in the direction perpendicular to the magnetic field is

$$K(\omega,k_\perp) = 1 - \frac{\omega_p^2}{k_\perp^2} \int_0^\infty dt \exp(-i\omega t) 2\pi \int_{-\infty}^{\infty} dv_\parallel \int_0^\infty v_\perp \, dv_\perp k_\perp \frac{\partial f_o}{\partial v_\perp}$$

$$\cdot \cos \frac{\omega_c t}{2} J_1 \left(2 \frac{k_\perp v_\perp}{\omega_c} \sin \frac{\omega_c t}{2} \right) . \qquad (3.3)$$

This expression can be put in a more convenient form if an integration by parts with respect to $v_\perp$ is carried out. The result is

$$K(\omega,k_\perp) = 1 + \frac{\omega_p^2}{\omega_c^2} \int_0^\infty d\tau \exp\left(-i \frac{\omega}{\omega_c} \tau\right) \sin \tau \, F_o(\tau) \quad , \qquad (3.4)$$

where

$$F_o(\tau) = \int \underset{\sim}{dv} \, f_o(v_\perp, v_\parallel) \, J_o \left(2 \frac{k_\perp v_\perp}{\omega_c} \sin \frac{\tau}{2} \right) \qquad (3.5)$$

$$= F_o(\tau + 2\pi) \quad . \qquad (3.6)$$

For convenience, τ has been set equal to $\omega_c t$. It is observed that Eq. (3.4) does not converge if $\mathrm{Im}(\omega) \geq 0$. In order to obtain the analytic continuation into this part of the complex plane, use is made of the periodicity of $F_o(\tau)$, and the fact that $\mathrm{Im}(\omega) < 0$, in order to transform Eq. (3.4) to the following equivalent forms:

$$K(\omega,k_\perp) = 1 + \frac{\omega_p^2}{\omega_c^2} \sum_{n=0}^{\infty} \int_{2\pi n}^{2\pi(n+1)} d\tau \exp\left(-i \frac{\omega}{\omega_c} \tau\right) \sin \tau \, F_o(\tau)$$

$$= 1 + \frac{\omega_p^2}{\omega_c^2} \left[\sum_{n=0}^{\infty} \exp\left(-2\pi n i \frac{\omega}{\omega_c}\right)\right] \int_0^{2\pi} d\tau \exp\left(-i \frac{\omega}{\omega_c} \tau\right) \sin \tau \, F_o(\tau)$$

$$= 1 + \frac{\omega_p^2}{\omega_c^2} \frac{1}{1 - \exp\left(-2\pi i \frac{\omega}{\omega_c}\right)} \int_0^{2\pi} d\tau \exp\left(-i \frac{\omega}{\omega_c} \tau\right) \sin \tau \, F_o(\tau)$$

$$= 1 + \frac{\omega_p^2}{\omega_c^2} \int_0^{\pi} d\tau \frac{\sin \Omega\tau}{\sin \Omega\pi} \sin \tau \, F_o(\tau + \pi) \, , \qquad (3.7)$$

where Ω has been written for (ω/ω_c). Clearly, the last expression is defined for all ω, except possibly at the points $\omega = n\omega_c$, and hence is the proper analytic continuation of $K(\omega,k_\perp)$. This form is particularly convenient for computational purposes since there are many efficient algorithms that can be used to integrate numerically, such as Simpson's method. Before solving the dispersion relation exactly, we will examine two limiting forms of that equation.

1. Cold-Plasma Limit

In this case the electrons have no motion in the unperturbed state of the plasma, and hence we can write

$$f_o(v_\perp, v_\parallel) = \frac{1}{2\pi v_\perp} \delta(v_\perp) \, \delta(v_\parallel) \, . \qquad (3.8)$$

Substituting this expression in Eq. (3.2), we find

$$a_n = \begin{cases} \frac{1}{2}, & n = \pm 1, \\ 0, & n = \pm 2, \pm 3, \ldots, \end{cases} \tag{3.9}$$

which, when combined with Eq. (3.1), leads to the familiar cold-plasma dielectric constant perpendicular to the magnetic field

$$K_c(\omega) = 1 - \frac{\omega_p^2}{\omega^2 - \omega_c^2} . \tag{3.10}$$

Clearly, the equation $K_c(\omega) = 0$ has a root at the upper hybrid frequency, $\omega_H = (\omega_p^2 + \omega_c^2)^{1/2}$. Since there is no dependence on the wave number $k_\perp$, the oscillation at ω_H persists without spatial dispersion.

2. Cutoffs and Resonances

If the unperturbed velocity of the electrons is nonzero, Eq. (3.1) indicates that the plasma supports space-charge waves which propagate perpendicular to the magnetic field. The cutoff $(k_\perp \to 0)$ and resonant $(k_\perp \to \infty)$ frequencies of these waves are obtainable from the small and large argument expansions of the plasma dielectric constant. If $k_\perp$ is small, we use the approximation [26]

$$J_n(z) \approx \frac{1}{|n|!} \left(\frac{z}{2}\right)^{|n|} , \tag{3.11}$$

in Eq. (3.2) to obtain

$$a_n \approx \frac{1}{2} c_n k_\perp^{2(|n|-1)} , \tag{3.12}$$

where

$$c_n = \frac{-1}{2^{2|n|-1}(|n|!)^2 \omega_c^{2(|n|-1)}} \int d\underset{\sim}{v}\, v_\perp^{2|n|-1} \frac{\partial f_o}{\partial v_\perp} . \tag{3.13}$$

Substituting Eq. (3.12) in Eq. (3.1), the limit of $K(\omega,k_\perp)$ as $k_\perp \to 0$ then has the form

$$K(\omega,k_\perp) = \begin{cases} 1 - \dfrac{\omega_p^2}{\omega^2 - \omega_c^2}, & \omega \neq n\omega_c, \qquad (3.14a) \\ 1 - \dfrac{\omega_p^2}{\omega^2 - \omega_c^2} - \dfrac{c_n k_\perp^{2(|n|-1)}}{2} \dfrac{\omega_p^2}{\omega_c^2} \dfrac{n\omega_c}{\omega - n\omega_c}, & \omega \approx n\omega_c, \qquad (3.14b) \end{cases}$$

for all $|n| > 1$. Clearly, the dispersion relation $K(\omega,k_\perp) = 0$ has roots in this approximation at the frequencies

$$\omega = \pm\left(\omega_p^2 + \omega_c^2\right)^{1/2}, \qquad (3.15)$$

and

$$\omega = n\omega_c \left(1 + \frac{1}{2} \frac{c_n}{K_c(\omega)} \frac{\omega_p^2}{\omega_c^2} k_\perp^{2(|n|-1)}\right), \qquad (3.16)$$

where $K_c(\omega)$ is defined by Eq. (3.10). Thus, cutoffs occur at the positive and negative upper hybrid frequency and at all harmonics of the electron cyclotron frequency excluding $n = \pm 1$.

As $k_\perp \to \infty$, the plasma dielectric constant approaches a form that is obtainable by substituting in Eq. (3.2) the large argument approximation of the Bessel function [26],

$$J_n(z) \sim \sqrt{\frac{2}{\pi z}} \cos\left(z - \frac{\pi}{4} - \frac{n\pi}{2}\right), \qquad (3.17)$$

and combining the result with Eq. (3.1). Assuming $\omega \approx n\omega_c$, it is sufficient to retain only the n^{th} term in the infinite series and write for large $k_\perp$

$$K(\omega,k_\perp) \approx 1 - \frac{d_n}{k_\perp^3}\frac{\omega_p^2}{\omega_c^2}\frac{n\omega_c}{\omega - n\omega_c} = 0 , \qquad (3.18)$$

where

$$d_n = -\frac{2\omega_c^3}{\pi}\int \frac{dv}{v_\perp^2}\frac{\partial f_o}{\partial v_\perp}\cos^2\left(\frac{k_\perp v_\perp}{\omega_c} - \frac{\pi}{4} - \frac{n\pi}{2}\right). \qquad (3.19)$$

Clearly, in this limit, the dispersion relation has roots at

$$\omega = n\omega_c\left(1 + \frac{\omega_p^2}{\omega_c^2}\frac{d_n}{k_\perp^3}\right), \qquad n = \pm 1, \pm 2, \ldots , \qquad (3.20)$$

implying that a resonance is found at each harmonic of the electron cyclotron frequency.

B. Dispersion Characteristics for Perpendicular Propagation

If $k_\perp$ is finite and nonzero, the dispersion relation, Eq. (3.1), is difficult to solve as a result of the infinite series, and recourse must be made to a numerical solution in order to obtain a detailed description of the behavior of cyclotron harmonic wave propagation. However, simplifying assumptions can be made which enable us to obtain an analytical representation of the dispersion characteristics and hence facilitate our study of the waves in certain ranges. For example, consider the case where $(\omega_p^2/\omega_c^2) \ll 1$. Assuming now that $\omega \approx n\omega_c$, it is reasonable to approximate the infinite series in Eq. (3.1) by the n^{th} term and write the dispersion relation in the form

$$K(\omega,k_\perp) \approx 1 - \frac{\omega_p^2}{\omega_c^2} a_n(k_\perp) \frac{n\omega_c}{\omega - n\omega_c} = 0 \ . \qquad (3.21)$$

Solving for the frequency, we find

$$\omega(k_\perp) \approx n\omega_c \left[1 + \frac{\omega_p^2}{\omega_c^2} a_n(k_\perp)\right] \ , \qquad (3.22)$$

establishing that there is a mode near each harmonic of the electron cyclotron frequency if (ω_p^2/ω_c^2) is small, and hence confirming our original assumption that led to Eq. (3.22). Two forms of $a_n(k_\perp)$ are examined here. First, if the velocity distribution is such that $a_n(k_\perp)$ undulates about the line $a_n = 0$, the dispersion characteristics predicted by Eq. (3.22) will have the form shown in Fig. 5a. It is noted that the amplitude of the undulation in the dispersion diagram increases with (ω_p^2/ω_c^2). Consequently, it is possible that the loops above a given harmonic will approach the loops below the harmonic immediately following it and lead to coupling of the modes and hence instability. This possibility is examined more extensively below. On the other hand, if the velocity distribution is such that $a_n(k_\perp) > 0$ for all real values of the wave number, Eq. (3.22) indicates that the modes are confined to the frequency band $n\omega_c < \omega < (n+1)\omega_c$ as shown in Fig. 5b. If this result is true for (ω_p^2/ω_c^2) arbitrarily large, no mode coupling is possible, suggesting that instability does not occur in this case. There is, in fact, a theorem which guarantees the stability of the plasma if $a_n(k_\perp) > 0$ for all n and which can be stated in the following way: A sufficient condition that a magnetoplasma--characterized by an electron velocity distribution $f_o(v_\perp, v_\parallel)$ and a background of immobile ions--supports stable cyclotron harmonic waves propagating perpendicular to the magnetic field is

$$a_n(k_\perp) = -\frac{\omega_c^2}{k_\perp^2} \int d\underset{\sim}{v} \frac{1}{v_\perp} \frac{\partial f_o}{\partial v_\perp} J_n^2\left(\frac{k_\perp v_\perp}{\omega_c}\right) > 0 \ , \qquad (3.23)$$

for all $|n| > 0$.

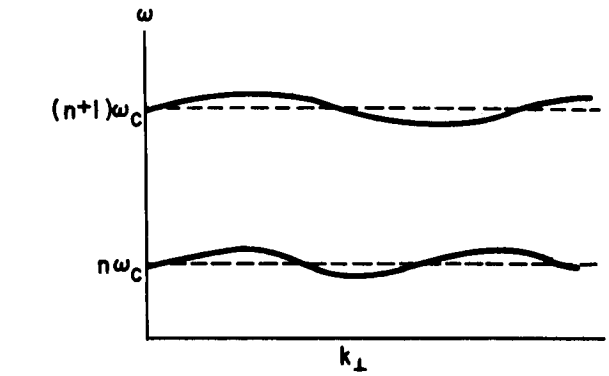

(a) Potentially unstable

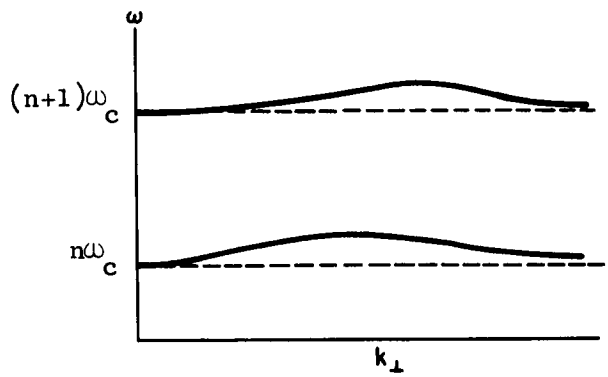

(b) Absolutely stable

Fig. 5. TYPICAL DISPERSION CHARACTERISTICS OF CYCLOTRON HARMONIC WAVES PROPAGATING PERPENDICULAR TO THE MAGNETIC FIELD.

In order to prove this theorem, let $\omega = \omega_r + i\omega_i$, and then separate the dispersion relation, Eq. (3.1), into its real and imaginary parts:

$$\text{Re } (K) = 1 - \frac{\omega_p^2}{\omega_c^2} \sum_{n=1}^{\infty} \left(\omega_r^2 - \omega_i^2 - n^2\omega_c^2\right) a_n \frac{2n^2\omega_c^2}{D(\omega_r,\omega_i)} = 0 \quad , \quad (3.24)$$

$$\text{Im } (K) = -2\omega_i\omega_r \frac{\omega_p^2}{\omega_c^2} \sum_{n=1}^{\infty} a_n \frac{2n^2\omega_c^2}{D(\omega_r,\omega_i)} = 0 \quad , \quad (3.25)$$

where

$$D(\omega_r,\omega_i) = \left(\omega_r^2 - \omega_i^2 - n^2\omega_c^2\right)^2 + 4\omega_r^2\omega_i^2 \quad . \tag{3.26}$$

Here, use has been made of the symmetry condition $a_n = a_{-n}$. Assume now that $a_n > 0$ for all $n > 1$. As a consequence of this assumption, Re (K) can vanish only if $\omega_r \neq 0$, while Im (K) will vanish only if $(\omega_r\omega_i) = 0$. Hence, we conclude that $\omega_i \equiv 0$, proving that if $k_\perp$ is real, all solutions of the dispersion relation, $\omega(k_\perp)$, must be real in this case. This implies plasma stability. If more than one particle species is taken into consideration, it is clear that the conclusion of the theorem is still correct so long as each velocity distribution satisfies a condition analogous to Eq. (3.23). It should be pointed out that Baldwin and Rowlands [27] have also obtained this theorem in a paper published during the preparation of this manuscript.

One class of velocity distributions that satisfy Eq. (3.23) is defined by the condition

$$\frac{\partial f_o(v_\perp, v_\parallel)}{\partial v_\perp} < 0 \quad , \tag{3.27}$$

for all $v_\perp > 0$. Hence a necessary condition for instability is that the inequality

$$\frac{\partial f_o(v_\perp, v_\parallel)}{\partial v_\perp} > 0 \tag{3.28}$$

must be satisfied for some range of $v_\perp$. It is difficult to determine whether or not an instability does indeed exist in the general case. In regard to this, it may be useful to approximate the dispersion relation [Eq. (3.1)], by two terms of the series, giving

$$K(\omega,k_\perp) \approx 1 - \frac{\omega_p^2}{\omega_c^2}\left[a_n \frac{n\omega_c}{\omega - n\omega_c} + a_{n+1}\frac{(n+1)\omega_c}{\omega - (n+1)\omega_c}\right] = 0 \quad , \tag{3.29}$$

which can be transformed to a quadratic equation,

$$\omega^2 - q_1\omega_c\omega + q_2\omega_c^2 = 0 \ , \tag{3.30}$$

where

$$q_1 = (2n + 1) + \frac{\omega_p^2}{\omega_c^2}\left[na_n + (n + 1)a_{n+1}\right] \ , \tag{3.31}$$

and

$$q_2 = n(n + 1)\left[1 + \frac{\omega_p^2}{\omega_c^2}(a_n + a_{n+1})\right] . \tag{3.32}$$

Equation (3.29) describes the interaction between the two modes shown in Fig. 5 for relatively small values of (ω_p^2/ω_c^2), and it is clear from Eq. (3.30) that the frequency is not necessarily real. Complex solutions are found if

$$q_2 > \frac{1}{4} q_1^2 \ , \tag{3.33}$$

implying that instabilities are present. However, this result depends on the validity of the approximation that was used to obtain Eq. (3.29).

In order to obtain a more detailed picture of the propagation characteristics of cyclotron harmonic waves, we will devote the rest of this chapter to computations which lead to an exact numerical solution of the dispersion relation. This will enable us to obtain exact threshold conditions for instability and a clear interpretation of the instabilities in terms of mode coupling. Four electron velocity distributions are chosen for study. The first is the ring distribution which describes a monoenergetic collection of electrons that move only in the plane perpendicular to the magnetic field and are uniformly distributed in velocity space on a circle with radius $v_{o\perp}$, as shown in Fig. 6a. This is to be distinguished from a delta function distribution in which all electrons

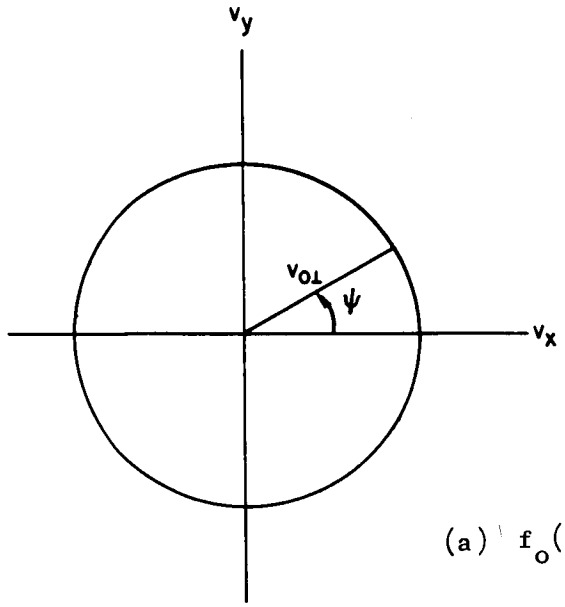

$$(a)\quad f_o(\underset{\sim}{v}) = \frac{1}{2\pi v_{o\perp}}\,\delta(v_\perp - v_{o\perp})\,\delta(v_\parallel)$$

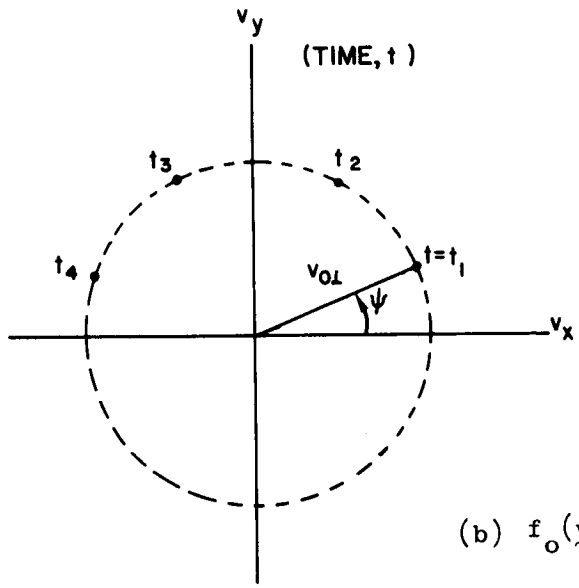

$$(b)\quad f_o(\underset{\sim}{v}) = \frac{1}{v_{o\perp}}\,\delta(v_\perp - v_{o\perp})\,\delta(\psi - \omega_c t)\,\delta(v_\parallel)$$

Fig. 6. RING (a) AND DELTA FUNCTION (b) VELOCITY DISTRIBUTIONS.

have the same phase at every instant of time, and consequently, the state of the plasma is represented in velocity space by a single dot which rotates about the origin at the cyclotron frequency, as illustrated in Fig. 6b. It will be noted that the delta function distribution is time dependent and hence is not a member of the class of velocity distributions examined in Chapter II.

The ring distribution occurs naturally in the earth's magnetosphere [28] when high-energy charged particles, streaming in from the sun, are trapped by the earth's magnetic field at the bow shock. This distribution may also be found in laboratory plasmas in connection with experimental studies on controlled thermonuclear fusion. An example of this is the DCX [29] where high-energy particles, injected perpendicular to the magnetic field, are ionized by interacting with a cooler background plasma. The resulting charged particles are trapped by the magnetic field with their transverse energy exceeding their longitudinal energy on the average.

It should be pointed out that plasmas with anisotropic velocity distributions may not remain in this state for a relatively long period of time. In the event that there is a background of heavy neutral particles, collisions between electrons and the neutrals may play an important role. For example, if only momentum is transferred during a collision, the electron velocity distribution will have the form of a spherical shell after approximately one collision period. If energy is also transferred during the collisions, the distributions will evolve toward a Maxwellian. For this reason, the dispersion characteristics associated with the spherical shell and Maxwellian distributions will also be examined below. Finally, a mixture of the ring and Maxwellian distributions will be considered since this condition is often found in devices such as the DCX [29].

1. Ring Distribution

The analytic representation of this distribution is conveniently written in terms of delta functions as

$$f_o(v_\perp, v_\parallel) = \frac{1}{2\pi v_{o\perp}} \delta(v_\perp - v_{o\perp}) \, \delta(v_\parallel) \quad . \tag{3.34}$$

After substituting this expression in Eqs. (3.2) and (3.5) and carrying out the integration with respect to the velocity, we find

$$a_n(k_\perp) = \frac{1}{\mu_\perp} \frac{\partial J_n^2(\mu_\perp)}{\partial \mu_\perp} \quad , \tag{3.35}$$

and

$$F_o(\tau) = J_o\left(2\mu_\perp \sin\frac{\tau}{2}\right) \quad , \tag{3.36}$$

where $\mu_\perp$ has been written for $(k_\perp v_{o\perp}/\omega_c)$. Substitution of Eqs. (3.35) and (3.36) into Eqs. (3.1) and (3.7), respectively, yield the dispersion relation associated with the ring distribution,

$$K(\omega,k_\perp) = 1 - \frac{\omega_p^2}{\omega_c^2}\sum_{n=-\infty}^{\infty}\frac{1}{\mu_\perp}\frac{\partial J_n^2(\mu_\perp)}{\partial\mu_\perp}\frac{n\omega_c}{\omega - n\omega_c} \tag{3.37a}$$

$$= 1 + \frac{\omega_p^2}{\omega_c^2}\int_0^\pi d\tau\,\frac{\sin\Omega\tau}{\sin\Omega\pi}\sin\tau\,J_o\left(2\mu_\perp\cos\frac{\tau}{2}\right) = 0 \cdot \tag{3.37b}$$

Figure 7a-g shows the dispersion characteristics for (ω_p^2/ω_c^2) set equal to 1, 3, 5, 8, 10, 20, and ∞ that were obtained by solving Eq. (3.37b) numerically. Cutoffs are observed at each harmonic of the electron cyclotron frequency, excluding the first, and at the upper hybrid frequency. Resonances occur at all harmonics of ω_c. These observations are consistent with the results of Section A.

If (ω_p^2/ω_c^2) is small, each mode is accurately described by Eq. (3.22). For the ring distribution, the coefficient $a_n(k_\perp)$ is given by Eq. (3.35), and hence, in this approximation, the frequency of the mode is

$$\omega(k_\perp) = n\omega_c\left[1 + \frac{\omega_p^2}{\omega_c^2}\,\frac{1}{\mu_\perp}\,\frac{\partial J_n^2(\mu_\perp)}{\partial\mu_\perp}\right] \quad , \tag{3.38}$$

which accounts for the undulations seen in Fig. 7. It will be noted that Eq. (3.38) predicts that the modes pass through points defined by

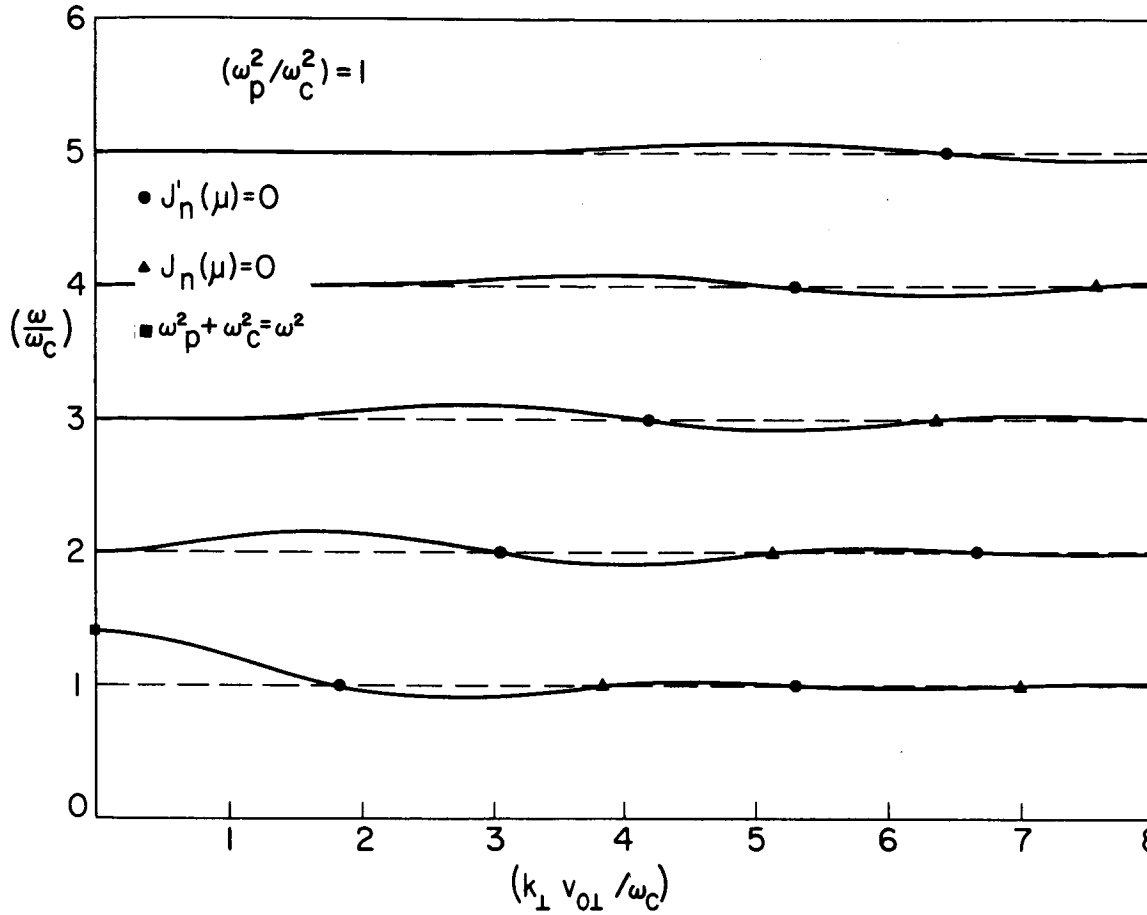

(a)

Fig. 7. DISPERSION CHARACTERISTICS OF PERPENDICULARLY PROPAGATING ELECTRON CYCLOTRON HARMONIC WAVES FOR RING DISTRIBUTION.

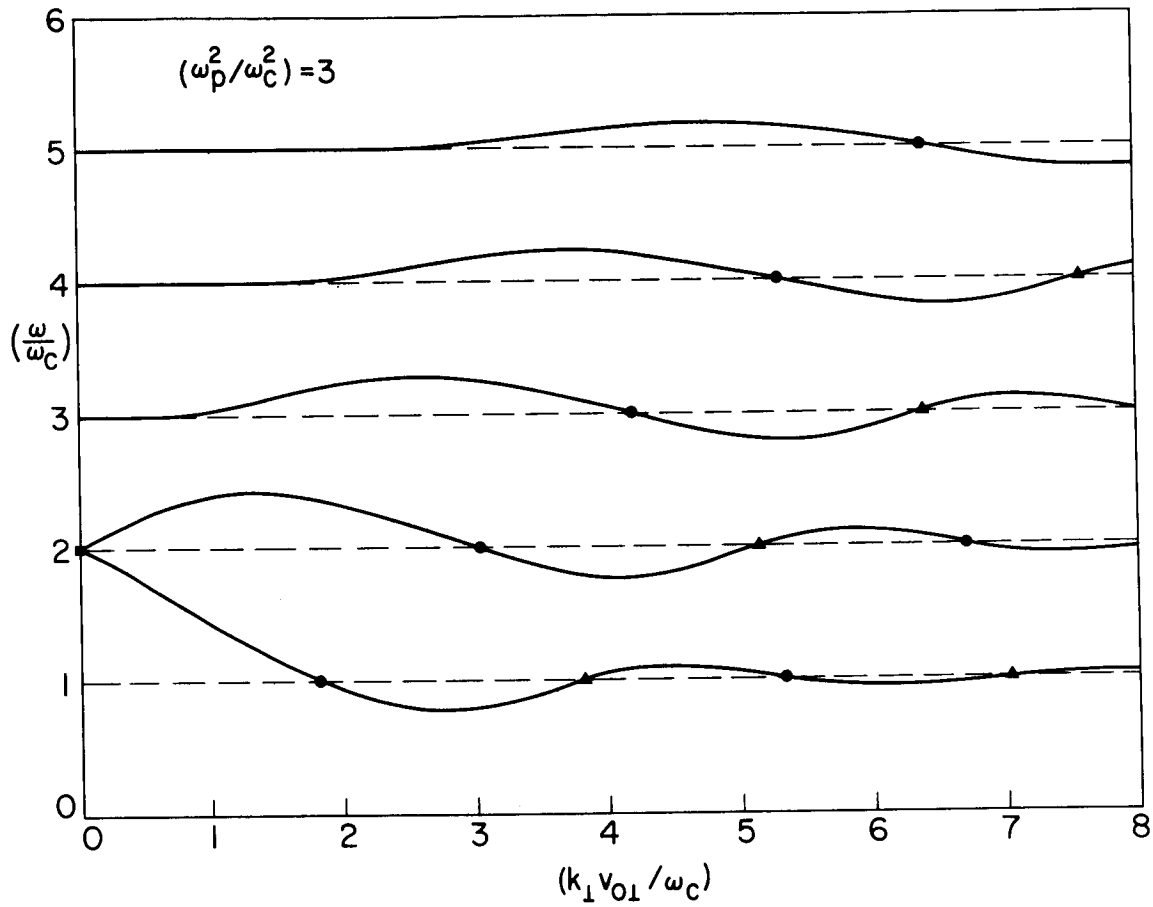

(b)

Fig. 7. CONTINUED.

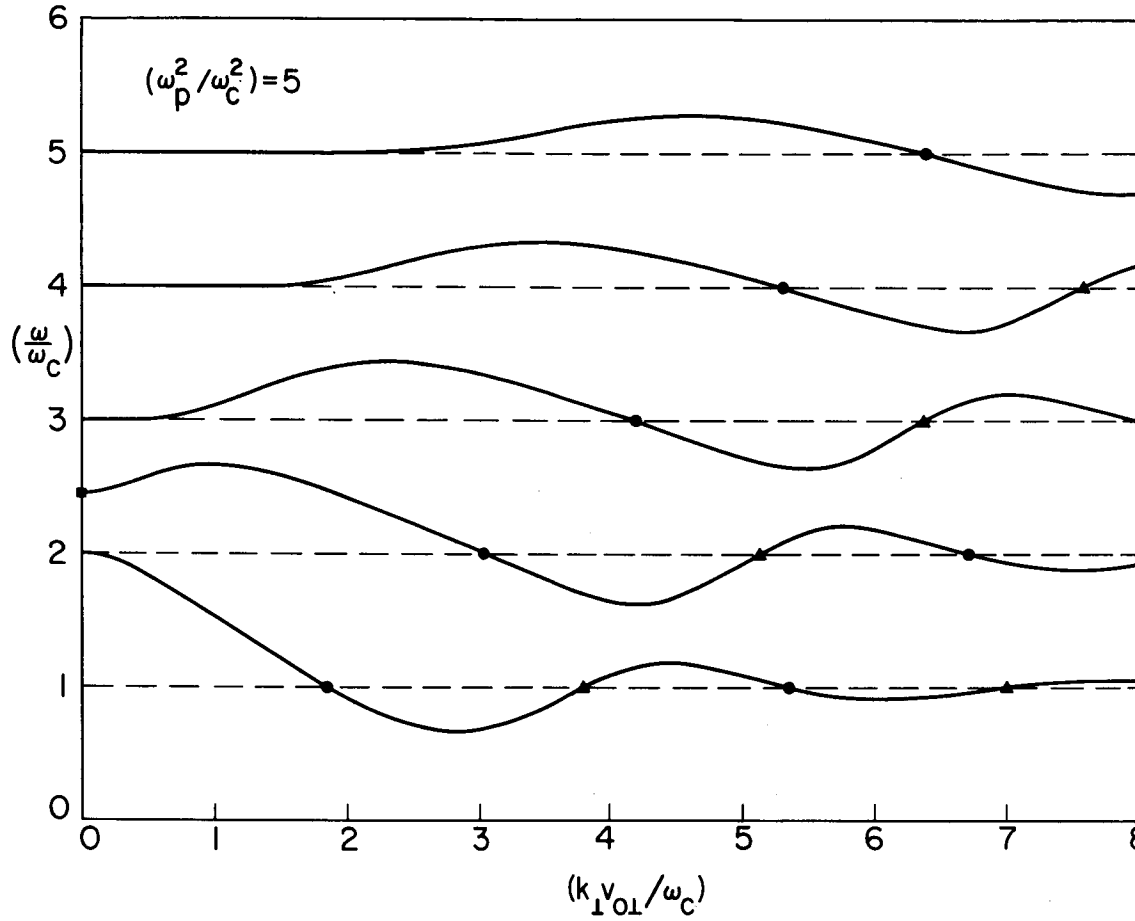

(c)

Fig. 7. CONTINUED.

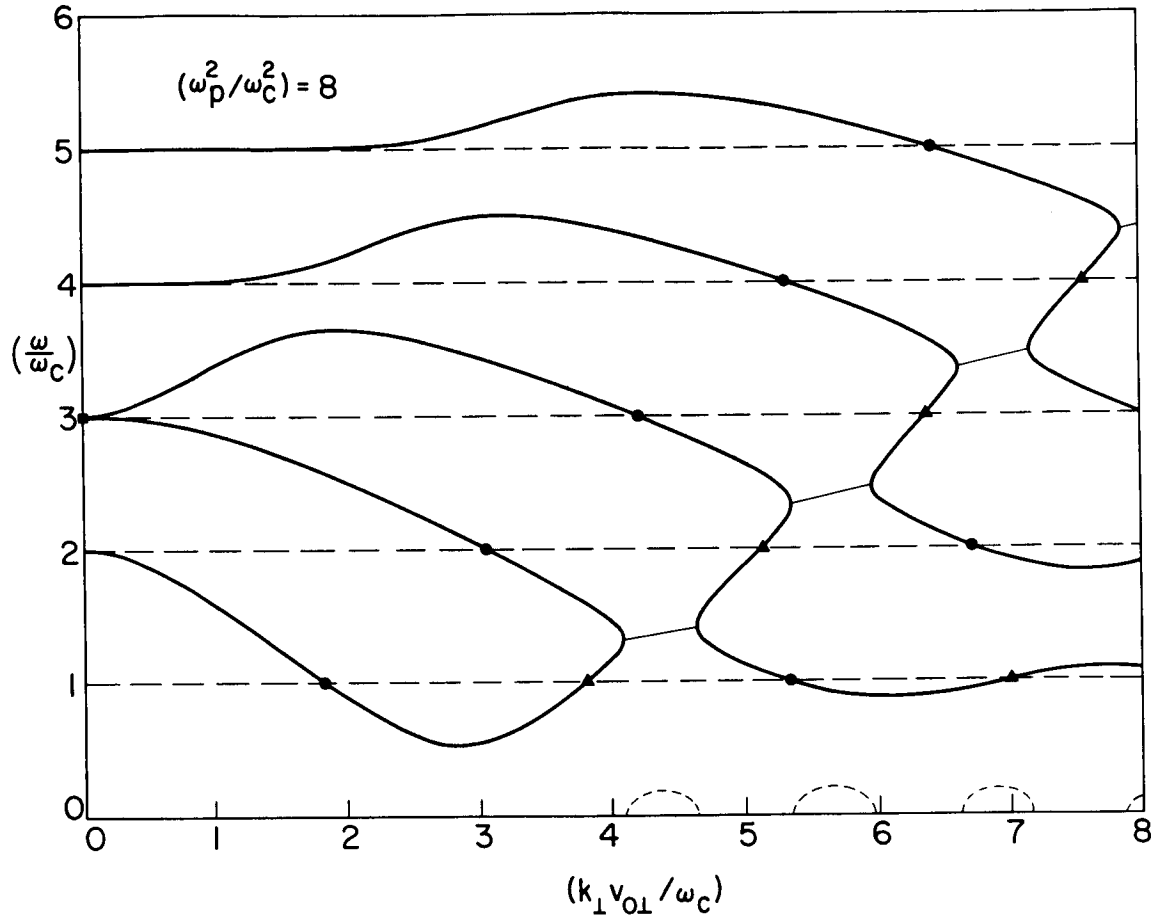

(d)

Fig. 7. CONTINUED.

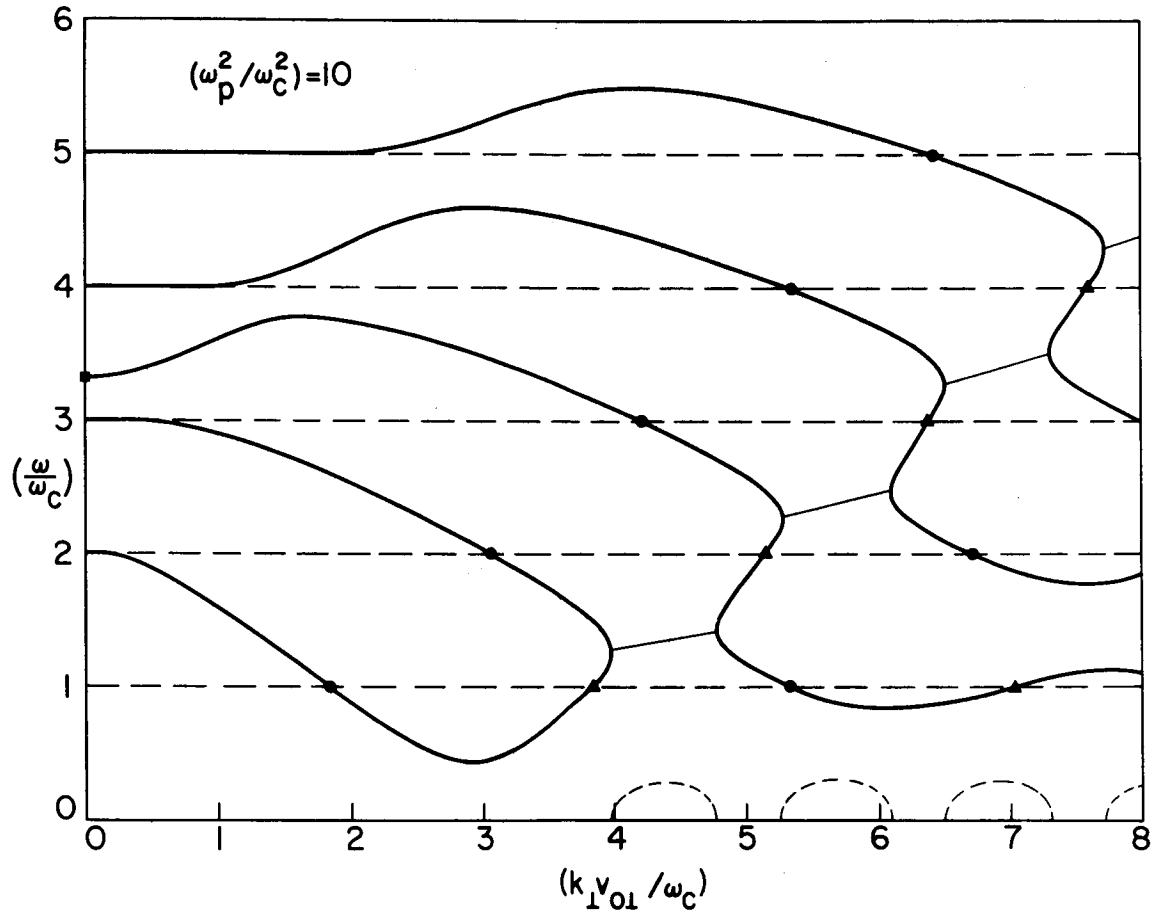

(e)

Fig. 7. CONTINUED.

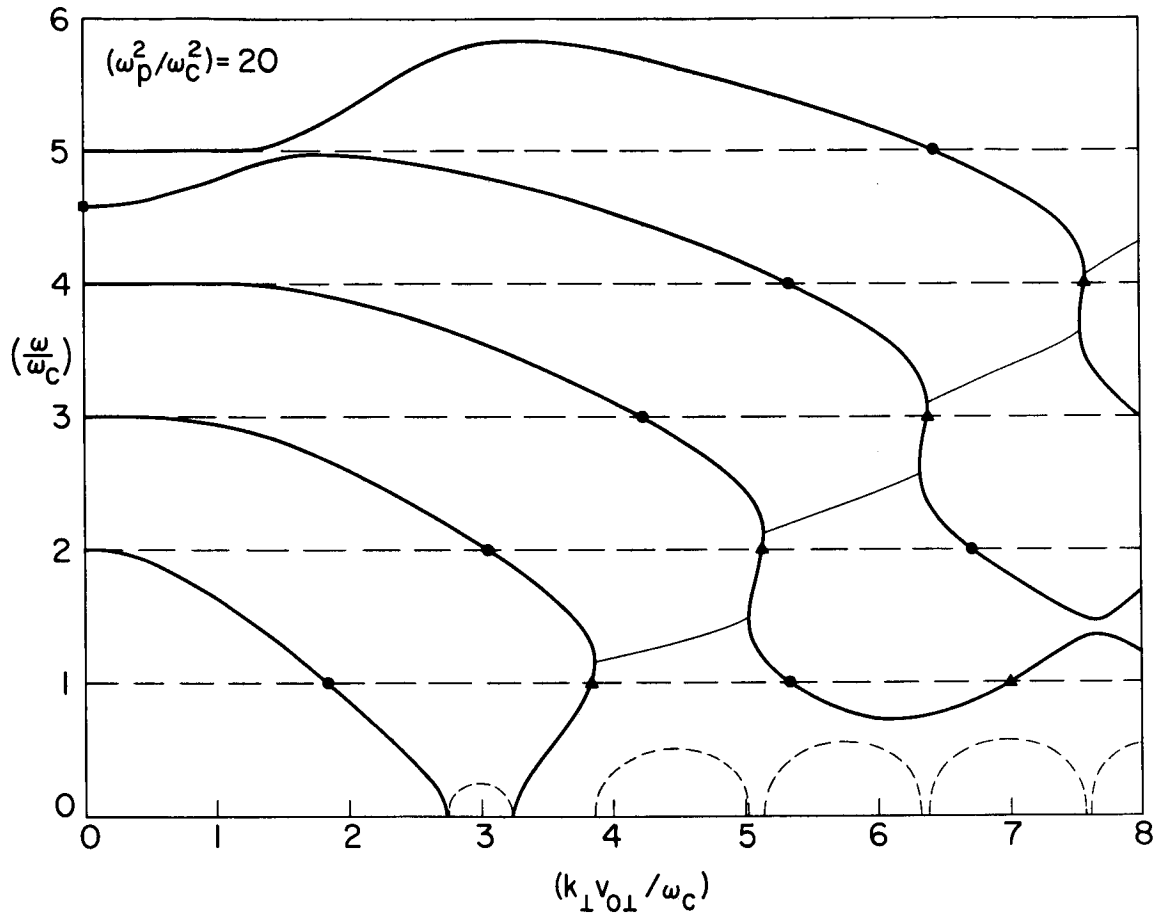

(f)

Fig. 7. CONTINUED.

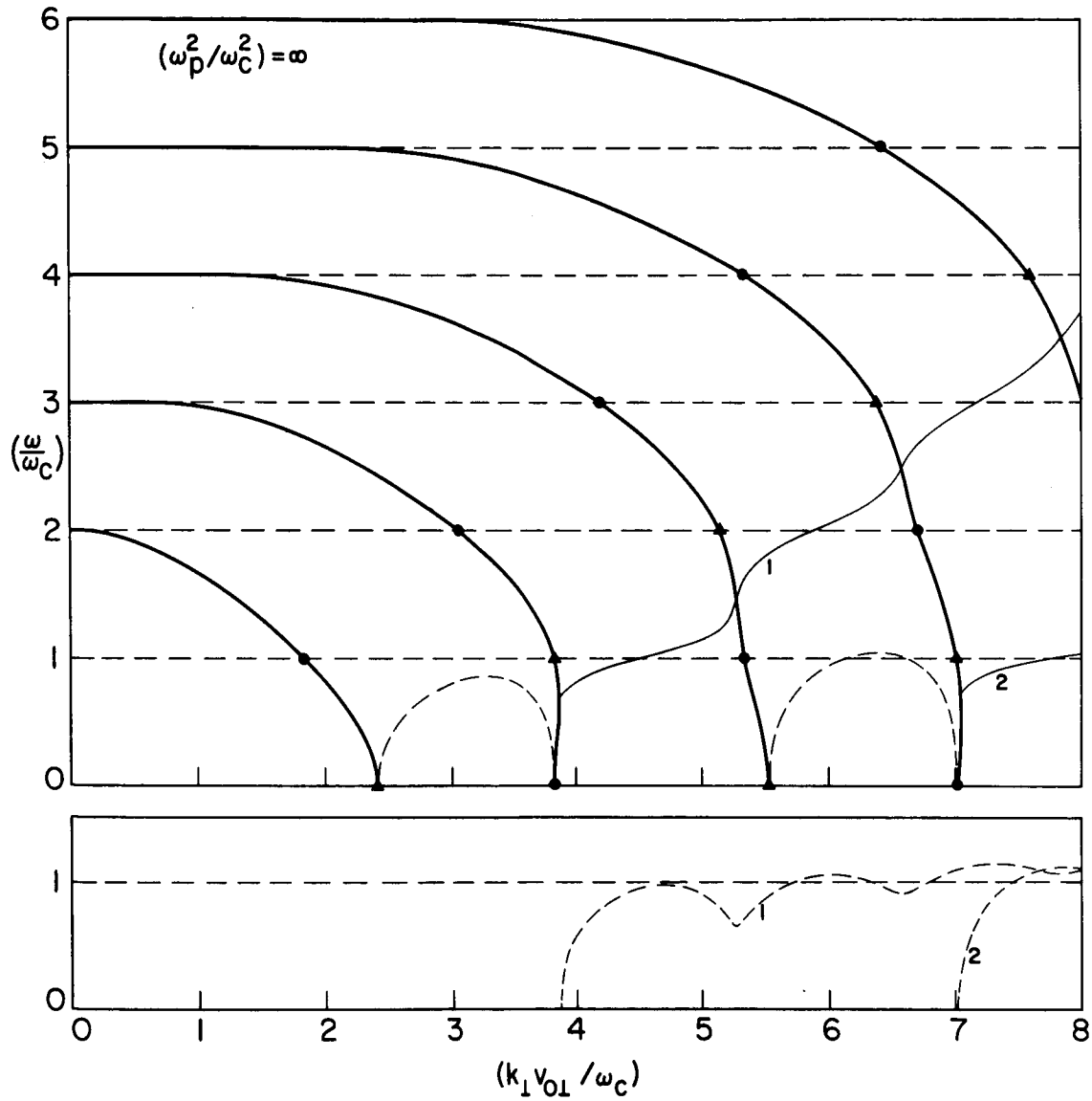

(g)

Fig. 7. CONTINUED.

$[\omega = n\omega_c,\ J_n(\mu_\perp) = 0]$ and $[\omega = n\omega_c,\ (\partial J_n/\partial \mu_\perp) = 0]$, in agreement with the exact numerical solution. In order to prove that this is true for arbitrary values of (ω_p^2/ω_c^2), it is only necessary to substitute in Eq. (3.37b) the identity

$$\sin \tau\, J_o\left(2\mu_\perp \cos\frac{\tau}{2}\right) = \frac{1}{\mu_\perp} \frac{\partial^2 J_n^2\left(2\mu_\perp \cos\frac{\tau}{2}\right)}{\partial \mu_\perp\, \partial \tau} , \qquad (3.39)$$

and then integrate by parts with respect to τ. This leads to an alternate representation of the dispersion relation

$$K(\omega, k_\perp) = 1 - \frac{\omega_p^2}{\omega_c^2} \frac{\Omega\pi}{\sin \Omega\pi} \frac{\partial}{\partial \mu_\perp} \left[J_\Omega(\mu_\perp)\, J_{-\Omega}(\mu_\perp)\right] = 0 , \qquad (3.40)$$

where use has been made of the Bessel function identity [26]

$$\frac{2}{\pi} \int_0^{\pi/2} J_{\mu+\nu}(2z \cos\tau) \cos(\mu-\nu)\tau\, d\tau = J_\mu(z)\, J_\nu(z) .$$

Clearly, if $\Omega\ [\equiv(\omega/\omega_c)]$ is an integer n, Eq. (3.40) implies

$$J_n(\mu_\perp) \frac{\partial J_n(\mu_\perp)}{\partial \mu_\perp} = 0 ,$$

verifying that the modes pass through harmonics of the electron cyclotron frequency when $\mu_\perp$ is a zero of the n^{th}-order Bessel function or its first derivative.

As (ω_p^2/ω_c^2) increases, the loops above a given harmonic approach the loops below the harmonic immediately following it. The points at which the loops can couple must always lie between α_{nm} and $\alpha_{(n+1)m}$, where α_{nm}

represents the m^{th} zero of $J_n(\mu_\perp)$. The first point at which two loops touch is $(\omega_p^2/\omega_c^2) = 6.62$ when the $(n = 3)$ mode touches the $(n = 2)$ mode for the first time. This is followed very rapidly by touching of the $(n = 1)$ and $(n = 2)$ modes at $(\omega_p^2/\omega_c^2) = 6.81$. After coupling has occurred, there are ranges of $\mu_\perp$ in which purely real solutions for ω do not exist. It is very important to investigate the complex solutions to the dispersion relation in these regions. The real parts of the complex conjugate roots for frequency are indicated by fine lines and the corresponding imaginary parts are shown dotted in Fig. 7d-g. The presence of these imaginary parts has the important practical significance that an individual propagating mode will grow in time to an amplitude limited only by the validity of the small-signal theory which has been used in obtaining the dispersion relation. It is pointed out that the imaginary frequency components can become very strong indeed. For example, when the imaginary component of (ω/ω_c) reaches unity, growth rates of the order of 50 dB per cyclotron period $(= 2\pi/\omega_c)$ are implied. It is an interesting feature of the complex roots that the lowest modes do not show the highest temporal growth rates. This is indicated particularly clearly by Fig. 7g.

A further point to note is the possibility of an instability with zero real part. This can be seen from a study of the behavior of the downward loops of the $(n = 1)$ mode. As (ω_p^2/ω_c^2) increases, this loop approaches the $(\omega = 0)$ axis, and finally touches it when $(\omega_p^2/\omega_c^2) = 17.02$. Beyond this value, purely imaginary solutions can be found. These are indicated in Fig. 7f,g. The threshold conditions for this instability are obtained by setting ω equal to zero in Eq. (3.37a) and expressing the result in the form

$$-\frac{1}{2}\,\frac{1}{\left(\omega_p^2/\omega_c^2\right)} = \frac{J_o(\mu_\perp)\,J_1(\mu_\perp)}{\mu_\perp}\ , \tag{3.41}$$

where the right-hand side is plotted in Fig. 8. Since $\mu_\perp$ is real, this equation can be satisfied only if the line

$$-\frac{1}{2}\frac{1}{\left(\omega_p^2/\omega_c^2\right)} = \text{const.} \quad ,$$

exceeds a minimum of $[J_o(\mu_\perp)\, J_1(\mu_\perp)/\mu_\perp]$. When this occurs, there exist purely imaginary roots of the dispersion relation, implying that plasma fluctuations will grow in time without propagation. It is clear from Fig. 8 that this can occur only if $\mu_\perp$ lies between succeeding pairs of zeros of J_o and J_1.

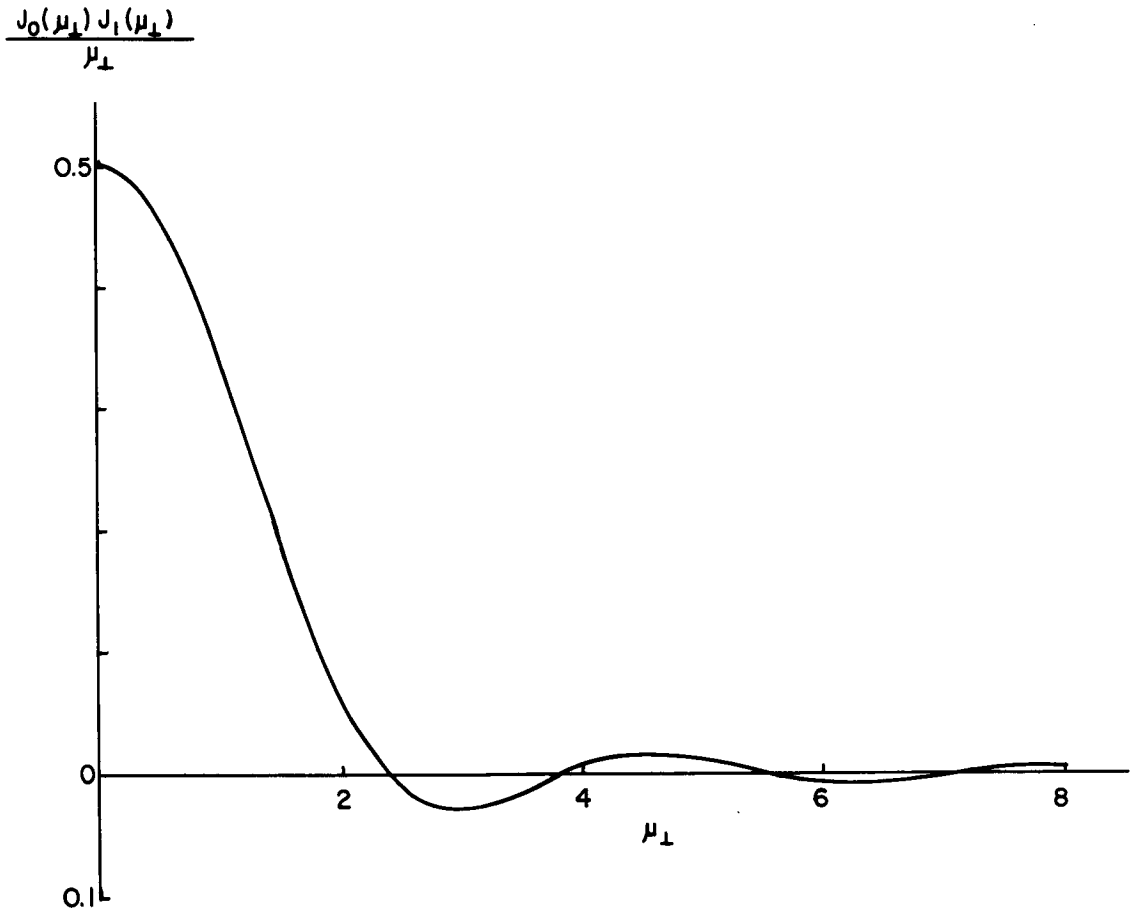

Fig. 8. PLOT OF $[J_o(\mu_\perp)\, J_1(\mu_\perp)/\mu_\perp]$ VS $v_\perp$.

In order to summarize these results, we list in Table 1 the lowest threshold conditions for instability in the first four frequency bands.

Table 1

INSTABILITY THRESHOLD CONDITIONS FOR RING DISTRIBUTION

Frequency Band	Values of (ω_p^2/ω_c^2) for Onset of Instability
$0 < (\omega/\omega_c) < 1$	17.02
$1 < (\omega/\omega_c) < 2$	6.81
$2 < (\omega/\omega_c) < 3$	6.62
$3 < (\omega/\omega_c) < 4$	6.94

2. Spherical Shell Distribution

The spherical distribution can be expressed in the form

$$f_o(v_\perp, v_\parallel) = \frac{1}{4\pi v_o^2}\,\delta(v - v_o)\ , \tag{3.42}$$

where $v = \sqrt{v_\perp^2 + v_\parallel^2}$. This describes a plasma in which all electrons have the same speed, v_o, and are isotropically distributed in velocity space on a sphere of radius v_o. The ring distribution would, in principle, relax to this case after the electrons have undergone collisions in which only momentum is transferred.

In order to evaluate Eq. (3.2) for this case, it is convenient to work with spherical coordinates, (v,Θ,ψ), in velocity space. The coefficient a_n can then be written in the form

$$a_n(k_\perp) = -2\pi\,\frac{\omega_c^2}{k_\perp^2}\int_0^\infty dv\,\frac{\partial f_o}{\partial v}\,v\int_0^\pi d\Theta\,J_n^2\left(\frac{k_\perp v}{\omega_c}\sin\Theta\right)\sin\Theta\ . \tag{3.43}$$

Since $f_o(v_\perp, v_\parallel) \equiv f_o(v)$, use has been made of the relationship

$$\frac{1}{v_\perp}\frac{\partial f_o}{\partial v_\perp} = \frac{1}{v}\frac{\partial f_o}{\partial v}\ . \tag{3.44}$$

The integration in Eq. (3.43) can be carried out in four steps:

(a) Subsitute the identity [26]

$$J_n^2\left(\frac{k_\perp v_\perp}{\omega_c}\sin\Theta\right) = \frac{1}{\pi}\int_0^\pi d\alpha\, J_o\left(2\,\frac{k_\perp v}{\omega_c}\sin\Theta\sin\alpha\right)\cos 2n\alpha\ ; \tag{3.45}$$

(b) Integrate with respect to Θ using the Bessel function integral [25]

$$\int_0^{\pi/2} d\Theta\, J_o\,(z\sin\Theta)\sin\Theta = \frac{\sin z}{z}\ ; \tag{3.46}$$

(c) Substitute the velocity distribution, Eq. (3.42), in the result and integrate with respect to v;

(d) Integrate over α with the identity [25]

$$J_{2n}(z) = \frac{2}{\pi}\int_0^{\pi/2} d\alpha\cos\,(z\sin\alpha)\cos 2n\alpha\ . \tag{3.47}$$

This procedure leads to the expression

$$a_n(k_\perp) = \frac{J_{2n}(2\xi_\perp)}{\xi_\perp^2}\quad , \tag{3.48}$$

and hence the dispersion relation, Eq. (3.1), is

$$K(\omega,k_\perp) = 1 - \frac{\omega_p^2}{\omega_c^2}\sum_{n=-\infty}^{\infty}\frac{J_{2n}(2\xi_\perp)}{\xi_\perp^2}\,\frac{n\omega_c}{\omega - n\omega_c}\ , \tag{3.49}$$

where $\xi_\perp$ has been written for $(k_\perp v_o/\omega_c)$. This expression is readily transformed to other forms. For example, an integral representation is obtainable from Eq. (3.7) after the function $F_o(\tau)$, defined be Eq. (3.5), is evaluated. For the spherical shell distribution, that function is given by

$$F_o(\tau) = \frac{\sin\left(2\xi_\perp \sin\frac{\tau}{2}\right)}{2\xi_\perp \sin\frac{\tau}{2}} , \qquad (3.50)$$

where use has been made of Eq. (3.46). Hence an alternate form of the dispersion relation is

$$K(\omega,k_\perp) = 1 + \frac{\omega_p^2}{\omega_c^2}\int_0^\pi d\tau \frac{\sin\Omega\tau \sin\frac{\tau}{2} \sin\left(2\xi_\perp \cos\frac{\tau}{2}\right)}{\xi_\perp \sin\Omega\pi} , \qquad (3.51)$$

which is also expressible in terms of Lommel's function [25]

$$s_{-1,\nu}(z) = \frac{-1}{\nu \sin\frac{\nu\pi}{2}}\int_0^{\pi/2} d\tau \cos\nu\tau \cos(z\cos\tau) , \qquad (3.52)$$

if the identity

$$\sin\frac{\tau}{2}\sin\left(2\xi_\perp \cos\frac{\tau}{2}\right) = \frac{1}{\xi_\perp}\frac{d}{d\tau}\left[\cos\left(2\xi_\perp \cos\frac{\tau}{2}\right)\right] , \qquad (3.53)$$

is substituted in Eq. (3.51) and an integration by parts is carried out. This yields the representation

$$K(\omega,k_\perp) = 1 + \frac{1}{\xi_\perp^2}\left[1 + 4\left(\frac{\omega_p^2}{\omega_c^2}\right)s_{-1,2\Omega}(2\xi_\perp)\right] . \qquad (3.54)$$

The computed dispersion characteristics are given in Fig. 9. When (ω_p^2/ω_c^2) is small, the n^{th} mode is represented by the function

$$\omega(k_\perp) = n\omega_c\left[1 + \frac{\omega_p^2}{\omega_c^2}\frac{J_{2n}(2\xi_\perp)}{\xi_\perp^2}\right] , \qquad (3.55)$$

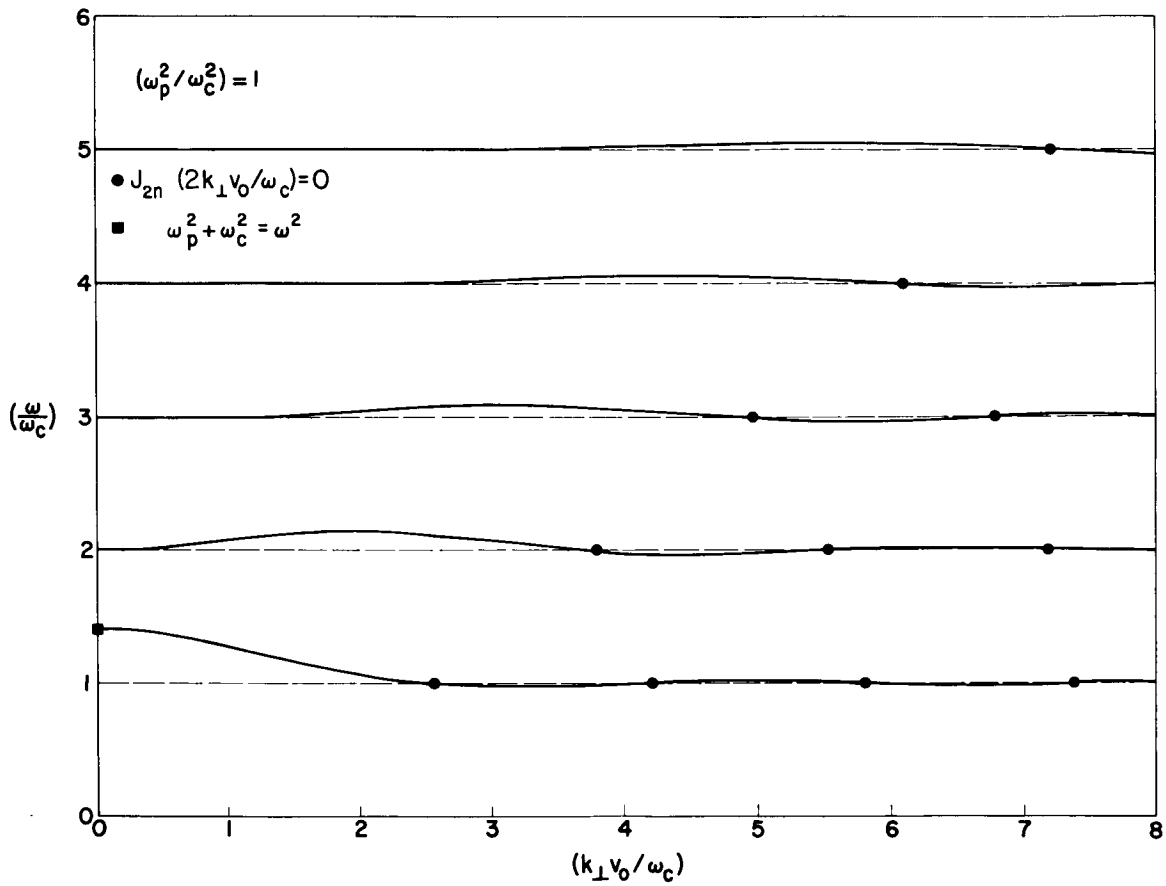

(a)

Fig. 9. DISPERSION CHARACTERISTICS OF PERPENDICULARLY PROPAGATING CYCLOTRON HARMONIC WAVES FOR SPHERICAL SHELL DISTRIBUTION.

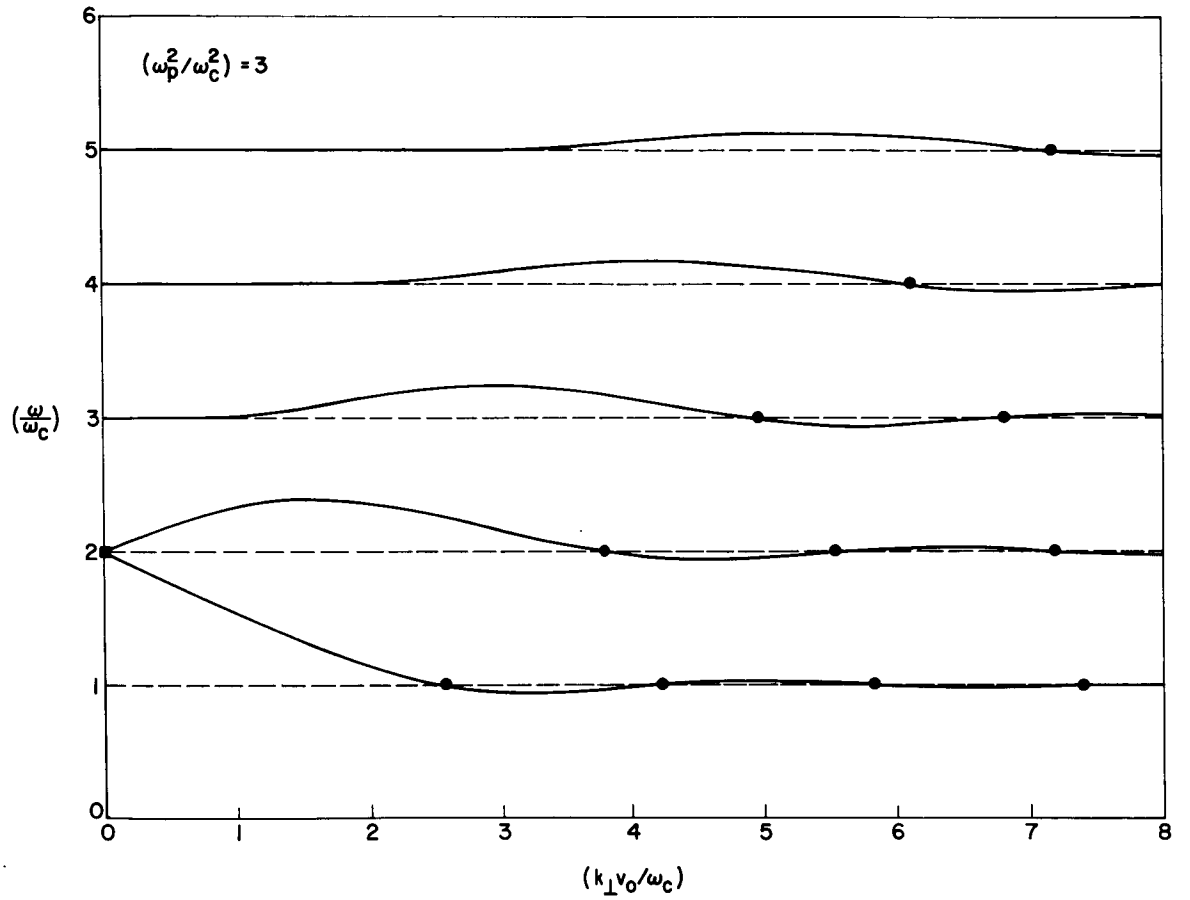

(b)

Fig. 9. CONTINUED.

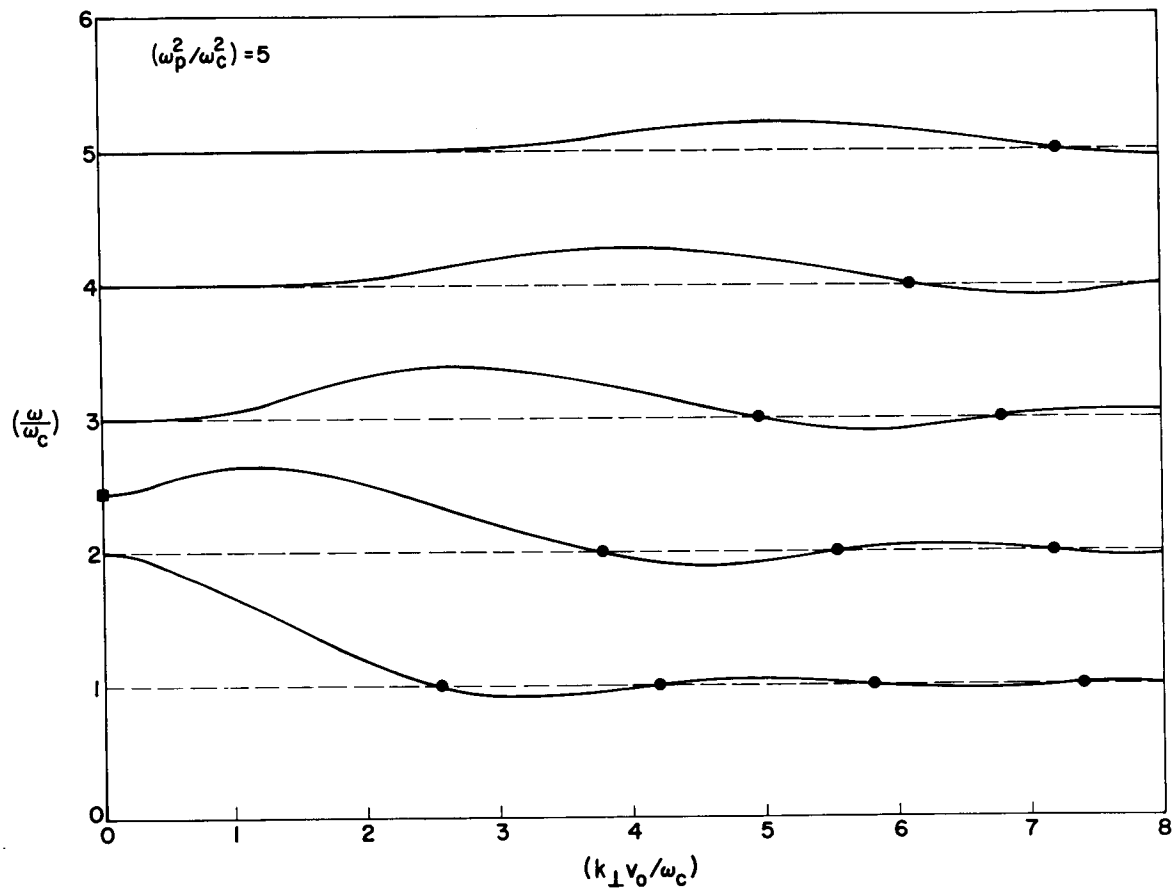

(c)

Fig. 9. CONTINUED.

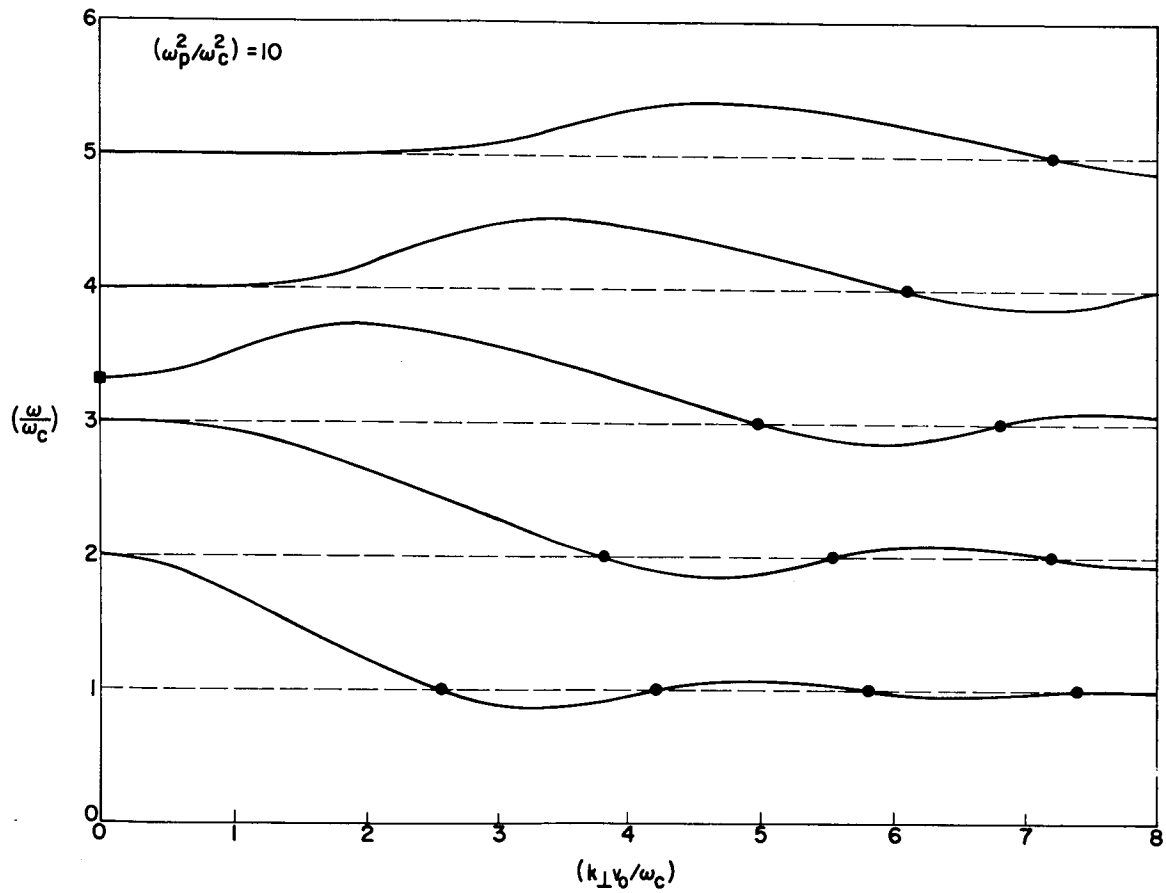

(e)

Fig. 9. CONTINUED.

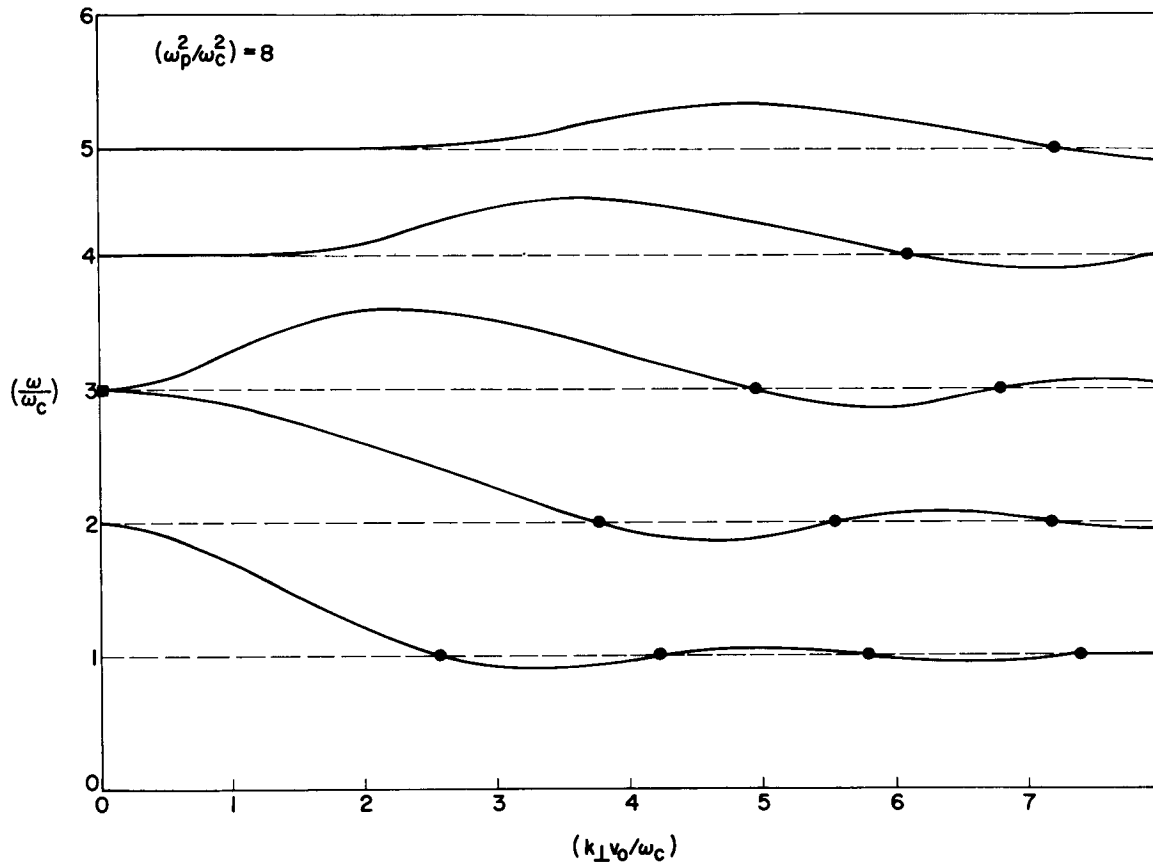

(d)

Fig. 9. CONTINUED.

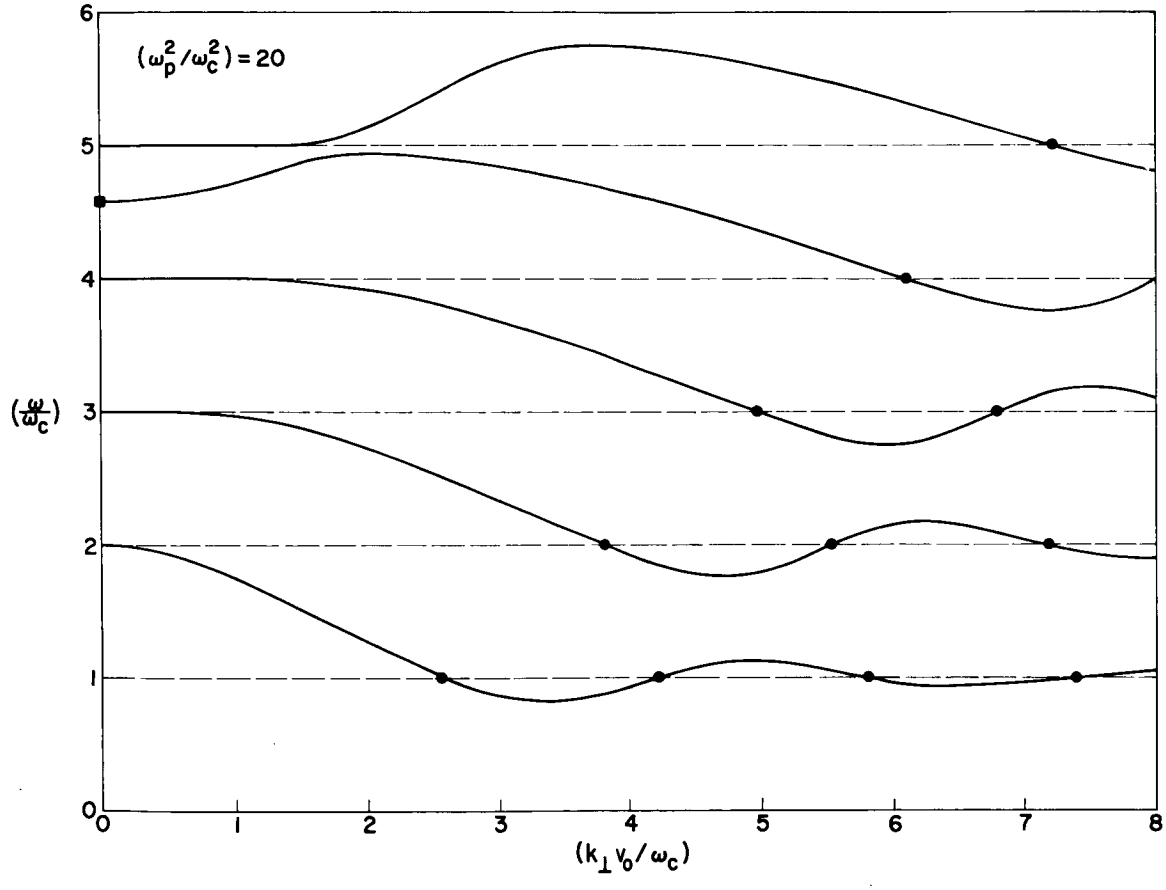

(f)

Fig. 9. CONTINUED.

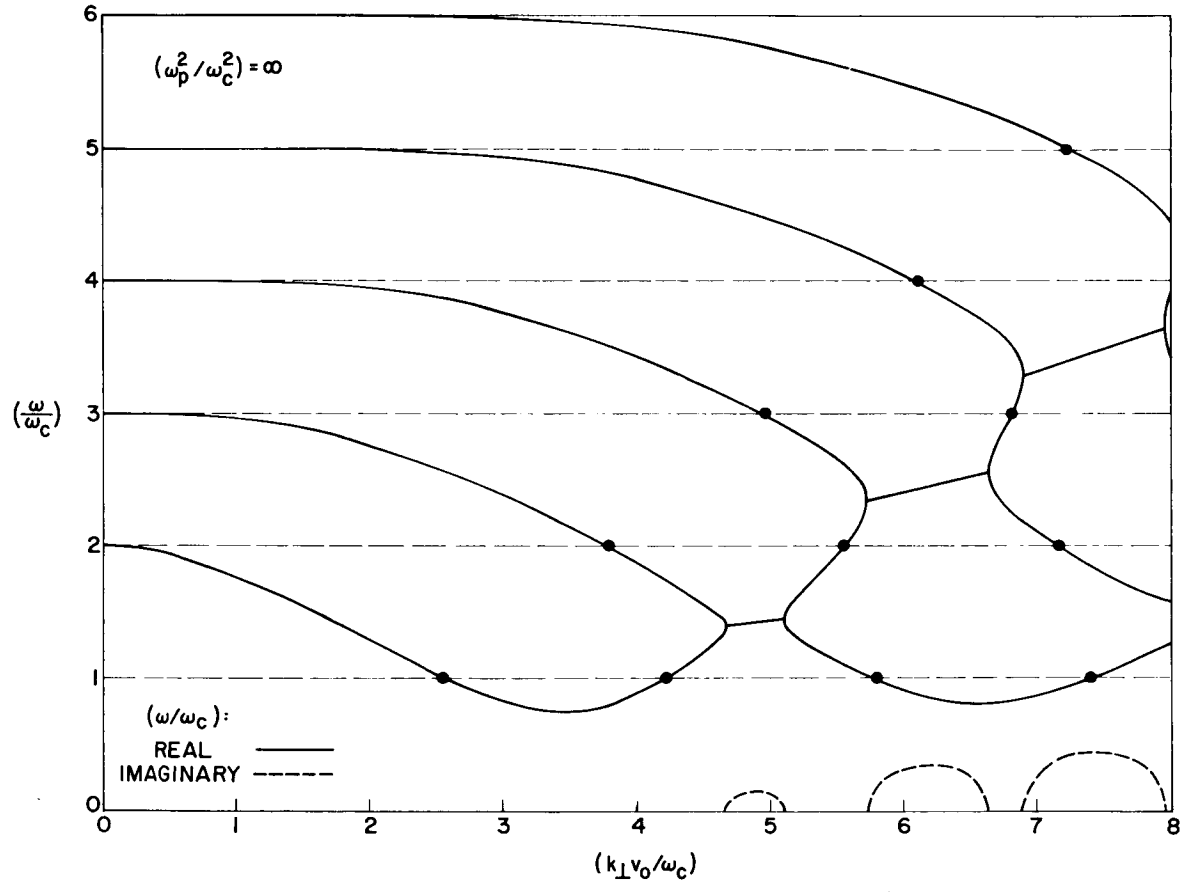

(g)

Fig. 9. CONTINUED.

which has been obtained by combining Eqs. (3.22) and (3.48). This expression indicates that the dispersion curve undulates about $\omega = n\omega_c$, passing through the harmonic when the equation, $J_{2n}(2\xi_\perp) = 0$, is satisfied, which is in agreement with the exact solutions in Fig. 9. As (ω_p^2/ω_c^2) increases, the amplitude of the undulation also increases, leading to mode coupling and hence instability. The lowest threshold conditions for these instabilities in the first four frequency bands are given in Table 2. When these results are compared with the numerical instability criteria for the ring distribution (Table 1), two important differences are observed: (1) the threshold conditions for instability in a plasma with a spherical-shell electron velocity distribution greatly exceed that of the ring distribution; and (2) unlike the ring distribution, no zero-frequency instability is associated with the spherical shell. The stringent requirements for instability of the spherical shell are closely related to the fact that electron energy is no longer confined solely to the transverse plane, but is also distributed parallel to the magnetic field.

Table 2

INSTABILITY THRESHOLD CONDITIONS FOR SPHERICAL SHELL DISTRIBUTION

Frequency Band	Values of (ω_p^2/ω_c^2) for Onset of Instability
$0 < (\omega/\omega_c) < 1$	Plasma absolutely stable
$1 < (\omega/\omega_c) < 2$	215.38
$2 < (\omega/\omega_c) < 3$	57.05
$3 < (\omega/\omega_c) < 4$	47.91

The absence of the zero-frequency instability in this case is apparent in Fig. 9g. This can also be established from the dispersion relation if ω is set equal to zero in Eq. (3.49). After using the identity [26]

$$\sum_{n=-\infty}^{\infty} J_{2n}(z) = 1 \ , \qquad (3.56)$$

the dispersion relation and the threshold condition for this instability reduce to

$$1 + \frac{\omega_p^2}{\omega_c^2} \frac{1 - J_o(2\xi_\perp)}{\xi_\perp^2} = 0 \ . \tag{3.57}$$

Since the left-hand side of this expression is positive definite for real and nonzero $\xi_\perp$, instability can never set in.

3. Maxwellian Distribution

It is important to consider the Maxwellian distribution since it may be closely approached in many laboratory plasmas. Its analytic representation is given by

$$f_o(v_\perp, v_\parallel) = \left(\frac{1}{2\pi v_t^2}\right)^{3/2} \exp\left(-\frac{v_\perp^2 + v_\parallel^2}{2v_t^2}\right) \ , \tag{3.58}$$

where v_t is the electron thermal velocity $(\kappa T_e/m_e)^{1/2}$. After substituting this expression in Eqs. (3.2) and (3.5), and making use of the identities [25]

$$\int_0^\infty dt \exp\left(-\frac{t^2}{2p^2}\right) J_n^2(t^2)t = p^2 \exp(-p^2) I_n(p^2) \ , \tag{3.59}$$

and

$$\int_0^\infty dt \exp\left(-\frac{t^2}{2p^2}\right) J_o(at)t = p^2 \exp\left(-\frac{a^2p^2}{2}\right) , \tag{3.60}$$

the functions $a_n(k_\perp)$ and $F_o(\tau)$ have the form

$$a_n(k_\perp) = \frac{\exp(-\lambda) I_n(\lambda)}{\lambda} \ , \tag{3.61}$$

$$F_o(\tau) = \exp\left(-2\lambda \sin^2 \frac{\tau}{2}\right) , \tag{3.62}$$

where $\lambda = (k_\perp v_t/\omega_c)^2$. Hence, from Eqs. (3.1) and (3.7), the dispersion relation is

$$K(\omega,k_\perp) = 1 - \frac{\omega_p^2}{\omega_c^2} \sum_{n=-\infty}^{\infty} \frac{\exp(-\lambda)\, I_n(\lambda)}{\lambda} \frac{n\omega_c}{\omega - n\omega_c} \tag{3.63}$$

$$= 1 + \frac{\omega_p^2}{\omega_c^2} \int_0^\pi d\tau \frac{\sin \Omega\tau}{\sin \Omega\pi} \sin \tau \exp\left(-2\lambda \cos^2 \frac{\tau}{2}\right) = 0 \ . \tag{3.64}$$

Equations (3.63) and (3.64) are equivalent to representations given by Bernstein [3], when he demonstrated that all solutions of those equations correspond to stable waves. This conclusion is consistent with the theorem proved at the beginning of this section since it is readily established from Eq. (3.61) that $a_n > 0$ for all n.

The dispersion curves associated with the Maxwellian distribution are shown in Fig. 10. It is clearly seen that each mode is confined to a specific band. As $(\omega_p^2/\omega_c^2) \to \infty$, the frequency of the n^{th} mode increases from

$$\omega(k_\perp) = n\omega_c \left[1 + \frac{\omega_p^2}{\omega_c^2} \frac{\exp(-\lambda)\, I_n(\lambda)}{\lambda}\right] , \tag{3.65}$$

when the plasma density is low, to the limiting values shown in Fig. 10. No mode coupling ever occurs, implying that the plasma is absolutely stable.

4. Mixed Distributions

If a group of electrons with an isotropic Maxwellian velocity distribution is added to the ring distribution of Section B1, the dispersion relation for purely perpendicular propagation is, in the notation of Eqs. (3.37) and (3.63),

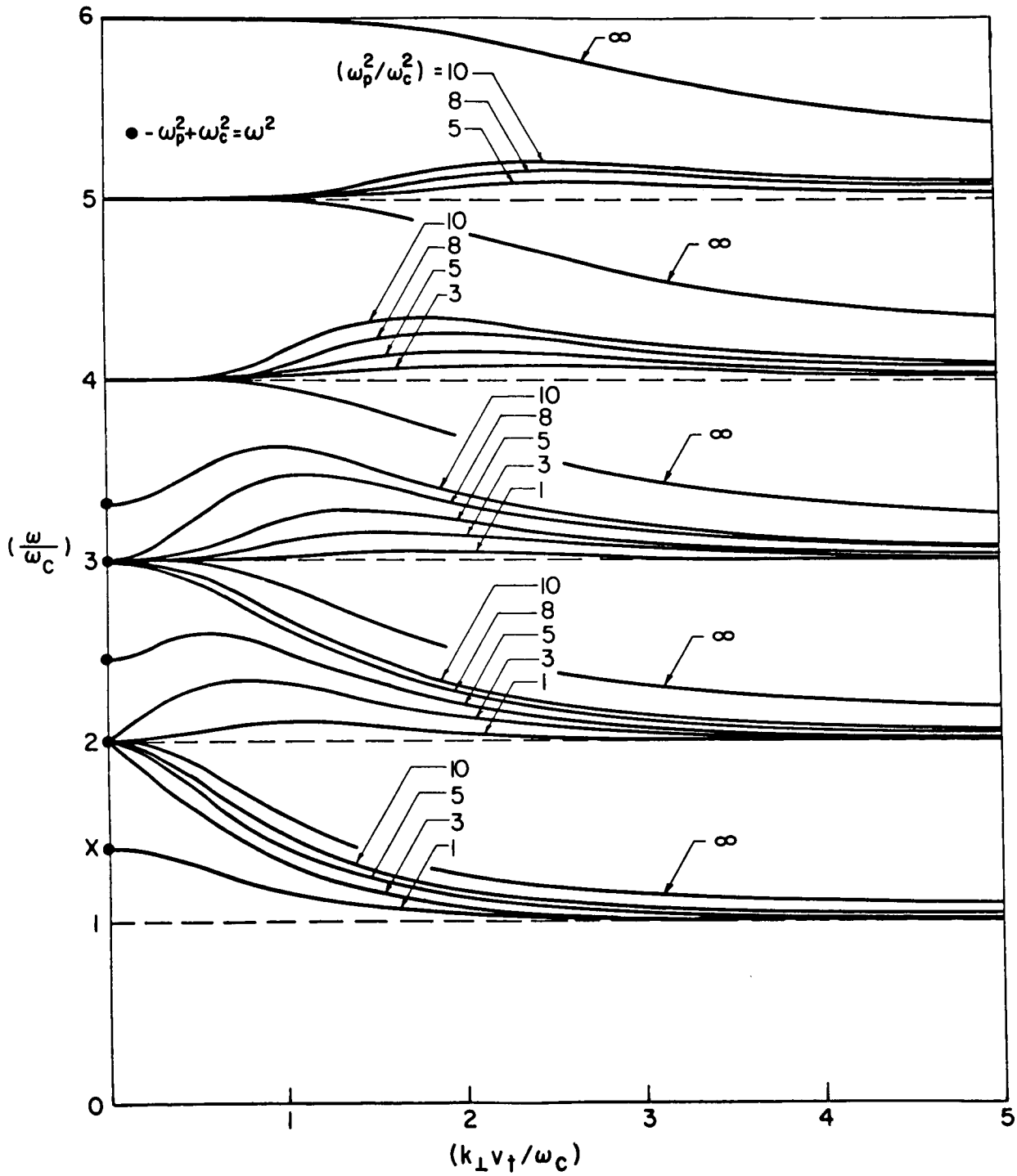

Fig. 10. DISPERSION CHARACTERISTICS OF PERPENDICULARY PROPAGATING CYCLOTRON HARMONIC WAVES FOR MAXWELLIAN DISTRIBUTION.

$$K(\omega,k_\perp) = 1 - \frac{\omega_p^2}{\omega_c^2}\left[\alpha \sum_{n=-\infty}^{\infty} \frac{\exp(-\lambda)\, I_n(\lambda)}{\lambda} \frac{n\omega_c}{\omega - n\omega_c}\right.$$

$$\left. + (1-\alpha) \sum_{n=-\infty}^{\infty} \frac{1}{\mu_\perp} \frac{\partial J_n^2(\mu_\perp)}{\partial \mu_\perp} \frac{n\omega_c}{\omega - n\omega_c}\right] = 0 \ , \qquad (3.66)$$

where α defines the proportion of the total electron density that is Maxwellian. As pointed out previously, situations similar to this may be approached in certain laboratory plasmas, for example in the DCX [29].

A study has been made of this dispersion relation to determine the threshold conditions for instability, in the first four frequency bands, due to mode coupling of the type indicated in Figs. 7 and 9. Two modes just couple in that case when the following equations are satisfied:

$$\frac{\partial \omega(k_\perp,\eta)}{\partial k_\perp} = 0 \ , \qquad (3.67)$$

$$\frac{\partial \omega(k_\perp,\eta)}{\partial \eta} = \infty \ , \qquad (3.68)$$

where $\omega(k_\perp,\eta)$ satisfies the dispersion relation,

$$K[\omega(k_\perp,\eta),k_\perp,\eta] = 0 \ , \qquad (3.69)$$

and η has been written for (ω_p^2/ω_c^2). The results are shown in Fig. 11. When $\alpha = 0$ (that is, the electrons are exclusively in the ring group), we retrieve the critical values of (ω_p^2/ω_c^2) that are given in Table 1. As α increases, the threshold conditions become strongly dependent on the velocity ratio parameter $\beta = (v_{o\perp}/v_t)$. In the first frequency band, Fig. 11a indicates that (ω_p^2/ω_c^2) increases monotonically with β. The remaining three bands have a more complicated structure.

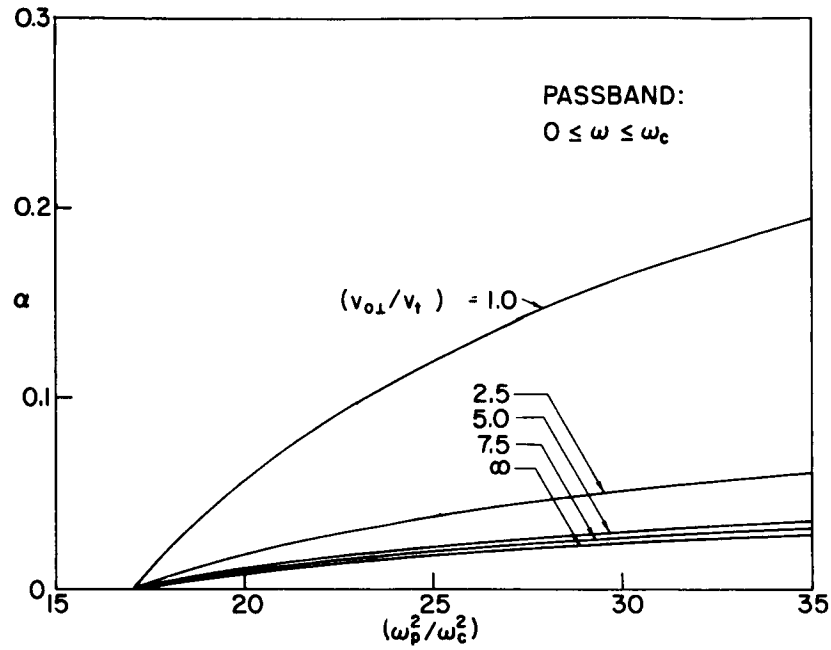

(a)

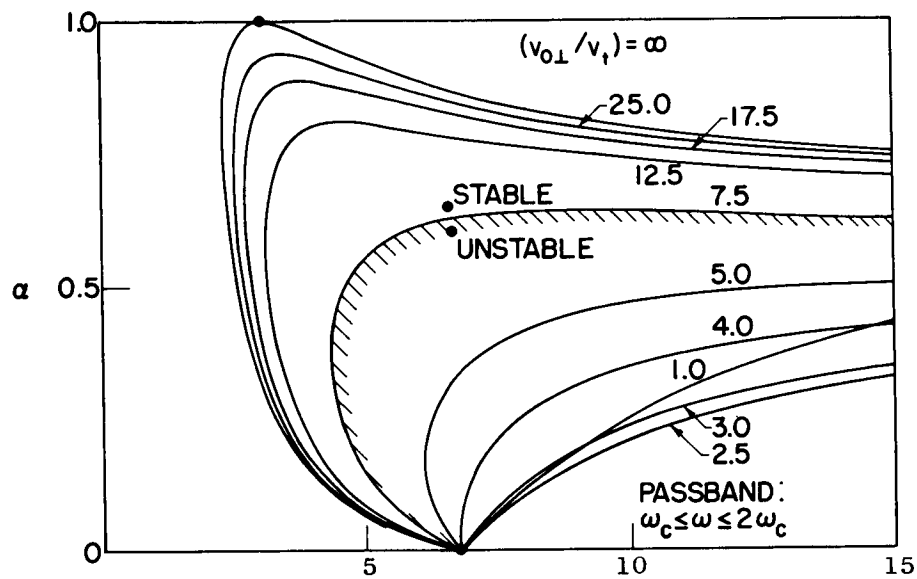

(b)

Fig. 11. CRITERIA FOR THE ONSET OF INSTABILITY FOR PERPENDICULARLY PROPAGATING CYCLOTRON HARMONIC WAVE IN A MIXTURE OF (α) MAXWELLIAN AND $(1-\alpha)$ RING ELECTRON VELOCITY DISTRIBUTIONS.

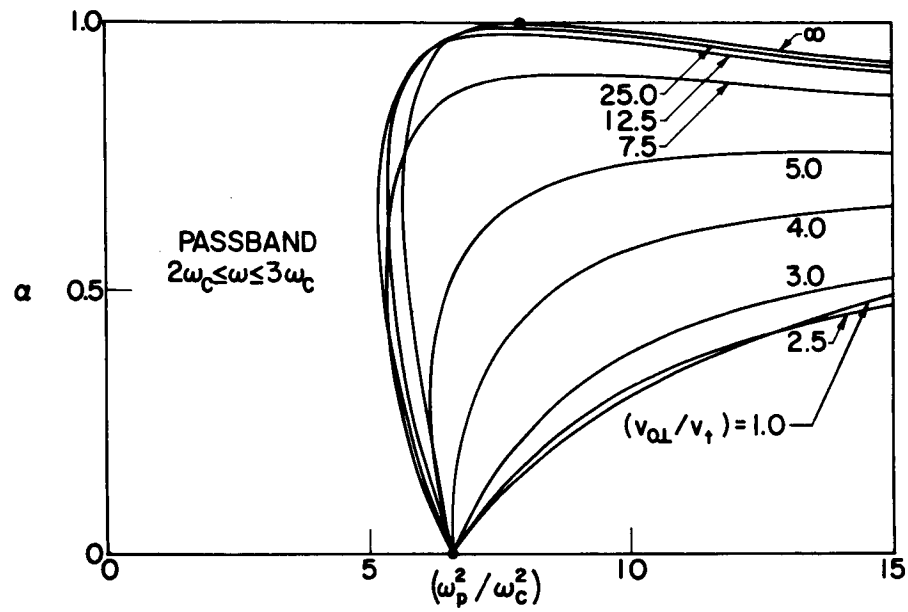

(c)

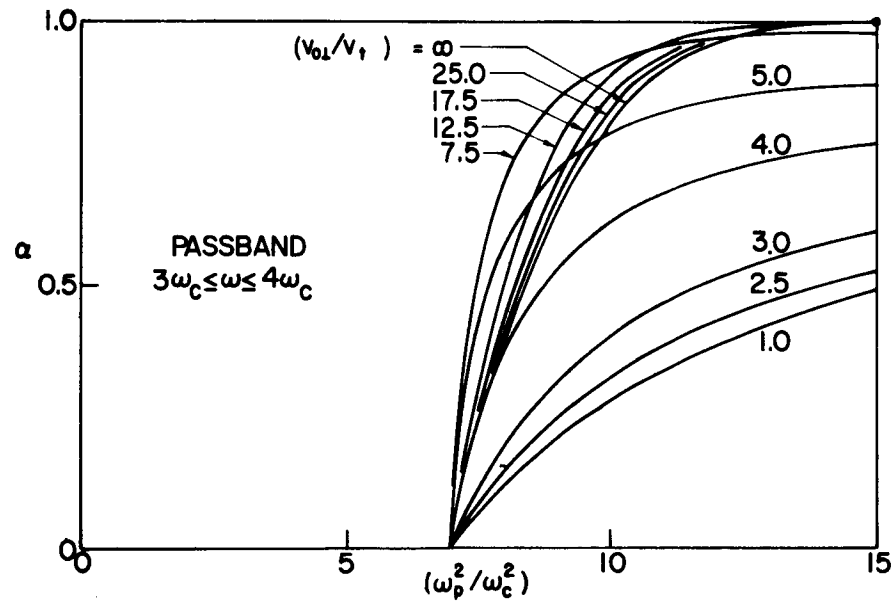

(d)

Fig. 11. CONTINUED.

For a given value of α, the instability threshold condition may be lowered if β is sufficiently large. Indeed, Figs. 11b and 11c show that instabilities are predicted for values of (ω_p^2/ω_c^2) that correspond to stability when the electrons are exclusively in the ring group. This also has the effect of increasing the maximum attainable growth rate of instabilities in a given frequency band. This is clearly illustrated in Fig. 12 where the maximum value of (ω_i/ω_c) is plotted as a function of α. It is seen that the growth rate of instabilities associated with the ring distribution can be increased by adding to that distribution a group of Maxwellian electrons.

C. Classification of Instabilities

The uniformity of the plasma model that is under investigation has permitted us to look for solutions of the linearized differential equations that have the form

$$\exp\left\{i[\omega(\underset{\sim}{k})t - \underset{\sim}{k}\cdot\underset{\sim}{r}]\right\}, \tag{3.70}$$

where the frequency and wave number are connected through the dispersion relation,

$$K[\omega(\underset{\sim}{k}),\underset{\sim}{k}] = 0 . \tag{3.71}$$

If $\underset{\sim}{k}$ is real and $\mathrm{Im}\,[\omega(\underset{\sim}{k})] < 0$, Eq. (3.70) implies that the amplitude of the perturbation will increase exponentially with time for any $\underset{\sim}{r}$. Hence, within the validity of the linearized theory, the plasma is unstable and no steady state conditions appear possible. However, it was clearly pointed out by Sturrock [30] that there are two distinct types of instabilities, one of which does lead to a steady state. This distinction becomes apparent only after a spectrum of waves is superimposed by inverting the Fourier and Laplace transformations. This inversion can be written in the form

$$\int_C \frac{d\omega}{2\pi}\int \frac{d\underset{\sim}{k}}{(2\pi)^3}\,\underset{\sim}{A}(\omega,\underset{\sim}{k})\,\exp\,[i(\omega t - \underset{\sim}{k}\cdot\underset{\sim}{r})] , \tag{3.72}$$

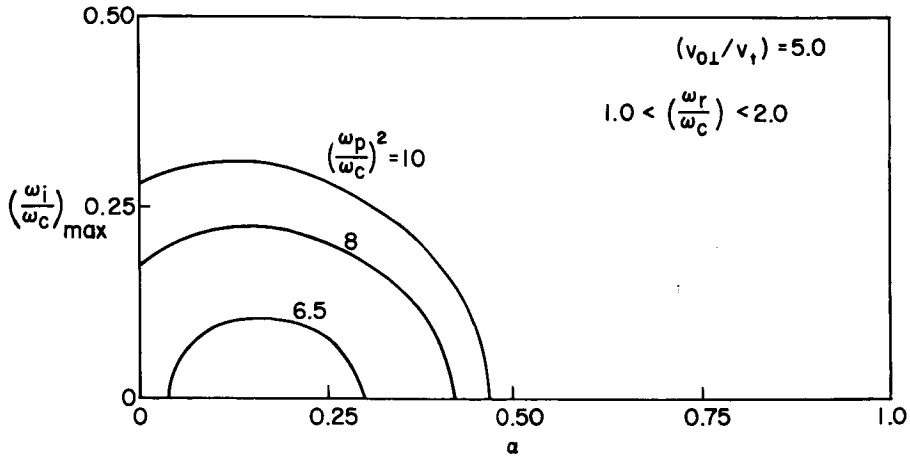

(a)

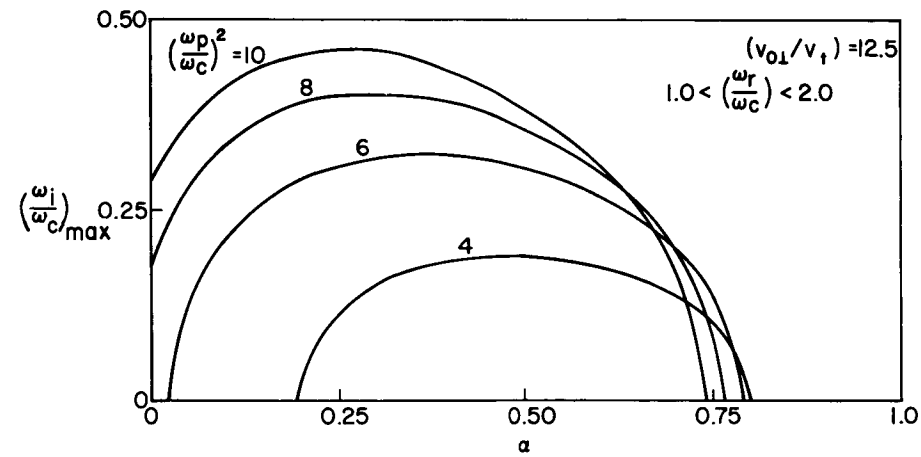

(b)

Fig. 12. MAXIMUM INSTABILITY GROWTH RATES FOR A MIXTURE OF MAXWELLIAN AND RING ELECTRON VELOCITY DISTRIBUTIONS.

where $\underset{\sim}{A}\,(\omega,\underset{\sim}{k})$ is the associated amplitude of the wave. As $t \to \infty$, Eq. (3.72) may take on one of two forms as illustrated in Fig. 13. The disturbance may grow in time at every point in space, or, if the speed of the pulse is sufficiently large, it may propagate away from a region of space while growing with time, leaving the plasma unperturbed. The

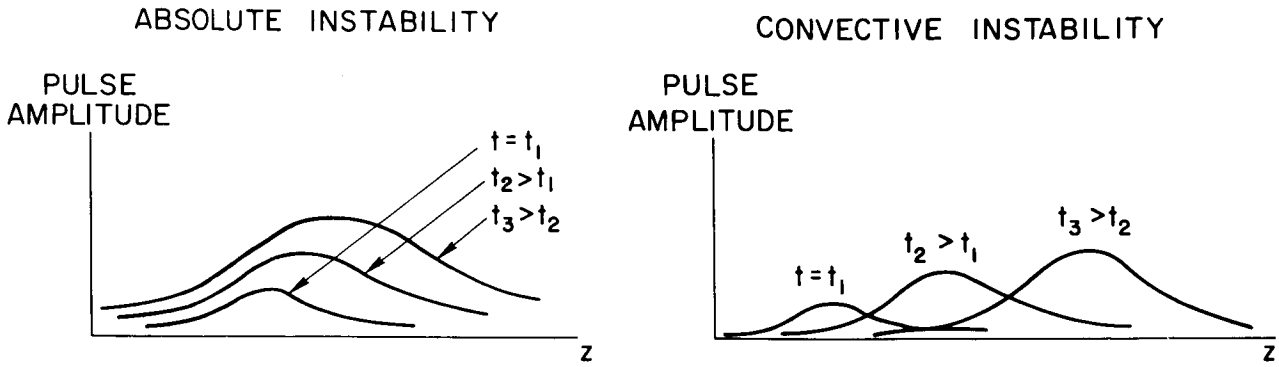

Fig. 13. SKETCHES ILLUSTRATING ABSOLUTE AND CONVECTIVE INSTABILITIES.

former situation is referred to as an absolute instability and the latter, as a convective instability.

The importance of making this distinction should now be clear. If the plasma is convectively unstable, a steady state exists and hence it should be possible to excite sinusoidal oscillations, characterized by a real frequency and the corresponding complex wave number solutions of the dispersion relation. This effect will be totally washed out if an absolute instability is present.

This section is devoted to a classification of the electrostatic instabilities of cyclotron harmonic waves propagating perpendicular to the applied magnetic field. To carry this out, we will use the now well-established method that was developed by Derfler [31], [32], Bers and Briggs [33], and Briggs [34]. The stability criterion is based on the form that is acquired by Eq. (3.72) as $t \to \infty$. If that limit increases with time for any $\underset{\sim}{r}$, the plasma is absolutely unstable; if the limit approaches zero for a fixed $\underset{\sim}{r}$, the instability is convective. In the following subsection, we will describe how that limit is obtained, and then apply the results to unstable cyclotron harmonic waves.

1. Stability Criterion

For purposes of illustrating the basic concepts governing the stability criterion, we will derive the asymptotic form of the electric field when spatial variations occur only along the x axis, perpendicular

to the magnetic field. In this case, $\underset{\sim}{A}(\omega,\underset{\sim}{k})$ is given by Eq. (2.49) which, under the cited restriction, has the form

$$\underset{\sim}{A}(\omega,\underset{\sim}{k}) \equiv \underset{\sim}{E}_1(\omega,\underset{\sim}{k}) = \hat{x}\,\frac{ig(k_\perp)\,f(\omega)}{\epsilon_o k_\perp K(\omega,k_\perp)} \tag{3.73}$$

where we assume that the source can be written as $\rho_s(k_\perp,\omega) = g(k_\perp)f(\omega)$, and $\hat{x}$ is a unit vector along the x axis. After performing an inverse transformation on Eq. (3.73), the electric field becomes

$$E_1(x,t) = \int_C \frac{d\omega}{2\pi} \int_{-\infty}^{\infty} \frac{dk_\perp}{2\pi} \frac{ig(k_\perp)\,f(\omega)}{\epsilon_o k_\perp K(\omega,k_\perp)} \exp\,[i(\omega t - k_\perp x)] \tag{3.74}$$

$$= \int_C \frac{d\omega}{2\pi} \exp\,(i\omega t)\,F(\omega,x)\,f(\omega)\ , \tag{3.75}$$

where

$$F(\omega,x) = i \int_{-\infty}^{\infty} \frac{dk_\perp}{2\pi} \frac{\exp\,(-ik_\perp x)\,g(k_\perp)}{\epsilon_o k_\perp K(\omega,k_\perp)}\ , \tag{3.76}$$

and $E_1(x,t)$ is defined by the expression, $\underset{\sim}{E}_1(\underset{\sim}{r},t) = \hat{x}E_1(x,t)$. As $t \to \infty$, the limiting form of Eq. (3.74) is derived by first deforming the Laplace contour in the usual manner into the upper half complex ω plane, around the singularities of the integrand, as shown in Fig. 14. This yields

$$\lim_{t\to\infty} E_1(x,t) = i \sum \text{Res}\,[\exp(i\omega t)\,F(\omega,x)\,f(\omega)]$$

$$+ \int_{C_b} \frac{d\omega}{2\pi} \exp\,(i\omega t)\,F(\omega,x)\,f(\omega)\ , \tag{3.77}$$

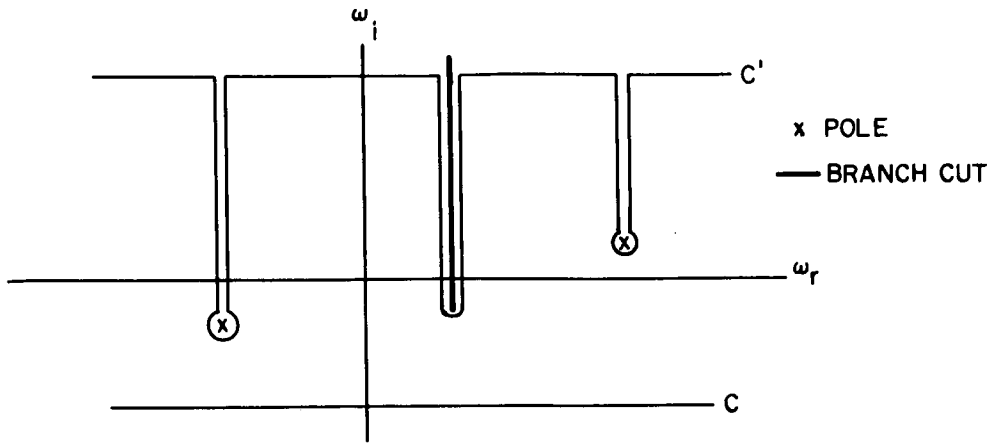

Fig. 14. ORIGINAL (C) AND DEFORMED (C') LAPLACE CONTOUR OF INTEGRATION.

where the first expression is a sum over the residues of poles, and C_b is a contour around the branch cuts.

The singularities of the source function, $f(\omega)$, are usually simple poles. For example, if $f(t) = \exp(i\omega_o t)$, then its Laplace transformation is given by $f(\omega) = -i/(\omega - \omega_o)$. The term in Eq. (3.77) corresponding to this singularity is

$$\exp(i\omega_o t)\, F(\omega_o, x) , \tag{3.78}$$

showing that a steady oscillation is excited at the real frequency ω_o.

To find the singularities of the function $F(\omega,x)$, use is made of a technique that has widespread applications in quantum field theory [35]. When ω is on the Laplace contour C, it is assumed that the integrand of Eq. (3.76) is analytic on the real $k_\perp$ axis, which for convenience we define as Γ, and that it has singularities in the complex plane at $k_i(\omega)$, where

$$K[\omega, k_i(\omega)] = 0 . \tag{3.79}$$

It is further assumed that the only singularities of the integrand are simple poles. In the process of deforming C to C', these singularities follow a continuous path, and the integration remains well-defined so long as the singularities do not move onto Γ. This possibility can be avoided by deforming Γ to $\tilde{\Gamma}$ ahead of an advancing singularity, as illustrated in Fig. 15, and thus obtaining the analytic continuation of

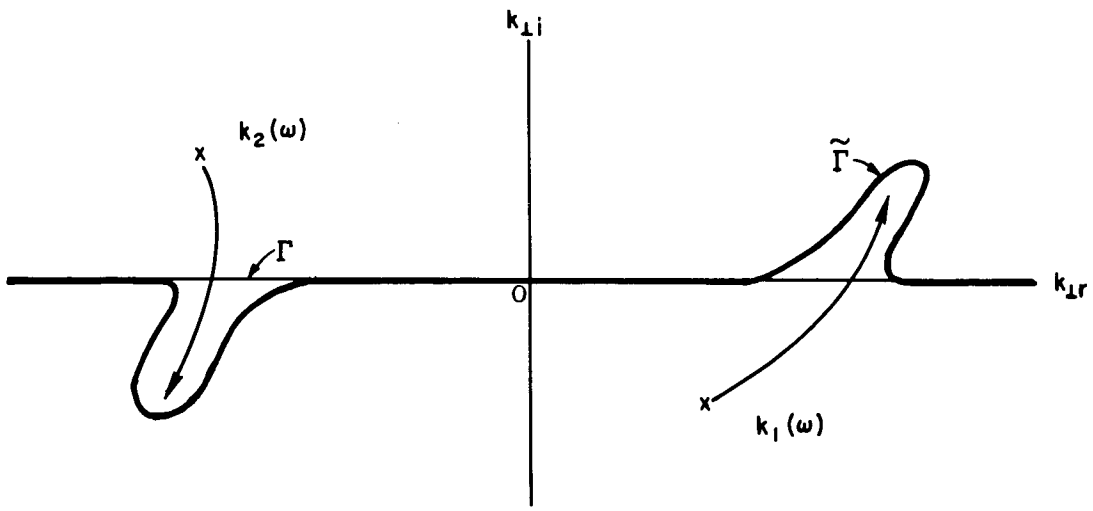

Fig. 15. ANALYTIC CONTINUATION OF INTEGRAL REPRESENTATION OF $F(\omega,x)$ BY CONTINUOUS DEFORMATION OF CONTOUR OF INTEGRATION Γ, AHEAD OF ADVANCING SINGULARITIES AT $k_1(\omega)$ AND $k_2(\omega)$.

Eq. (3.76). This deformation will be necessary if the dispersion relation has solutions with $\mathrm{Im}(\omega) < 0$ and $k_\perp$ real, corresponding to our previous requirement for instability. However, useful deformation is impossible if two or more singularities, coming from opposite sides of the contour of integration, "pinch" $\tilde{\Gamma}$ at k_o when $\omega = \omega_o$. This is illustrated in Fig. 16 with two singularities, $k_1(\omega)$ and $k_2(\omega)$. In this case Eq. (3.79) possesses a double root at $k_\perp(\omega_o)$, implying

$$\left(\frac{\partial K}{\partial k_\perp}\right)_{\omega=\omega_o} = 0 \,. \tag{3.80}$$

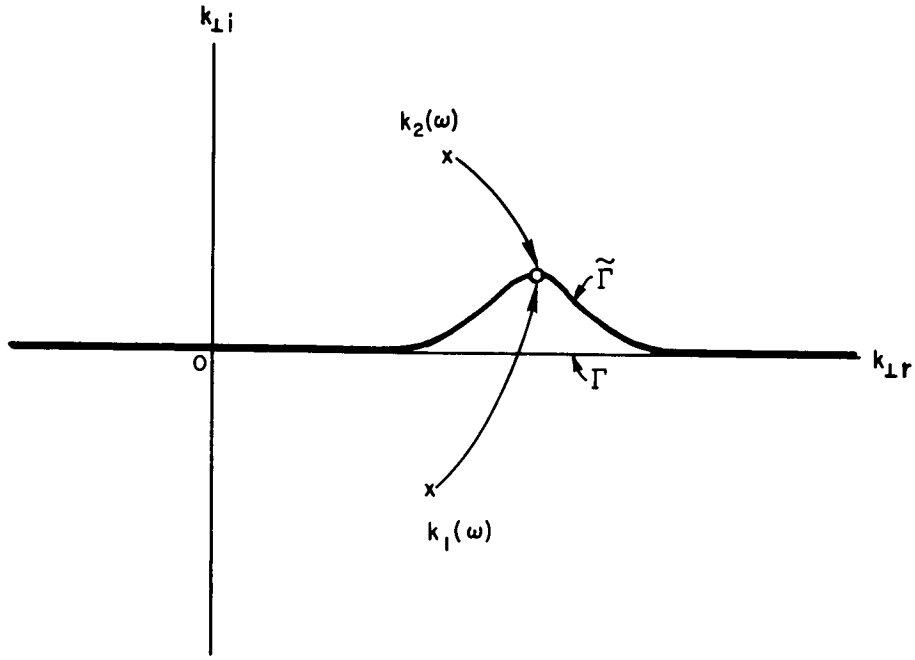

Fig. 16. SKETCH ILLUSTRATING ORIGIN OF SINGULARITIES IN $F(\omega,x)$.

When ω is near ω_o, the most significant contribution to Eq. (3.76) will come from that part of $\tilde{\Gamma}$ which is near k_o and where the following expansion is valid:

$$K(\omega,k_\perp) \approx K_\omega(\omega_o,k_o)(\omega - \omega_o) + \frac{1}{2} K_{k_\perp k_\perp}(\omega_o,k_o)(k_\perp - k_o)^2 \ . \qquad (3.81)$$

Substituting this in Eq. (3.76) and evaluating the integral by the method of residues yields

$$F(\omega,x) \approx \left[\frac{\exp(-ik_\perp x)\, g(k_\perp)}{\epsilon_o k_\perp \left(-2K_\omega K_{k_\perp k_\perp}\right)^{1/2}}\right]_{\omega_o,k_o} \frac{1}{(\omega - \omega_o)^{1/2}} \ , \qquad (3.82)$$

which shows that a branch pole exists at ω_o. This expression is correct to within a plus or minus sign, the appropriate one being determined only

after $K(\omega,k_\perp)$ is specified. It is important to realize that Eq. (3.82) specifies the form of the function $F(\omega,x)$ near ω_o only if the two zeros of Eq. (3.81) lie on opposite sides of the contour $\tilde{\Gamma}$ since only in this case will pinching occur. If this condition is not satisfied, $F(\omega,x)$ will be analytic at ω_o.

We now can substitute Eq. (3.82) in (3.77) and integrate around the branch cut to find that the asymptotic form of the electric field has a component which varies in time and space as

$$\frac{1}{t^{1/2}} \exp\left[i(\omega_o t - k_o x)\right] . \tag{3.83}$$

Hence, if $\mathrm{Im}(\omega_o) < 0$, the oscillation will grow with time for any x, implying that the plasma is absolutely unstable. If no such point is found in the lower half ω plane, $F(\omega,x)$ will be analytic there, implying that a steady state exists. It should be clear that a singularity will still occur at ω_o if more than two roots of the dispersion relation pinch $\tilde{\Gamma}$, but the form of $F(\omega,x)$ near that point will be different from what is given by Eq. (3.82).

In the light of this discussion, the stability criterion can be stated in the following manner: Map that part of the lower half complex ω plane which is bounded by the real axis and the Laplace contour C, into the complex $k_\perp$ plane with the dispersion relation. If, in the process of doing this, the contour Γ (that is, the real $k_\perp$ axis) is deformed and pinched by two or more zeros of the dispersion relation, the plasma is absolutely unstable and no steady state is possible.

2. Application of the Stability Criterion

In this section we will use this criterion to determine if a steady state exists when one-dimensional space-charge oscillations are excited perpendicular to the applied magnetic field. Briggs [34] has pointed out that a convenient method that can be used to search for pinching singularities is to map contours of constant ω_i into the complex wave number plane and look for saddlepoints of the function $\omega(k_\perp)$, that is, points where

$$\frac{d\omega(k_\perp)}{dk_\perp} = 0 \ . \tag{3.84}$$

By writing

$$\frac{d\omega}{dk_\perp} = \frac{K_{k_\perp}}{K_\omega} \ , \tag{3.85}$$

it is seen that if Eq. (3.84) is satisfied and K_ω is finite, the partial derivative $K_{k_\perp}$ must vanish, implying that the dispersion relation has a double root in the complex $k_\perp$ plane.

This technique has been used to classify the instabilities associated with the ring distribution. Some results are given in Fig. 17 for $(\omega_p^2/\omega_c^2) = 20$ and $1 < (\omega_r/\omega_c) < 2$. When contours A, B, C, and D

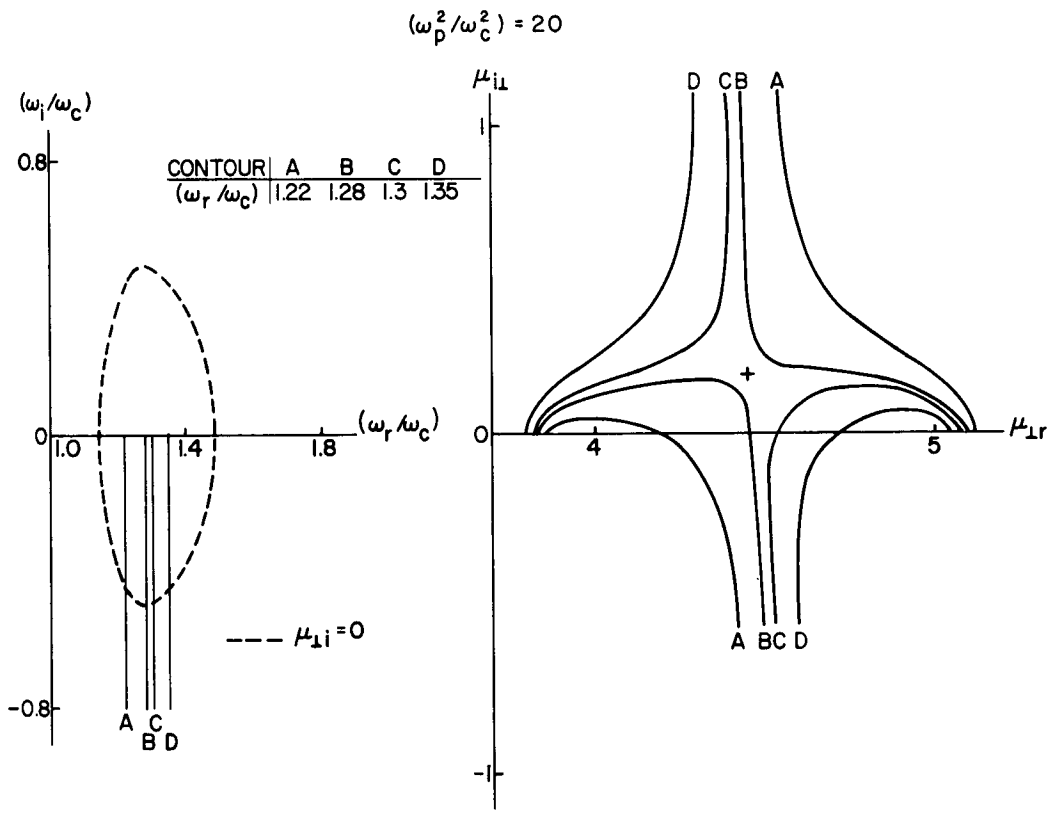

Fig. 17. CONFORMAL MAPPING OF CONTOURS A, B, C, AND D INTO COMPLEX $\mu_\perp$ PLANE PROVING THAT INSTABILITIES OF RING DISTRIBUTION ARE ABSOLUTE.

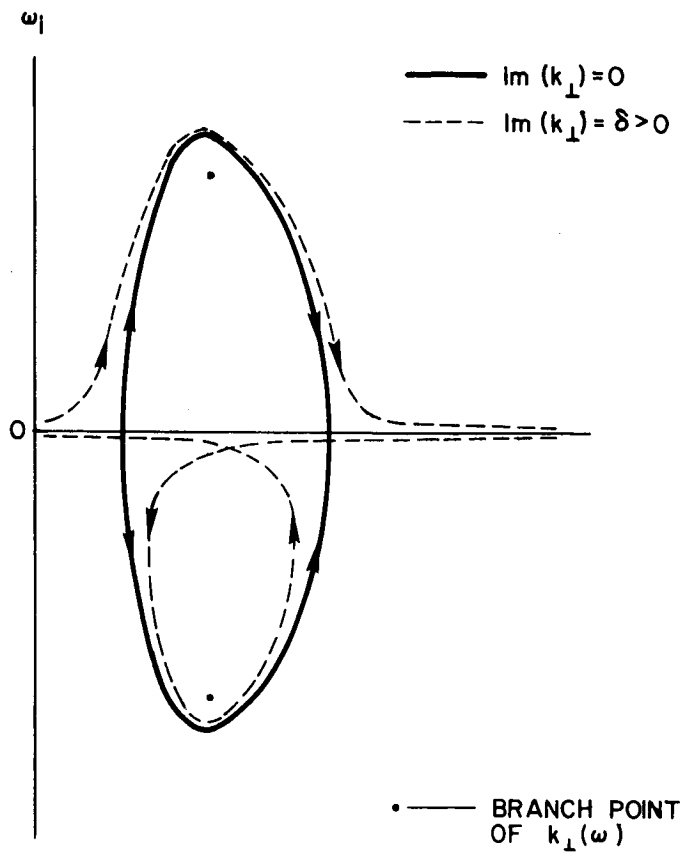

Fig. 18. LOCUS OF COMPLEX FREQUENCIES OF PERPENDICULARLY PROPAGATING CYCLOTRON HARMONIC WAVES.

is based on the restriction that instabilities arise from mode coupling of the type indicated in the computed dispersion diagrams. However, in all cases considered, this type of mode coupling does indeed occur.

This section has been concerned with singularities of $F(\omega,x)$ in the lower half ω plane since these points imply instability. However, this function may be singular elsewhere in the complex plane. Of particular importance are singularities on the real axis since, for stable distributions, they are the lowest singularities in the ω plane and hence determine the asymptotic form of the plasma response. This situation is examined further in Chapter V where we investigate the excitation of resonances in a magnetoplasma with a Maxwellian velocity distribution.

are mapped to the complex $k_\perp$ plane with Eq. (3.37b), a saddlepoint is found at $(k_{\perp o} v_{o\perp}/\omega_c) = 4.46 + i0.18$. The corresponding value of the frequency is $(\omega_o/\omega_c) = 1.29 - i0.47$. Since the saddlepoint is formed by the merging of two roots of the dispersion relation that originate on opposite sides of the real axis, the contour of integration is pinched at $k_\perp = k_o$ and $F(\omega,x)$ is singular in the lower half frequency plane at $\omega = \omega_o$. Hence the plasma in this case is absolutely unstable.

This result can be extended to more general situations. It was pointed out previously that Eq. (3.84) implies that the function $\omega(k_\perp)$ has a saddlepoint somewhere in the complex $k_\perp$ plane. However, that equation also implies that the inverse function, $k_\perp(\omega)$, has a branch point in the frequency plane. Derfler [31] has shown that this interpretation can be used to classify instabilities. If a mapping of the real wave number axis to the complex ω plane is a loop that is located entirely in the lower half of the plane, a branch point of $k_\perp(\omega)$ must be encircled, suggesting that $F(\omega,x)$ must also have a branch point at the same frequency and hence that the plasma is absolutely unstable. Derfler has shown that this interpretation is implied by the pinching criterion.

Figure 18 shows a sketch of a locus that the complex roots of the dispersion relation for cyclotron harmonic waves will follow as the wave number increases along the real axis. It is easy to see that all complex frequencies shown in the dispersion diagrams of Section B behave in this manner. In order to separate the two branches in Fig. 18, a second locus has been drawn along which the imaginary part of $k_\perp$ equals δ, where δ is a small positive number. The equation describing this locus is obtainable by expanding the frequency $\omega(k_{\perp r} + i\delta)$, in a Taylor series,

$$\omega(k_{\perp r} + i\delta) \approx \omega(k_{\perp r}) + i\delta \frac{\partial\omega(k_{\perp r})}{\partial k_{\perp r}} , \qquad (3.86)$$

where $\omega(k_{\perp r})$ and its first derivative can be found in the dispersion diagrams given earlier in this chapter. The appearance of a loop in the lower half plane leads to the immediate conclusion that cyclotron harmonic wave instabilities are absolutely unstable. Of course, this

D. Steady State Conditions and Collision Damping

If the plasma is free of absolute instabilities, it is possible to excite steady oscillations with a source operating at a real frequency, ω_o. The form of the electric field in this case is given by Eq. (3.78). In that expression, it is necessary to know the definition of the function $F(\omega,x)$ on the real ω axis. This can be obtained with the prescription described in the previous section: As ω approaches the real axis from the Laplace contour in the lower half complex plane, the contour of integration of Eq. (3.76) must be deformed ahead of an advancing root of the dispersion relation that may cross the real $k_\perp$ axis. This will occur if the dispersion relation has solutions with $Im(\omega) < 0$ and $k_\perp$ real. However, it was shown in Section C of this chapter that the plasma is absolutely unstable in these cases. In all other cases, a steady state does exist, but there are still solutions where the frequency and wave number are real and hence where the contour $\tilde{\Gamma}$, shown in Fig. 19, must be used to define $F(\omega,x)$ on the real frequency axis. In order to determine which roots of the dispersion relation approach the real axis from the upper or lower half $k_\perp$ plane as $\omega \to \omega_o$, it is only necessary to add a small, negative imaginary part, δ, to ω_o and

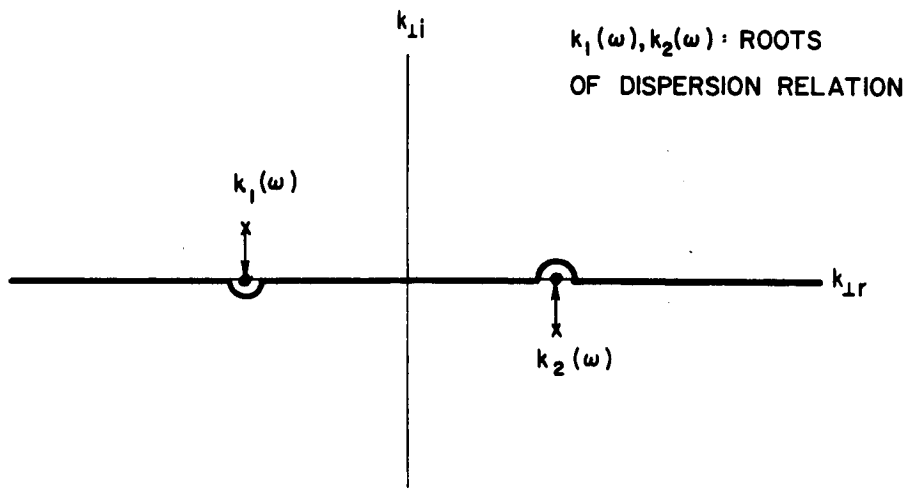

Fig. 19. DEFORMATION OF CONTOUR OF INTEGRATION WHEN ROOTS OF THE DISPERSION RELATION APPROACH REAL AXIS IN LIMIT AS $Im(\omega) \to 0$ FROM THE LOWER HALF COMPLEX PLANE.

then expand the function $k_\perp(\omega) = k_\perp(\omega_o + i\delta)$ in a Taylor series:

$$k_\perp(\omega_o + i\delta) \approx k_\perp(\omega_o) + i\delta \frac{\partial k_\perp(\omega_o)}{\partial \omega_o} . \tag{3.87}$$

Since $k_\perp(\omega_o)$ is real, dispersion curves with positive slope will approach the real $k_\perp$ axis from the lower half plane as $\delta \to 0$, and those with negative slope will approach the real axis from the upper half plane.

Based on the above discussion, Eq. (3.78) can be evaluated by the method of residues and put in the following form if $x > 0$:

$$E(x,t) = \sum_n E_n^o \exp\left\{i\left[\omega_o t - k_{\perp n}^o(\omega_o)x\right]\right\} + \sum_n E_n^- \exp\left\{i\left[\omega_o t - k_{\perp n}^-(\omega_o)x\right]\right\} , \tag{3.88}$$

where $k_{\perp n}^o$ and $k_{\perp n}^-$ are those roots of the dispersion relation with zero and negative imaginary parts, respectively, and where the amplitude of each wave is

$$E_n^{\underline{o}} = \left[\frac{g(k_\perp)}{i\epsilon_o k_\perp K(\omega,k_\perp)}\right]_{(\omega_o, k_{\perp n}^{\underline{o}})} . \tag{3.89}$$

The first sum in Eq. (3.88) includes only those real roots of the dispersion relation for which $(\partial k_\perp/\partial\omega) < 0$. If $x < 0$, only roots located above the deformed contour are included in the residue summation. It can be inferred from Eq. (3.88) that space charge oscillations propagating perpendicular to the magnetic field in a plasma with a steady state must attenuate in space if $k_\perp(\omega_o)$ is complex, while the amplitude of the oscillation is independent of the spatial coordinates if $k_\perp(\omega_o)$ is real.

In this section, computations are presented which show the complex solutions of the dispersion relation for $k_\perp$ as a function of real ω for a plasma having a Maxwellian electron velocity distribution. The

dispersion characteristics for this distribution were partially examined in Section B3 in which it was found that there are frequency bands where the wave number is real (see Fig. 10). However, in other frequency bands, the wave number is complex, corresponding to evanescent propagation, as shown in Fig. 20. The high damping rates indicated imply that, experimentally, detection of these waves will be difficult.

In practice, the degree of ionization of the plasma is often low, and hence even the unattenuated modes that are predicted in a collisionless Maxwellian plasma can suffer from damping as a result of electron-neutral collisions. To take this effect into account in the derivation

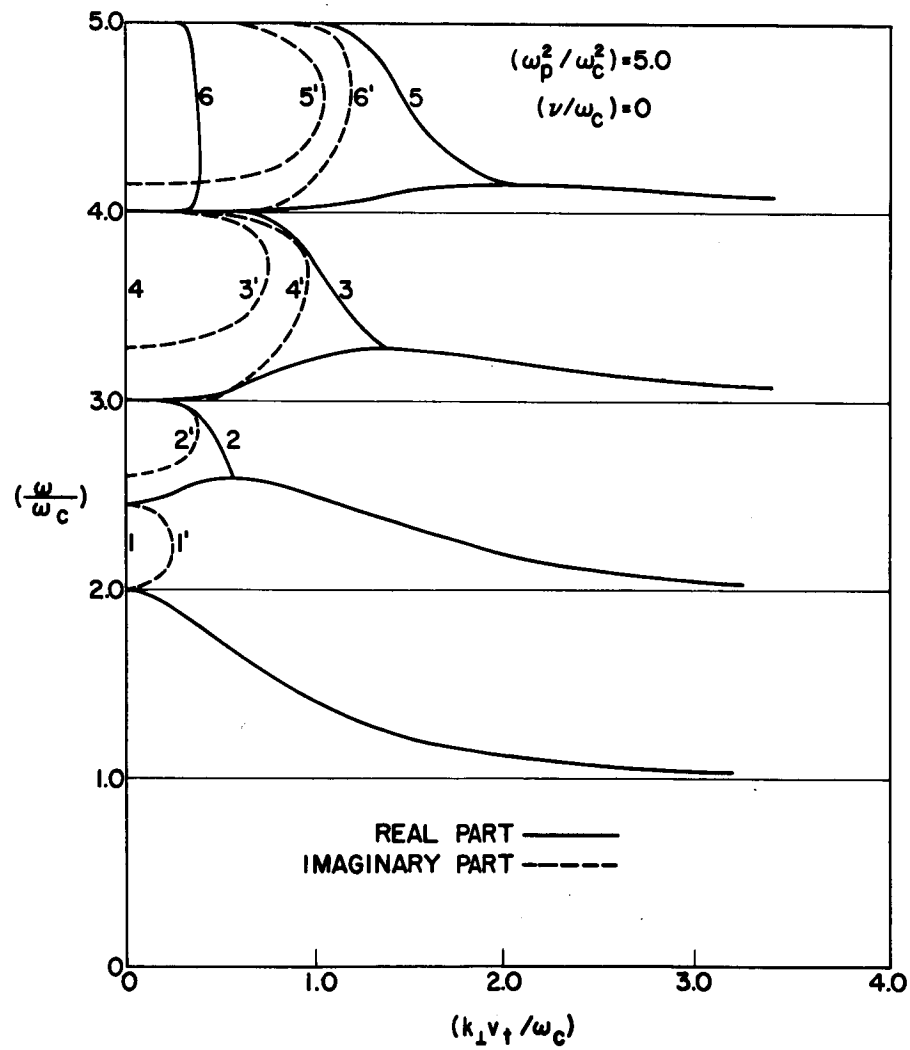

Fig. 20. DISPERSION CURVES FOR PERPENDICULARLY PROPAGATING CYCLOTRON HARMONIC WAVES IN A MAXWELLIAN PLASMA.

of the cyclotron harmonic wave dispersion relation, it is necessary to solve Boltzmann's equation,

$$\frac{\partial f}{\partial t} + \underset{\sim}{v} \cdot \nabla f + \frac{q}{m} (\underset{\sim}{E} + \underset{\sim}{v} \times \underset{\sim}{B}) \cdot \frac{\partial f}{\partial \underset{\sim}{v}} = \left(\frac{\partial f}{\partial t}\right)_c , \tag{3.90}$$

for the velocity distribution $f(\underset{\sim}{r},\underset{\sim}{v},t)$, instead of Vlasov's equation that was used in Chapter II. The right-hand side of Eq. (3.90) represents the rate of change of the velocity distribution due to collisions. A correct form of this term should conserve energy, momentum, and particles, but this leads to a complicated integrodifferential equation for f. A suitable approximate form of the collision term is that given by Bhatnagar, Gross, and Krook [36],

$$\left(\frac{\partial f}{\partial t}\right)_c = -\nu \left[f - \frac{n}{n_o} f_o \right] , \tag{3.91}$$

where $n(\equiv n_o \int d\underset{\sim}{v} f)$ is the particle density and ν is a velocity-independent phenomenological collision frequency. (Quantities with a subscript zero refer to the equilibrium state of the plasma.) This collision term conserves particles, allowing them to relax in position space to the local density rather than the unperturbed density, n_o. However, it has the defect that neither momentum nor energy is conserved, and consequently can be regarded as an approximation for collisions between electrons and heavy neutral particles.

The modifications in the theory of cyclotron harmonic wave propagation, when use is made of Eqs. (3.90) and (3.91), are given elsewhere [37]. It can be shown that the dispersion relation with collisions can be obtained correctly from that with no collisions by replacing ω_p^2 with $\omega_p^2[1 - i(\nu/\omega)]$ and replacing ω with $(\omega - i\nu)$. For perpendicular propation in a Maxwellian plasma, Eq. (3.63) is then replaced by

$$K(\omega,k_\perp) = 1 - \left(1 - i\frac{\nu}{\omega}\right)\frac{\omega_p^2}{\omega_c^2}\sum_{n=-\infty}^{\infty}\frac{\exp(-\lambda)\, I_n(\lambda)}{\lambda}\frac{n\omega_c}{\omega - i\nu - n\omega_c} = 0 \,. \tag{3.92}$$

Figure 21 shows the solutions for complex $k_\perp$ as a function of real ω and nonzero collision frequency. Eight independent modes of propagation are indicated. Modes 1, 2, 3, and 4 are present if $x > 0$, while modes 1', 2', 3', and 4' are excited if $x < 0$. It is pointed out that the imaginary part of $k_\perp$ for the primed modes is the negative of that for the unprimed modes. It will be observed that the spatial decay rate, $\mathrm{Im}(k_\perp)$, is increasingly heavy in the higher frequency bands and may easily be of the order of tens of decibels per wavelength for the value of (ν/ω_c) chosen. Similarly, heavy damping is indicated for all modes as $\omega \to n\omega_c$ and $\mathrm{Re}(k_\perp) \to \infty$. It should be noted that Fig. 21 does not show all modes. Indeed, since the dispersion relation is a transcendental function, one can always find an infinite number for a specified ω. Only those modes with the smallest damping rate are indicated in that figure.

E. Discussion

In this chapter the dispersion relation for perpendicularly propagating cyclotron harmonic waves has been solved numerically for several electron velocity distributions that are of current interest in plasma physics. Criteria for the existence of instabilities have been derived, and the results show that the necessary conditions are (i) $(\partial f_o/\partial v_\perp) > 0$ for some $v_\perp > 0$, and (ii) $(\omega_p^2/\omega_c^2) > \varkappa$, where $\varkappa$ is a critical number that is obtained from the numerical solution of the dispersion relation. An analysis of the instabilities has shown them to be absolute. The effects of electron-neutral collisions in a plasma with a Maxwellian electron velocity distribution have also been considered. The results show heavy damping for frequencies near the harmonics of the electron cyclotron frequency. In addition, the damping becomes progressively heavy in the higher frequency bands, suggesting that it would be difficult to observe these modes experimentally.

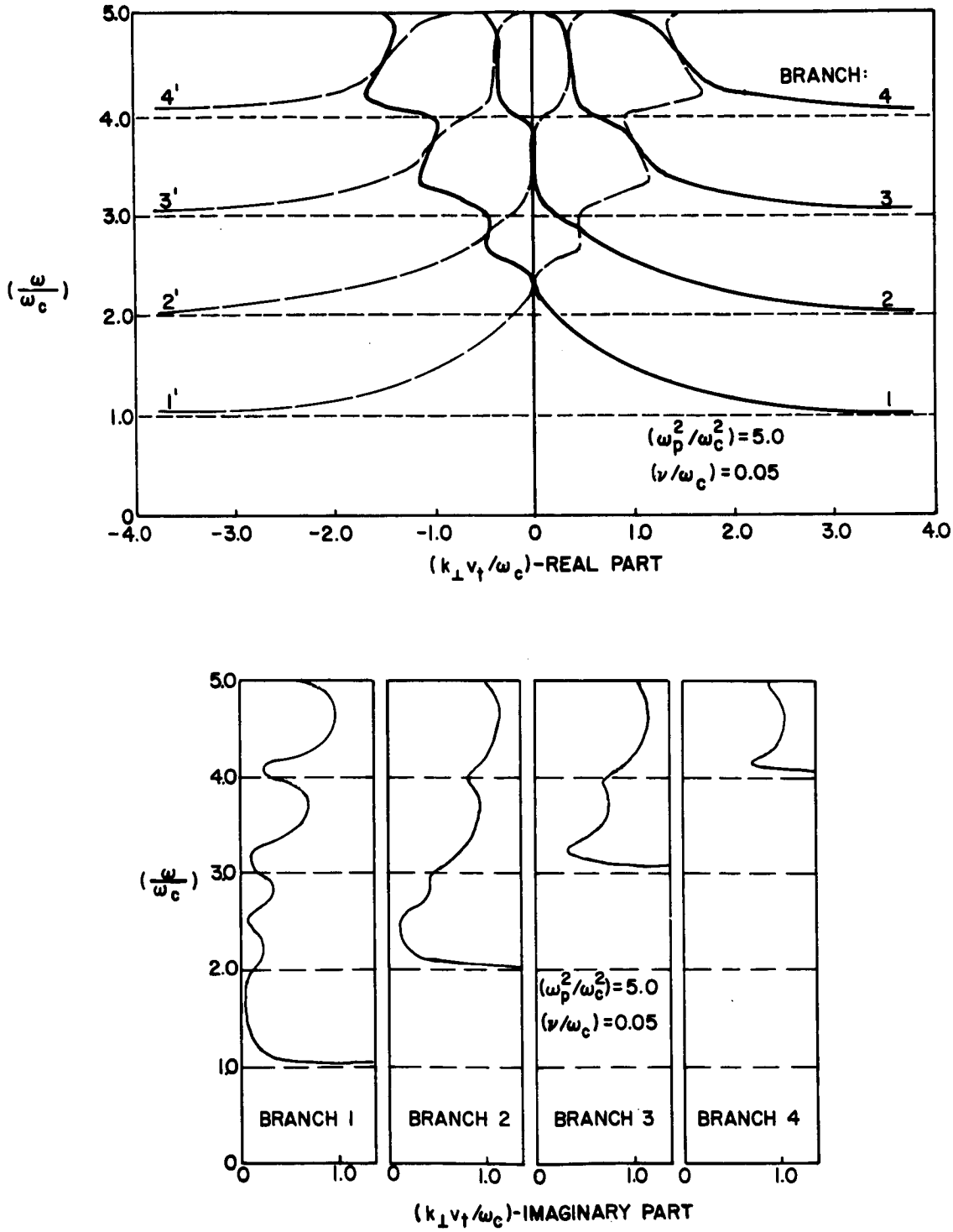

Fig. 21. DISPERSION CURVES FOR PERPENDICULAR PROPAGATION IN A MAXWELLIAN PLASMA, WITH COLLISIONS.

Up to this point, no mention has been made of the experiments on cyclotron harmonic wave excitation and detection. Unfortunately, only limited work has been done in this area. The most conclusive results come from the experiments of Mantei [20], Harp [38], and Crawford [39]. Figure 22 shows some of the data obtained by Mantei, and excellent agreement is observed between theory and experiment. Because of the nature of the experiment, it was convenient to hold (ω_p^2/ω^2) constant along each curve rather than (ω_p^2/ω_c^2). Experiments with unstable distributions are almost nonexistent. Anastassiades and Marshall [40] appear to have obtained some data that agree with the theoretical dispersion diagram of the ~~cylindrical shell~~ ring dispersion relation, but no conclusive observation of the predicted instabilities can be found in the literature.

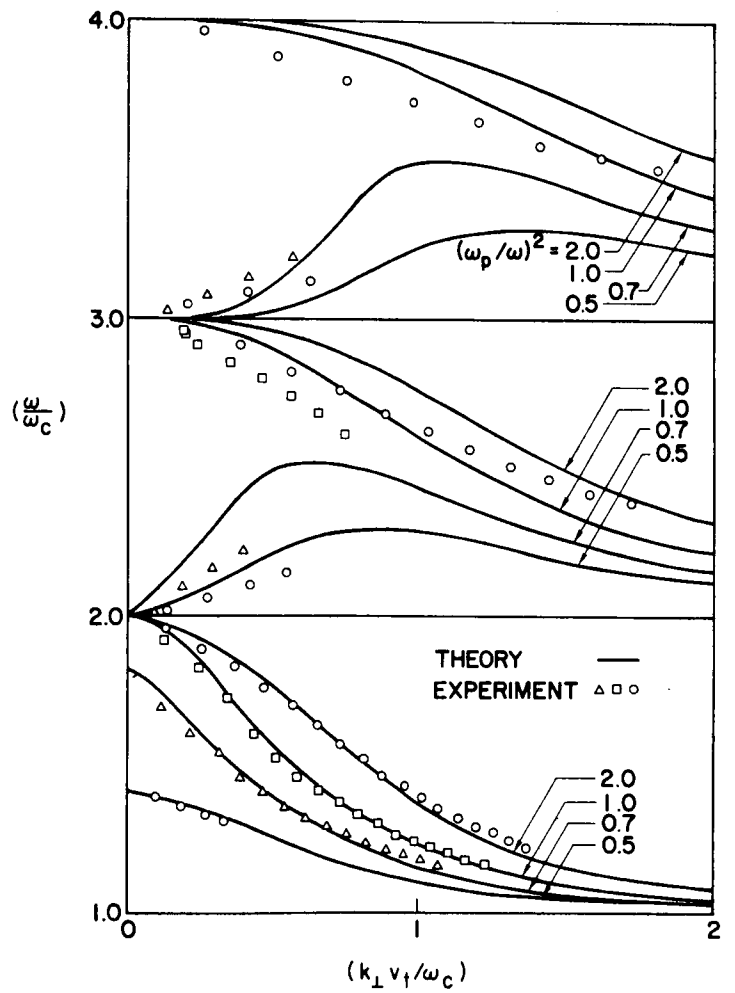

Fig. 22. EXPERIMENTAL CONFIRMATION OF CYCLOTRON HARMONIC WAVE PROPAGATION IN A MAXWELLIAN PLASMA. (From Mantei [20].)

IV. OBLIQUE PROPAGATION OF CYCLOTRON HARMONIC WAVES

The dispersion characteristics of cyclotron harmonic waves propagating oblique to the magnetic field are examined in this chapter. Specific electron velocity distributions are considered which clearly show how and at what frequencies instabilities set in. Furthermore, it is shown that electron velocity distributions which are stable for perpendicular propagation can be unstable if the propagation occurs oblique to the magnetic field. Instabilities of this type are essentially those investigated by Harris [4], [5] and are found in magnetoplasmas when the transverse energy of the gyrating charged particles greatly exceeds the longitudinal energy. An important finding of this chapter is that the threshold conditions for instability in oblique propagation are much less stringent than those of perpendicular propagation.

The dispersion relation is solved in Section A for a class of velocity distributions describing a plasma with no electron motion parallel to the magnetic field. As in Chapter III, the motion of the ions is ignored. Section B treats the more general situation where a spread exists in $v_{\parallel}$, the component of the electron velocity along the magnetic field. An approximate expression for the imaginary part of the frequency is derived in Section C for the case in which the propagation is close to an angle of $(\pi/2)$ to the magnetic field. This formula is then compared with the exact numerical solution of the dispersion relation for the case of an isotropic Maxwellian velocity distribution. In Section D the instabilities are classified as either absolute or convective, and the chapter ends in Section F with a discussion of the results.

A. Plasma with No Electron Motion Parallel to the Magnetic Field

The dispersion relation for cyclotron harmonic waves propagating at an arbitrary angle to the magnetic field is given by Eq. (2.68). As demonstrated in Chapter II, that expression takes on a characteristically different form if all charged particles of a given species, α, move parallel to the magnetic field with the same speed, $v_{\parallel o}$. The velocity distribution

in this situation can then be written as

$$f_o(v_\perp, v_{||}) = f_\perp(v_\perp)\, \delta(v_{||} - v_{o||}) \ , \tag{4.1}$$

leading to the dispersion relation given by Eq. (2.77) and repeated here for convenience:

$$K(\omega, \underset{\sim}{k}) = 1 - \frac{\omega_p^2}{\omega_c^2} \sum_\alpha \left[\frac{k_\perp^2}{k^2} \sum_{n=-\infty}^{\infty} p_n \frac{n\omega_c}{\omega - v_{o||} k_{||} - n\omega_c} \right.$$

$$\left. + \frac{k_{||}^2}{k^2} \sum_{n=-\infty}^{\infty} q_n \frac{\omega_c^2}{(\omega - v_{o||} k_{||} - n\omega_c)^2} \right]$$

$$= 0 \ , \tag{4.2}$$

where the coefficients p_n and q_n are defined as follows:

$$p_n = -2\pi \frac{\omega_c^2}{k_\perp^2} \int_0^\infty dv_\perp \frac{df_\perp(v_\perp)}{dv_\perp} J_n^2\left(\frac{k_\perp v_\perp}{\omega_c}\right) \ , \tag{4.3a}$$

$$q_n = 2\pi \int_0^\infty dv_\perp \, f_\perp(v_\perp) \, J_n^2\left(\frac{k_\perp v_\perp}{\omega_c}\right) v_\perp \ . \tag{4.3b}$$

It is clear from Eq. (4.2) that if the wave vector $\underset{\sim}{k}$ is real, the frequency $\omega(\underset{\sim}{k})$ must either be real or occur in complex conjugate pairs.

In this section Eq. (4.2) is solved for the frequency, and the threshold conditions for instability are calculated. For convenience in notation, $v_{o||}$, the drift speed of the charged particles parallel to the magnetic field, is set equal to zero. This introduces little loss in generality since the frequency of plasma oscillations when $v_{o||}$ is nonzero can be recovered by a simple doppler shift, whereby ω is replaced

with $(\omega - v_{o\parallel} k_{\parallel})$. Clearly, this frequency change does not affect the growth rate of any instability if $k_{\parallel}$ is real since the quantity $v_{o\parallel} k_{\parallel}$ is also real. In order to gain some insight into the form of the dispersion characteristics predicted by Eq. (4.2), a specific electron velocity distribution is considered first, namely, the ring distribution that was introduced in Chapter III. The motion of the ions will be neglected in this study due to the relatively large mass of these particles. The ring distribution is followed by a treatment of the more general situation where a distribution exists in the transverse energy of the gyrating electrons.

1. Ring Distribution

The ring distribution describes a plasma where all electrons are confined to the plane perpendicular to the magnetic field and rotate with the same speed, $v_{o\perp}$, at the cyclotron frequency. In terms of a delta function, we can then write

$$f_{\perp}(v_{\perp}) = \frac{\delta(v_{\perp} - v_{o\perp})}{2\pi v_{o\perp}} . \tag{4.4}$$

Substituting this expression in Eq. (4.3), integrating with respect to $v_{\perp}$, and combining the results with Eq. (4.2) yields the dispersion relation

$$K(\omega,\underset{\sim}{k}) = 1 - \frac{\omega_p^2}{\omega_c^2}\left[\frac{k_{\perp}^2}{k^2}\sum_{n=-\infty}^{\infty}\frac{1}{\mu_{\perp}}\frac{dJ_n^2(\mu_{\perp})}{d\mu_{\perp}}\frac{n\omega_c}{\omega - n\omega_c}\right.$$

$$\left. + \frac{k_{\parallel}^2}{k^2}\sum_{n=-\infty}^{\infty} J_n^2(\mu_{\perp})\frac{\omega_c^2}{(\omega - n\omega_c)^2}\right]$$

$$= 0 , \tag{4.5}$$

where $v_{o\parallel}$ has been set equal to zero and $\mu_\perp$ has been written for $(k_\perp v_{o\perp}/\omega_c)$. Since ion motion is neglected, the summation over particle species α is not required, and the quantities ω_p, ω_c, and $v_{o\perp}$ refer to the electrons. Note that if $k_\parallel$ is identically equal to zero, we retrieve Eq. (3.37a), the dispersion relation for perpendicular propagation.

Since the dielectric constant in the direction oblique to the magnetic field is a function of three variables, namely, ω, $k_\perp$, and $k_\parallel$, a second condition must be specified before the propagation is uniquely determined. In this section two examples of plasma wave propagation are examined. In the first example the component of the wave vector perpendicular to the magnetic field is a constant number, and the dispersion relation is solved for $\omega(k_\parallel)$. This situation corresponds to propagation parallel to the magnetic field in a bounded plasma. In the second example the angle of propagation $\theta = \tan^{-1}(k_\perp/k_\parallel)$, as defined in Fig. 3, is constant, and the dispersion relation

$$K(\omega,\underset{\sim}{k}) = 1 - \frac{\omega_p^2}{\omega_c^2}\left[\sin^2\theta \sum_{n=-\infty}^{\infty} \frac{1}{\mu_\perp}\frac{\partial J_n^2(\mu_\perp)}{\partial \mu_\perp}\frac{n\omega_c}{\omega - n\omega_c}\right.$$

$$\left. + \cos^2\theta \sum_{n=-\infty}^{\infty} J_n^2(\mu_\perp)\frac{\omega_c^2}{(\omega - n\omega_c)^2}\right]$$

$$= 0 \quad , \tag{4.6}$$

is solved for $\omega(k)$, where $k = |\underset{\sim}{k}|$. This describes plane wave propagation in an infinite plasma at a fixed angle θ to the magnetic field. Each example will now be considered separately.

a. Bounded Geometry

To solve the dispersion relation in this geometry it is convenient to use the relation, $k^2 = k_\perp^2 + k_\parallel^2$, and rewrite Eq. (4.5) in the form

$$k_{\parallel}^2 = -k_{\perp}^2 \frac{1 - \frac{\omega_p^2}{\omega_c^2} \sum_{n=-\infty}^{\infty} \frac{1}{\mu_{\perp}} \frac{\partial J_n^2(\mu_{\perp})}{\partial \mu_{\perp}} \frac{n\omega_c}{\omega - n\omega_c}}{1 - \frac{\omega_p^2}{\omega_c^2} \sum_{n=-\infty}^{\infty} J_n^2(\mu_{\perp}) \frac{\omega_c^2}{(\omega - n\omega_c)^2}} , \tag{4.7}$$

which explicitly shows the dependency of the wave number $k_{\parallel}$ on both the frequency and the constant $k_{\perp}$. This representation of the dispersion relation has a distinct advantage in that the cutoff $(k_{\parallel} = 0)$ and resonant $(k_{\parallel} = \infty)$ frequencies are immediately identifiable. The wave number vanishes first when the numerator is zero, and the denominator nonzero, giving the expression

$$1 - \frac{\omega_p^2}{\omega_c^2} \sum_{n=-\infty}^{\infty} \frac{1}{\mu_{\perp}} \frac{\partial J_n^2(\mu_{\perp})}{\partial \mu_{\perp}} \frac{n\omega_c}{\omega - n\omega_c} = 0 . \tag{4.8}$$

This equation was solved in Chapter III, and the results can be summarized in the following manner: If (ω_p^2/ω_c^2) is small, the cutoff frequency is accurately given by

$$\omega(\mu_{\perp}) = n\omega_c \left[1 - \frac{\omega_p^2}{\omega_c^2} \frac{1}{\mu_{\perp}} \frac{\partial J_n^2(\mu_{\perp})}{\partial \mu_{\perp}} \right] . \tag{4.9}$$

As (ω_p^2/ω_c^2) increases, the detailed behavior of the solution of Eq. (4.8) can only be obtained numerically. The salient features of these solutions are illustrated in Fig. 23 with (ω_p^2/ω_c^2) equal to 5 and 20. It is seen that the roots of Eq. (4.8) may be complex in certain ranges of $\mu_{\perp}$ for (ω_p^2/ω_c^2) sufficiently large. The real part of the frequency is shown as a fine solid line, and the imaginary as a fine dashed line. Since all complex solutions must occur in conjugate pairs if $\mu_{\perp}$ is real, we conclude that long-wavelength space-charge oscillations may grow with time. The threshold conditions for these instabilities are found in Table 1.

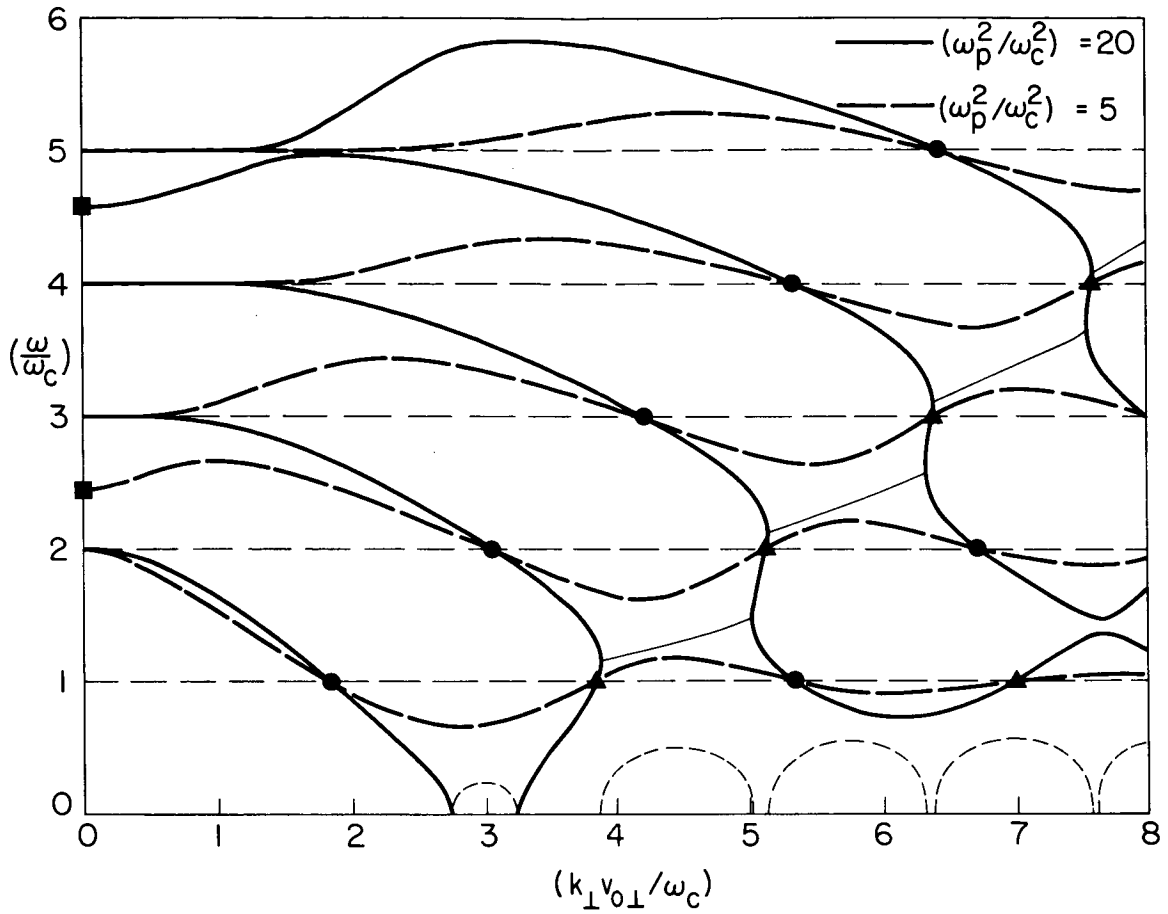

Fig. 23. CUTOFF FREQUENCIES FOR OBLIQUELY PROPAGATING CYCLOTRON HARMONIC WAVES WITH $k_\perp$ CONSTANT; RING DISTRIBUTION FOR $(\omega_p^2/\omega_c^2) = 5, 20$.

A second class of cutoffs can be predicted with Eq. (4.7). These are obtained by assuming $\omega \approx n\omega_c$ and approximating that equation with the expression

$$\frac{k_\parallel^2}{k_\perp^2} = -\frac{2n^2 J_n'(\mu_\perp)}{\mu_\perp J_n(\mu_\perp)}\left(\frac{\omega - n\omega_c}{n\omega_c}\right) , \qquad (4.10)$$

where $J_n'(\mu_\perp)$ is the first derivative of $J_n(\mu_\perp)$. Clearly, $k_\parallel \to 0$ as $\omega \to n\omega_c$, implying that a cutoff is found at each harmonic of the electron cyclotron frequency.

A resonance $(k_{\parallel} = \infty)$ occurs when the demoninator of Eq. (4.7) vanishes, yielding the expression

$$1 - \frac{\omega_p^2}{\omega_c^2} \sum_{n=-\infty}^{\infty} J_n^2(\mu_\perp) \frac{\omega_c^2}{(\omega - n\omega_c)^2} = 0 \ . \qquad (4.11)$$

If (ω_p^2/ω_c^2) is small, we look for solutions near the n^{th} harmonic, where Eq. (4.11) has the approximate form

$$1 - \frac{\omega_p^2}{\omega_c^2} J_n^2(\mu_\perp) \frac{\omega_c^2}{(\omega - n\omega_c)^2} = 0 \ . \qquad (4.12)$$

Solving for the frequency yields the expression

$$\omega = n\omega_c \left[1 \pm \left(\frac{\omega_p}{\omega_c} \right) \frac{J_n(\mu_\perp)}{n} \right] \ . \qquad (4.13)$$

This result indicates that two branches undulate about the n^{th} harmonic, passing through the points defined by $(\omega = n\omega_c, \ \mu_\perp = \alpha_{nm})$, where α_{nm} is the m^{th} zero of the n^{th}-order Bessel function. Figure 24a shows the form of the branches near the second and third harmonic when $(\omega_p^2/\omega_c^2) = 0.25$. As (ω_p^2/ω_c^2) increases, a down-going and an up-going loop approach each other and eventually couple to form a gap where complex frequencies occur in conjugate pairs, one corresponding to growth and another to collisionless damping. This is clearly illustrated in Fig. 24b for (ω_p^2/ω_c^2) equal to 1. For convenience, the positive imaginary part of (ω/ω_c) has been plotted using the line, $(\omega/\omega_c) = n$, as a base, but the scale is identical to that of the real part. It has been found that for all cases considered, coupling occurs in the ranges $\alpha_{nm} < \mu_\perp < \alpha_{(n+1),m}$ and $\alpha_{(n+1),m} < \mu_\perp < \alpha_{n,(m+1)}$, assuming that the parameter (ω_p^2/ω_c^2) is sufficiently large. Some critical values of (ω_p^2/ω_c^2) are given in Table 3 for the first three frequency bands. By comparing this numerical criterion with that of Table 1, the onset conditions for complex cutoff

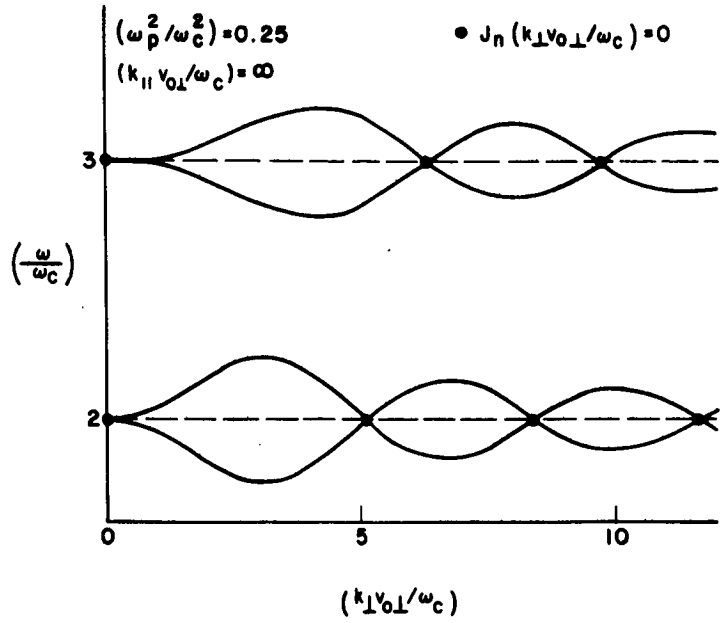

(a)

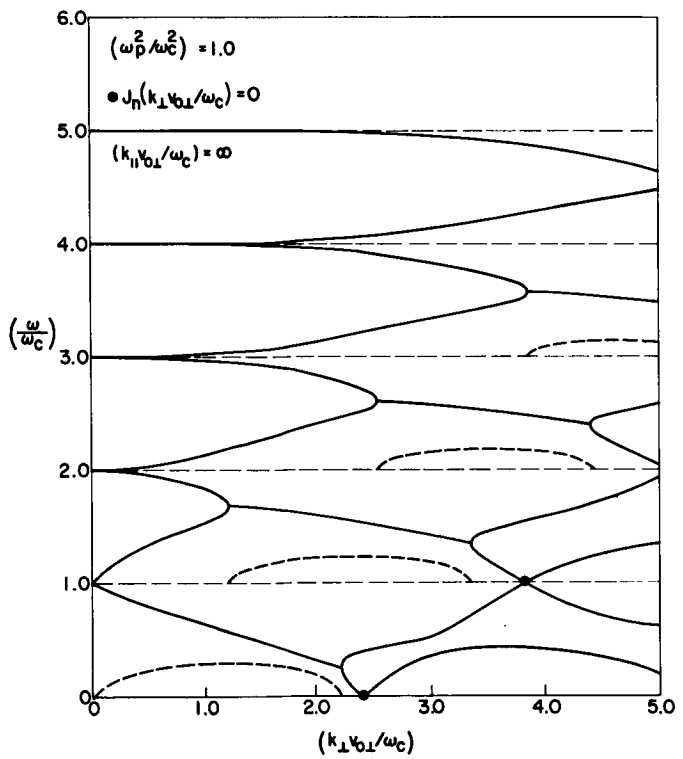

(b)

Fig. 24. RESONANT FREQUENCIES FOR OBLIQUELY PROPAGATING CYCLOTRON HARMONIC WAVES WITH $k_\perp$ CONSTANT; RING DISTRIBUTION FOR (a) $(\omega_p^2/\omega_c^2) = 0.25$, AND (b) $(\omega_p^2/\omega_c^2) = 1$.

Table 3

THRESHOLD CONDITIONS FOR ZERO-WAVELENGTH INSTABILITIES

Frequency Band	Range of $\mu_\perp$	Critical Value of (ω_p^2/ω_c^2) for Onset of Instability
$0 < \omega < \omega_c$	0 - 2.40	0.34
	2.40 - 3.83	1.07
	3.83 - 5.52	1.38
$\omega_c < \omega_c < 2\omega_c$	0 - 3.83	0.53
	3.83 - 5.14	1.70
	5.14 - 7.02	1.62
$2\omega_c < \omega < 3\omega_c$	0 - 5.14	0.66
	5.14 - 6.38	2.29
	6.38 - 8.42	1.82

frequencies, it is clear that space-charge oscillations with short wavelengths parallel to the applied magnetic field are, by far, more susceptible to instability than oscillations with long wavelengths. However, it should be pointed out that, in practice, there is a spread in the electron velocity components parallel to the magnetic field. This may wipe out the short-wavelength instabilities and hence modify the relatively weak threshold conditions for instability due to oblique propagation.

Next, we consider the case where $k_\parallel$ is finite and non-zero. Three distinct values of $\mu_\perp$ have been chosen to indicate the characteristic behavior of propagation in a bounded plasma. The first ($\mu_\perp = 1.0$) is in a region where no growth can occur when $k_\parallel = 0$ as seen in Fig. 33. The second ($\mu_\perp = 3.0$) is in a region in which the only instability that can occur is that at zero frequency. The third ($\mu_\perp = 4.5$) is in the region where loops from $n = 1$ and $n = 2$ may

couple $[(\omega_p^2/\omega_c^2) > 6.81]$. We shall examine the effect on the dispersion curves $[(\omega/\omega_c)/(k_{||} v_{o\perp}/\omega_c)]$ as (ω_p^2/ω_c^2) is varied.

Case 1 $(\mu_\perp = 1.0)$. The results are shown in Fig. 25. For low values of (ω_p^2/ω_c^2) the dispersion curves show no instabilities. Each passband $n = 1, 2, \ldots$ has a slow and a fast space-charge wave associated with it, the frequency spread about $n\omega_c$ decreasing rapidly with increasing n.

As (ω_p^2/ω_c^2) increases, the plasma branch (n = 0 mode) couples to the slow space-charge wave of the n = 1 mode and instability occurs as indicated in Fig. 25b for $(\omega_p^2/\omega_c^2) = 1$, and in Fig. 25c-g for higher values of (ω_p^2/ω_c^2). This instability first occurs for propagation at about 45° to the magnetic field, and the imaginary part (ω_i/ω_c) increases asymptotically to about 0.3. In assessing the strength of the instabilities it is worth remembering that $(\omega_i/\omega_c) = 1$ represents a growth rate of 55 dB per cyclotron period $(= 2\pi/\omega_c)$.

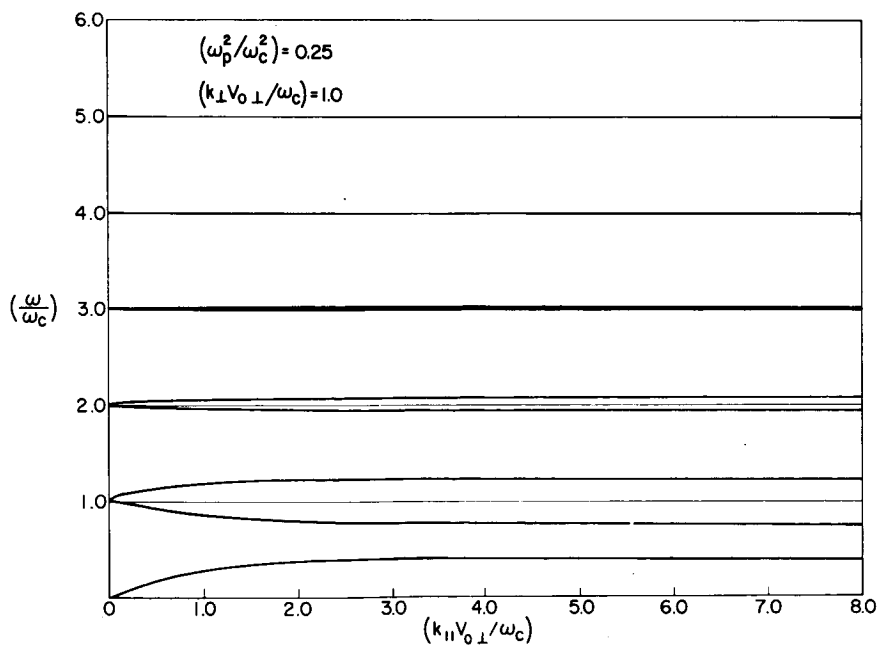

(a)

Fig. 25. DISPERSION CHARACTERISTICS OF OBLIQUELY PROPAGATING CYCLOTRON HARMONIC WAVES; RING DISTRIBUTION FOR $\mu_\perp = 1.0$ AND $(\omega_p^2/\omega_c^2) = 0.25$, 1.0, 3.0, 5.0, 8.0, 20.0, ∞.

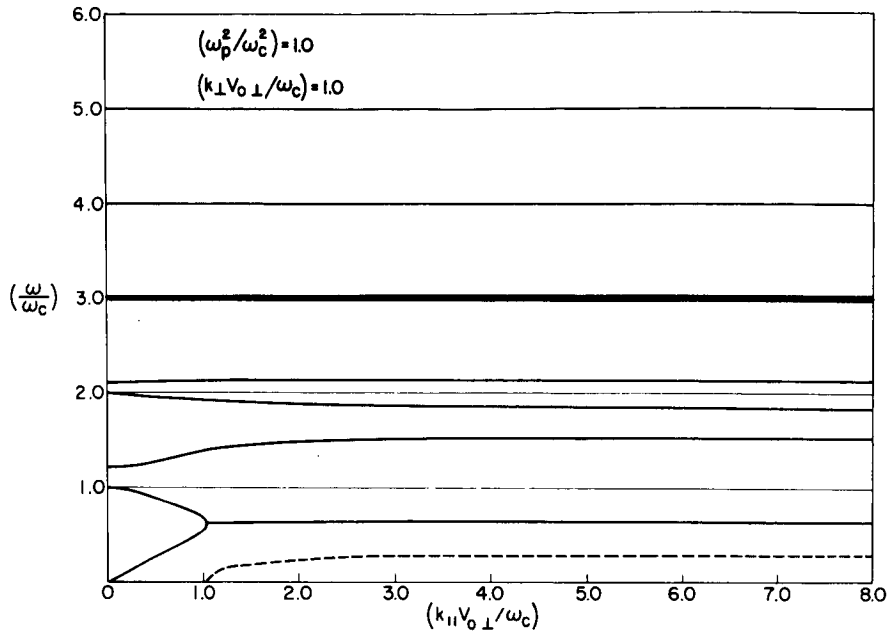

(b)

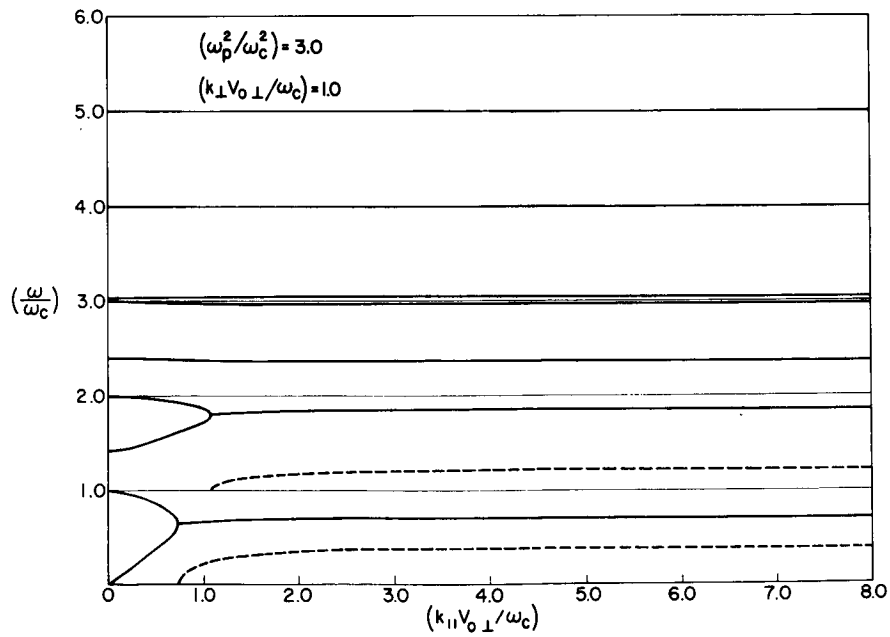

(c)

Fig. 25. CONTINUED.

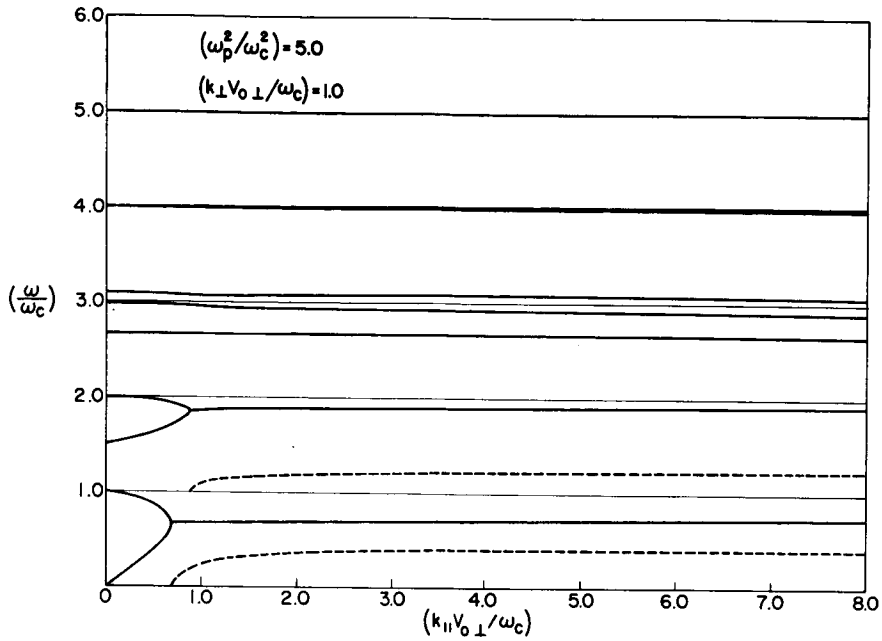

(d)

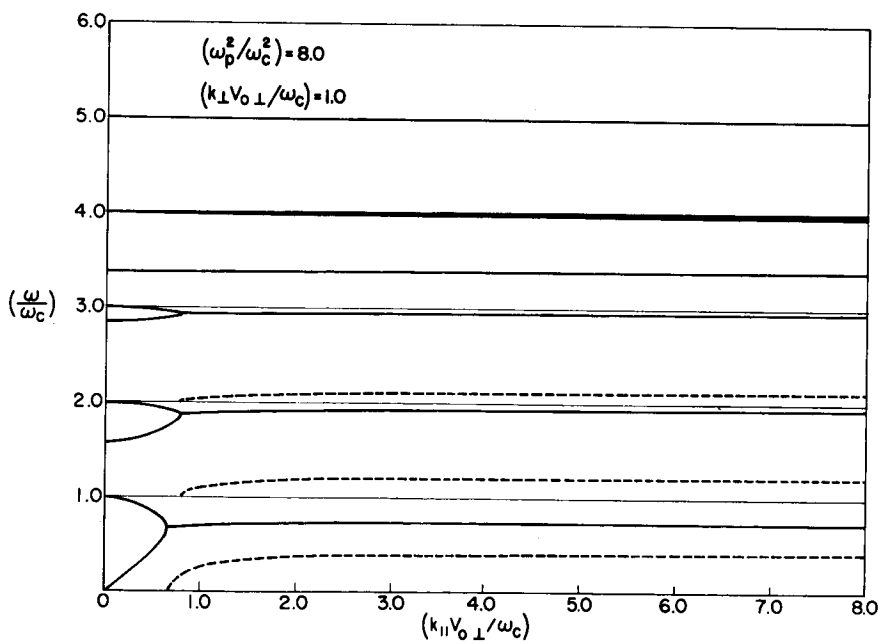

(e)

Fig. 25. CONTINUED.

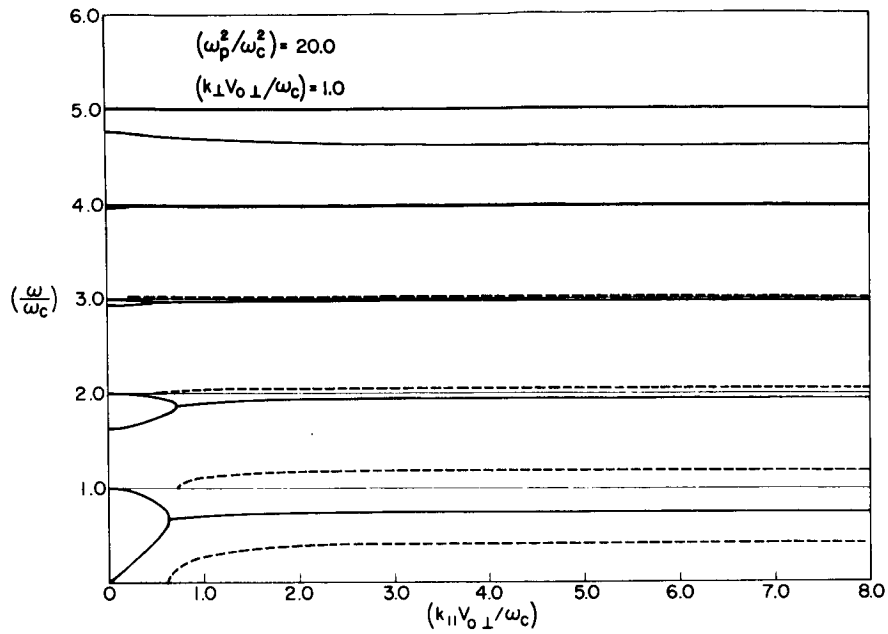

(f)

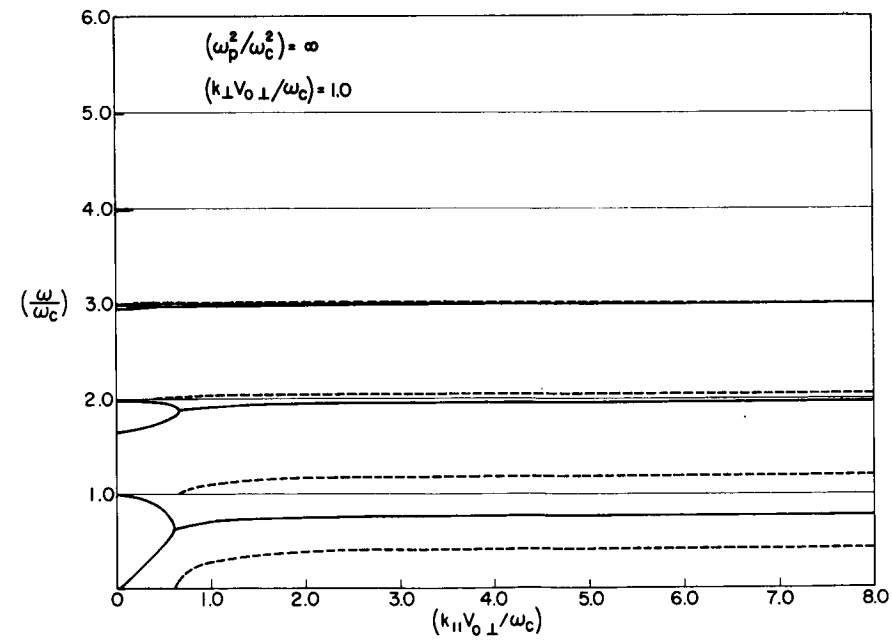

(g)

Fig. 25. CONTINUED.

It will be noted from Fig. 25b that the upward progress of the upper hybrid frequency with increasing (ω_p^2/ω_c^2) has the effect of raising the fast space-charge wave of the $n = 1$ mode toward the slow space-charge wave associated with the $n = 2$ mode. These ultimately couple and give rise to a new absolute instability in the range $1 < (\omega/\omega_c) < 2$. This is clearly indicated in Fig. 25c for $(\omega_p^2/\omega_c^2) = 3$. For convenience, the imaginary part of (ω/ω_c) is shown dashed using $(\omega/\omega_c) = 1$ as zero line and its scale is identical to that of the real part. It will be noted that again real propagation is possible only for angles greater than $(\pi/4)$ to the magnetic field and that the growth rate is not much smaller than that in the $0 < (\omega/\omega_c) < 1$ frequency band. For the case of Fig. 25c the asymptotic growth rates are approximately 0.2 and 0.4.

Figure 25d for $(\omega_p^2/\omega_c^2) = 5$ indicates the increasing angular range over which absolutely unstable propagation occurs and also that the growth rates increase steadily. It will be observed that the location of the upper hybrid resonance, now located in the band $2 < (\omega/\omega_c) < 3$, has the effect of carrying the fast space-charge wave of the $n = 2$ passband toward the slow space-charge wave of the $n = 3$ passband. The coupling of these modes is indicated in Fig. 25e for $(\omega_p^2/\omega_c^2) = 8$.

Figures 25f and 25g for $(\omega_p^2/\omega_c^2) = 20$ and ∞ indicate that there is very little essential difference in behavior as (ω_p^2/ω_c^2) increases to large values. Successive passbands become unstable roughly for $(\omega_p^2 + \omega_c^2) > (n\omega_c)^2$, but the growth rates are small except in the first few passbands even as $(\omega_p^2/\omega_c^2) \to \infty$. The asymptotic limits in the first three passbands are approximately $(\omega_i/\omega_c) = 0.6, 0.2, 0.1$.

Case 2 $(\mu_\perp = 3)$. These results are shown in Fig. 26. For $(\omega_p^2/\omega_c^2) = 0.25$, curves similar to those of Fig. 25a are obtained except that the frequency spreads about $\omega = n\omega_c$ in the passbands for which $n > 1$ are appreciably greater. This reflects the periodic behavior of the loops in the various passbands indicated in Fig. 23.

As (ω_p^2/ω_c^2) increases, instability occurs first not in the lowest passband, as for $\mu = 1$, but in the second and third passbands at propagation angles of about $(\pi/6)$ to the magnetic field. This is indicated in Fig. 26b. A further increase to $(\omega_p^2/\omega_c^2) = 3$ (Fig. 26c) introduces

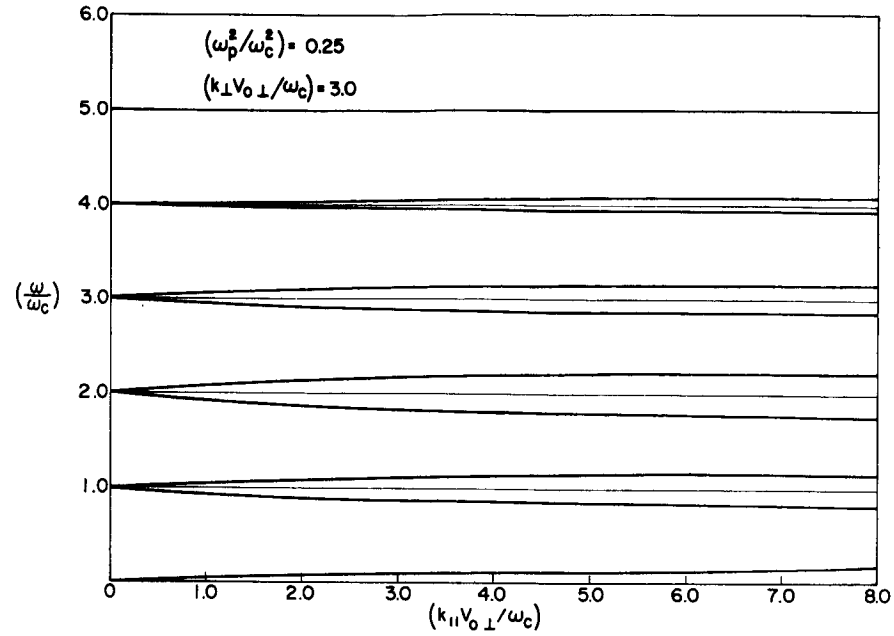

(a)

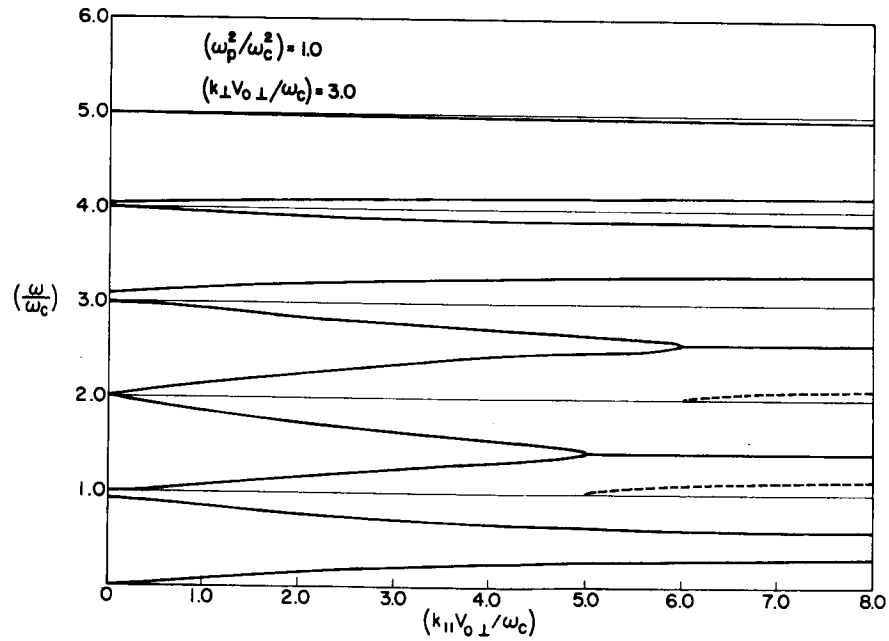

(b)

Fig. 26. DISPERSION CHARACTERISTICS OF OBLIQUELY PROPAGATING CYCLOTRON HARMONIC WAVES; RING DISTRIBUTION FOR $\mu_\perp = 3.0$ AND $(\omega_p^2/\omega_c^2) = 0.25$, 1.0, 3.0, 5.0, 8.0, 20.0, ∞.

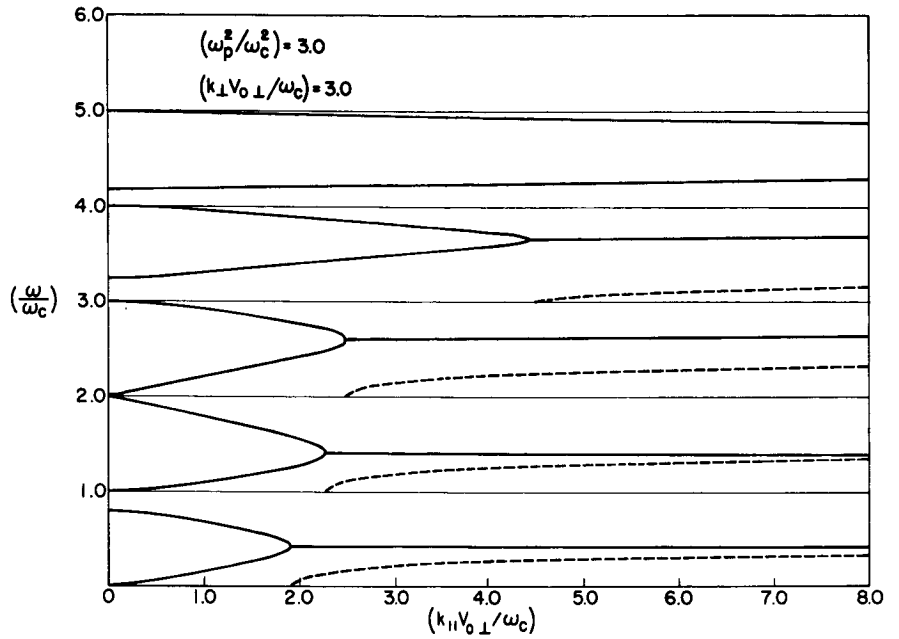

(c)

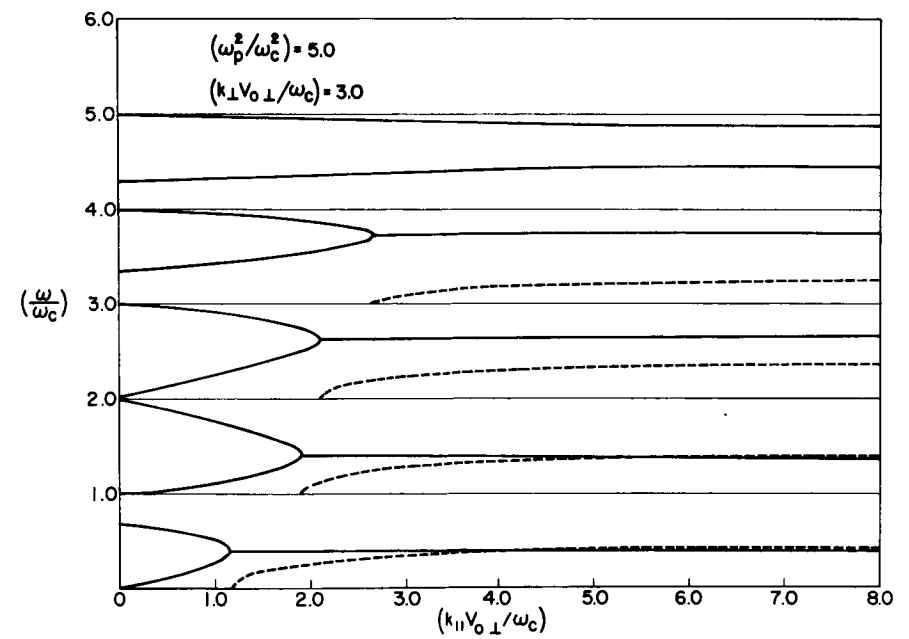

(d)

Fig. 26. CONTINUED.

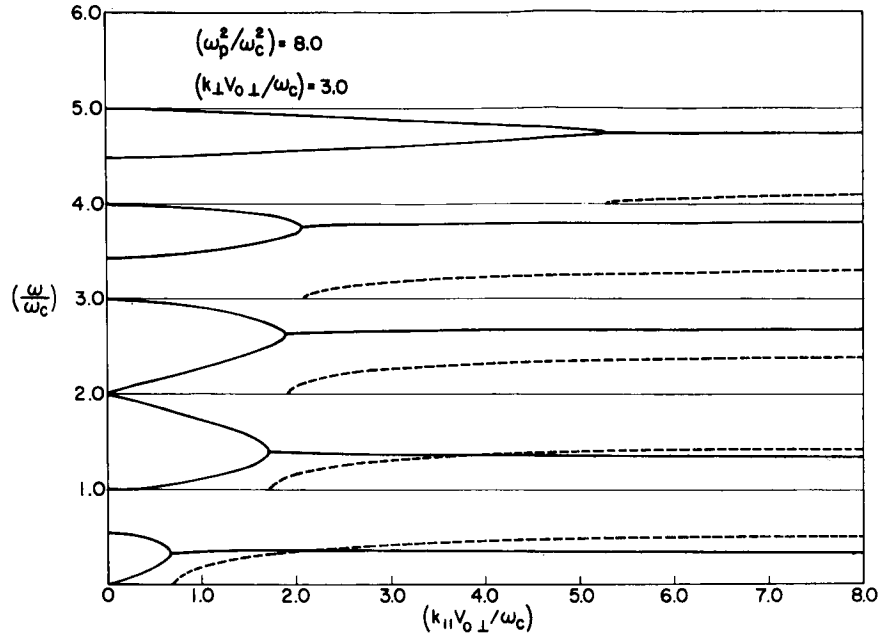

(e)

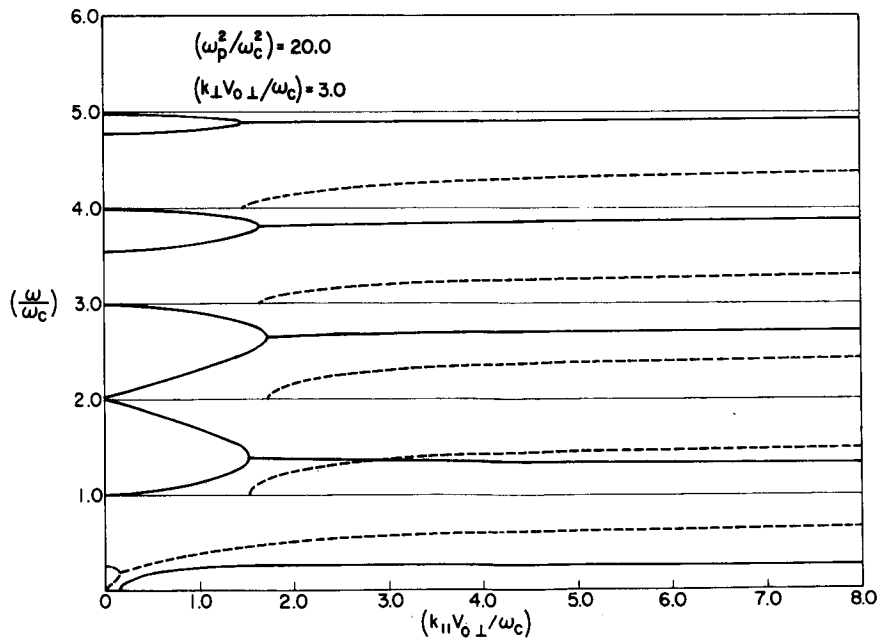

(f)

Fig. 26. CONTINUED.

absolute instability into two further passbands. The curves should be compared with those of Fig. 25c. Although the growth is slightly less for $\mu_\perp = 3$ than for $\mu_\perp = 1$ in the first passband, the instabilities in the second and higher passbands are more serious. By the time $(\omega_p^2/\omega_c^2) = 5$, the growth rate even in the first passband is higher for the $\mu = 3$ case. Further increases confirm these basic trends. Comparison of Figs. 25e-g and 26e-g indicates wider ranges of instability and higher growth rates for $\mu_\perp = 3$.

Above $(\omega_p^2/\omega_c^2) = 17.02$ we expect new phenomena to show in the dispersion curves due to the zero frequency instability mentioned earlier. This is indicated in Fig. 26f,g. At very small values of $k_\parallel$, two pairs of complex roots are found. As $k_\parallel$ increases, one pair disappears and a complex root with very rapid growth rate remains. Increasing (ω_p^2/ω_c^2) flattens the real branch to zero leaving purely imaginary solutions for all values of $k_\parallel$.

Case 3 $(\mu_\perp = 4.5)$. The results for this case are shown in Fig. 27. It is interesting to compare the results of Figs. 26a and 27a for $(\omega_p^2/\omega_c^2) = 0.25$. It will be seen that the frequency spread in the various passbands is in some cases larger for $\mu_\perp = 4.5$ and in others smaller. This depends, of course, on the heights of the loops in the various passbands for $k_\parallel = 0$. Continuing the comparison, we note that whereas Fig. 26b shows instability at $(\omega_p^2/\omega_c^2) = 1$, no such instability is indicated in Fig. 27b. For $(\omega_p^2/\omega_c^2) = 3$ or 5, the situation is rather different. The wider range of instabilities is then exhibited for $\mu_\perp = 4.5$, though the growth rates in some passbands are lower than for $\mu_\perp = 3.0$.

At $(\omega_p^2/\omega_c^2) = 6.81$, coupling between the $n = 2$ and $n = 1$ modes occurs for $k_\parallel = 0$. This is reflected in the curves of Fig. 27e, where absolute instability is indicated in the second passband for all values of $k_\parallel$. It will be noted that this particular instability has the highest growth rate of all the passbands over the entire range $0 < k_\parallel < \infty$. This becomes even more marked at very high values of (ω_p^2/ω_c^2) as is shown by Fig. 27f,g.

It will be remarked that the real frequency component in the second passband drops to almost exactly $(\omega_r/\omega_c) = 1$ for $k_\parallel = 0$. For other

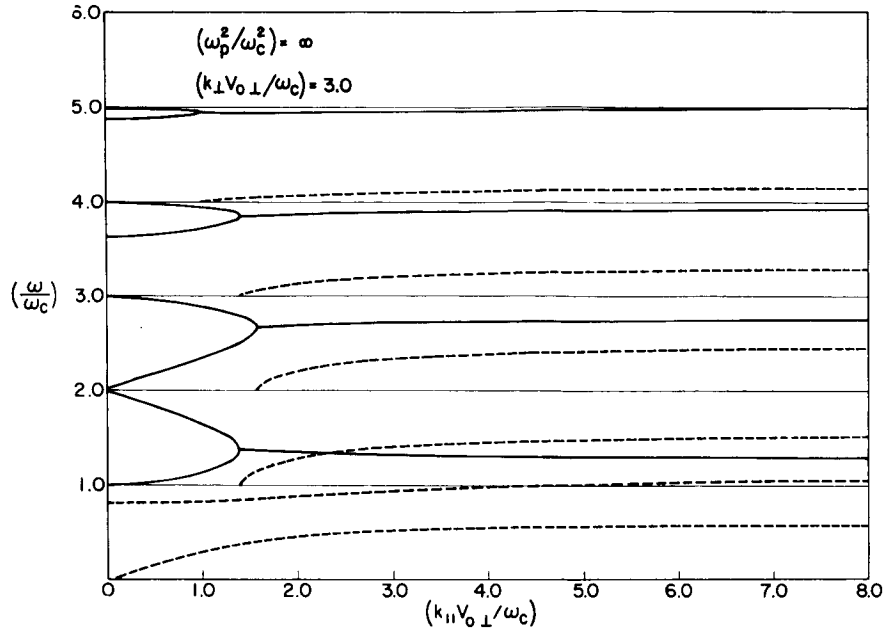

(g)

Fig. 26. CONTINUED.

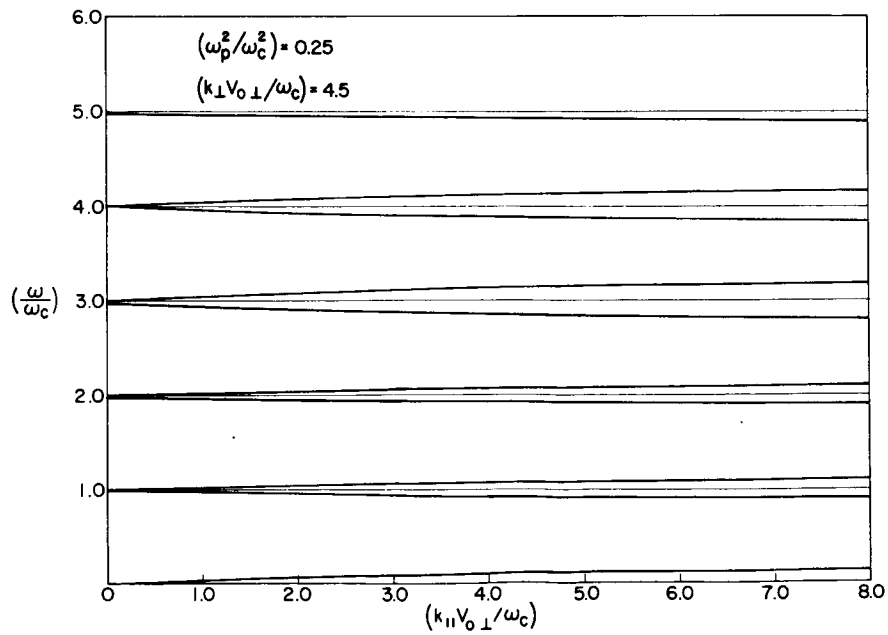

(a)

Fig. 27. DISPERSION CHARACTERISTICS OF OBLIQUELY PROPAGATING CYCLOTRON HARMONIC WAVES; RING DISTRIBUTION FOR $\mu_\perp = 4.5$ AND $(\omega_p^2/\omega_c^2) = 0.25$, 1.0, 3.0, 5.0, 8.0, 20.0, ∞.

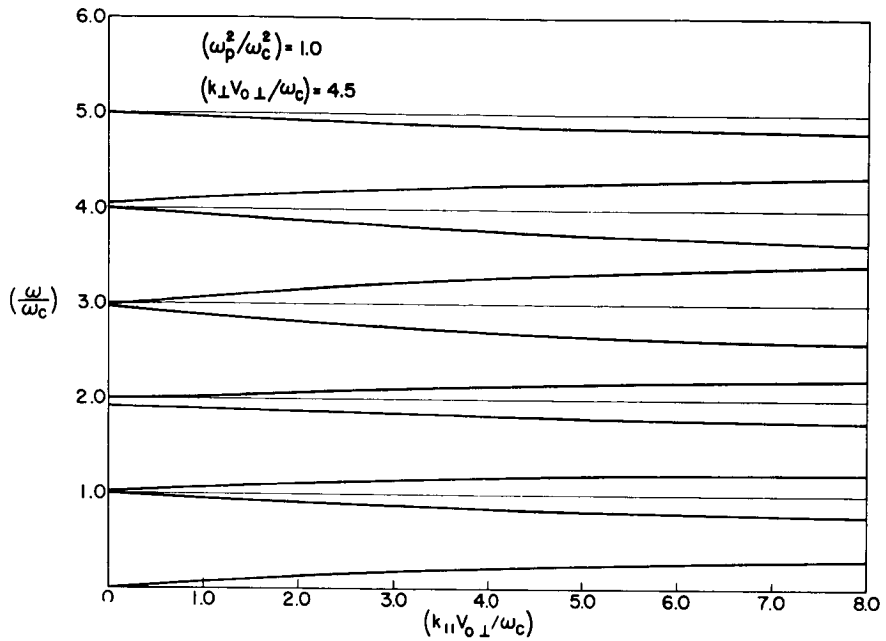

(b)

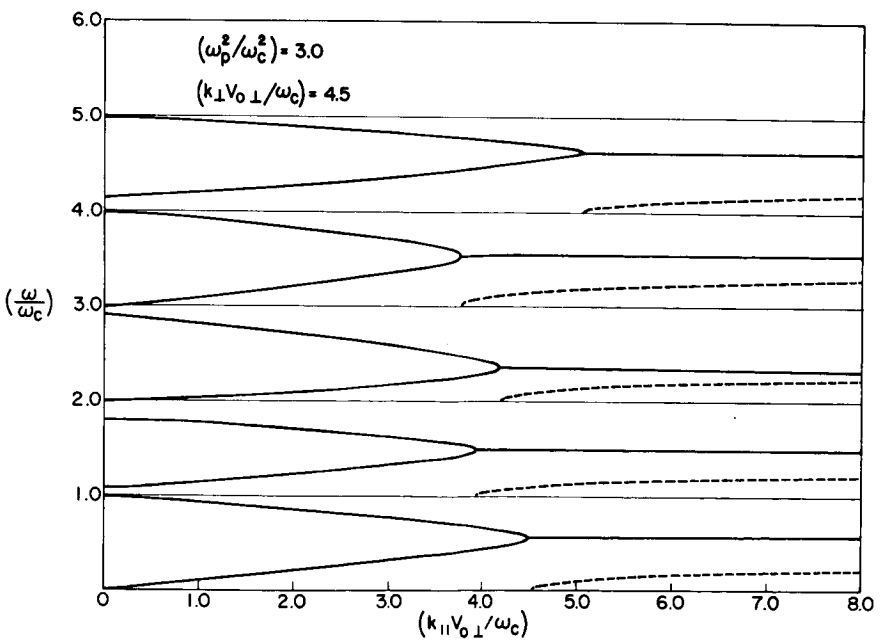

(c)

Fig. 27. CONTINUED.

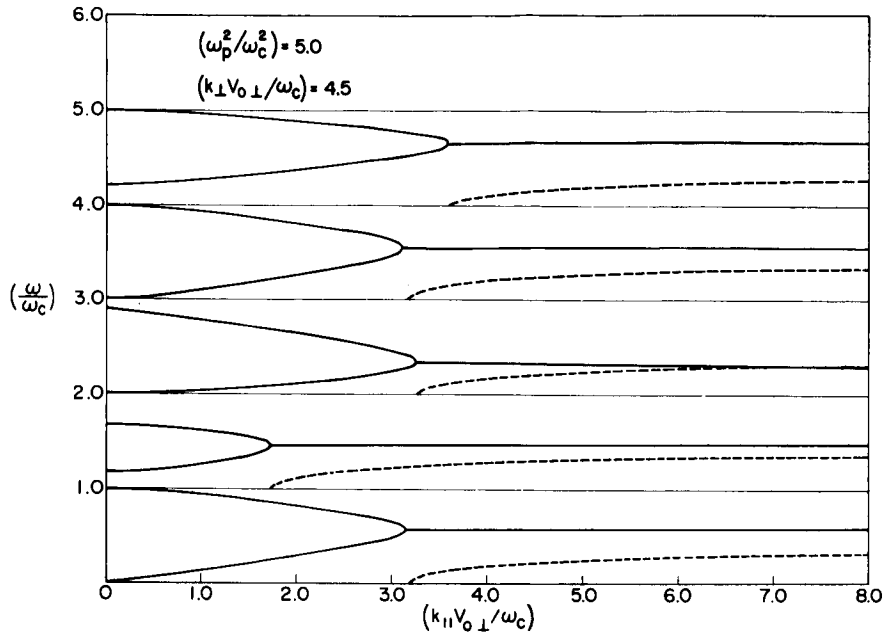

(d)

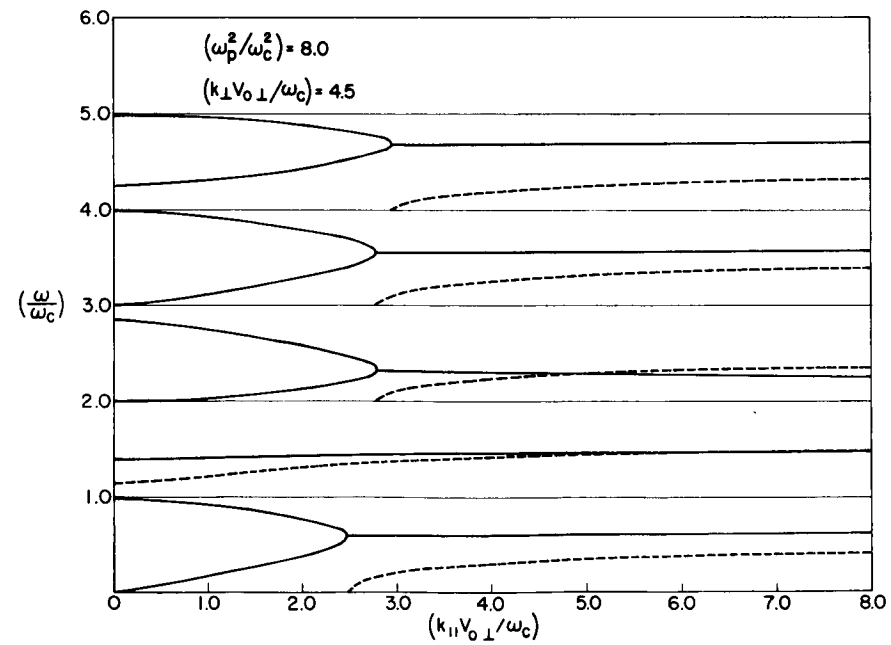

(e)

Fig. 27. CONTINUED.

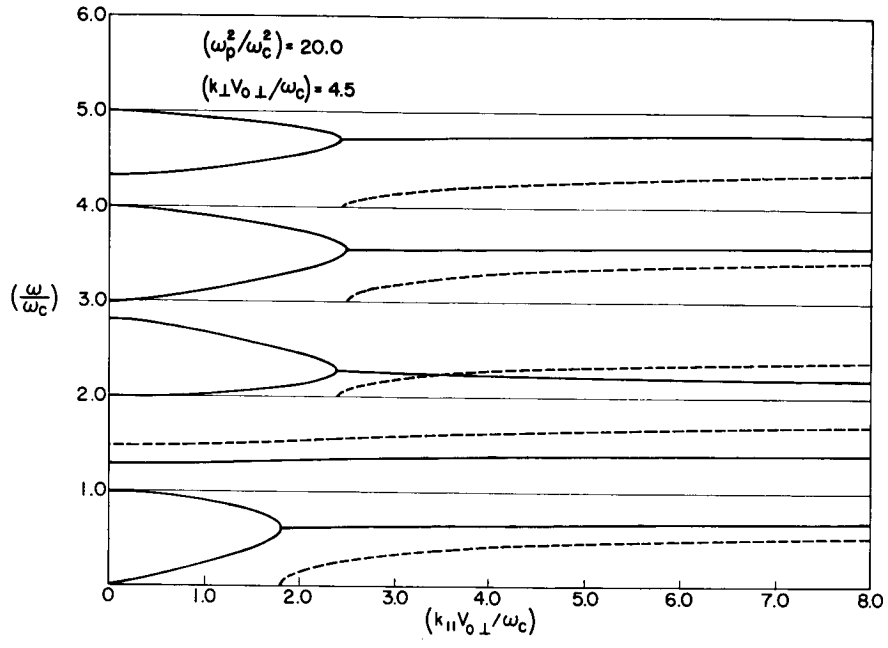

(f)

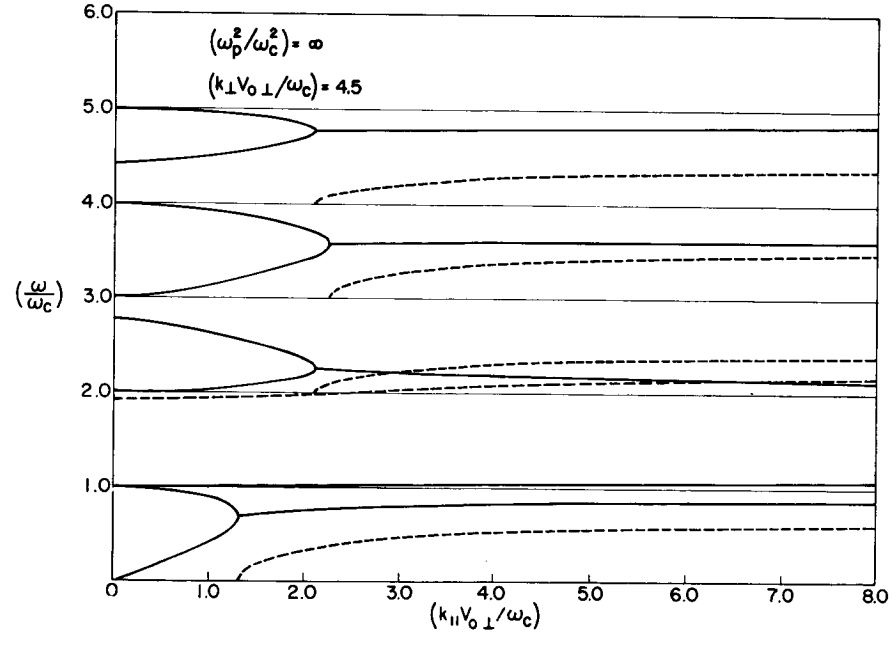

(g)

Fig. 27. CONTINUED.

values of $\mu_\perp$ it is actually possible for the real part to lie below unity. There is then no real frequency component at all in the second passband.

b. Unbounded Plasma

In this section we will consider the dispersion characteristics of plane cyclotron harmonic waves, propagating at a fixed angle θ to the applied magnetic field, in a plasma with a ring electron velocity distribution. The dispersion relation in this case is given by Eq. (4.6). The solutions to this dispersion relation may be obtained from curves in Figs. 25-27 after θ and μ ($\equiv kv_{o_\perp}/\omega_c$) are specified and if the corresponding value of $\mu_\perp$ ($\equiv \mu \cos\theta$) is either 1, 3, or 4.5. However, it is more convenient to solve Eq. (4.6) directly for $\omega(k)$. Some results which illustrate the basic features of the dispersion curves are given in Fig. 28 for $(\omega_p^2/\omega_c^2) = 1$ and $\theta = 70°$, $45°$, and $15°$, respectively. Cutoffs and resonances are observed at all harmonics of the electron cyclotron frequency. In addition, a cutoff is found at the frequencies which satisfy the following equation:

$$1 - \frac{\omega_p^2}{\omega_c^2}\left(\sin^2\theta\,\frac{\omega_c^2}{\omega^2 - \omega_c^2} + \cos^2\theta\,\frac{\omega_c^2}{\omega^2}\right) = 0 \quad , \tag{4.14}$$

which is obtained from Eq. (~~4.16~~ 4.6) by setting k identically equal to zero. Solving for ω yields the expression

$$\omega^2 = \frac{1}{2}\left(\omega_c^2 + \omega_p^2\right)\left\{1 \pm \left[1 - \frac{4\omega_p^2\omega_c^2\cos^2\theta}{\left(\omega_p^2 + \omega_c^2\right)^2}\right]^{1/2}\right\} . \tag{4.15}$$

When k is finite and nonzero, Fig. 28 shows that two modes are found near harmonics, as could have been deduced from Figs. 25 to 27. However, in this case the modes undulate about the frequency $\omega = n\omega_c$

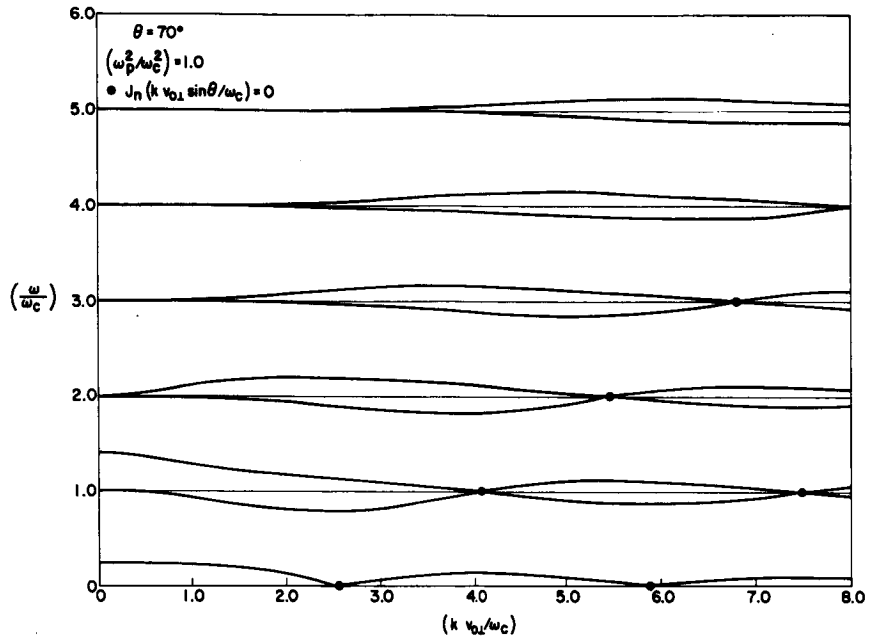

(a)

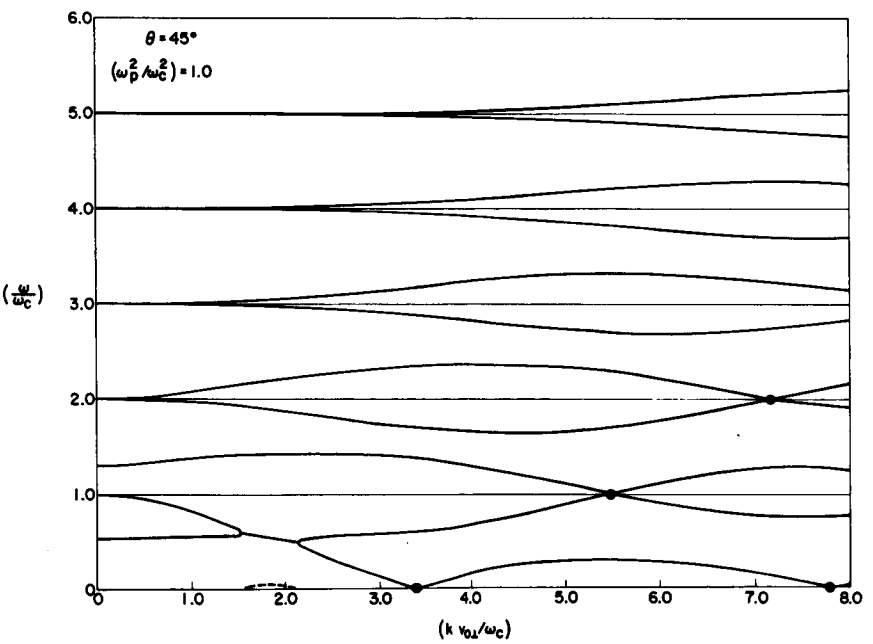

(b)

Fig. 28. DISPERSION CHARACTERISTICS OF OBLIQUELY PROPAGATING CYCLOTRON HARMONIC WAVES; RING DISTRIBUTION FOR $(\omega_p^2/\omega_c^2) = 1$; $\theta = 70°, 45°, 15°$.

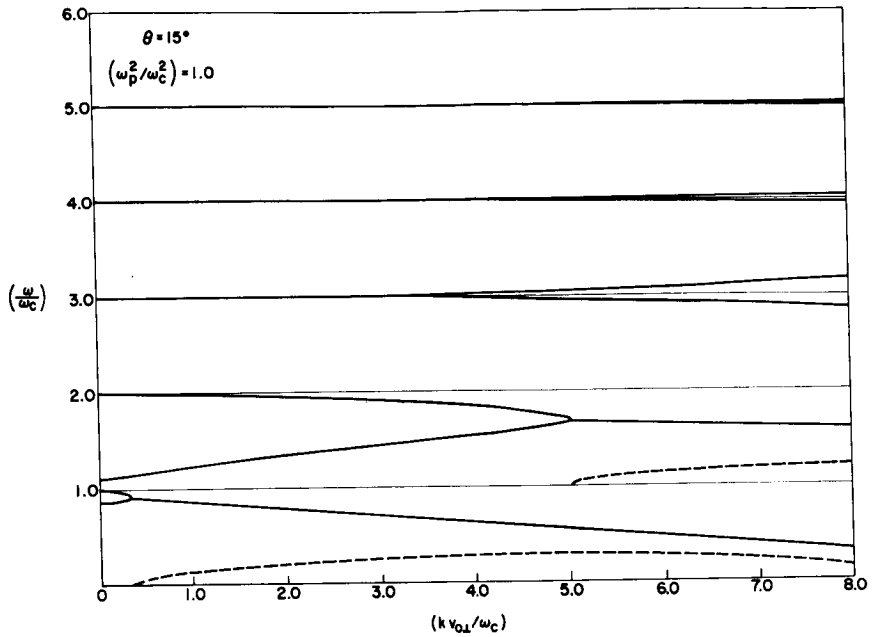

(c)

Fig. 28. CONTINUED.

and pass through the harmonic when μ satisfies the equation, $J_n(\mu \sin \theta) = 0$. Note that as θ decreases, a down-going and an up-going mode couple to produce complex frequencies for a small band of wave numbers. The complex roots must occur in conjugate pairs so that one mode grows exponentially with time at the indicated rate and the other decays with time. As θ decreases further from 45° to 15°, additional modes couple and the growth rates become larger.

It is now apparent that the propagating modes in bounded and unbounded plasmas have similar characteristics. In each case there are two modes between $n\omega_c$ and $(n+1)\omega_c$. Furthermore, both classes of modes are very unstable and exhibit complex frequencies for much smaller values of (ω_p^2/ω_c^2) than was possible for purely perpendicular propagation. The main difference between the two classes is that the unbounded plasma exhibits modes which undulate about the harmonics of the cyclotron frequency while the frequency of the modes of the bounded plasma vary monotonically with $k_{\parallel}$.

2. Distributions in Transverse Electron Speed

The results of the previous subsection indicate that a magnetoplasma with a monoenergetic ring distribution is capable of supporting a large class of electrostatic instabilities. However, this plasma model may be too idealistic since there is usually particle motion parallel to the magnetic field and distributions in the particle velocity that influence the stability characteristics of the plasma. At this time we consider a more general problem and examine the propagation characteristics of cyclotron harmonic waves when there is a distribution in the components of the electron velocity perpendicular to the magnetic field. As in the first subsection, we will assume that there is no particle motion parallel to the magnetic field. Our objectives are to obtain the basic form of the dispersion characteristics for oblique propagation in this case and to determine the factors that influence the stability of the plasma. The effects of electron motion parallel to the magnetic field are considered in Section B.

When the motion of the charged particles parallel to the magnetic field is neglected, the most general form of the dispersion relation is obtainable from Eq. (4.2) by setting $v_{o_{||}}$ equal to zero. Solving explicitly for $k_{||}^2$ yields the expression

$$k_{||}^2 = - k_{\perp}^2 \frac{N(\omega,k_{\perp})}{D(\omega,k_{\perp})} \quad , \tag{4.16}$$

where use has been made of the relation, $k^2 = k_{\perp}^2 + k_{||}^2$, and the functions $N(\omega,k_{\perp})$ and $D(\omega,k_{\perp})$ are defined as follows:

$$N(\omega,k_{\perp}) = 1 - \frac{\omega_p^2}{\omega_c^2} \sum_{n=-\infty}^{\infty} p_n \frac{n\omega_c}{\omega - n\omega_c} \quad , \tag{4.17a}$$

$$D(\omega,k_{\perp}) = 1 - \frac{\omega_p^2}{\omega_c^2} \sum_{n=-\infty}^{\infty} q_n \frac{\omega_c^2}{(\omega - n\omega_c)^2} \, . \tag{4.17b}$$

Only the case where $k_\perp$ is constant will be considered here since the form of the dispersion curves with the angle of propagation θ [$\equiv \tan^{-1}(k_\perp/k_\parallel)$] held constant can be inferred from the characteristics that will be described below. From Eq. (4.16), it is readily shown that, in the general case, cutoff frequencies are found first at the zeros of $N(\omega,k_\perp)$, that is, the frequencies of perpendicularly propagating waves), and second at harmonics of the electron cyclotron frequency. In addition, resonant frequencies occur at the zeros of $D(\omega,k_\perp)$. These solutions of the dispersion relation are reflected in the propagation curves shown in Figs. 25-27. For certain transverse velocity distributions $f_\perp(v_\perp)$, the cutoffs and resonances may be complex. This was the case, for example, for the ring distribution, and as a consequence, instability was excited in the plasma. Another distribution that can go unstable is the transverse Maxwellian:

$$f_\perp(v_\perp) = \left(\frac{1}{2\pi v_{t\perp}^2}\right) \exp\left(-\frac{v_\perp^2}{2v_{t\perp}^2}\right). \tag{4.18}$$

Although perpendicular propagation occurs, in this case, without growth, obliquely propagating waves can grow exponentially with time under the proper conditions. In order to determine what these conditions are, Eq. (4.18) is substituted into Eq. (4.2) and the integration with respect to $v_\perp$ is carried out, yielding the dispersion relation

$$K(\omega,\underset{\sim}{k}) = 1 - \frac{\omega_p^2}{\omega_c^2}\left[\sum_{n=-\infty}^{\infty} \frac{\exp(-\lambda)\, I_n(\lambda)}{\lambda} \frac{n\omega_c}{\omega - n\omega_c}\right.$$

$$\left. + \sum_{n=-\infty}^{\infty} \exp(-\lambda)\, I_n(\lambda) \frac{\omega_c^2}{(\omega - n\omega_c)^2}\right]$$

$$= 0 \quad , \tag{4.19}$$

where $\lambda = (k_\perp v_{t\perp}/\omega_c)^2$ and use has been made of the identity

$$\int_0^\infty dq \exp\left(-\frac{q^2}{2p^2}\right) J_n^2(q)q = p^2 I_n(p^2) \exp(-p^2) . \qquad (4.20)$$

Alternately, Eq. (4.19) can be rewritten in the form given by Eq. (4.16), in which case the functions $N(\omega,k_\perp)$ and $D(\omega,k_\perp)$ become:

$$N(\omega,k_\perp) = 1 - \frac{\omega_p^2}{\omega_c^2} \sum_{n=-\infty}^{\infty} \frac{\exp(-\lambda)\, I_n(\lambda)}{\lambda} \frac{n\omega_c}{\omega - n\omega_c} , \qquad (4.21a)$$

$$D(\omega,k_\perp) = 1 - \frac{\omega_p^2}{\omega_c^2} \sum_{n=-\infty}^{\infty} \exp(-\lambda)\, I_n(\lambda) \frac{\omega_c^2}{(\omega - n\omega_c)^2} . \qquad (4.21b)$$

The equation $N(\omega,k_\perp) = 0$, which determines the cutoffs, is nothing more than the dispersion relation for perpendicular propagation that was considered in Chapter III. Figure 10 shows the computed dispersion diagram for this case where it will be noted that $\omega(k_\perp)$ is always real if $k_\perp$ is real. Consequently, no long-wavelength instabilities are excited. However, the resonant frequencies may be complex. To see how this comes about, it is assumed that (ω_p^2/ω_c^2) is small and that ω is near $n\omega_c$. It is then reasonable to approximate the series in Eq. (4.19b) by the n^{th} term. Solving the equation $D(\omega,k_\perp) = 0$ for ω yields the expression

$$\omega = n\omega_c \pm \omega_p \sqrt{\exp(-\lambda)\, I_n(\lambda)} , \qquad (4.22)$$

which is plotted in Fig. 29a for $(\omega_p/\omega_c) = 0.5$ and $n = 2$ and 3. For larger values of (ω_p^2/ω_c^2), numerical methods must be used to obtain the resonances. Results of these computations are shown in Fig. 29b with the case $(\omega_p^2/\omega_c^2) = 1$, where it is found that complex frequencies occur

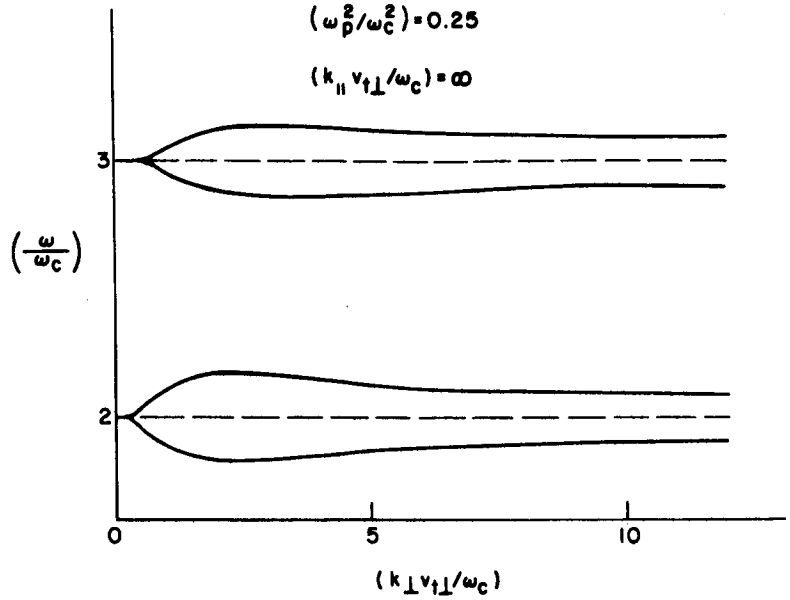

(a)

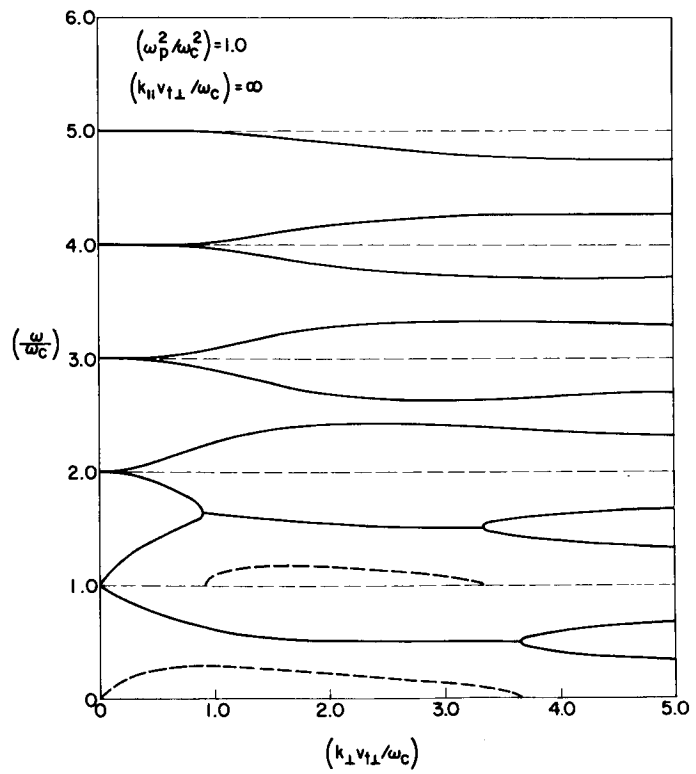

(b)

Fig. 29. RESONANT FREQUENCIES FOR OBLIQUELY PROPAGATING CYCLOTRON HARMONIC WAVES; TRANSVERSE MAXWELLIAN VELOCITY DISTRIBUTION FOR (a) $(\omega_p^2/\omega_c^2) = 0.25$, AND (b) $(\omega_p^2/\omega_c^2) = 1$.

in a single finite range of the parameter $(k_\perp v_{t\perp}/\omega_c)$. This result is in contrast with that of the ring distribution where several bands of $(k_\perp v_{o\perp}/\omega_c)$ produce complex solutions. It is important to note that these instabilities set in with the plasma frequency less than the cyclotron frequency.

Figure 30 shows the form of the complete dispersion diagram, computed from Eq. (4.19). The parameters (ω_p^2/ω_c^2) and $(k_\perp v_{t\perp}/\omega_c)$ were chosen so that some waves are unstable. The imaginary part of ω is shown dashed and drawn to the base, $\omega = n\omega_c$. These curves behave in essentially the same manner as that of the ring distribution in Figs. 25 to 27 with the exception that no long-wavelength instabilities occur, reflecting the discussion of the previous paragraph.

From the results of this and the previous section, we can conclude that oblique propagation may excite two classes of instability, one of which occurs only if the wavelength parallel to the magnetic field is relatively small and has no counterpart in exact perpendicular propagation.

B. Distributions in Longitudinal Electron Energy

In this section we obtain the real wave number solutions of the dispersion relation for cyclotron harmonic waves in the general case where a distribution exists in the electron velocity components parallel to the magnetic field. The expression that describes this situation is given by Eq. (2.67) and, for convenience, is rewritten in the form:

$$K(\omega,\underset{\sim}{k}) = 1 + \frac{\omega_p^2}{k^2} \sum_{n=-\infty}^{\infty} \int_{-\infty}^{\infty} dv_{\parallel} \frac{H_n(v_{\parallel})}{\omega - k_{\parallel} v_{\parallel} - n\omega_c} = 0 , \qquad \mathrm{Im}(\omega) < 0 , \tag{4.23}$$

where

$$H_n(v_{\parallel}) = 2\pi \int_0^{\infty} dv_\perp \left(\frac{n\omega_c}{v_\perp} \frac{\partial f_o}{\partial v_\perp} + k_{\parallel} \frac{\partial f_o}{\partial v_{\parallel}} \right) J_n^2 \left(\frac{k_\perp v_\perp}{\omega_c} \right) v_\perp . \tag{4.24}$$

Since only electron motion is being considered, the summation over particle species is redundant and hence was not included in Eq. (4.23). The analytic continuation of this representation of $K(\omega,\underset{\sim}{k})$ to the real ω axis and to the upper half complex plane is obtainable from Eq. (2.68).

Unlike the special case examined in Section A, the roots of Eq. (4.23) are in general complex, as will be appreciated from the complete definition of $K(\omega,\underset{\sim}{k})$ in Eq. (2.68). Consequently, the amplitude of electrostatic waves propagating oblique to the magnetic field grows or decays with time, depending on the sign of the imaginary part of ω. These complex roots result from the presence of electrons that can interact strongly with the electric field associated with the space-charge wave. The physics involved in this interaction have been considered elsewhere [22] and can be summarized as follows: An electron, spiralling about the magnetic field, sees the wave at the doppler-shifted frequency, $\omega' = (\omega - k_{\parallel} v_{\parallel})$. Since a spread in $v_{\parallel}$ exists, it is always possible to find an electron for which $\omega' = n\omega_c$, where n is an integer. By solving the equations of motion for such electrons, it is shown that in the linear regime there is a net energy exchange between the gyrating electron and the electric field of the space-charge wave. Damping of the coherent oscillations results if the charged particle gains energy, while instability is present if the particle loses energy. The net temporal change in the wave amplitude is determined by a superposition of all resonant electrons. Cyclotron damping or instability arises from those electrons which see the space-charge wave at nonzero harmonics of the cyclotron frequency, while if the particle sees a static field, corresponding to $n = 0$, Landau damping or instability results.

Little is known about the temporal rate at which the amplitude of cyclotron harmonic waves changes due to Landau and cyclotron damping or instability. In this section computations are presented which show the form of the dispersion characteristics when a spread in the parallel velocity component $v_{\parallel}$ exists. The basic features of the characteristics are illustrated with electron velocity distributions that have the form

$$f_o(v_{\perp},v_{\parallel}) = \left(\frac{1}{2\pi v_{t\perp}^2}\right) \exp\left(-\frac{v_{\perp}^2}{2v_{t\perp}^2}\right) f_{\parallel}(v_{\parallel}) \ , \qquad (4.25)$$

where $v_{t\perp}$ $[\equiv (\kappa T_\perp/m)^{1/2}]$ is the transverse thermal speed of the electrons, $T_\perp$ is the associated transverse temperature, and the function $f_\parallel(v_\parallel)$ has the normalization

$$\int_{-\infty}^{\infty} dv_\parallel \; f_\parallel(v_\parallel) = 1 \; . \tag{4.26}$$

The following functions are chosen to represent $f_\parallel(v_\parallel)$:

(i) Resonance

$$f_\parallel(v_\parallel) = \frac{v_{t\parallel}}{\pi(v_\parallel^2 + v_{t\parallel}^2)} \quad , \tag{4.27}$$

(ii) Maxwellian

$$f_\parallel(v_\parallel) = \left(\frac{1}{2\pi v_{t\parallel}^2}\right)^{1/2} \exp\left(-\frac{v_\parallel^2}{2v_{t\parallel}^2}\right) \quad , \tag{4.28}$$

where, for the Maxwellian, $v_{t\parallel}$ is rms parallel speed of the distribution. Since all moments of the resonance are infinite, $v_{t\parallel}$ in that case is interpreted as a measure of the spread of the distribution.

1. The Dispersion Relations

The form of the dispersion relation for each of the distributions cited above is found by first substituting Eq. (4.25) in Eq. (4.24) to obtain the function $H_n(v_\parallel)$. The integration with respect to $v_\perp$ is accomplished with the identity [25]

$$\int_0^{\infty} dq \exp\left(-\frac{q^2}{2p^2}\right) J_n^2(q)q = p^2 \exp(-p^2)\, I_n(p^2) \; , \tag{4.29}$$

yielding

$$H_n(v_{\parallel}) = - \exp(-\lambda)\, I_n(\lambda) \left[\frac{n\omega_c}{v_{t\perp}^2} f_{\parallel}(v_{\parallel}) - k_{\parallel} \frac{df_{\parallel}(v_{\parallel})}{dv_{\parallel}} \right] , \qquad (4.30)$$

where λ has been written for $(k_\perp^2 v_{t\perp}^2/\omega_c^2)$. If the resonance function is substituted for $f_{\parallel}(v_{\parallel})$, the velocity distribution has the form

$$f_o(v_\perp, v_{\parallel}) = \left(\frac{v_{t\parallel}}{2\pi^2 v_{t\perp}^2} \right) \frac{\exp\left(- \frac{v_\perp^2}{2v_{t\perp}^2} \right)}{(v_{\parallel}^2 + v_{t\parallel}^2)} , \qquad (4.31)$$

and, after combining Eqs. (4.23), (4.27), and (4.30), the dispersion relation becomes

$$K(\omega, \underset{\sim}{k}) = 1 - \frac{\omega_p^2}{\omega_c^2} \left[\frac{k_\perp^2}{k^2} \sum_{n=-\infty}^{\infty} \frac{\exp(-\lambda)\, I_n(\lambda)}{\lambda} \left(\frac{n\omega_c v_{t\parallel}}{\pi} \right) \int_{-\infty}^{\infty} \frac{dv_{\parallel}}{(v_{\parallel}^2 + v_{t\parallel}^2)(\omega - k_{\parallel} v_{\parallel} - n\omega_c)} \right.$$

$$\left. + \frac{k_{\parallel}^2}{k^2} \sum_{n=-\infty}^{\infty} \exp(-\lambda)\, I_n(\lambda) \left(\frac{2v_{t\parallel}\omega_c^2}{\pi k_{\parallel}} \right) \int_{-\infty}^{\infty} \frac{v_{\parallel}\, dv_{\parallel}}{(v_{\parallel}^2 + v_{t\parallel}^2)^2 (\omega - k_{\parallel} v_{\parallel} - n\omega_c)} \right]$$

$$= 0, \qquad \mathrm{Im}(\omega) < 0 . \qquad (4.32)$$

The integration with respect to $v_{\parallel}$ is readily accomplished by the method of residues, yielding for $k_{\parallel} > 0$,

$$K(\omega,\underset{\sim}{k}) = 1 - \frac{\omega_p^2}{\omega_c^2}\left[\frac{k_\perp^2}{k^2}\sum_{n=-\infty}^{\infty}\frac{\exp(-\lambda)\, I_n(\lambda)}{\lambda}\,\frac{n\omega_c}{\omega - ik_\parallel v_\parallel - n\omega_c}\right.$$

$$\left. + \frac{k_\parallel^2}{k^2}\sum_{n=-\infty}^{\infty}\exp(-\lambda)\, I_n(\lambda)\,\frac{\omega_c^2}{(\omega - ik_\parallel v_\parallel - n\omega_c)^2}\right]$$

$$= 0 \quad . \tag{4.33}$$

Clearly, this expression is analytic over the entire complex ω plane, except where $\omega = n\omega_c + ik_\parallel v_\parallel$.

In our second example the Maxwellian function is written in place of $f_\parallel(v_\parallel)$, leading to the velocity distribution

$$f_o(v_\perp, v_\parallel) = \left(\frac{1}{2\pi v_{t\perp}^2}\right)\left(\frac{1}{2\pi v_{t\parallel}^2}\right)^{1/2} \exp\left(-\frac{v_\perp^2}{2v_{t\perp}^2} - \frac{v_\parallel^2}{2v_{t\parallel}^2}\right) \quad . \tag{4.34}$$

From Eqs. (4.23), (4.28), and (4.30), the corresponding dispersion relation is

$$K(\omega,\underset{\sim}{k}) = 1 + \frac{\omega_p^2}{k^2 v_{t\parallel}^2}\left[1 + \sum_{n=-\infty}^{\infty}\exp(-\lambda)\, I_n(\lambda)\,\frac{\omega - (1-T)n\omega_c}{\sqrt{2}\, k_\parallel v_{t\parallel}}\, Z\left(\frac{\omega - n\omega_c}{\sqrt{2}\, k_\parallel v_{t\parallel}}\right)\right]$$

$$= 0 \quad , \tag{4.35}$$

where $T = (v_{t\parallel}^2/v_{t\perp}^2)$ and the function $Z(z)$, which arises from the $v_\parallel$ integration, has the following definition, in the notation of Fried and Conte [41]:

$$Z(z) = \frac{1}{\sqrt{\pi}}\, P\int_{-\infty}^{\infty}\frac{\exp(-t^2)}{t - z}\, dt - i\sigma\sqrt{\pi}\exp(-z^2) \, . \tag{4.36}$$

Here P signifies that the principal part of the integral is taken if z lies on the real t axis and σ has either of the values 0, 1, or 2, depending on whether the imaginary part of z is less than, equal to, or greater than zero, respectively. The second term on the right-hand side arises from the analytic continuation of the $v_{\parallel}$ integral from the lower to the upper half complex ω plane, in accordance with the definition given in Eq. (2.68).

2. Solutions of the Dispersion Relations

In order to appreciate the structure of the dispersion characteristics when a spread exists in $v_{\parallel}$, it is useful to return to the extreme anisotropic case where the electrons have no motion parallel to the magnetic field. Assuming that the transverse speed of the gyrating electrons has a Maxwellian distribution, the dispersion relation is given by Eq. (4.19) and the solutions are shown in Fig. 30. It is readily

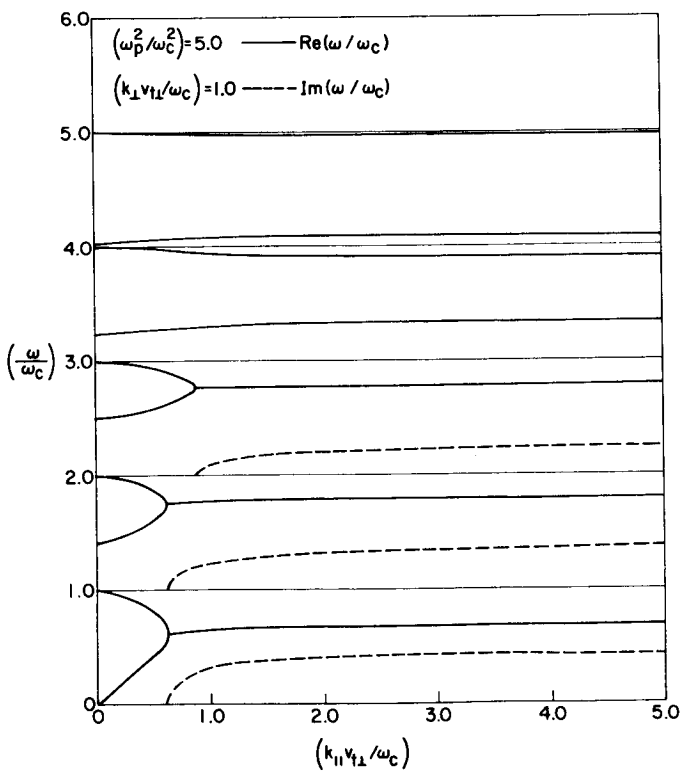

Fig. 30. DISPERSION CHARACTERISTICS OF OBLIQUELY PROPAGATING CYCLOTRON HARMONIC WAVES; TRANSVERSE MAXWELLIAN VELOCITY DISTRIBUTION.

established that both Eqs. (4.33) and (4.35) reduce to Eq. (4.19) in the limit as $v_{t\parallel} \to 0$. For Eq. (4.35), this limit is obtainable from the asymptotic expansion [41]

$$Z(z) \sim -\frac{1}{z} - \frac{1}{2z^3} - \ldots . \tag{4.37}$$

If temperature effects are introduced parallel to the magnetic field by means of a resonance distribution in the velocity component $v_{\parallel}$, a comparison of Eqs. (4.19) and (4.33) shows that the dispersion characteristics are then given by the expression

$$\omega(k_{\parallel}) = \omega_D(k_{\parallel}) + iv_{t\parallel}k_{\parallel} , \tag{4.38}$$

where the $\omega_D(k_{\parallel})$ are the complex frequency solutions of Eq. (4.19) that are shown in Fig. 30. Since $k_{\parallel}$ is greater than zero, each branch of the dispersion diagram has acquired a positive imaginary part which may transform growing waves to waves that decay with time if the parallel thermal speed $v_{t\parallel}$ is sufficiently large. This point is illustrated in Fig. 31 with a comparison of the imaginary part of $\omega(k_{\parallel})$ in the first five frequency bands for two values of the temperature ratio $(v_{t\parallel}/v_{t\perp})$. The curves corresponding to $(v_{t\parallel}/v_{t\perp}) = 0$ were obtained from Fig. 30, and the second set, corresponding to $(v_{t\parallel}/v_{t\perp}) = 0.2$, were computed from Eq. (4.38). It is seen that a parallel electron temperature is manifested in three characteristic ways:

1. As $k_{\parallel} \to \infty$, every mode acquires a large positive imaginary part which implies strong attenuation with time.
2. If the normalized wave number $(k_{\parallel}v_{t\perp}/\omega_c)$ is sufficiently small, each mode has a positive imaginary part that varies linearly with $k_{\parallel}$.
3. There may exist finite ranges of the normalized wave number $(k_{\parallel}v_{t\perp}/\omega_c)$ over which the imaginary part of ω is negative. The waves falling into this group are consequently unstable.

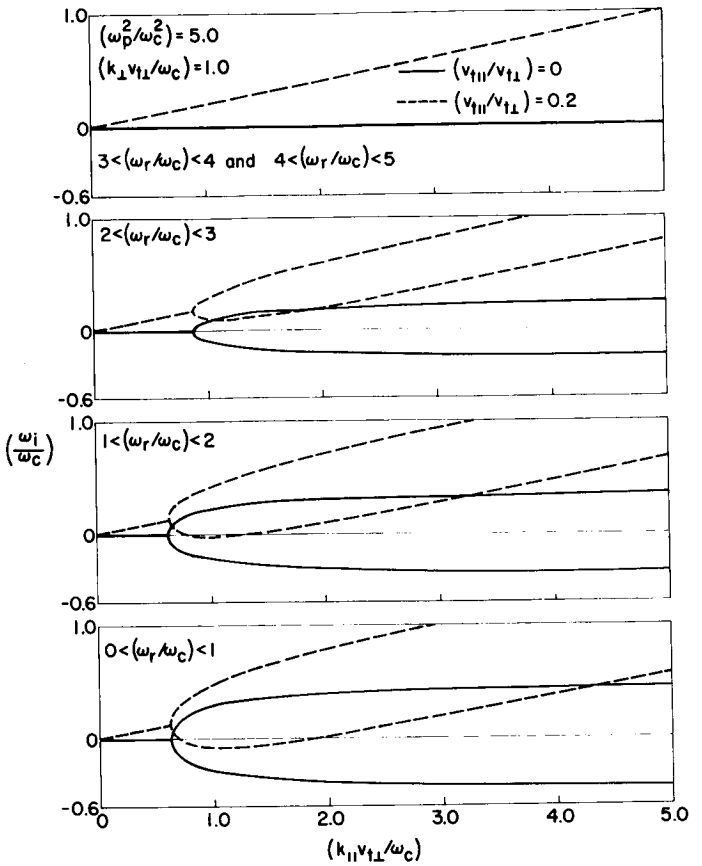

Fig. 31. IMAGINARY PART OF ω FOR OBLIQUE PROPAGATION OF CYCLOTRON HARMONIC WAVES. Here the parallel component of the electron velocity $v_\parallel$ is distributed according to a resonance function with effective thermal speed $v_{t\parallel}$, and the transverse components have a Maxwellian distribution with thermal speed $v_{t\perp}$.

When $v_\parallel$ is distributed according to the resonance function, the real part of the frequency is the same as that of a plasma with zero thermal electron speed parallel to the magnetic field, and hence is obtainable from the dispersion characteristics shown in Fig. 30.

It is seen from the above that instabilities can be expected only if the electron temperature is sufficiently anisotropic, as originally shown by Harris [4,5]. In the limiting case of an isotropic plasma where the velocity distribution of the electrons is a function only of $v\left[\equiv (v_\perp^2 + v_\parallel^2)^{1/2}\right]$, and where $(\partial f_o/\partial v) < 0$ for all $v > 0$, instability cannot be excited (see Appendix A). Space-charge oscillations decay exponentially with time in this case. For purposes of illustrating the dispersion characteristics

for an isotropic plasma, Eq. (4.35) has been solved numerically for $\omega(k_{\parallel})$ with the temperature parameter T equal to unity. The Maxwellian distribution occurs commonly in laboratory plasmas, and for this reason these computations are of particular significance. Figure 32 shows the resulting dispersion characteristics for ~~two~~ three values of (ω_p^2/ω_c^2) and of $(k_\perp v_t/\omega_c)$, where v_t $(= v_{t\perp} = v_{t\parallel})$ is the thermal speed of the isotropic Maxwellian distribution. To obtain these curves the function $Z(z)$ was generated numerically from a computer program written by H. Derfler and T. Simonen. It will be noted that, as in other cases, two modes are found in each passband. The damping rate, given by the imaginary part of ω, increases rapidly with $(k_{\parallel} v_t/\omega_c)$, particularly for modes that have a cutoff at harmonics of the electron cyclotron frequency. It is remarked that for modes between $n\omega_c$ and $(n+1)\omega_c$, (ω_i/ω_c) has been plotted with the line $\omega = n\omega_c$ as a base, and with the indicated scale. It can be concluded from these curves that for propagation more than about 10° off exact perpendicularity, attenuation of the order of 50 dB

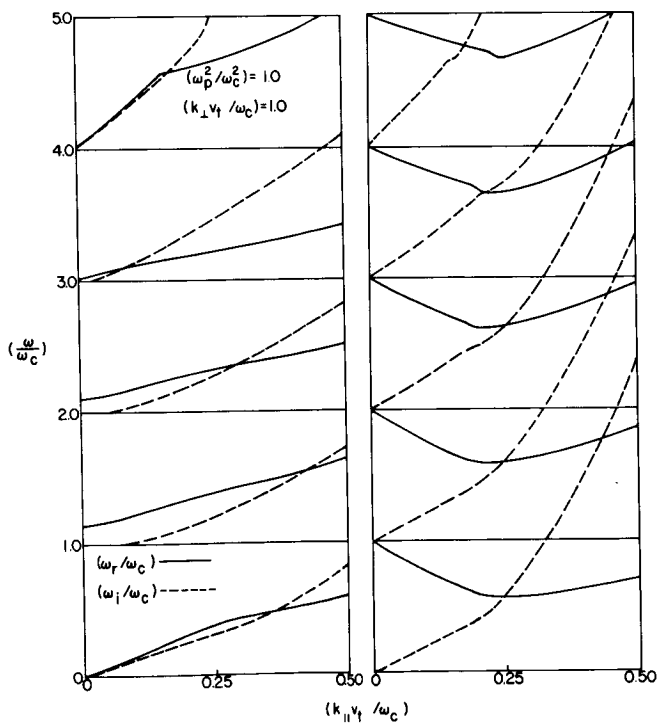

(a)

Fig. 32. DISPERSION CURVES FOR OBLIQUELY PROPAGATING CYCLOTRON HARMONIC WAVES IN A MAXWELLIAN PLASMA SHOWING CYCLOTRON AND LANDAU DAMPING EFFECTS.

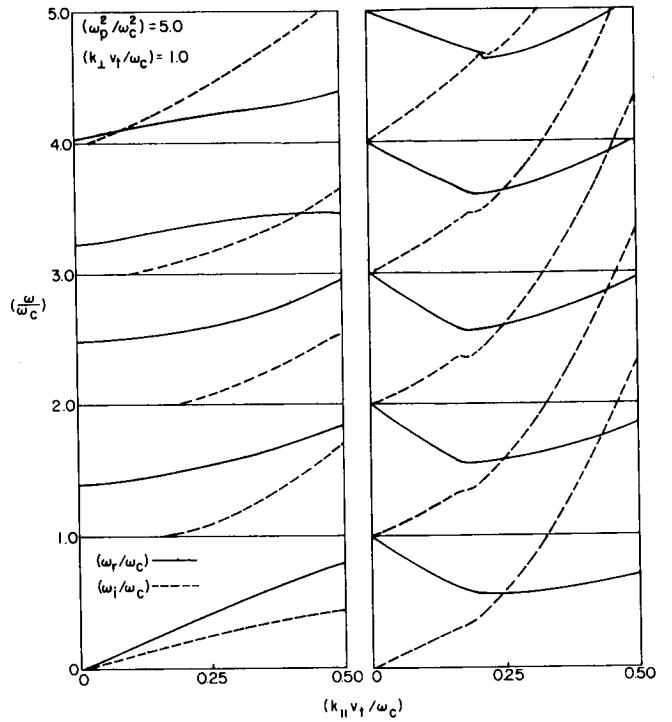

(b)

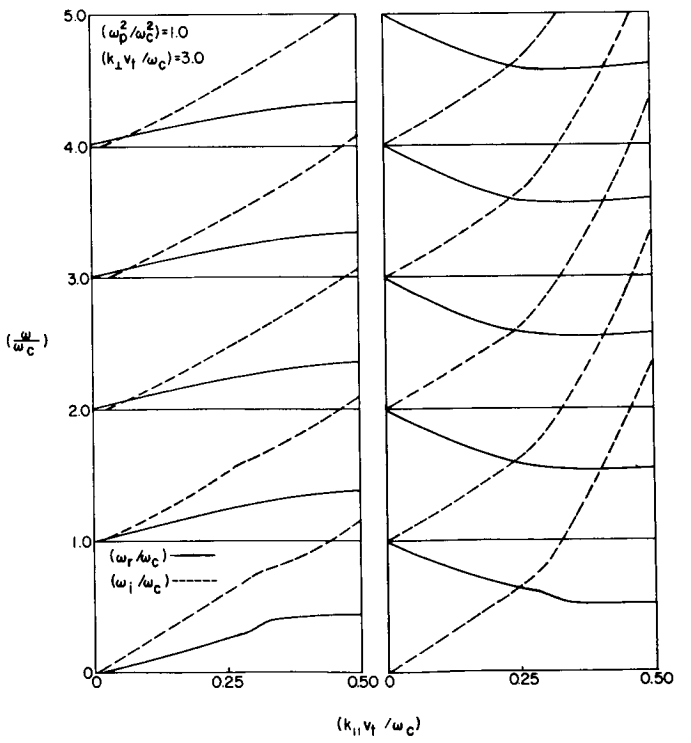

(c)

Fig. 32. CONTINUED.

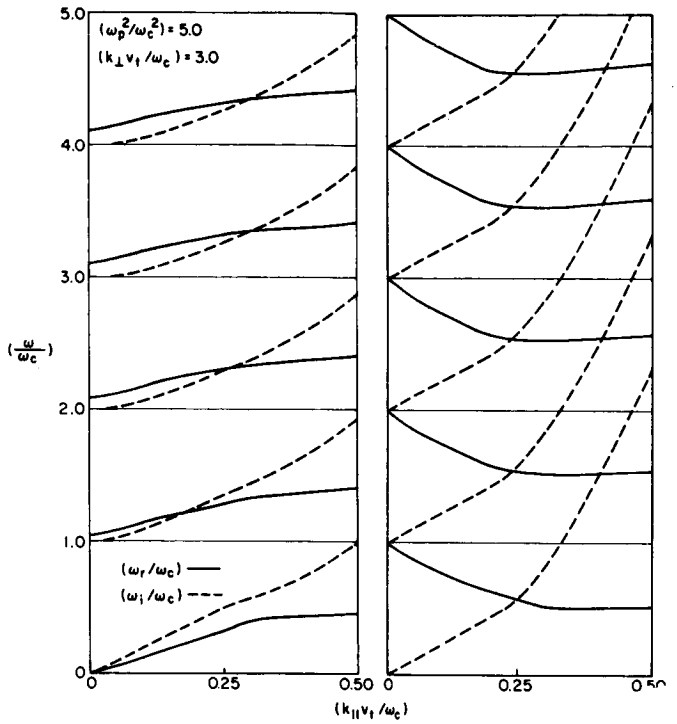

(d)

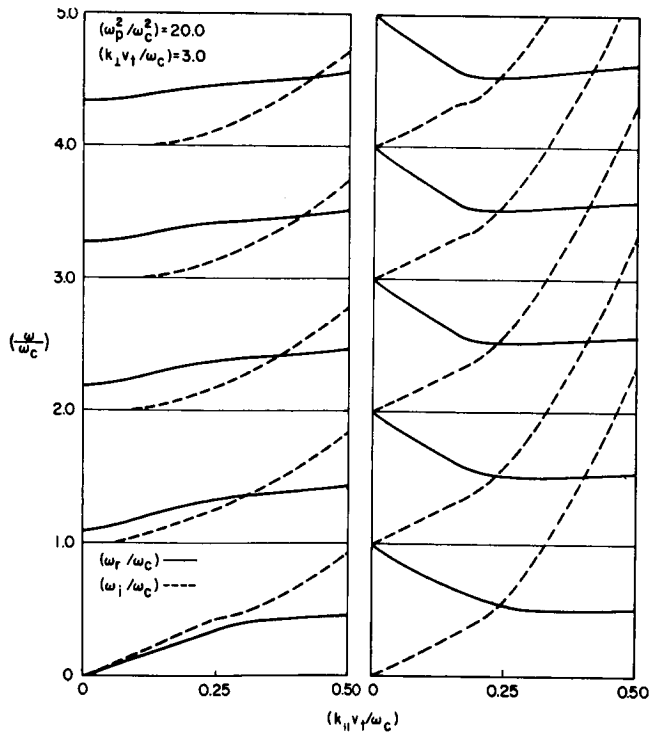

(e)

Fig. 32. CONTINUED.

per cyclotron period would be encountered. Consequently, oblique propagation will normally only be observable in a narrow angular range near $(\pi/2)$ to the magnetic field.

C. Nearly Perpendicular Propagation

It has been shown in the previous section that cyclotron harmonic waves propagating almost perpendicular to the magnetic field in a Maxwellian plasma are lightly damped due to Landau and cyclotron damping. In the limit of perpendicular propagation, this damping disappears and the waves can propagate without collisionless attenuation. In this section approximate expressions have been derived which give the rate of decay and the frequency of oscillation of cyclotron harmonic waves in the limit as $(k_{\parallel}/k_{\perp}) \to 0$, where $k_{\parallel}$ and $k_{\perp}$ are, respectively, the components of the wave vector $\underset{\sim}{k}$ parallel and perpendicular to the magnetic field. This limit corresponds to waves propagating at angles near $(\pi/2)$ to the magnetic field. The expressions are compared with the exact numerical solutions of the dispersion relation to determine when their validity breaks down.

The dispersion relation for cyclotron harmonic waves can be written in several equivalent forms. For the purposes of this work, the most convenient form is that given by Eq. (4.23):

$$K(\omega,\underset{\sim}{k}) = 1 - \frac{\omega_p^2}{k_{\parallel} k^2} \sum_{n=-\infty}^{\infty} \int_{-\infty}^{\infty} dv_{\parallel} \frac{H_n(v_{\parallel})}{v_{\parallel} - w_n} = 0, \qquad Im(\omega) < 0 \quad , \tag{4.39}$$

where

$$H_n(v_{\parallel}) = 2\pi \int_0^{\infty} dv_{\perp} \left(\frac{n\omega_c}{v_{\perp}} \frac{\partial f_o}{\partial v_{\perp}} + k_{\parallel} \frac{\partial f_o}{\partial v_{\parallel}} \right) J_n^2 \left(\frac{k_{\perp} v_{\perp}}{\omega_c} \right) v_{\perp} \quad . \tag{4.40}$$

Here w_n has been written for $(\omega - n\omega_c)/k_{\parallel}$. A background of singly charged ions, with a density equal to that of the electrons, is also present in the plasma, but the motion of these particles is neglected due to their

large mass. We now assume that the wave vector $\underset{\sim}{k}$ is real and look for roots of Eq. (4.39) that are close to the real ω axis and that are characterized by the inequalities,

$$|\omega_i/k_{\parallel}| \ll v_{t\parallel} \quad \text{and} \quad |(\omega_r - n\omega_c)/k_{\parallel}| \gg v_{t\parallel} , \tag{4.41}$$

for all n. Here the quantities ω_r and ω_i are, respectively, the real and imaginary parts of the complex frequency ω, and $v_{t\parallel}$ is the effective thermal speed of electrons along the magnetic field. Since $(\omega_i/k_{\parallel})$ is small, an approximate expression for these roots can be found by expanding the n^{th} integral in Eq. (4.39) in powers of the imaginary part of w_n, according to a prescription given by Jackson [42]:

$$\int_{-\infty}^{\infty} dv_{\parallel} \frac{H_n(v_{\parallel})}{v_{\parallel} - w_{nr} - iw_{ni}} = \sum_{m=0}^{\infty} \frac{(iw_{ni})^m}{m!} \left[P \int_{-\infty}^{\infty} dv_{\parallel} \frac{H_n(v_{\parallel})}{v_{\parallel} - w_{nr}} - \pi i H_n^{(m)}(w_{nr}) \right] . \tag{4.42}$$

Here we have made the substitution $w = w_{nr} + iw_{ni}$, and for definiteness, have assumed that $k_{\parallel}$ is greater than zero. Equation (4.42) is now substituted in Eq. (4.39) and the real and imaginary parts of $D(\omega,\underset{\sim}{k})$ are set equal to zero, giving us the expressions,

$$\mathrm{Re}[K(\omega,\underset{\sim}{k})] = 1 - \frac{\omega_p^2}{k_{\parallel} k^2} \sum_{n=-\infty}^{\infty} \left[P \int_{-\infty}^{\infty} dv_{\parallel} \frac{H_n(v_{\parallel})}{v_{\parallel} - w_{nr}} + \pi w_{ni} H_n^{(1)}(w_{nr}) + O(w_{ni}^2) \right] = 0 , \tag{4.43a}$$

$$\mathrm{Im}[K(\omega,\underset{\sim}{k})] = -\frac{\omega_p^2}{k_\parallel k^2}\sum_{n=-\infty}^{\infty}\left[w_{ni}\,P\int_{-\infty}^{\infty}dv_\parallel\,\frac{H_n^{(1)}(v_\parallel)}{v_\parallel - w_{nr}}\right.$$

$$\left. - \pi H_n(w_{nr}) + O(w_{ni}^2)\right] = 0 \quad , \qquad (4.43b)$$

where only terms up to the order of w_{ni} have been retained. To lowest significant order in w_{ni}, the solution of these equations for ω_i is

$$\omega_i = \frac{\pi k_\parallel \sum_{n=-\infty}^{\infty} H_n\left(\frac{\omega_r - n\omega_c}{k_\parallel}\right)}{\sum_{n=-\infty}^{\infty} P\int_{-\infty}^{\infty}dv_\parallel\,\frac{H_n^{(1)}(v_\parallel)}{v_\parallel - (\omega_r - n\omega_c)/k_\parallel}} \quad , \qquad (4.44)$$

where ω_r is determined by the expression

$$1 - \frac{\omega_p^2}{k_\parallel k^2}\sum_{n=-\infty}^{\infty} P\int_{-\infty}^{\infty}dv_\parallel\,\frac{H_n(v_\parallel)}{v_\parallel - (\omega_r - n\omega_c)/k_\parallel} = 0 \quad . \qquad (4.45)$$

In obtaining these expressions, use has been made of the definitions, $w_{ni} = \omega_i/k_\parallel$ and $w_{nr} = (\omega_r - n\omega_c)/k_\parallel$. Since, from Eq. (4.41), the quantity $(\omega_r - n\omega_c)/k_\parallel$ greatly exceeds $v_{t\parallel}$, the parallel component of the electron thermal velocity, the singularities on the real $v_\parallel$ axis in Eqs. (4.44) and (4.45) are located where $H_n(v_\parallel)$ is vanishingly small. Consequently, it is reasonable to neglect the contribution of the pole and use the expansion

$$\frac{1}{v_\parallel - (\omega_r - n\omega_c)/k_\parallel} = \frac{-k_\parallel}{\omega_r - n\omega_c}\sum_{m=0}^{M}\frac{v_\parallel^m k_\parallel^m}{(\omega_r - n\omega_c)^m} \quad , \qquad (4.46)$$

M being the total number of terms in the approximate series,

to obtain an asymptotic expansion of the principal value integrals as $k_{\parallel} \to 0$. Combining Eqs. (4.40), (4.45), and (4.46), and noting the symmetry condition $f_o(v_\perp, -v_\parallel) = f_o(v_\perp, v_\parallel)$ it is readily established, after judiciously integrating by parts, that the real part of the frequency is determined by the equation,

$$1 - \frac{\omega_p^2}{\omega_c^2}\left[\frac{k_\perp^2}{k^2}\sum_{n=-\infty}^{\infty} a_n \frac{n\omega_c}{\omega_r - n\omega_c} + \frac{k_\parallel^2}{k^2}\sum_{n=-\infty}^{\infty} b_n \frac{\omega_c^2}{(\omega_r - n\omega_c)^2}\right.$$

$$\left. + \frac{k_\parallel^2}{k^2}\sum_{n=-\infty}^{\infty} c_n \frac{n\omega_c^3}{(\omega_r - n\omega_c)^3} + 3\frac{k_\parallel^4}{k^4}\sum_{n=-\infty}^{\infty} d_n \frac{\omega_c^4}{(\omega_r - n\omega_c)^4} + \ldots\right] = 0 \,, \tag{4.47}$$

where the dimensionless coefficients a_n, b_n, c_n, and d_n are defined as follows:

$$a_n = -\frac{\omega_c^2}{k_\perp^2}\int d\underset{\sim}{v}\, \frac{1}{v_\perp}\frac{\partial f_o}{\partial v_\perp} J_n^2\left(\frac{k_\perp v_\perp}{\omega_c}\right) \,, \tag{4.48a}$$

$$b_n = \int d\underset{\sim}{v}\, f_o\, J_n^2\left(\frac{k_\perp v_\perp}{\omega_c}\right) \,, \tag{4.48b}$$

$$c_n = -\int d\underset{\sim}{v}\, \frac{1}{v_\perp}\frac{\partial f_o}{\partial v_\perp} J_n^2\left(\frac{k_\perp v_\perp}{\omega_c}\right) v_\parallel^2 \,, \tag{4.48c}$$

$$d_n = \frac{k^2}{\omega_c^2}\int d\underset{\sim}{v}\, f_o\, J_n^2\left(\frac{k_\perp v_\perp}{\omega_c}\right) v_\parallel^2 \,. \tag{4.48d}$$

In deriving these expressions, it is necessary to make the assumption that the function $v_{\parallel}^{3} f_o(v_\perp, v_\parallel)$ approaches zero as $|v_\parallel|$ approaches ∞. Equation (4.47) can be regarded as an expansion of the dispersion relation in terms of the mean thermal speed of the electrons along the magnetic field. If only the first two terms of the expansion are retained, the dispersion relation will have the form

$$1 - \frac{\omega_p^2}{\omega_c^2}\left[\frac{k_\perp^2}{k^2}\sum_{n=-\infty}^{\infty} a_n \frac{n\omega_c}{\omega_r - n\omega_c} + \frac{k_\parallel^2}{k^2}\sum_{n=-\infty}^{\infty} b_n \frac{\omega_c^2}{(\omega_r - n\omega_c)^2}\right] = 0 , \quad (4.49)$$

which will be recognized as the dispersion relation of a plasma in which the electrons have no motion parallel to the magnetic field. This case was treated in Section A of this chapter. The remaining two terms in the expansion in Eq. (4.47) represent the lowest order thermal correction to Eq. (4.49).

In Eq. (4.44) the denominator is an infinite series of principal value integrals. Each integral can be evaluated in a manner similar to that used above since the pole at $v_\parallel = (\omega_r - n\omega_c)/k_\parallel$ is far out on the real axis where, we assume, $H_n^{(1)}(v_\parallel)$, the first derivative of $H_n(v_\parallel)$, is vanishingly small. Combining the n^{th} integral in the denominator with Eq. (4.46) and using Eq. (4.40) we find, after integrating judiciously by parts,

$$P\int_{-\infty}^{\infty} dv_\parallel \frac{H_n^{(1)}(v_\parallel)}{v_\parallel - (\omega_r - n\omega_c)/k_\parallel} = -\frac{k_\parallel^2}{\omega_c^2}\left[k_\perp^2 \sum_{n=-\infty}^{\infty} a_n \frac{n\omega_c}{(\omega_r - n\omega_c)^2}\right.$$

$$+ 2k_\parallel^2 \sum_{n=-\infty}^{\infty} b_n \frac{\omega_c^2}{(\omega_r - n\omega_c)^3} + 3k_\parallel^2 \sum_{n=-\infty}^{\infty} c_n \frac{n\omega_c^3}{(\omega_r - n\omega_c)^4}$$

$$\left. + 12\frac{k_\parallel^4}{\omega_c^2}\sum_{n=-\infty}^{\infty} d_n \frac{\omega_c^4}{(\omega_r - n\omega_c)^5} + \ldots\right] . \quad (4.50)$$

It is also necessary to assume that certain derivatives of $f_o(v_\perp, v_\parallel)$ vanish as $|v_\parallel| \to \infty$. This expansion has been carried out to the same order in the electron thermal speed along the magnetic field as Eq. (4.47).

In order to determine the accuracy of our approximate formulas, we now consider a specific velocity distribution and compare the dispersion characteristics obtainable from Eqs. (4.44) and (4.45) with the exact numerical solution of Eq. (4.39). We assume that the electrons have an isotropic Maxwellian velocity distribution:

$$f_o(v_\perp, v_\parallel) = \left(\frac{1}{2\pi v_t^2}\right)^{3/2} \exp\left(-\frac{v_\perp^2 + v_\parallel^2}{2v_t^2}\right). \tag{4.51}$$

Substituting this expression in Eqs. (4.40) and (4.48), and integrating with the aid of the identity [25],

$$\int_0^\infty \exp(-\gamma^2 t^2)\, J_n^2(\alpha t)\, t\, dt = \frac{1}{2\gamma^2} \exp\left(-\frac{\alpha^2}{2\gamma^2}\right) I_n\left(\frac{\alpha^2}{2\gamma^2}\right), \tag{4.52}$$

yields

$$H_n(v_\parallel) = -\frac{\exp(-\lambda)\, I_n(\lambda)}{\sqrt{\pi}\, v_t^2} \frac{\exp(-v_\parallel^2/2v_t^2)}{\sqrt{2}\, v_t} (n\omega_c + k_\parallel v_\parallel), \tag{4.53}$$

$$a_n = \frac{\exp(-\lambda)\, I_n(\lambda)}{\lambda}, \tag{4.54a}$$

$$b_n = \exp(-\lambda)\, I_n(\lambda), \tag{4.54b}$$

$$c_n = \exp(-\lambda)\, I_n(\lambda), \tag{4.54c}$$

$$d_n = \left(\frac{k^2 v_t^2}{\omega_c^2}\right) \exp(-\lambda)\, I_n(\lambda), \tag{4.54d}$$

where λ has been written for $(k_\perp v_t/\omega_c)^2$. The dispersion relation for the isotropic Maxwellian distribution is given by Eq. (4.35) and solutions for $\omega(k_\parallel)$ are shown in Fig. 32. As a first approximation to these curves, we use Eqs. (4.44) and (4.45), and Eqs. (4.49) and (4.50). For the plasma under discussion,

$$\omega_i = \frac{\sqrt{\pi}\,\omega_r \sum_{n=-\infty}^{\infty} \exp(-\lambda)\, I_n(\lambda)\, \frac{\exp\left[-(\omega_r - n\omega_c)^2/2v_t^2k_\parallel^2\right]}{\sqrt{2}\, v_t k_\parallel}}{\sum_{n=-\infty}^{\infty} \exp(-\lambda)\, I_n(\lambda)\, \frac{n\omega_c}{(\omega_r - n\omega_c)^2} + 2\left(\frac{k_\parallel^2 v_t^2}{\omega_c^2}\right) \sum_{n=-\infty}^{\infty} \exp(-\lambda)\, I_n(\lambda)\, \frac{\omega_c^2}{(\omega_r - n\omega_c)^3}} \tag{4.55}$$

where the real part of the frequency is determined by the equation,

$$1 - \frac{\omega_p^2}{\omega_c^2}\left[\frac{k_\perp^2}{k^2} \sum_{n=-\infty}^{\infty} \frac{\exp(-\lambda)\, I_n(\lambda)}{\lambda} \frac{n\omega_c}{\omega_r - n\omega_c} + \frac{k_\parallel^2}{k^2} \sum_{n=-\infty}^{\infty} \exp(-\lambda)\, I_n(\lambda)\, \frac{\omega_c^2}{(\omega_r - n\omega_c)^2}\right] = 0 \quad . \tag{4.56}$$

It is pointed out that only the first two terms of Eq. (4.50) have been retained in order to be consistent with the order of the expansion of Eq. (4.49). Figure 30 shows typical solutions of Eq. (4.56) for ω_r. It is seen that for certain ranges of $(k_\parallel v_t/\omega_c)$, ω_r may be complex (the imaginary part is shown as a dashed line and drawn to the base $\omega_r = n\omega_c$), which is completely inconsistent with our initial assumption that ω_r is real. However, when $(k_\parallel v_t/\omega_c)$ is sufficiently small, ω_r is real and,

qualitatively, has the same dependence on the wave number as the frequencies shown in Fig. 32. A comparison between the exact and approximate solutions of the dispersion relation shows that good agreement is possible only in the limit as $k_{\parallel} \to 0$. This is illustrated in Fig. 33a with the imaginary part of ω. Equations (4.55) and (4.56) were used to compute the approximate curves, and the mode beginning at $(\omega_r/\omega_c) = 1.409$, when $k_{\parallel} \equiv 0$, was chosen. It is seen that even when (ω_i/ω_c) is as small as 10^{-15}, a discrepancy between the two curves is present. Better agreement can be attained if we expand the approximate formulas to a higher order in the thermal speed of the electrons, as given by Eqs. (4.47) and (4.50). For an isotropic Maxwellian distribution, Eq. (4.44) then has the form,

$$\omega_i = \frac{\sqrt{\pi}\,\omega_r \sum_{n=-\infty}^{\infty} \exp(-\lambda)\, I_n(\lambda)\, \dfrac{\exp\left[-(\omega_r - n\omega_c)^2/2v_t^2 k_{\parallel}^2\right]}{\sqrt{2}\, v_t k_{\parallel}}}{G(\omega_r)} \tag{4.57}$$

where the real part of the frequency is determined by

$$1 - \frac{\omega_p^2}{\omega_c^2}\left[\frac{k_{\perp}^2}{k^2}\sum_{n=-\infty}^{\infty}\frac{\exp(-\lambda)\, I_n(\lambda)}{\lambda}\frac{n\omega_c}{\omega_r - n\omega_c} + \frac{k_{\parallel}^2}{k^2}\sum_{n=-\infty}^{\infty}\exp(-\lambda)\, I_n(\lambda)\frac{\omega_c^2}{(\omega_r - n\omega_c)^2}\right.$$

$$+ \frac{k_{\parallel}^2}{k^2}\sum_{n=-\infty}^{\infty}\exp(-\lambda)\, I_n(\lambda)\frac{n\omega_c^3}{(\omega_r - n\omega_c)^3}$$

$$\left. + 3\left(\frac{k^2 v_t^2}{\omega_c^2}\right)\frac{k_{\parallel}^4}{k^4}\sum_{n=-\infty}^{\infty}\exp(-\lambda)\, I_n(\lambda)\frac{\omega_c^4}{(\omega_r - n\omega_c)^4}\right] = 0\,, \tag{4.58}$$

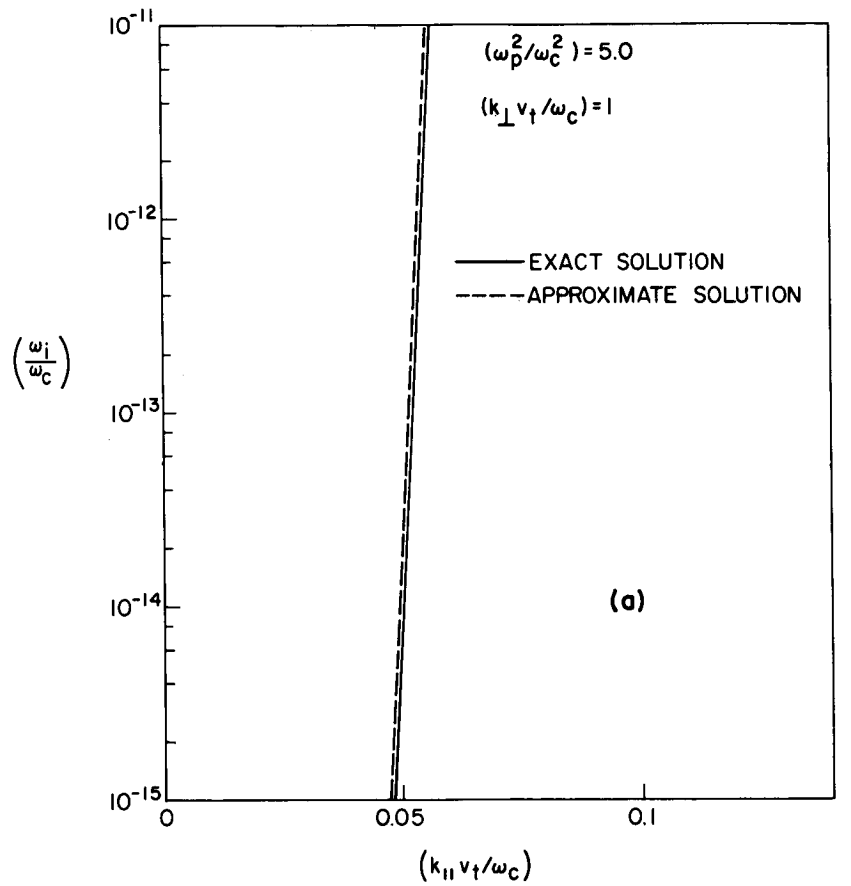

Fig. 33. IMAGINARY PART OF ω FOR OBLIQUELY PROPAGATING CYCLOTRON HARMONIC WAVES IN A MAXWELLIAN PLASMA. In (a), the dashed line was computed from an approximate formula which neglects the thermal motion of the electrons parallel to the magnetic field when the real part of ω is computed; in (b), the real part of ω is evaluated to lowest order in the parallel thermal speed of the electron.

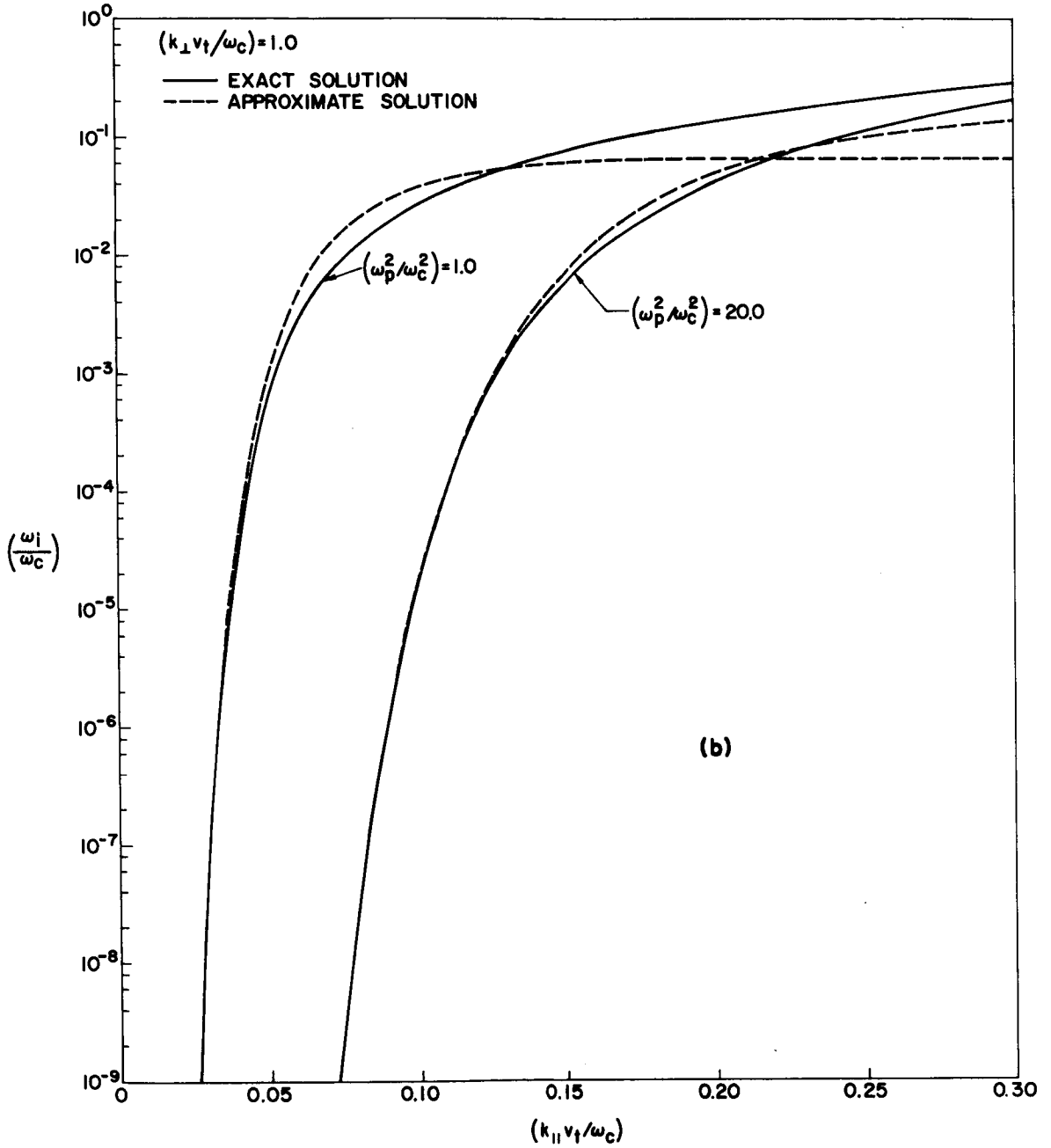

Fig. 33. CONTINUED.

and the function $G(\omega_r)$ is defined as follows:

$$G(\omega_r) = \sum_{n=-\infty}^{\infty} \exp(-\lambda)\, I_n(\lambda)\, \frac{n\omega_c}{(\omega_r - n\omega_c)^2} + 2\left(\frac{k_{\parallel}^2 v_t^2}{\omega_c^2}\right) \sum_{n=-\infty}^{\infty} \exp(-\lambda)\, I_n(\lambda)\, \frac{\omega_c^2}{(\omega_r - n\omega_c)^3}$$

$$+ 3\left(\frac{k_{\parallel}^2 v_t^2}{\omega_c^2}\right) \sum_{n=-\infty}^{\infty} \exp(-\lambda)\, I_n(\lambda)\, \frac{n\omega_c^3}{(\omega_r - n\omega_c)^4}$$

$$+ 12\left(\frac{k_{\parallel}^4 v_t^4}{\omega_c^4}\right) \sum_{n=-\infty}^{\infty} \exp(-\lambda)\, I_n(\lambda)\, \frac{\omega_c^4}{(\omega_r - n\omega_c)^5} \quad . \tag{4.59}$$

Figure 33b compares Eq. (4.57) with the imaginary part of ω obtained from the exact numerical solution of the dispersion relation. These curves correspond to the same mode examined in Fig. 33a. For $(\omega_p^2/\omega_c^2) = 1$, exact agreement is seen for $(k_{\parallel} v_t/\omega_c)$ out to approximately 0.034, corresponding to an angle of propagation of 88.5° with respect to the direction of the magnetic field. This angular range can be increased by increasing the parameter (ω_p^2/ω_c^2). For $(\omega_p^2/\omega_c^2) = 20.0$, exact agreement occurs out to 85°.

The approximate formulas that have been derived in this report are not capable of reproducing the dispersion characteristics of the modes that are found near the harmonics of the electron cyclotron frequency. Indeed, for ω near $n\omega_c$, Eqs. (4.55) and (4.57) predict that ω_i is less than zero, implying temporal growth. However, this cannot occur in a plasma with an isotropic Maxwellian velocity distribution. The reason for this breakdown is that our initial assumptions, Eq. (4.41), are not valid near the harmonics. This is readily established by using Eq. (4.49) to show that

$$\lim_{k_{\parallel} \to 0} \frac{\omega_r - n\omega_c}{k_{\parallel}} = 0 \quad . \tag{4.60}$$

D. Classification of Instabilities

It was pointed out in Chapter III that instabilities can take on one of two forms, as illustrated in Fig. 13. If the amplitude of a plasma disturbance increases indefinitely with time at any point in space, the instability is absolute and hence no steady state can be maintained. However, it is possible that an excited pulse will propagate away from a region of space while the amplitude of the pulse will grow with time. This situation will leave the plasma in a quiescent condition, implying that a steady state is possible. Instabilities of the latter type are called convective. In this section the instabilities associated with obliquely propagating cyclotron harmonic waves are classified according to this prescription.

The basic ideas that are relevant to the classification are summarized in Chapter III (Section C). The main part of the criterion is a mapping of the lower half complex frequency plane onto the complex wave number plane via the dispersion relation. If this mapping shows that two or more roots of the dispersion relation, which are located on opposite sides of the real wave number axis when ω is on the Laplace contour, merge to a single point as ω approaches some frequency with negative imaginary part, absolute instability is present. If this merging does not occur, the instability is convective.

Before applying this criterion, it is important to note that the representation of the dielectric constant given by Eq. (4.23) is not a unique function, but one with two branches if $k_{\parallel}$ is real. The two branches are readily identifiable if use is made of the identity

$$\frac{1}{v_{\parallel} - w_n} = -i \int_0^{\pm\infty} d\zeta \, \exp\left[i(v_{\parallel} - w_n)\zeta\right] , \qquad (4.61)$$

where w_n has been written for $(\omega - n\omega_c)/k_{\parallel}$. In order to insure convergence of the integral, the plus sign is chosen if $\mathrm{Im}(w_n) < 0$, and the negative sign if $\mathrm{Im}(w_n) > 0$. Substituting Eq. (4.61) in Eq. (4.23) and assuming that the imaginary part of ω is less than zero leads to the following expression:

$$K(\omega,\underset{\sim}{k}) = \begin{cases} K^{+}(\omega,k_{\perp},k_{\parallel}) = 1 + 2\pi i \dfrac{\omega_p^2}{k_{\parallel}k^2} \displaystyle\sum_{n=-\infty}^{\infty} H_n^{+}\left(\dfrac{\omega - n\omega_c}{k_{\parallel}}, k_{\perp}, k_{\parallel}\right), & k_{\parallel} > 0 , \quad (4.61a) \\ K^{-}(\omega,k_{\perp},k_{\parallel}) = 1 - 2\pi i \dfrac{\omega_p^2}{k_{\parallel}k^2} \displaystyle\sum_{n=-\infty}^{\infty} H_n^{-}\left(\dfrac{\omega - n\omega_c}{k_{\parallel}}, k_{\perp}, k_{\parallel}\right), & k_{\parallel} < 0 , \quad (4.61b) \end{cases}$$

where the positive and negative "frequency" parts of H_n, respectively, are defined as

$$H_n^{+}(w_n,k_{\perp},k_{\parallel}) = \int_0^{\infty} \frac{d\zeta}{2\pi} \exp\,(-iw_n\zeta)\, \bar{H}_n(\zeta,k_{\perp},k_{\parallel}) \qquad (4.62a)$$

and

$$H_n^{-}(w_n,k_{\perp},k_{\parallel}) = \int_{-\infty}^{0} \frac{d\zeta}{2\pi} \exp\,(-iw_n\zeta)\, \bar{H}_n(\zeta,k_{\perp},k_{\parallel}) \,. \qquad (4.62b)$$

In these expressions the function $\bar{H}_n(t,k_{\perp},k_{\parallel})$ is the Fourier transform of $H_n(v_{\parallel},k_{\perp},k_{\parallel})$, that is,

$$\bar{H}_n(\zeta,k_{\perp},k_{\parallel}) = \int_{-\infty}^{\infty} dv_{\parallel} \exp\,(iv_{\parallel}\zeta)\, H_n(v_{\parallel},k_{\perp},k_{\parallel}) \,. \qquad (4.63)$$

It is remarked that the two branches, K^{+} and K^{-}, are not independent but are connected by the relationship

$$K^{+}(-\omega^{*},k_{\perp},k_{\parallel}) = K^{-}(\omega,k_{\perp},-k_{\parallel})^{*} \,, \qquad (4.64)$$

as shown in Appendix B.

As a result of the decomposition in $K(\omega,k_\perp,k_\parallel)$ in Eq. (4.61), the instability criterion stated in Chapter III must be modified slightly. Derfler [32] has given the appropriate changes when a dispersion function has properties similar to those indicated by Eqs. (4.61) and (4.64). For purposes of discussion, we assume that $k_\perp$ is a fixed, real number and that the propagation is parallel to the magnetic field with frequency ω and wave number $k_\parallel$. Then, it can be inferred from Derfler's work that absolute instability is present if (1) zeros of $K^+(\omega,k_\perp,k_\parallel)$ collide across the positive $k_\parallel$ axis--rather than the entire $k_\parallel$ axis--as ω varies along some contour in the lower half complex plane, or if (2) zeros of $K^-(\omega,k_\perp,k_\parallel)$ collide across the negative $k_\parallel$ axis as the frequency varies in the lower half plane.

For purposes of illustrating the type of instabilities that can be expected for oblique propagation, we consider the following electron velocity distribution,

$$f_o(v_\perp,v_\parallel) = \frac{v_{t\parallel}^3}{\pi^2 v_{t\perp}^2} \frac{\exp\,(-v_\perp^2/2v_{t\perp}^2)}{(v_\parallel^2 + v_{t\parallel}^2)^2} , \qquad (4.65)$$

implying that the transverse velocity components have a Maxwellian distribution while the parallel components have a second-order resonance distribution. In order to obtain the positive frequency component of $K(\omega,\underset{\sim}{k})$, Eq. (4.65) is substituted in Eq. (4.23) and the integration is first carried out with respect to $v_\perp$ using Eq. (4.29), and then with respect to $v_\parallel$ by the method of residues under the assumption that $\mathrm{Im}(\omega) < 0$ and $k_\parallel > 0$. This procedure yields the dispersion relation,

$$K^+(\omega,\underset{\sim}{k}) = 1 - \frac{\omega_p^2}{\omega_c^2}\left[F(\omega - iv_{t\parallel}k_\parallel,k_\perp,k_\parallel)\right.$$

$$\left. + iv_{t\parallel}k_\parallel \frac{\partial F(\omega - iv_{t\parallel}k_\parallel,k_\perp,k_\parallel)}{\partial\omega}\right] = 0 , \qquad (4.66)$$

where

$$F(\omega,k_\perp,k_{||}) = \frac{k_\perp^2}{k^2} \sum_{n=-\infty}^{\infty} \frac{\exp(-\lambda)\, I_n(\lambda)}{\lambda} \frac{n\omega_c}{\omega - n\omega_c}$$

$$+ \frac{k_{||}^2}{k^2} \sum_{n=-\infty}^{\infty} \exp(-\lambda)\, I_n(\lambda) \frac{\omega_c^2}{(\omega - n\omega_c)^2} \quad . \qquad (4.67)$$

In Eq. (4.67) the variable λ has been written for $(k_\perp v_{t\perp}/\omega_c)$. In order to show where instability can be expected in this case, the complex frequency solutions of Eq. (4.66) are plotted in Fig. 34 for positive, real $k_{||}$. As in previous examples, there exist two propagating modes

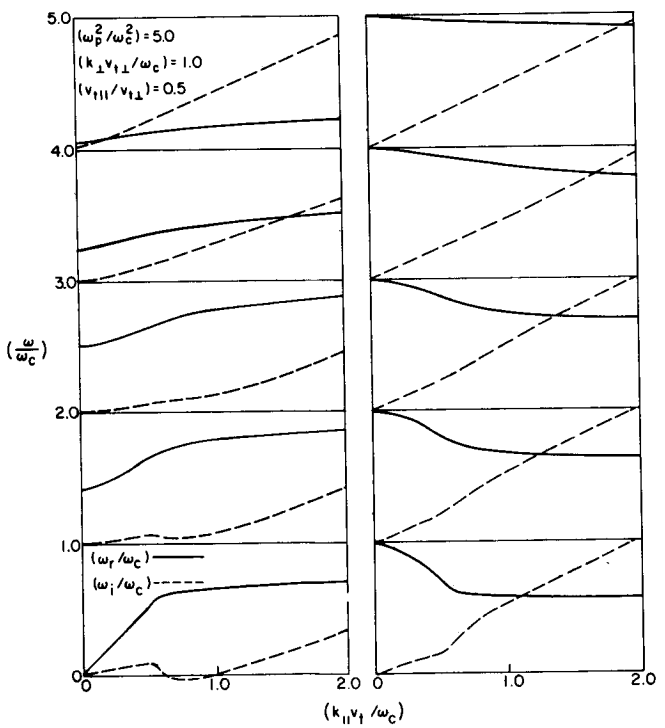

Fig. 34. DISPERSION CHARACTERISTICS FOR OBLIQUELY PROPAGATING CYCLOTRON HARMONIC WAVES; MAXWELLIAN DISTRIBUTION IN THE TRANSVERSE VELOCITY COMPONENT $v_\perp$ AND A SECOND-ORDER RESONANCE DISTRIBUTION IN THE PARALLEL VELOCITY COMPONENT $v_{||}$.

in each passband, one of which may go unstable as a result of a dip in the imaginary part of ω. Instability occurs when the minimum of the dip passes the line, $\omega_i = 0$. Figure 35 shows the variation of one unstable mode (dashed line) in the complex ω plane as a function of the velocity ratio $(v_{t\parallel}/v_{t\perp})$. The four contours, A, B, C, D, are now mapped onto the complex $\mu_\parallel$ plane and a search is made for saddle-points where $(\partial K^+/\partial k_\parallel) = 0$, corresponding to the merging of two zeros of $K^+(\omega,\underset{\sim}{k})$. If these zeros originate from opposite sides of the real $k_\parallel$ axis, an absolute instability is present. For the case where $(v_{t\parallel}/v_{t\perp}) = 0.42$, a saddlepoint is found at $\mu_{\parallel o} = 6.81 + i1.65$ when $(\omega/\omega_c)_o = 1.405 - i0.03$. Since the positive wave number axis is also pinched, an absolute instability is present. If the velocity ratio is now increased to 0.43, the contour of integration is again pinched, but the frequency at which this occurs is located above the real axis. Therefore, the instability in this case is convective since there are still complex frequency solutions with $\mathrm{Im}(\omega/\omega_c) < 0$ and real wave number. A further increase in the velocity ratio to 0.5 completely stabilizes the plasma.

E. Discussion

The main features of this chapter can be summarized as follows: Electrostatic waves propagating in a bounded magnetoplasma with a ring electron velocity distribution support a large class of instabilities that have onset conditions that are far less stringent than for purely perpendicular propagation. In a given frequency passband there is found a series of bounded regions in $\mu_\perp (\equiv k_\perp v_{o\perp}/\omega_c)$ where growing waves are predicted. The regions are defined by

$$\alpha_{nm} < \mu_\perp < \alpha_{n+1,m} \quad , \tag{4.68}$$

where α_{nm} is the m^{th} zero of the Bessel function of order n. For other values of $\mu_\perp$ the waves propagate without growth or attenuation. If temperature is first introduced in the plane perpendicular to the magnetic field, only one range of $\mu_\perp$ predicts growing oscillations. Temperature effects parallel to the magnetic field are manifested by

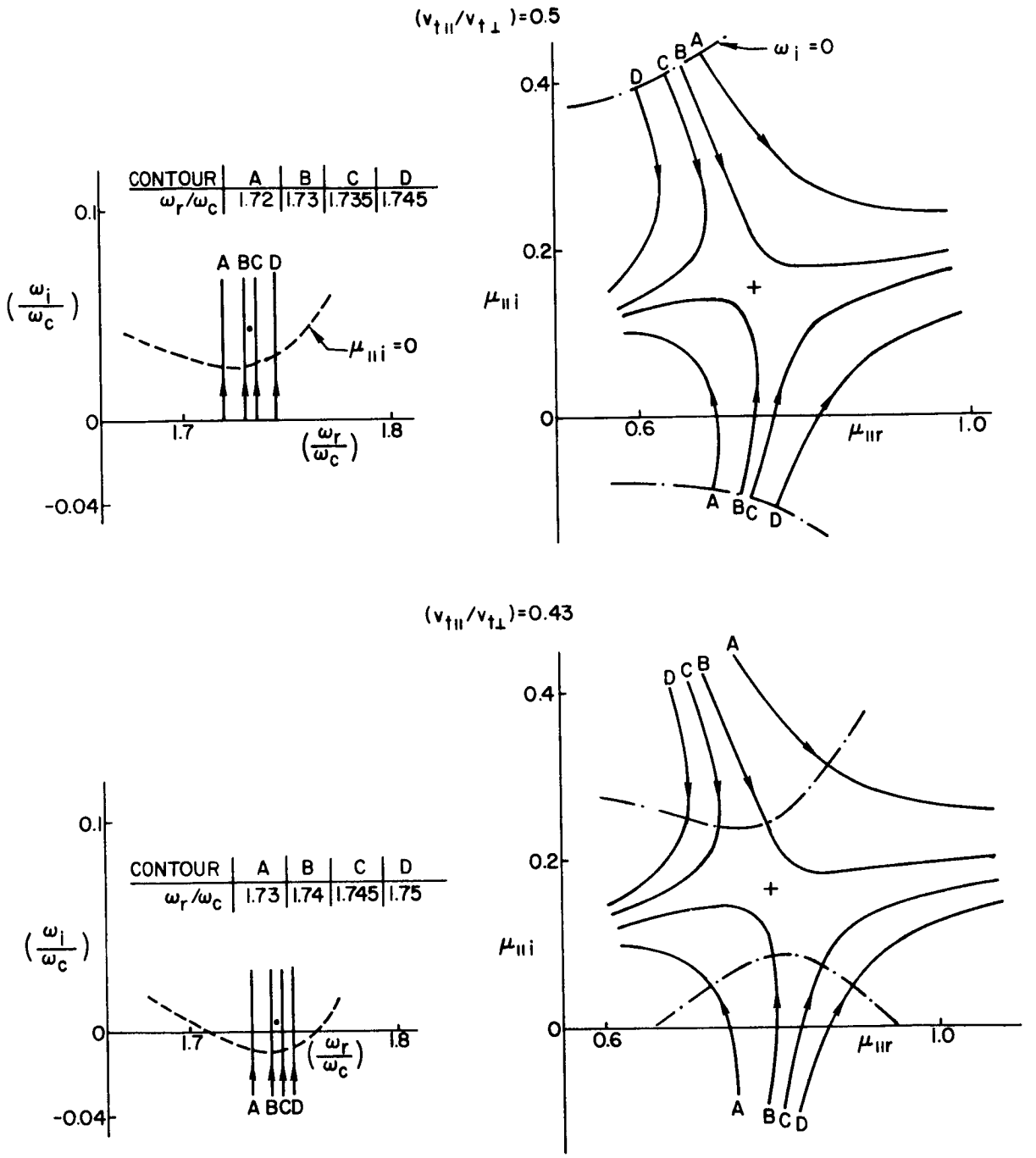

Fig. 35. CONFORMAL MAPPING OF CONTOURS A, B, C, D, TO COMPLEX $k_{\parallel}$ PLANE VIA THE EQUATION $K^{+}(\omega,\underset{\sim}{k}) = 0$, ESTABLISHING THE TYPE OF INSTABILITY EXCITED BY OBLIQUELY PROPAGATING CYCLOTRON HARMONIC WAVES. The instability is convective for $(v_{t\parallel}/v_{t\perp}) = 0.43$, absolute for $(v_{t\parallel}/v_{t\perp}) = 0.42$, while the plasma is stable for $(v_{t\parallel}/v_{t\perp}) = 0.5$.

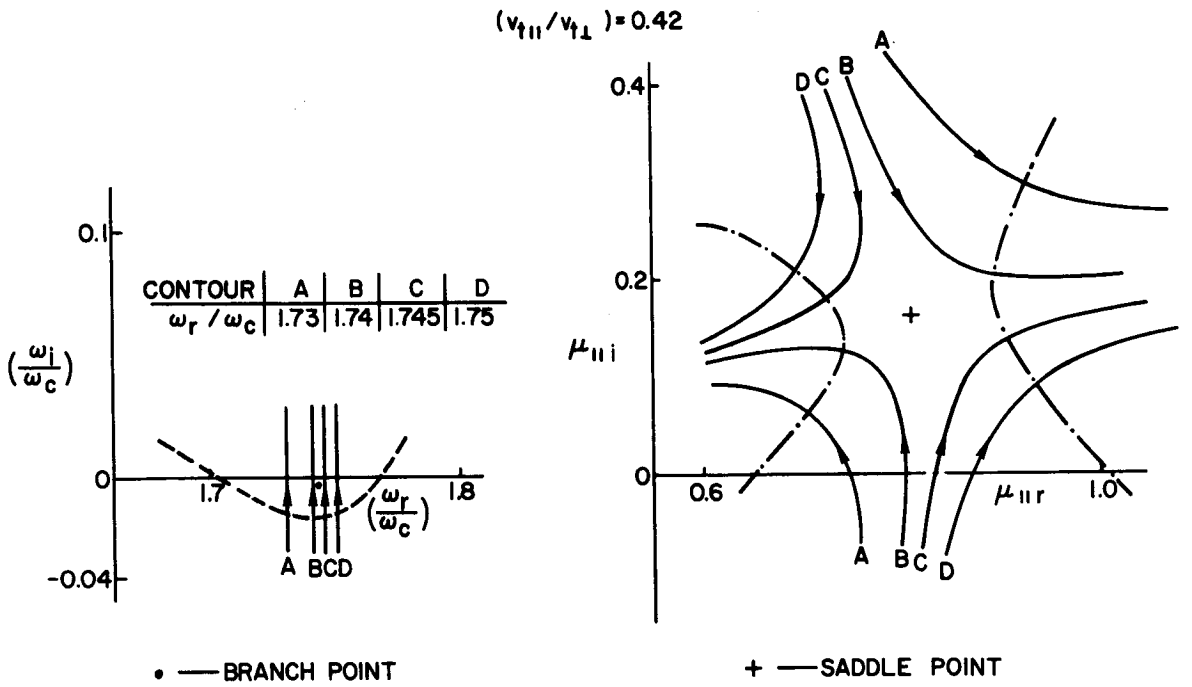

Fig. 35. CONTINUED.

strong damping of waves with small wavelengths and by weak damping for propagation nearly perpendicular to the magnetic field. Also, if the velocity distribution is sufficiently anisotropic, instability is predicted for a finite band in $\mu_{\parallel} (\equiv k_{\parallel} v_{t\parallel}/\omega_c)$. Finally, the instabilities were classified as being either convective or absolute. It was demonstrated that for a sufficiently low temperature parallel to the magnetic field, the instabilities are absolute. However, as the ratio $(v_{t\parallel}/v_{t\perp})$ approaches unity, the instability becomes convective and then damping sets in.

V. EXCITATION OF ELECTROSTATIC RESONANCES IN A HOT MAGNETOPLASMA

In recent years a considerable amount of experimental evidence has been accumulated, from both laboratory and ionospheric studies, which indicates the presence of strong resonant effects, or prolonged ringing, in magnetoplasmas. Resonances have been detected at harmonics of the electron cyclotron frequency, at the plasma frequency, and at the upper hybrid frequency. In this chapter it is shown that within the range of the electrostatic approximation, resonant plasma oscillations can be excited perpendicular to the magnetic field at frequencies which agree with experimental observations.

The background and some introductory considerations of the problem are given in Section A. This is followed in Section B by the definition of the plasma Green's function and a study of its analyticity in the complex ω plane. In Section C we obtain the asymptotic form of the excited electric field as $t \to \infty$. We examine in Section D the dependence of the resonances on the spatial form of the source and, in particular, we consider a source that is periodic in space. The results are discussed in Section E.

A. Basic Equations

The theory which describes the behavior of plasmas in the presence of a uniform magnetic field, in the electrostatic approximation, has been given in Chapter II. If external charges are present with density $\rho_s(\underset{\sim}{r},t)$, space-charge oscillations can be excited in this medium with the associated fluctuating electric field obtainable from Eq. (2.49) by performing inverse Fourier and Laplace transformations. In this chapter the asymptotic behavior of the electric field is examined as t approaches infinity to determine the components of this field after the uninteresting transients have died out. The following assumptions are made concerning the plasma model: (a) The plasma is composed of electrons and ions with equal density, but the motion of the ions is neglected due to the relatively large mass of these particles; (b) the space-charge

oscillations are one-dimensional and directed along the x axis perpendicular to the magnetic field; and (c) the electron velocity distribution is an isotropic Maxwellian. Under these restrictions, only $E(x,t)$, the x component of the electric field, survives. Thus, by inverting Eq. (2.49), we find that our basic equation that must be evaluated is

$$E(x,t) = \int_C \frac{d\omega}{2\pi} \exp(i\omega t)\, F(\omega,x)\, f(\omega) \quad , \tag{5.1}$$

where

$$F(\omega,x) = i \int_{-\infty}^{\infty} \frac{dk_\perp}{2\pi} \frac{\exp(-ik_\perp x)\, g(k_\perp)}{\epsilon_o k_\perp K(\omega,k_\perp)} \quad , \tag{5.2}$$

and, from Eq. (3.63), the plasma dielectric constant perpendicular to the magnetic field is

$$K(\omega,k_\perp) = 1 - \frac{\omega_p^2}{\omega_c^2} \sum_{n=-\infty}^{\infty} \frac{\exp(-\lambda)\, I_n(\lambda)}{\lambda} \frac{n\omega_c}{\omega - n\omega_c} \, . \tag{5.3}$$

Here, C is the Laplace contour running parallel to the real axis in the lower half complex ω plane; λ has been written for $(k_\perp v_{t\perp}/\omega_c)$, where $v_{t\perp}$ is the thermal speed of the electrons; and the source has been expressed as $\rho_s(x,t) = g(x)\, f(t)$, which is transformed to $\rho_s(k_\perp,\omega) = g(k_\perp)\, f(\omega)$. As t approaches infinity, the asymptotic form of Eq. (5.1) is determined by the singularities of the integrand. In this chapter we assume for convenience that $f(\omega)$ is analytic in the entire complex ω plane, thus representing excitation of the resonances by a temporal pulse. The singularities in the function $F(\omega,x)$ can be found with a technique introduced to plasma stability studies by Derfler [31], [32] and by Bers [33] and Briggs [34], and used in this report to classify cyclotron harmonic wave instabilities as either absolute or convective. These singularities arise from the deformation and pinching

of the contour of integration of Eq. (5.2) by two or more zeros of $K(\omega,k_\perp)$ as ω varies along some path in the complex plane. The basic parts of the technique are explained in Section III-C.

It should be remarked at this point that the determination of resonances in this manner is closely related to the problem of absolute instabilities in plasmas. If the function $F(\omega,x)$ has a pinching singularity in the lower half complex ω plane, the plasma is absolutely unstable. A necessary condition for this situation to occur is that the dispersion relation, $K(\omega,k_\perp) = 0$ possess complex frequency roots (with negative imaginary parts) with real wave number. We are concerned here with cases where $F(\omega,x)$ is analytic in the lower half plane but singular at isolated points on the real axis. Situations of this type are of significant importance since the electric field that remains as $t \to \infty$ will contain a component that decays very slowly with time. This is evident in Eq. (3.83) where a decay rate of $(1/t^{1/2})$ is indicated. This condition of long-lived fields, or ringing as it is often called, is defined as a resonance and has been the subject of a great deal of experimental research in plasma physics in recent years [11, 20, 21, 39].

In what follows, the real frequency resonances of a magnetoplasma with a Maxwellian transverse electron velocity distribution will be located. Although there are other stable distributions that have some academic interest and hence could be considered, the Maxwellian is more appropriate because of its common occurrence in both laboratory and extraterrestrial plasmas. Having found the frequency of the resonances, this will bring us naturally to our main objective, the derivation of the long-time behavior of the electric field. It may appear at first that this is given by Eq. (3.83). However, that formula is based on the assumption that two roots of the dispersion relation pinch the contour of integration. If the number of such roots exceeds two, the singularity in $F(\omega,x)$ will be different from what is shown in Eq. (3.82) and hence the limit of the electric field as $t \to \infty$ must be recomputed.

It should be pointed out that this problem has been treated previously with a different technique. Sturrock [43], for example, finds resonances at each harmonic of the electron cyclotron frequency and at the cold-plasma, upper hybrid frequency, but does not include in his analysis adequate

justification that a resonance does indeed occur at the indicated frequencies. However, with the use of the pinching criterion, this justification is readily established and, in addition, other resonances are obtained that Sturrock did not predict. The approach adopted here appears to have been first used in plasma wave studies by Nuttall [44] when he examined electromagnetic resonances in a magnetoplasma.

B. Singularities of the Green's Function

It is convenient to excite the resonances with a sheet charge located at $x = 0$. The spatial form of the source is then given by the expression, $g(x) = \delta(x)$, and hence, $g(k_\perp) = 1$. Under this assumption, Eq. (5.2) reads

$$F(\omega,x) = G(\omega,x) \equiv i \int_{-\infty}^{\infty} \frac{dk_\perp}{2\pi} \frac{\exp(-i k_\perp x)}{\epsilon_o k_\perp K(\omega,k_\perp)} , \tag{5.4}$$

and is clearly identifiable as a Green's function. The response of the plasma to a source with arbitrary spatial form is obtained from the convolution integral

$$F(\omega,x) = \int_{-\infty}^{\infty} dx' \, G(\omega,x-x') \, g(x') . \tag{5.5}$$

The multiple zeros of $K(\omega,k_\perp)$ which pinch the contour of integration of Eq. (5.4) can be obtained from the dispersion characteristics shown in Fig. 10. As explained in Section III-C, this may occur at frequencies where the group velocity $(d\omega/dk_\perp)$ vanishes. For a Maxwellian plasma, this condition is found at the following points:

(i) $k_\perp = 0$ when $\omega = n\omega$ and $n = \pm 2, \pm 3, \ldots$.

(ii) $k_\perp = \pm\infty$ when $\omega = n\omega_c$ and $n = \pm 1, \pm 2, \ldots$.

(iii) $k_\perp$ finite and nonzero when $|n|\omega_c < \omega < (|n| + 1)\omega_c$ and $n = 2, 3, \ldots$. Note from Fig. 10 that this case is not present in every frequency band. In fact, if $|n|\omega_c < (\omega_p^2 + \omega_c^2)^{1/2} < (|n| + 1)\omega_c$, the dispersion curves show that the group velocity is nonzero for $\omega < |n|\omega_c$ and $0 < k_\perp < \infty$.

It is pointed out, however, that case (ii) will probably not occur in more realistic plasma models. For example, it was shown in Chapter IV that when electron-neutral collisions are introduced in the theory, the double root at $k_\perp = \infty$ is replaced by two distinct roots which are located far in the complex plane, on opposite sides of the real axis. Collisions will also affect the other multiple roots in a similar manner but not as strongly as that which occurs at $k_\perp = \infty$. For this reason, case (ii) will not be included in the forthcoming work. It is now shown that cases (i) and (iii) are responsible for the singularities of $F(\omega,x)$ on the real ω axis.

1. Pinching at $k_\perp = 0$

The zeros of $K(\omega,k_\perp)$ in the vicinity of the origin in the complex $k_\perp$ plane are obtained by expanding Eq. (5.3) in a power series about $k_\perp = 0$. For ω near $n\omega_c$, this yields

$$K(\omega,k_\perp) \approx 1 - \frac{\omega_p^2}{\omega^2 - \omega_c^2} - \frac{1}{2^n n!} \frac{\omega_p^2}{\omega_c^2} \frac{n\omega_c}{\omega - n\omega_c} \left(\frac{k_\perp v_{t\perp}}{\omega_c}\right)^{2(n-1)} , \qquad n \geq 2 \qquad (5.6)$$

where use has been made of the small argument approximations of the Bessel and exponential functions to obtain for positive n

$$\exp(-\lambda)\, I_n(\lambda) \approx \frac{1}{n!} \left(\frac{\lambda}{2}\right)^n . \qquad (5.7)$$

If ω is near $(-n\omega_c)$ where $n > 2$, the symmetry condition $I_{-n}(\lambda) = I_n(\lambda)$ implies that the correct form of $K(\omega,k_\perp)$ is obtained from Eq. (5.6) with the substitution

$$\omega \rightarrow -\omega . \qquad (5.8)$$

Hence, any resonance found on the positive real frequency axis has associated with it a mirror image on the negative axis. For this reason, it is sufficient to restrict our work to positive harmonics of the cyclotron frequency.

The zeros of Eq. (5.6) are located at

$$k_{\perp j} = \frac{\omega_c}{v_{t\perp}} \left[2^n n! \, \frac{\omega_c^2}{\omega_p^2} \left(1 - \frac{\omega_p^2}{\omega^2 - \omega_c^2} \right) \frac{\omega - n\omega_c}{n\omega_c} \right]^{\frac{1}{2(n-1)}}$$

$$\cdot \exp \left(i \, \frac{j-1}{n-1} \, \pi \right) , \qquad j = 1, \ldots, 2(n-1) . \quad (5.9)$$

Since ω is near $n\omega_c$ and in the lower half complex plane, it is convenient to write

$$\omega = n\omega_c + \delta \exp (i\theta) , \quad (5.10)$$

where δ is a small expansion parameter and θ is in the range $-\pi < \theta < 0$. Equation (5.9) then reads to lowest significant order in δ:

$$k_{\perp j} = \frac{\omega_c}{v_{t\perp}} \left[\frac{2^n n!}{n\omega_c} \, \frac{\omega_c^2}{\omega_p^2} \left(1 - \frac{1}{n^2 - 1} \, \frac{\omega_p^2}{\omega_c^2} \right) \delta \right]^{\frac{1}{2(n-1)}}$$

$$\cdot \exp \left[i \, \frac{2(j-1)\pi + \theta}{2(n-1)} \right] , \qquad j = 1, \ldots, 2(n-1) . \quad (5.11)$$

It is clearly seen that surrounding the origin in the complex $k_\perp$ plane there exist $2(n-1)$ poles of the integrand of Eq. (5.2), with $(n-1)$ above the real axis and $(n-1)$ below. Furthermore, it is seen that the poles are uniformly distributed on the circumference of a circle centered at $k_\perp = 0$ with radius

$$\xi = \frac{\omega_c}{v_{t\perp}} \left[\frac{2^n n!}{n\omega_c} \, \frac{\omega_c^2}{\omega_p^2} \left(1 - \frac{1}{n^2 - 1} \, \frac{\omega_p^2}{\omega_c^2} \right) \delta \right]^{\frac{1}{2(n-1)}} . \quad (5.12)$$

Clearly, as $\delta \to 0$, that is, as $\omega \to n\omega_c$, the poles converge toward the origin to form a $2(n-1)^{th}$ root of the dispersion relation that pinches the real axis, and hence the contour of integration, at $k_\perp = 0$.

It is now a simple matter to find the form of $G(\omega,x)$ near the harmonics of the electron cyclotron frequency. Because of the presence of poles surrounding the origin the most significant contribution to Eq. (5.2) will come from values of $k_\perp$ near zero. Therefore, for ω sufficiently close to $n\omega_c$, an approximation to the integral will be obtained by substituting for the integrand its small argument expansion. Before doing this, it is convenient to separate $\exp(-ik_\perp x)$ into its real and imaginary parts to obtain, after invoking the symmetry condition $K(\omega,-k_\perp) = K(\omega,k_\perp)$

$$G(\omega,x) = \int_{-\infty}^{\infty} \frac{dk_\perp}{2\pi} \frac{\sin k_\perp x}{\epsilon_o k_\perp K(\omega,k_\perp)} \quad . \tag{5.13}$$

Substituting Eq. (5.6) for $K(\omega,k_\perp)$ and $k_\perp x$ for $\sin k_\perp x$, this expression reads, for ω in the lower half complex plane and near $n\omega_c$,

$$G(\omega,x) = -\frac{\alpha x}{2\pi\epsilon_o} (\omega - n\omega_c) \int_{-\infty}^{\infty} \frac{dk_\perp}{k_\perp^{2(n-1)} - \alpha K_c(\omega)(\omega - n\omega_c)} \quad , \tag{5.14}$$

where we have introduced the variables

$$K_c(\omega) = 1 - \frac{\omega_p^2}{\omega^2 - \omega_c^2} \quad , \qquad \alpha = \frac{2^n n!}{n\omega_c} \frac{\omega_c^2}{\omega_p^2} \left(\frac{\omega_c}{v_{t\perp}}\right)^{2(n-1)} \quad . \tag{5.15}$$

It will be noted that $K_c(\omega)$ is the effective cold-plasma dielectric constant in the direction perpendicular to the magnetic field.

The integration in Eq. (5.14) is accomplished with Cauchy's residue theorem, which permits us to write

$$G(\omega,x) = \frac{\alpha x}{i\epsilon_o} (\omega - n\omega_c) \sum_j \text{Res } [k_{\perp j}^+(\omega)] \ , \qquad (5.16)$$

where the summation extends over the residues of the poles located in the upper half complex plane at $k_{\perp j}^+$. Equation (5.9) gives the position of all poles near the origin, while those above the real axis are listed in Table 4 for three different positions of the hybrid frequency. It is

Table 4

POLES IN UPPER HALF $k_\perp$ PLANE FOR ω NEAR $n\omega_c$

Position of Hybrid Frequency ω_H	Poles above the Real $k_\perp$ Axis
$\omega_H < n\omega_c$	$k_{\perp j}^+ = \left[\alpha \left(1 - \frac{1}{n^2 - 1} \frac{\omega_p^2}{\omega_c^2}\right)\delta\right]^{\frac{1}{2(n-1)}} \exp\left[i \frac{2(j-1)\pi + \theta}{2(n-1)}\right]$, $j = 2, \ldots, n$
$\omega_H = n\omega_c$	$k_{\perp j}^+ = \left[\alpha \frac{2n\omega_c}{(n^2 - 1)\omega_c^2} \delta^2\right]^{\frac{1}{2(n-1)}} \exp\left[i \frac{(j-1)\pi + \theta}{n-1}\right]$, $j = 2, \ldots, n$
$\omega_H > n\omega_c$	$k_{\perp j}^+ = \left[\alpha\left(\frac{1}{n^2 - 1} \frac{\omega_p^2}{\omega_c^2} - 1\right) \delta\right]^{\frac{1}{2(n-1)}} \exp\left[i \frac{(2j-1)\pi + \theta}{2(n-1)}\right]$, $j = 1, \ldots, n-1$

pointed out that when deriving this table, ω was set equal to $n\omega_c + \delta \exp(i\theta)$ with $-\pi < \theta < 0$, and the dielectric constant was approximated by its value near $n\omega_c$:

$$K(\omega) \approx \begin{cases} 1 - \dfrac{1}{n^2 - 1}\dfrac{\omega_p^2}{\omega_c^2}\,, & \omega_H \neq n\omega_c\,, \qquad (5.17a) \\ \dfrac{2n\omega_c}{(n^2 - 1)\omega_c^2}\,(\omega - n\omega_c)\,, & \omega_H = n\omega_c\,. \qquad (5.17b) \end{cases}$$

It is readily established from Eq. (5.14) that

$$\text{Res}\,[k_{\perp j}] = \frac{1}{2(n-1)k_{\perp j}^{2n-3}}\,. \qquad (5.18)$$

Hence, after substituting this result in Eq. (5.16) and making use of Table 4, we obtain

$$G(\omega,x) = \frac{x\alpha^{\frac{1}{2(n-1)}}}{i\epsilon_o} \begin{cases} \dfrac{1}{\beta_1}\dfrac{(\omega - n\omega_c)^{\frac{1}{2(n-1)}}}{2(n-1)} \displaystyle\sum_{j=2}^{n} \exp\left[-i(j-1)\frac{2n-3}{n-1}\pi\right], \\ \qquad \omega_H < n\omega_c\,, \qquad (5.19a) \\ \dfrac{1}{\beta_2}\dfrac{(\omega - n\omega_c)^{-\frac{n-2}{n-1}}}{2(n-1)} \displaystyle\sum_{j=2}^{n} \exp\left[-i(j-1)\frac{2n-3}{n-1}\pi\right], \\ \qquad \omega_H = n\omega_c\,, \qquad (5.19b) \\ \dfrac{1}{\beta_3}\dfrac{(\omega - n\omega_c)^{\frac{1}{2(n-1)}}}{2(n-1)} \displaystyle\sum_{j=1}^{n-1} \exp\left[-i(2j-1)\frac{2n-3}{2(n-1)}\pi\right], \\ \qquad \omega_H > n\omega_c\,, \qquad (5.19c) \end{cases}$$

$$\beta_1 = \left(1 - \frac{1}{n^2 - 1}\frac{\omega_p^2}{\omega_c^2}\right)^{\frac{2n-3}{2n-2}} , \quad \beta_2 = \left[\frac{2n\omega_c}{(n^2 - 1)\omega_c^2}\right]^{\frac{2n-3}{2n-2}} ,$$

$$\beta_3 = \left(\frac{1}{n^2 - 1}\frac{\omega_p^2}{\omega_c^2} - 1\right)^{\frac{2n-3}{2n-2}} . \qquad (5.20)$$

The finite sums are closed with the identity

$$\sum_{k=1}^{n} \exp(ik\varphi) = \frac{\sin\frac{n\varphi}{2}}{\sin\frac{\varphi}{2}} \exp\left(i\frac{n+1}{2}\varphi\right) , \qquad (5.21)$$

yielding the formula

$$\sum_{j=2}^{n} \exp\left[-i(j-1)\frac{2n-3}{n-1}\pi\right] = \frac{i \exp\left[i\frac{\pi}{2(n-1)}\right]}{\sin\frac{\pi}{2(n-1)}} , \qquad (5.22)$$

$$\sum_{j=1}^{n-1} \exp\left[-i(2j-1)\frac{2n-3}{2(n-1)}\pi\right] = \frac{1}{i \sin\frac{\pi}{2(n-1)}} . \qquad (5.23)$$

After substituting in Eqs. (5.19a-c), the form of the Green's function near the n^{th} harmonic reads

$$G(\omega,x) = \frac{x\alpha^{\frac{1}{2(n-1)}}}{i\epsilon_o} \begin{cases} \dfrac{1}{\beta_1} \dfrac{i \exp\left[i \dfrac{\pi}{2(n-1)}\right]}{2(n-1) \sin \dfrac{\pi}{2(n-1)}} (\omega - n\omega_c)^{\frac{1}{2(n-1)}}, \\ \qquad \omega_H < n\omega_c, \qquad (5.24a) \\ \dfrac{1}{\beta_2} \dfrac{i \exp\left[i \dfrac{\pi}{2(n-1)}\right]}{2(n-1) \sin \dfrac{\pi}{2(n-1)}} (\omega - n\omega_c)^{-\frac{n-2}{n-1}}, \\ \qquad \omega_H = n\omega_c, \qquad (5.24b) \\ \dfrac{1}{\beta_3} \dfrac{-i}{2(n-1) \sin \dfrac{\pi}{2(n-1)}} (\omega - n\omega_c)^{\frac{1}{2(n-1)}}, \\ \qquad \omega_H > n\omega_c. \qquad (5.24c) \end{cases}$$

Clearly, there exists a singularity at integral multiples of ω_c except the first. When $\omega_H \neq n\omega_c$, the singularities are branch points which are replaced by branch poles when ω_H is identical with $n\omega_c$. It will be observed, however, in Eq. (5.24b) that an exception to this rule occurs at the second harmonic when the hybrid is equal to that frequency. In this case, $G(\omega,x)$ is regular at $2\omega_c$ and hence no resonance will be found at that frequency.

In addition to the singularities found above, the Green's function has an additional one at the upper hybrid frequency. The form of $G(\omega,x)$ near this point is found by substituting in Eq. (5.6) the power series expansion of $K(\omega,k_\perp)$. For $\omega \approx \omega_H \neq n\omega_c$, this has the form, to lowest significant order in $k_\perp$,

$$K(\omega,k_\perp) \approx \frac{2\omega_H}{\omega_p^2} (\omega - \omega_H) - \left(\frac{3\omega_c^2}{\omega_p^2 - 3\omega_c^2}\right)\left(\frac{k_\perp v_{t\perp}}{\omega_c}\right)^2 . \qquad (5.25)$$

Clearly, this expression has zeros at

$$k_\perp = \begin{cases} \pm \left[\frac{2}{3} \frac{\delta\omega_H(\omega_p^2 - 3\omega_c^2)}{\omega_p^2 v_{t\perp}^2} \right]^{1/2} \exp\left(i\frac{\theta}{2}\right), & \omega_p^2 > 3\omega_c^2 \quad , \qquad (5.26a) \\ \pm i \left[\frac{2}{3} \frac{\delta\omega_H(3\omega_c^2 - \omega_p^2)}{\omega_p^2 v_{t\perp}^2} \right]^{1/2} \exp\left(i\frac{\theta}{2}\right), & \omega_p^2 < 3\omega_c^2 \quad , \qquad (5.26b) \end{cases}$$

which pinch the real axis as $\delta \to 0$. Here we have made the substitution

$$\omega = \omega_H + \delta \exp(i\theta) , \qquad -\pi < \theta < 0 . \qquad (5.27)$$

Thus, for ω near ω_H, residue evaluation of Eq. (5.6) yields

$$G(\omega,x) = \begin{cases} i \frac{x\gamma_1}{2\epsilon_o} \frac{1}{(\omega - \omega_H)^{1/2}}, & \omega_p^2 > 3\omega_c^2 \quad , \qquad (5.28a) \\ - \frac{x\gamma_2}{2\epsilon_o} \frac{1}{(\omega - \omega_H)^{1/2}}, & \omega_p^2 < 3\omega_c^2 \quad , \qquad (5.28b) \end{cases}$$

where we have introduced the variables

$$\gamma_1 = \left[\frac{\omega_p^2(\omega_p^2 - 3\omega_c^2)}{6\omega_H^2 v_{t\perp}^2} \right]^{1/2} , \qquad \gamma_2 = \left[\frac{\omega_p^2(3\omega_c^2 - \omega_p^2)}{6\omega_H^2 v_{t\perp}^2} \right]^{1/2} . \qquad (5.29)$$

A branch pole is clearly evident at the upper hybrid frequency.

2. Pinching at Finite and Nonzero $k_\perp$

The dispersion characteristics of the Maxwellian distribution have branches which are typically of the form illustrated in Fig. 36.

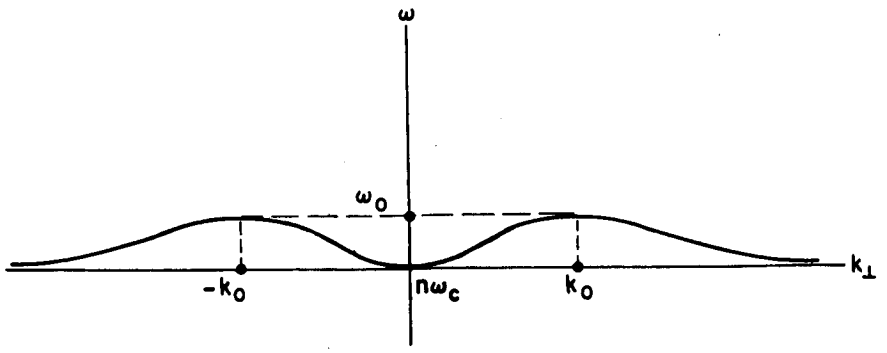

Fig. 36. PORTION OF DISPERSION DIAGRAM FOR PERPENDICULAR PROPAGATION IN A MAXWELLIAN PLASMA SHOWING TWO POINTS WHERE THE SLOPE $d\omega/dk_\perp$ VANISHES FOR FINITE AND NONZERO WAVE NUMBER.

Modes of this type are characterized by two points (ω_o, k_o) and $(\omega_o, -k_o)$, where the slope $(d\omega/dk_\perp)$ vanishes and hence where

$$K_{k_\perp}(\omega, k_\perp) = 0 \ . \tag{5.30}$$

This conclusion is based on the assumption that $K_\omega \neq 0$ at both points. However, this is clearly satisfied for the Maxwellian distribution since from Eq. (5.3)

$$K_\omega(\omega, k_\perp) = \frac{\omega_p^2}{\omega_c^2} \sum_{n=-\infty}^{\infty} \frac{\exp(-\lambda)\, I_n(\lambda)}{\lambda} \frac{n\omega_c}{(\omega - n\omega_c)^2} > 0 \ , \tag{5.31}$$

for all ω and $k_\perp$.

If, as indicated in Fig. 36, the dispersion relation has only a double root at k_o for $\omega = \omega_o$, it is readily established that $K_{k_\perp k_\perp}(\omega_o, k_o) = K_{k_\perp k_\perp}(\omega_o, -k_o) > 0$. Hence, the Taylor series expansion of $K(\omega, k_\perp)$ about the point (ω_o, k_o) yields, with the use of Eq. ~~(5.28a)~~ 5.30, the approximation

$$K(\omega, k_\perp) \approx K_\omega(\omega_o, k_o)\,(\omega - \omega_o) + \frac{1}{2} K_{k_\perp k_\perp}(\omega_o, k_o)\,(k_\perp - k_o)^2 \ . \tag{5.32}$$

For ω in the lower half complex plane at

$$\omega = \omega_o + \delta \exp(i\theta) , \qquad -\pi < \theta < 0 , \tag{5.33}$$

Eq. (5.32) has two zeros on opposite sides of the real axis at

$$k_\perp = k_o \pm i \left[\frac{2\delta K_\omega(\omega_o, k_o)}{K_{k_\perp k_\perp}(\omega_o k_o)} \right]^{1/2} \exp\left(i \frac{\theta}{2}\right) , \tag{5.34}$$

which converge to k_o as $\delta \to 0$ to form a double root that pinches the contour of integration of Eq. (5.13). Similarly, there exist two zeros of $K(\omega, k_\perp)$ near $(-k_o)$ which behave identically to those in Eq. (5.34) and are located at

$$k_\perp = -k_o \pm i \left[\frac{2\delta K_{k_\perp k_\perp}(\omega_o, k_o)}{K_\omega(\omega_o, k_o)} \right]^{1/2} \exp\left(i \frac{\theta}{2}\right) . \tag{5.35}$$

Thus, for ω near ω_o, residue evaluation of Eq. (5.13) yields

$$G(\omega, x) \approx \frac{\sin k_o x}{\epsilon_o k_o (2K_\omega K_{k_\perp k_\perp})^{1/2}} \frac{1}{(\omega - \omega_o)^{1/2}} , \tag{5.36}$$

and reveals a branch pole at ω_o. The partial derivatives in this expression are evaluated at the point (ω_o, k_o).

C. The Long-Time Behavior of the Electric Field

The asymptotic form of the electric field can now be obtained by deforming the Laplace contour in the usual manner around the singularities of the Green's function. Then in the limit as $t \to \infty$, Eq. (5.1) reduces to

$$E(x,t) \sim \sum_k \int_{\Gamma_k} \frac{d\omega}{2\pi} \exp(i\omega t)\, G(\omega,x)\, f(\omega) \quad , \tag{5.37}$$

where the summation is over the branch points of the Green's function and the contour Γ_k extends around the k^{th} branch cut as shown in Fig. 37. Here we have assumed that $f(\omega)$ is an analytic function of ω, corresponding to pulse excitation of the resonances. It should be pointed out that not all singularities are indicated in this figure. For purposes of clarity we have excluded those singularities of Section B with finite and nonzero wave number. We now examine the k^{th} term in Eq. (5.37) at each branch point.

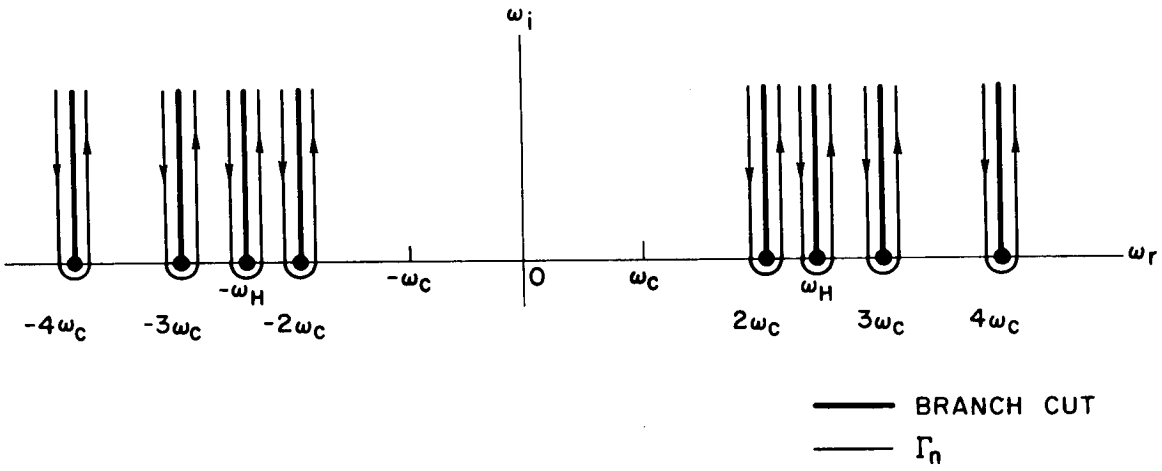

Fig. 37. CONTOUR OF INTEGRATION AROUND SINGULARITIES OF THE GREEN'S FUNCTION.

Case 1 ($\omega = n\omega_c$, $\omega_H \neq n\omega_c$). Since the contribution to the integral from the part of Γ_k in the upper half complex plane vanishes exponentially as $t \to \infty$, it is sufficient to expand the integrand about $\omega = n\omega_c$ and retain only the most significant parts. Hence, in this limit, the k^{th} term of Eq. (5.37) approaches, for $\omega_H < n\omega_c$,

$$E_k(x,t) = \frac{x\alpha^{\frac{1}{2(n-1)}}\, f(n\omega_c)}{\epsilon_o \beta_1} \frac{\exp\left[in\omega_c t + i\,\frac{\pi}{2(n-1)}\right]}{2(n-1)\,\sin\frac{\pi}{2(n-1)}}$$

$$\cdot \int_{\Gamma_k} \frac{d\omega}{2\pi} \exp\,[i(\omega - n\omega_c)t]\,(\omega - n\omega_c)^{\frac{1}{2(n-1)}}\,, \qquad (5.38)$$

where Eq. (5.24a) has been written for $G(\omega,x)$. Figure 38 shows that the integration along Γ_k can be written as a sum of three terms:

$$I_{\Gamma_k} = I_{AB} + I_{BCD} + I_{DE}\,, \qquad (5.39)$$

where

$$I_{\Gamma_k} = \int_{\Gamma_k} \frac{d\omega}{2\pi} \exp\,[i(\omega - n\omega_c)t]\,(\omega - n\omega_c)^{\frac{1}{2(n-1)}}\,. \qquad (5.40)$$

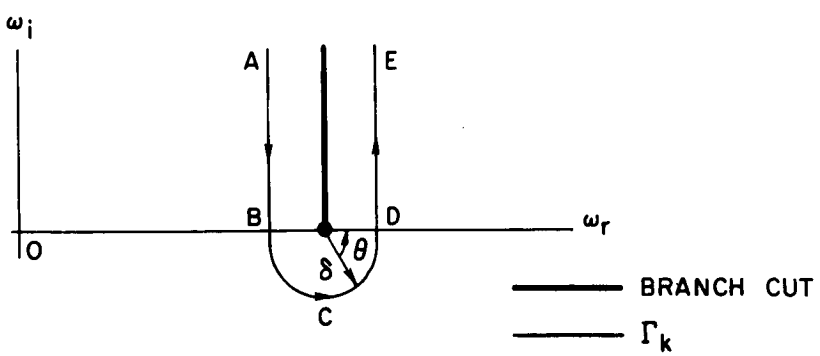

Fig. 38. CONTOUR OF INTEGRATION Γ_k AROUND A BRANCH POINT IN THE GREEN'S FUNCTION.

Writing

$$\omega = n\omega_c + \delta \exp(i\theta), \qquad -\frac{3\pi}{2} < \theta < \frac{\pi}{2} , \tag{5.41}$$

it is clear that

$$\lim_{\delta \to 0} I_{BCD} \to i\delta^{\frac{2n-1}{2n-2}} \int_{-\pi}^{0} \frac{d\theta}{2\pi} \exp\left(i \frac{2n-1}{2n-2} \theta\right) \tag{5.42}$$

$$= 0 , \tag{5.43}$$

while in the same limit,

$$I_{AB} + I_{DE} = i \exp\left[-i \frac{3\pi}{4(n-1)}\right] \int_{\infty}^{0} \frac{d\omega_i}{2\pi} \exp(-\omega_i t)\, \omega_i^{\frac{1}{2(n-1)}}$$

$$+ i \exp\left[i \frac{\pi}{4(n-1)}\right] \int_{0}^{\infty} \frac{d\omega_i}{2\pi} \exp(-\omega_i t)\, \omega_i^{\frac{1}{2(n-1)}} \tag{5.44a}$$

$$= -2 \exp\left[-i \frac{\pi}{4(n-1)}\right] \sin \frac{\pi}{2(n-1)} \int_{0}^{\infty} \frac{d\omega_i}{2\pi}$$

$$\cdot \exp(-\omega_i t)\, \omega_i^{\frac{1}{2(n-1)}} . \tag{5.44b}$$

Here, the integration with respect to ω_i [$\equiv \mathrm{Im}(\omega)$] has been extended to ∞ for convenience. This step is purely formal and will introduce no error in the limit as $t \to \infty$. The integration in Eq. (5.44b) is accomplished with the identity

$$\int_0^\infty dx\, x^p \exp(-qx) = \frac{\Gamma(p+1)}{q^{p+1}} , \qquad (q < 0;\ p + 1 > 0) , \tag{5.45}$$

where $\Gamma(z)$ is the familiar gamma function. Hence, after combining Eqs. (5.43) and (5.44b) with Eq. (5.39) and substituting the result in Eq. (5.38), the component of the electric field at $\omega = n\omega_c$ is, in the limit as $t \to \infty$,

$$E_k(x,t) = -\frac{x\alpha^{\frac{1}{2(n-1)}}\,\Gamma\left(\frac{2n-1}{2n-2}\right) f(n\omega_c)}{2\pi(n-1)\epsilon_o\beta_1}\;\frac{\exp\left[in\omega_c t + i\,\frac{\pi}{4(n-1)}\right]}{t^{\frac{2n-1}{2n-2}}}\,. \tag{5.46}$$

If $\omega_H > n\omega_c$, the only change in this expression occurs in the phase, and it is readily established, from Eq. (5.24c), that the asymptotic form of the electric field is

$$E_k(x,t) = \frac{x\alpha^{\frac{1}{2(n-1)}}\,\Gamma\left(\frac{2n-1}{2n-2}\right) f(n\omega_c)}{2\pi(n-1)\epsilon_o\beta_3}\;\frac{\exp\left[in\omega_c t - i\,\frac{\pi}{4(n-1)}\right]}{t^{\frac{2n-1}{2n-2}}}\,. \tag{5.47}$$

Case 2 $(\omega = n\omega_c,\ \omega_H = n\omega_c)$. This case requires a recomputation of the branch cut integral. From Eqs. (5.24b) and (5.37), the correct expression for the electric field, as $t \to \infty$, is

$$E_k(x,t) = \frac{x\alpha^{\frac{1}{2(n-1)}}\, f(n\omega_c)}{\epsilon_o\beta_2}\;\frac{\exp\left[in\omega_c t + i\,\frac{\pi}{2(n-1)}\right]}{2(n-1)\sin\frac{\pi}{2(n-1)}}$$

$$\cdot\int_{\Gamma_k}\frac{d\omega}{2\pi}\exp\left[i(\omega - n\omega_c)t\right](\omega - n\omega_c)^{-\frac{n-2}{n-1}}\,, \tag{5.48}$$

where the contour Γ_k is shown in Fig. 38. Following the integration in Case 1, we define

$$I_{\Gamma_k} = \int_{\Gamma_k} \frac{d\omega}{2\pi} \exp\left[i(\omega - n\omega_c)t\right] (\omega - n\omega_c)^{-\frac{n-2}{n-1}} \tag{5.49a}$$

$$= I_{AB} + I_{BCD} + I_{DE} \, . \tag{5.49b}$$

In the limit as $\delta \to 0$, the components of the branch cut integration reduce to

$$I_{BCD} = i\delta^{\frac{1}{n-1}} \int_{-\pi}^{0} \frac{d\theta}{2\pi} \exp\left(i \frac{1}{n-1} \theta\right) \to 0 \quad , \tag{5.50}$$

$$I_{AB} + I_{DE} = i \exp\left(i \frac{n-2}{n-1} \frac{3\pi}{2}\right) \int_{\infty}^{0} \frac{d\omega_i}{2\pi} \exp\left(-\omega_i t\right) \omega_i^{-\frac{n-2}{n-1}}$$

$$+ i \exp\left(-i \frac{n-2}{n-1} \frac{\pi}{2}\right) \int_{0}^{\infty} \frac{d\omega_i}{2\pi} \exp\left(-\omega_i t\right) \omega_i^{-\frac{n-2}{n-1}} \tag{5.51a}$$

$$= \frac{i}{\pi} \exp\left[-i \frac{\pi}{2(n-1)}\right] \sin \frac{\pi}{n-1} \frac{\Gamma\left(\frac{1}{n-1}\right)}{t^{\frac{1}{n-1}}} \quad , \tag{5.51b}$$

where Eq. (5.41) was written for ω in Eq. (5.50), and the integration with respect to ω_i was accomplished with Eq. (5.45). Hence, the component of the electric field at the n^{th} harmonic reads

$$E_k(x,t) = \frac{x\alpha^{\frac{1}{2(n-1)}} \Gamma\left(\frac{1}{n-1}\right) f(n\omega_c) \cos \frac{\pi}{2(n-1)}}{\pi(n-1)\epsilon_o \beta_2} \frac{\exp\left(in\omega_c t + i \frac{\pi}{2}\right)}{t^{\frac{1}{n-1}}} \, . \tag{5.52}$$

It is observed that E_k is identically zero when $n = 2$, indicating that no resonance exists at the second harmonic in this case. This is a manifestation of the analyticity of the Green's function, Eq. (5.24b), in the region about $2\omega_c$ when the upper hybrid frequency also equals $2\omega_c$.

Case 3 $(\omega = \omega_H \neq n\omega_c)$. The component of the electric field excited at this frequency is obtained by combining Eq. (5.28a) or (5.28b) with the k^{th} term in Eq. (5.37). This yields the expression

$$E_k(x,t) = \frac{xf(\omega_H)}{2\epsilon_o} \begin{bmatrix} i\gamma_1 \\ \bar{\gamma}_2 \end{bmatrix} \exp\ (i\omega_H t) \int_{\Gamma_k} \frac{d\omega}{2\pi} \exp\ [i(\omega - \omega_H)t\ ]\ (\omega - \omega_H)^{-1/2}\ , \tag{5.53}$$

where the top entry in the brackets is chosen if $\omega_p^2 > 3\omega_c^2$, while the bottom entry is chosen if $\omega_p^2 < 3\omega_c^2$. The branch cut integral will be recognized as a special case of Eq. (5.49a), namely, the case $n = 3$, and hence we take advantage of the result of the integration, Eq. (5.51b), to obtain

$$E_k(x,t) = \begin{cases} \dfrac{x\gamma_1 f(\omega_H)}{2\sqrt{\pi\epsilon_o}} \dfrac{\exp\left(i\omega_H t + i\,\frac{3\pi}{4}\right)}{t^{1/2}}\ , & \omega_p^2 > 3\omega_c^2\ , \qquad (5.54a) \\ \dfrac{x\gamma_2 f(\omega_H)}{2\sqrt{\pi\epsilon_o}} \dfrac{\exp\left(i\omega_H t - i\,\frac{3\pi}{4}\right)}{t^{1/2}}\ , & \omega_p^2 < 3\omega_c^2\ , \qquad (5.54b) \end{cases}$$

where use has been made of the identity $\Gamma(1/2) = \sqrt{\pi}$.

Case 4 $(\omega = \omega_o)$. This case corresponds to the singularities described in Section B2. They are found only at frequencies larger than the hybrid and have an associated finite and nonzero wave number k_o.

A comparison of Eqs. (5.36) and either (5.28a) or (5.28b) indicates that the singularity at ω_o is of the same type and form as the one at the upper hybrid frequency ω_H. Hence it is readily established from the computations of case 3 that the electric field excited at ω_o is

$$E_k(x,t) = \frac{f(\omega_o)\ \sin k_o x}{\epsilon_o k_o (2K_\omega K_{k_\perp} k_\perp)^{1/2}} \exp(i\omega_o t) \int_{\Gamma_k} \frac{d\omega}{2\pi} \exp[i(\omega - \omega_o)t]\ (\omega - \omega_o)^{-1/2} \tag{5.55a}$$

$$= \frac{f(\omega_o)\ \sin k_o x}{\epsilon_o k_o (2\pi K_\omega K_{k_\perp} k_\perp)^{1/2}} \frac{\exp\left(i\omega_o t + i\frac{\pi}{4}\right)}{t^{1/2}}, \tag{5.55b}$$

where the partial derivatives are evaluated at (ω_o, k_o).

In order to summarize the results obtained here and in the previous section, Table 5 lists the frequencies at which the Green's function is singular, the form of $G(\omega,x)$ near these points, and the time and spatial dependence of the electric field excited at each resonant frequency. It is seen that the decay rate of that field at $n\omega_c$ is critically dependent on the hybrid frequency. If $\omega_H \neq n\omega_c$, the decay rate decreases from $(1/t^{3/2})$ at $n = 2$ to $(1/t)$ in the limit as $n \to \infty$. However, these rates can be decreased significantly by setting the upper hybrid frequency identically equal to $n\omega_c$. Indeed, the decay rates in this case are always slower than $(1/t)$ and vary from $(1/t^{1/2})$ when $n = 3$ to a limit of a time-invariant amplitude as $n \to \infty$. When $n = 2$, Eq. (5.52) indicates that the electric field is identically zero, and hence the entry in Table 5 corresponding to this case is not applicable at the second harmonic. It will be recalled from Section B that in addition to the resonances found here, an equal number of resonances are found on the negative frequency axis which are mirror images to those at positive frequencies. The correct form of the Green's function in the vicinity of these points is obtainable from previously derived formulas by replacing ω by $(-\omega)$; and similarly, the correct form of the electric field is found by replacing ω_c, ω_H, and ω_o by their negative values. After

Table 5

FORM OF $G(\omega,x)$ AND $E(x,t)$ AT RESONANCES

Frequency	$G(\omega,x)$	$\lim_{t \to \infty} E(x,t)$
$\omega = n\omega_c$ $\omega_H \neq n\omega_c$	$(\omega - n\omega_c)^{\frac{1}{2(n-1)}}$	$\frac{x \exp(in\omega_c t)}{t^{\frac{2n-1}{2n-2}}}$
$\omega = n\omega_c$ $\omega_H = n\omega_c$	$(\omega - n\omega_c)^{-\frac{n-2}{n-1}}$	$\frac{x \exp(in\omega_c t)}{t^{\frac{1}{n-1}}}$
$\omega = \omega_H$ $\omega_H \neq n\omega_c$	$(\omega - \omega_H)^{-1/2}$	$\frac{x \exp(i\omega_H t)}{t^{1/2}}$
$\omega = \omega_o$	$(\omega - \omega_o)^{-1/2}$	$\frac{\exp i(\omega_o t - k_o x)}{t^{1/2}}$

making these substitutions, n is still restricted to positive integers greater than one.

An important factor that should be considered in plasma resonance studies is the spatial form of the source. Up to this point, this effect was neglected, and the resonances that were obtained depend only on the properties of the plasma medium. In the next section, we will illustrate with a hypothetical, though instructive, example how a spatial distribution in the source can completely change the results of this and the previous sections.

D. Excitation by Spatially Periodic Sources

When the spatial form of the source is taken into consideration through the function $g(x)$, the frequency response of the plasma is obtainable from either Eq. (5.2) or (5.5), i.e., from

$$F(\omega,x) = \int_{-\infty}^{\infty} dx'\, G(\omega,x - x')\, g(x') \,, \qquad \mathrm{Im}(\omega) < 0 \,, \tag{5.56a}$$

$$= i \int_{-\infty}^{\infty} \frac{dk_\perp}{2\pi} \frac{\exp\,(-ik_\perp x)\, g(k_\perp)}{\epsilon_o k_\perp K(\omega,k_\perp)} \,, \qquad \mathrm{Im}(\omega) < 0 \,, \tag{5.56b}$$

where $G(\omega,x)$ is the Green's function and $g(k_\perp)$ is the Fourier transform of $g(x)$. Clearly, if $g(k_\perp)$ is analytic on the real axis, the only change in the results of the last section is the replacement of x by

$$\lim_{k_\perp \to k_{\perp o}} \left[\frac{\exp\,(ik_\perp x)\, g(k_\perp)}{k_\perp}\right] \,, \tag{5.57}$$

where $k_{\perp o}$ is the point on the real axis where pinching occurs. However, if the condition of analyticity is not satisfied, the nature of the resonance can be changed significantly.

In order to illustrate this, consider a source that is periodic in space with period L. The function $g(x)$ now satisfies the condition

$$g(x + L) = g(x) \,, \tag{5.58}$$

and hence possesses a Fourier transform which can be written in the form

$$g(k_\perp) = 2\pi \sum_{n=-\infty}^{\infty} h_n \delta\left(k_\perp - \frac{2\pi n}{L}\right) \,, \tag{5.59}$$

where $\delta(k_\perp)$ is the Dirac delta function and h_n is the n^{th} coefficient in the Fourier series expansion of $g(x)$, that is,

$$h_n = \frac{1}{L} \int_0^L dx\, \exp\left(i\,\frac{2\pi n x}{L}\right) g(x) \,. \tag{5.60}$$

By choosing a coordinate system in space such that the average of $g(x)$ over one period is zero, the coefficient corresponding to $n = 0$ clearly must vanish. This convention will be adopted here. After substituting Eq. (5.60) in Eq. (5.56b) and performing the integration over $k_\perp$ with $\mathrm{Im}(\omega) < 0$, the frequency response of the plasma has the form

$$F(\omega,x) = \sum_{\substack{n=-\infty \\ n \neq 0}}^{\infty} \frac{i \exp(-ink_{\perp 1}x)h_n}{\epsilon_o nk_{\perp 1} K(\omega, nk_{\perp 1})} , \tag{5.61}$$

where $k_{\perp 1}$ has been written for $(2\pi/L)$. Clearly, this also defines $F(\omega,x)$ for $\mathrm{Im}(\omega) \geq 0$ as long as the radius of convergence of the infinite series includes this part of the complex ω plane.

It is now evident that a spatially periodic source quantizes the wave number, restricting its values to integral multiples of $(2\pi/L)$. As a consequence of this, singularities in $F(\omega,x)$ no longer occur at harmonics of the electron cyclotron frequency. Indeed, for $\omega \approx m\omega_c$ and $k_\perp \neq 0$, Eq. (5.3) implies that

$$K(\omega,k_\perp) \approx \frac{\omega_p^2}{\omega_c^2} \frac{\exp(-\lambda)\, I_n(\lambda)}{\lambda} \frac{m\omega_c}{\omega - m\omega_c} , \tag{5.62}$$

and hence the expression for $F(\omega,x)$ reduces to

$$F(\omega,x) \approx -\frac{\omega - m\omega_c}{m\omega_c} \frac{\omega_c^2}{\omega_p^2} \sum_{\substack{n=-\infty \\ n \neq 0}}^{\infty} \frac{i \exp(-ink_{\perp 1}x)h_n}{\epsilon_o nk_{\perp 1}} \cdot \frac{n^2\lambda_1}{\exp(-n^2\lambda_1)\, I_m(n^2\lambda_1)} , \tag{5.63}$$

where λ_1 has been written for $(k_{\perp 1} v_{t\perp}/\omega_c)^2$. Clearly, $F(\omega,x)$ has a simple zero at each harmonic of the cyclotron frequency, including the first, implying that no resonances occur in the electric field at those frequencies.

However, Eq. (5.61) does have singularities at other frequencies, namely, where ω satisfies the equation

$$K(\omega, nk_{\perp 1}) = 0 \ . \tag{5.64}$$

This is the dispersion relation for perpendicularly propagating cyclotron harmonic waves, and the roots at $\omega_m(nk_{\perp 1})$ can be obtained from the curves shown in Chapter III. For ω in the vicinity of ω_m, it is necessary to retain only the n^{th} term in Eq. (5.61) and hence, with the use of the Taylor series expansion

$$K(\omega, nk_{\perp 1}) \approx K_\omega(\omega_m, nk_{\perp 1})(\omega - \omega_m) \ , \tag{5.65}$$

the expansion for $F(\omega,x)$ has the approximate form

$$F(\omega,x) \approx \frac{i \exp(-ink_{\perp 1}x)h_n}{\epsilon_o nk_{\perp 1} K_\omega(\omega_m, nk_{\perp 1})} \frac{1}{\omega - \omega_m} \ , \tag{5.66}$$

to reveal the presence of a simple pole. The distribution of the poles along the real ω axis is obtainable from Fig. 39, where the dispersion relation for a Maxwellian plasma is plotted for $(\omega_p^2/\omega_c^2) = 8$. In this figure, an arbitrary value of $k_{\perp 1}$ is indicated along with integral multiples of this constant. It is clearly seen that the frequency response of the plasma has an infinite number of poles between $n\omega_c$ and $(n + 1)\omega_c$, the density increasing indefinitely near the bottom of the band.

To obtain the time response, the Laplace contour is deformed around the singularities on the real frequency and into the upper portion of the complex plane. Taking the limit as $t \to \infty$, Eq. (5.1), in conjunction with Eq. (5.66), reduces to

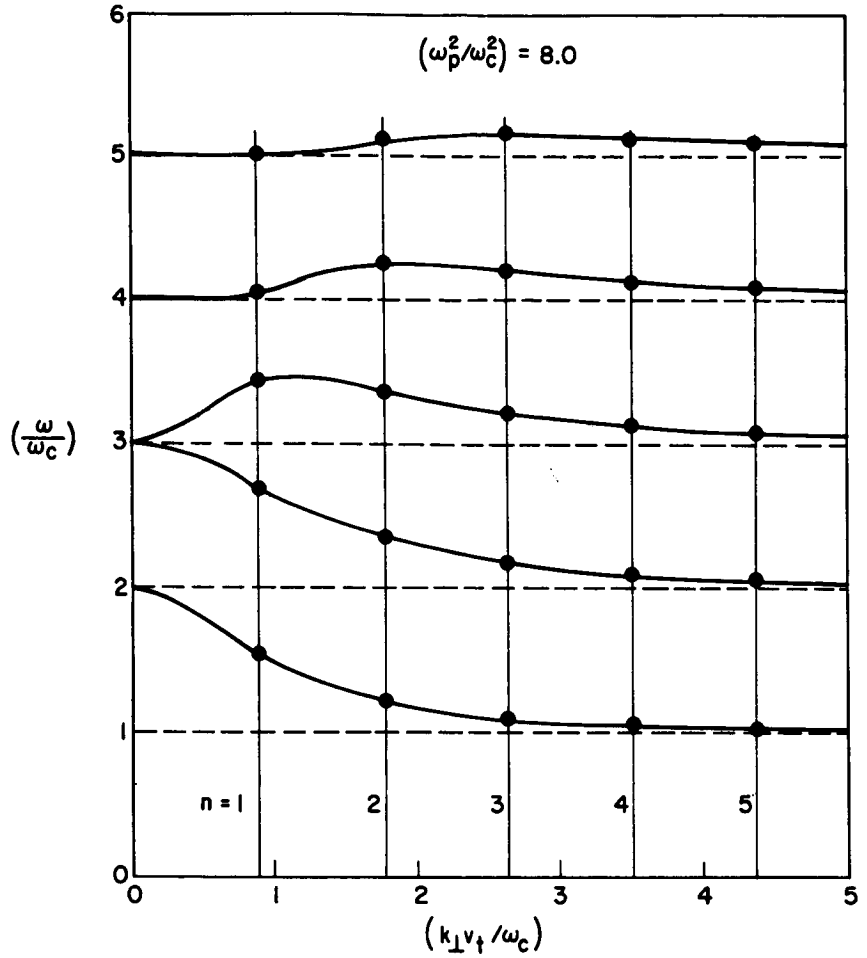

Fig. 39. ORIGIN OF SINGULARITIES IN $F(\omega,x)$ WHEN SOURCE IS SPATIALLY PERIODIC.

$$E(x,t) = - \sum_{m,n\neq 0} \frac{h_n f(\omega_m) \exp i(\omega_m t - nk_{\perp 1} x)}{\epsilon_o nk_{\perp 1} K_\omega(\omega_m, nk_{\perp 1})} , \qquad (5.67)$$

showing that a propagating wave is excited at frequencies where $F(\omega,x)$ is singular. It will be seen, by comparing this expression with the results in Section C, that unlike the fields excited by a nonperiodic source, Eq. (5.67) does not attenuate with time.

The example considered here is only one of many others that demonstrate the same point: the behavior of the electric field that is excited at a resonance may depend critically on the type of source that is used.

E. Discussion

The results of this chapter show that the one-dimensional Green's function $G(\omega,x)$ for a Maxwellian plasma is singular at (i) $\omega = n\omega_c$ for $n = \pm 2, \pm 3, \ldots$; (ii) $\omega = \pm(\omega_p^2 + \omega_c^2)^{1/2}$; and (iii) an intermediate frequency ω_o between $|n|\omega_o$ and $(|n| + 1)\omega_c$ if $(\omega_p^2 + \omega_c^2)^{1/2} < (|n| + 1)\omega_c$. As a consequence of this, application of a temporal pulse to the plasma will excite components of the electric field at those frequencies. These components have the important property that the temporal decay rate is small, suggesting that experimental observation may be possible for an appreciable length of time. It is pointed out that the form of the singularities, and hence the time dependence of the excited fields, will change with the type of source that is assumed. This was clearly illustrated in Section D where the source was spatially periodic. The results show that resonances in the electric field no longer occur at harmonics of the electron cyclotron frequency. Instead, the periodicity of the source quantizes the wave number, restricting its values to integral multiples of $(2\pi/L)$, where L is the period. For each allowed value, a propagating wave is excited in each band of frequencies bounded by $n\omega_c$ and $(n + 1)\omega_c$. Unlike the examples with nonperiodic sources, the fields in this case are free of attenuation.

Chapter VI

CONCLUDING REMARKS

Plasmas in which the constituent charged particles have a distribution in velocity can exhibit strong and important effects that have no counterpart in the cold plasma approximation. This was first brought to light by Landau in his classic paper [2] when he showed that longitudinal space-charge waves, propagating in a Maxwellian plasma with no magnetic field, decay with time. The existence of these waves has since been verified experimentally by several workers [45-47]. The introduction of a magnetic field leads to new effects that may have far-reaching significance in areas of plasma research as widely separated as controlled thermonuclear fusion and ionospheric phenomena. These effects include (1) the presence of longitudinal space-charge waves, called cyclotron harmonic waves, near harmonics of the cyclotron frequency of each particle species, (2) the existence of such waves that propagate perpendicular to the magnetic field without collisionless damping, and (3) the excitation of electrostatic instabilities by anisotropies in the plasma temperature. These basic properties of hot magnetoplasmas were established predominantly by Bernstein [3] and by Harris [4,5]. However, due to the complexity of the dispersion relation which determines the propagation of cyclotron harmonic waves, detailed properties, which would be required if theory is to be compared with experimental observations, have been difficult to obtain. This work has been devoted to an analysis of a hot magnetoplasma in the quasi-static approximation in order to determine the exact form of the dispersion characteristics of cyclotron harmonic waves, to derive exact threshold conditions for instability, and to examine the steady state conditions of the plasma.

A somewhat idealized model, but one that is closely approached in many experimental situations, has been treated here. We have considered a time-invariant and uniform plasma that is immersed in a constant magnetic field and that is free of electric fields. Two types of charged particles, with equal number density, are present: electrons and singly charged ions. However, the motion of the ions has been neglected due to the relatively large mass of these particles. Under these assumptions, the Vlasov

equation was solved simultaneously with Maxwell's equation in the quasi-static approximation to derive a dispersion relation for cyclotron harmonic waves. For purposes of illustrating the basic features of the propagation, a series of electron velocity distributions has been considered. The dispersion relation has been solved for each case numerically and, when possible, analytically. Our results indicate that for perpendicular propagation, a mode is found near each harmonic of the electron cyclotron frequency which may go unstable if $(\partial f_o/\partial v_\perp)$ is greater than zero for some range of $v_\perp$ and if the parameter (ω_p^2/ω_c^2) is sufficiently large. Using a well-established criterion, we have found that these instabilities are absolute. In cases where instability is not excited, space-charge waves which propagate perpendicular to the magnetic field with a real wave number are free from collisionless damping. However, in practice, collisions between the constituent particles are present, which could seriously limit the spectrum of waves that would be detected experimentally. This was illustrated in the report with electron-neutral collisions, and it was found that waves with large frequencies relative to the cyclotron frequency, or waves with short wavelengths, are heavily damped as a result of these collisions.

Oblique propagation has additional features that have no counterpart in exact perpendicular propagation. The primary new feature is the presence of an additional mode in each frequency passband bounded by succeeding harmonics of the electron cyclotron frequency. This new mode leads to a second class of instabilities that have onset conditions that are less severe than those of perpendicular propagation, and are found only if the effective temperature of the electrons perpendicular to the magnetic field is sufficiently greater than the temperature along the magnetic field. These instabilities can be either convective or absolute, depending on the values of the parameters that characterize the plasma.

An important problem considered in this work was that of the steady state conditions of the plasma in the quasi-static approximation. In situations where absolute instability is excited, the plasma cannot return to equilibrium since the amplitude of an arbitrary disturbance grows indefinitely with time at any point in space. However, in cases where

all instabilities are convective or where instability is not present, the plasma response contains components that decay very slowly with time. This resonance condition, or ringing of the plasma, occurs at harmonics of the electron cyclotron frequency, at the upper hybrid frequency, and at some intermediate frequencies, and is the result of singularities of the Laplace transform of the plasma Green's function.

It was mentioned earlier that the plasma model considered in this study may be approached in many experimental situations. The excellent agreement between the theoretical predictions of this work and the experimental observations of perpendicular propagation (see Fig. 22) adds confidence to our model. However, there are situations where external factors, such as confining walls, could alter our results significantly. For example, in an infinite uniform magnetoplasma, cyclotron harmonic waves propagate perpendicular to the magnetic field without collisionless damping since the periodicity of the electron trajectory in the plane transverse to the magnetic field leads to the periodic regeneration of the initial form of disturbance of the plasma. If walls are present, the periodicity of some electron orbits will be destroyed, leading to phase mixing of the normal modes that make up the disturbance, and hence to damping. Harker et al [48] are presently carrying out computations to determine the importance of this effect. In connection with the instabilities predicted in this research, nonlinear processes (which were neglected here) may limit the growth rate and lead to an equilibrium condition. These are but a few of the many effects which should be considered in a complete study but which are difficult to treat as a result of the complexity of the basic equations that determine the spatial and temporal behavior of the plasma. Consequently, many of these important problems may remain intractable in an analysis which involves the solution of Boltzmann's equation, and recourse might have to be made to alternative treatments, such as computer simulation of plasmas.

Appendix A

DIELECTRIC CONSTANT OF A MAGNETOPLASMA WITH A SPHERICALLY SYMMETRIC VELOCITY DISTRIBUTION

It is demonstrated in this appendix that the dielectric constant of a magnetoplasma

$$K(\omega,\underset{\sim}{k}) = 1 - \sum_{\alpha} \frac{\omega_p^2}{k^2} \int d\underset{\sim}{v}\, \frac{1}{v} \frac{\partial f_o}{\partial v} + \sum_{\alpha} \frac{\omega_p^2}{k^2} \sum_{n=-\infty}^{\infty} \int d\underset{\sim}{v}\, \frac{\omega}{v} \frac{\partial f_o}{\partial v} \frac{J_n^2\left(\frac{k_\perp v_\parallel}{\omega_c}\right)}{\omega - k_\parallel v_\parallel - n\omega_c} ,$$

$$\mathrm{Im}\,(\omega) < 0 , \qquad (A.1)$$

with $\underset{\sim}{k}$ real is not equal to zero if the velocity distribution of each particle species is spherically symmetric and satisfies the condition

$$\frac{\partial f_o(v)}{\partial v} < 0 . \qquad (A.2)$$

Bernstein [3] proves this theorem for the special case of a plasma consisting of electrons, with a Maxwellian velocity distribution, and stationary ions. We now follow his proof, but with these restrictions relaxed.

Let $\omega = \omega_r + i\omega_i$ in Eq. (A.1). Then the real and imaginary parts of K are, respectively,

$$K_r(\omega,\underset{\sim}{k}) = 1 - \sum_{\alpha} \frac{\omega_p^2}{k^2} \int d\underset{\sim}{v}\, \frac{1}{v} \frac{\partial f_o}{\partial v}$$

$$+ \sum_{\alpha} \frac{\omega_p^2}{k^2} \int d\underset{\sim}{v}\, \frac{1}{v} \frac{\partial f_o}{\partial v} \sum_{n=-\infty}^{\infty} J_n^2\left(\frac{k_\perp v_\perp}{\omega_c}\right) \frac{\omega_r(\omega_r - k_\parallel v_\parallel - n\omega_c) + \omega_i^2}{(\omega_r - k_\parallel v_\parallel - n\omega_c)^2 + \omega_i^2} ,$$

(A.3)

$$K_i(\omega,\underset{\sim}{k}) = \sum_{\alpha} \frac{\omega_p^2}{k^2} \int d\underset{\sim}{v}\, \frac{1}{v} \frac{\partial f_o}{\partial v} \sum_{n=-\infty}^{\infty} J_n^2\left(\frac{k_\perp v_\perp}{\omega_c}\right) \frac{\omega_i(-k_\parallel v_\parallel - n\omega_c)}{(\omega_r - k_\parallel v_\parallel - n\omega_c)^2 + \omega_i^2} \quad . \tag{A.4}$$

We now add K_r to $(\omega_r/\omega_i)K_i$ and then use the identity

$$\sum_{n=-\infty}^{\infty} J_n^2\left(\frac{k_\perp v_\perp}{\omega_c}\right) = 1 \quad , \tag{A.5}$$

to arrive at the sum

$$K_r + \left(\frac{\omega_r}{\omega_i}\right) K_i = 1 - 2\pi \sum_{\alpha} \frac{\omega_p^2}{k^2} \int_0^{\infty} dv\, v \frac{\partial f_o}{\partial v} \int_0^{\pi} d\Theta \sin\Theta$$

$$\cdot \sum_{n=-\infty}^{\infty} J_n^2\left(\frac{k_\perp v}{\omega_c} \sin\Theta\right) \frac{(k_\parallel v \cos\Theta + n\omega_c)^2}{(\omega_r - k_\parallel v \cos\Theta - n\omega_c)^2 + \omega_i^2} \quad , \tag{A.6}$$

where spherical variables have been introduced in the velocity integration. Clearly, the right-hand side of this equation is greater than zero due to Eq. (A.2), and hence K_r and K_i cannot both be zero. This confirms the statement made at the beginning of the appendix that $K(\omega,\underset{\sim}{k})$ is nonzero if $\underset{\sim}{k}$ is real and $\mathrm{Im}\,(\omega) < 0$.

Appendix B

THE CONNECTION BETWEEN K^+ AND K^-

It is the purpose of this appendix to derive the formula that connects the positive and negative "frequency" components of the dielectric constant of a magnetoplasma in the electrostatic approximation. These functions were defined in Chapter IV and are repeated here for convenience:

$$K^+(\omega,k_\perp,k_\parallel) = 1 + 2\pi i \frac{\omega_p^2}{k_\parallel k^2} \sum_{n=-\infty}^{\infty} H_n^+\left(\frac{\omega - n\omega_c}{k_\parallel}, k_\perp, k_\parallel\right) \tag{4.61a}$$

$$K^-(\omega,k_\perp,k_\parallel) = 1 - 2\pi i \frac{\omega_p^2}{k_\parallel k^2} \sum_{n=-\infty}^{\infty} H_n^-\left(\frac{\omega - n\omega_c}{k_\parallel}, k_\perp, k_\parallel\right) \tag{4.61b}$$

where we introduce

$$H_n^+(w_n,k_\perp,k_\parallel) = \int_0^\infty \frac{d\zeta}{2\pi} \exp(-iw_n\zeta)\ \bar{H}_n(\zeta,k_\perp,k_\parallel) \tag{B.1a}$$

$$H_n^-(w_n,k_\perp,k_\parallel) = \int_{-\infty}^0 \frac{d\zeta}{2\pi} \exp(-iw_n\zeta)\ \bar{H}_n(\zeta,k_\perp,k_\parallel)\ . \tag{B.1b}$$

The Fourier transform of $H_n(v_\parallel,k_\perp,k_\parallel)$ is

$$\bar{H}_n(\zeta,k_\perp,k_\parallel) = \int_{-\infty}^\infty dv_\parallel \exp(iv_\parallel\zeta)\ H_n(v_\parallel,k_\perp,k_\parallel) \tag{B.2}$$

where from Eq. (2.69)

$$H_n(v_\parallel,k_\perp,k_\parallel) = 2\pi \int_0^\infty dv_\perp v_\perp \left(\frac{n\omega_c}{v_\perp}\frac{\partial f_o}{\partial v_\perp} + k_\parallel \frac{\partial f_o}{\partial v_\parallel}\right) J_n^2\left(\frac{k_\perp v_\perp}{\omega_c}\right) \tag{B.3}$$

An identity that will be useful in this appendix is

$$\bar{H}_n(-\zeta,k_\perp,-k_\parallel) = -\bar{H}_{-n}(\zeta,k_\perp,k_\parallel)^* \tag{B.4}$$

which is derived from Eq. (B.2) by assuming that $k_\perp$ and $k_\parallel$ are real and by making use of

$$H_n(v_\parallel, k_\perp, -k_\parallel) = -H_{-n}(v_\parallel, k_\perp, k_\parallel) \ . \tag{B.5}$$

Consider now the function

$$\bar{H}_n^-\left(\frac{\omega - n\omega_c}{-k_\parallel}, k_\perp, -k_\parallel\right) = \int_{-\infty}^{0} \frac{d\zeta}{2\pi} \exp\left(-i \frac{\omega - n\omega_c}{-k_\parallel} \zeta\right) \bar{H}_n(\zeta, k_\perp, -k_\parallel)$$

$$= \int_0^{\infty} \frac{d\zeta}{2\pi} \exp\left(-i \frac{\omega - n\omega_c}{k_\parallel} \zeta\right) \bar{H}_n(-\zeta, k_\perp, -k_\parallel) \ . \tag{B.6}$$

After introducing Eq. (B.4), the right-hand side of Eq. (B.6) takes the form

$$- \int_0^{\infty} \frac{d\zeta}{2\pi} \exp\left(-i \frac{\omega - n\omega_c}{k_\parallel} \zeta\right) \bar{H}_{-n}(\zeta, k_\perp, k_\parallel)^* \tag{B.7}$$

and therefore we can write

$$\bar{H}_{-n}^-\left(\frac{\omega + n\omega_c}{-k_\parallel}, k_\perp, -k_\parallel\right)^* = - \int_0^{\infty} \frac{d\zeta}{2\pi} \exp\left(-i \frac{-\omega^* - n\omega_c}{k_\parallel} \zeta\right) \bar{H}_n(\zeta, k_\perp, k_\parallel)$$

$$= -H_n^+\left(\frac{-\omega^* - n\omega_c}{k_\parallel}, k_\perp, k_\parallel\right) \ . \tag{B.8}$$

Replacing n by $-n$ in Eq. (4.61b) and taking the complex conjugate of that function, we find with the help of Eq. (B.8) that

$$K^+(-\omega^*, k_\perp, k_\parallel) = K^-(\omega, k_\perp, -k_\parallel)^* \ . \tag{B.9}$$

This relates the positive and negative frequency components of the dielectric constant if $k_\perp$ and $k_\parallel$ are real.

REFERENCES

1. L. Tonks and I. Langmuir, "Oscillations in Ionized Gases," Phys. Rev. 33, 195 (1929).

2. L. Landau, "On the Vibrations of the Electron Plasma," J. Phys. (U.S.S.R.) 10, 45 (1946).

3. I. B. Bernstein, "Waves in a Plasma in a Magnetic Field," Phys. Rev. 109, 10 (1958).

4. E. G. Harris, "Unstable Plasma Oscillations in a Magnetic Field," Phys. Rev. Lett. 2, 34 (1959).

5. E. G. Harris, "Plasma Instabilities Associated with Anisotropic Velocity Distributions," J. Nucl. Energy, Pt. C, 2, 138 (1961).

6. C. B. Wharton, "Microwave Radiation Measurements of Very Hot Plasmas," Proc. 4th Intern. Conf. on Ionization Phenomena in Gases, Uppsala (North-Holland Publishing Co., Amsterdam, 1959) 2, 737 (1960).

7. G. Landauer, "Generation of Harmonics of the Electron Gyrofrequency in a Penning Discharge," J. Nucl. Energy, Pt. C, 4, 395 (1962).

8. G. Bekefi et al, "Microwave Emission and Absorption at Cyclotron Harmonics of a Warm Plasma," Phys. Rev. Lett. 9, 6 (1962).

9. G. Bekefi and E. G. Hooper, "Cyclotron Radiation of an Hg Plasma Generated by an Electron Beam," Appl. Phys. Lett. 4, 135 (1964).

10. J. L. Hirshfield and J. M. Wachtel, "Electron Cyclotron Maser," Phys. Rev. Lett. 12, 533 (1964).

11. G. E. K. Lockwood, "Plasma Cyclotron Spike Phenomena Observed in Top-Side Ionograms," Can. J. Phys. 41, 190 (1963).

12. F. W. Crawford, "A Review of Cyclotron Harmonic Phenomena in Plasmas," Nucl. Fusion 5, 73 (1965).

13. S. Tanaka, K. Mitani and H. Kubo, "Microwave Radiation from a Plasma in a Magnetic Field," Institute of Plasma Physics Report No. 13, Nagoya University, Nagoya, Japan (1963).

14. S. Tanaka, H. Kubo, and K. Mitani, "Microwave Radiation Near Electron Cyclotron Harmonics," J. Phys. Soc. Japan 20, 462 (1965).

15. E. Canobbio and R. Croci, "Harmonics of the Electron Cyclotron Frequency in a PIG-Discharge," Proc. 6th Intern. Conf. on Ionization Phenomena in Gases, Paris (SERMA Publishing Co., Paris, 1963) 3, 269 (1964). Also in Phys. Fluids 9, 549 (1966).

16. E. G. Harris, "The Electron Cyclotron Instability," Rept. No. GA-5581, John Jay Hopkins Laboratory for Pure and Applied Science, San Diego, Calif. (1964).

17. Y. Ozawa, I. Kaji, and M. Kito, "Stability Criterion for Longitudinal Plasma Waves in a Magnetic Field," J. Nucl. Energy, Pt.C, 4, 271 (1962).

18. T. Kammash and W. Heckrotte, "Stable Longitudinal Oscillations in Anisotropic Plasma," Phys. Rev. 131, 2129 (1963).

19. L. S. Hall, W. Heckrotte, and T. Kammash, "Ion Cyclotron Electrostatic Instabilities," Phys. Rev. 139, A1117 (1965).

20. T. Mantei, "Cyclotron Harmonic Wave Phenomena," Institute for Plasma Research Rept. No. 194, Stanford Electronics Laboratories, Stanford, Calif. (1967).

21. F. W. Crawford, R. S. Harp, and T. D. Mantei, "Pulsed Transmission and Ringing Phenomena in a Warm Magnetoplasma," Phys. Rev. Lett. 17, 626 (1966).

22. T. H. Stix, The Theory of Plasma Waves (McGraw-Hill Book Company, New York, 1962), Chaps. 8 and 9.

23. F. W. Crawford, "Cyclotron Harmonic Waves in Warm Plasmas," J. Res. Natl. Bur. Stds. 69D (Radio Science), 789 (1965).

24. A. A. Vlasov, "Vibrational Properties of an Electron Gas," J. Exp. Theoret. Phys. (U.S.S.R.) 8, 291 (1938).

25. A. Erdélyi et al, Higher Transcendental Functions (McGraw-Hill Book Company, New York, 1953), pp. 7, 102, 68, 81, 84, and 50.

26. G. N. Watson, A Treatise on the Theory of Bessel Functions (Cambridge University Press, Cambridge, England, 1966) 2d ed., pp. 31, 16, 195, 150, and 32.

27. D. E. Baldwin and G. Rowlands, "Plasma Oscillations Perpendicular to a Weak Magnetic Field," Phys. Fluids 9, 2444 (1966).

28. C. F. Kennel and H. E. Petschek, "Limit on Stably Trapped Particle Fluxes," J. Geophys. Res. 71, 1 (1966).

29. J. L. Dunlap et al, "Radiation and Ion Energy Distribution of the DCX-1 Plasma," Nucl. Fusion, Suppl. 1, 233 (1962).

30. P. A. Sturrock, "Kinematics of Growing Waves," Phys. Rev. 112, 1488 (1958).

31. H. Derfler, "Theory of R-F Probe Measurements in a Fully Ionized Plasma," Proc. of 5th Intern. Conf. on Ionization Phenomena in Gases, Munich (North-Holland Publishing Co., Amsterdam, 1962) 2, 1423 (1961).

32. H. Derfler, "Growing Wave and Instability Criteria for Hot Plasmas," Phys. Lett. 24A, 763 (1967). Also in Proc. of 8th Intern. Conf. on Phenomena in Ionized Gases, Vienna, 1967 (to be published).

33. A. Bers and R. J. Briggs, "Criteria for Determining Absolute Instabilities and Distinguishing between Amplifying and Evanescent Waves," M.I.T. Res. Lab. Electronics, Quarterly Status Rept. 71, p. 21 (1963).

34. R. J. Briggs, Electron-Stream Interaction with Plasmas (The M.I.T. Press, Cambridge, Mass., 1964), Chap. 2.

35. R. J. Eden, "Complex Variable Theory and Elementary Particle Physics," 1961 Brandeis University Summer Institute, Lectures in Theoretical Physics (W. A. Benjamin, Inc., New York, 1962) 1, 1 (1961).

36. P. L. Bhatnagar, E. P. Gross, and M. Krook, "A Model for Collision Processes in Gases. I. Small Amplitude Processes in Charged and Neutral One-Component System," Phys. Rev. 94, 511 (1954).

37. J. A. Tataronis and F. W. Crawford, "Cyclotron and Collision Damping of Propagating Waves in a Magnetoplasma," Proc. 7th Intern. Conf. on Phenomena in Ionized Gases, Belgrade (Gradevinska Knjiga Publishing House, Belgrade, 1966) 2, 244 (1965).

38. R. S. Harp, "The Dispersion Characteristics of Longitudinal Plasma Oscillations near Cyclotron Harmonics," Proc 7th Intern. Conf. on Phenomena in Ionized Gases, Belgrade (Gradevinska Knjiga Publishing House, Belgrade, 1966) 2, 294 (1965)

39. F. W. Crawford, R. S. Harp, and T. Mantei, "On the Interpretation of Ionospheric Resonances Stimulated by Alouette I," J. Geophys. Res. 72, 57(1967).

40. A. J. Anastassiades and T. C. Marshall, "Scattering of Microwaves from Plasma Space-Charge Waves near the Harmonics of the Electron Gyrofrequency," Phys. Rev. Lett. 18, 1117 (1967).

41. B. D. Fried and S. D. Conte, The Plasma Dispersion Function (Academic Press, New York, 1961).

42. J. D. Jackson, "Longitudinal Plasma Oscillations," J. Nucl. Energy, Pt.C, 1, 171 (1960).

43. P. A. Sturrock, "Dipole Resonances in Homogeneous Plasma in a Magnetic Field," Phys. Fluids 8, 88 (1965).

44. J. Nuttall, "Singularities of the Green's Function for a Collisionless Magnetoplasma," Phys. Fluids 8, 286 (1965).

45. H. Derfler and T. C. Simonen, "Landau Waves: An Experimental Fact," Phys. Rev. Lett. 17, 175 (1966).

46. G. Van Hoven, "Observation of Plasma Oscillations," Phys. Rev. Lett. 17, 169 (1966).

47. J. H. Malmberg and C. B. Wharton, "Dispersion of Electron Plasma Waves," Phys. Rev. Lett. 17, 172 (1966).

48. K. J. Harker, D. L. Eitelbach and F. W. Crawford, "Impedance of a Coaxial Magnetoplasma Capacitor," Bull. Am. Phys. Soc. 12, 1137 (1967).

49. P. Diament, "Magnetoplasma Wave Properties," SU-IPR Report No. 119, Institute for Plasma Research, Stanford University, Stanford, Calif. (February, 1967).

N68-20176
CR-93818

2

SU-IPR Report No. 205 by J. A. Tataronis

ERRATA

Page	Item	Should be
8	$r'_{\alpha 0}$ in Eq. (2.22)	$\underset{\sim}{r}'_{\alpha 0}$
8	$v'_{\alpha 0}$ in Eq. (2.22)	$\underset{\sim}{v}'_{\alpha 0}$
24	v_z in Eq. (2.76)	$v_{\|}$
32	$a_n(k_{\|})$ in fourth line after Eq.(3.22)	$a_n(k_{\perp})$
37	(3.7) in line following Eq. (3.34)	(3.5)
66	x in second line following Eq. (3.71)	$\underset{\sim}{r}$
69	k in Eq. (3.74)	$k_{\perp}$
83	"cylindrical-shell" in line 11	"ring"
90	α_{nn} in fifth line from bottom	α_{nm}
92	Fig. 21 in third line from bottom	Fig. 23
106	Eq. (4.16) in line following Eq. (4.14)	Eq. (4.6)
116	Eq. (4.24) in line following Eq. (4.31)	Eq. (4.23)
121	"two" in line 5	"three"
128	ω_n in Eq. (4.49)	ω_r
131	k^3 in Eq. (4.58)	k^2
135	Eq. (4.1) in third line from bottom	Eq. (4.23)
143	$(k_{\perp} v_t/\omega_c)$ in second line following Eq. (5.3)	$(k_{\perp} v_{t\perp}/\omega_c)$
143	v_t in third line following Eq. (5.3)	$v_{t\perp}$
147	v_t in Eq. (5.12)	$v_{t\perp}$
151	$\exp\left[-i(j-1)\frac{2n-3}{n-1}\right]$ in Eq. (5.22)	$\exp\left[-i(j-1)\frac{2n-3}{n-1}\pi\right]$
151	$\exp\left[-i(2j-1)\frac{2n-3}{2(n-1)}\right]$ in Eq. (5.23)	$\exp\left[-i(2j-1)\frac{2n-3}{2(n-1)}\pi\right]$

ERRATA (Cont)

Page	Item	Should be
154	Eq. (5.28a) in second line above Eq. (5.32)	Eq. (5.30)
161	$i\gamma_2$ in Eq. (5.53)	$-\gamma_2$
164	$g(\lambda)$ in line above Eq. (5.58)	$g(x)$
165	k in second line above Eq. (5.61)	$k_\perp$
175	$H_n^-\left(\frac{\omega - n\omega_c}{-k_\parallel}, k_\perp, k_\parallel\right)$ in Eq. (B.6)	$H_n^-\left(\frac{\omega - n\omega_c}{-k_\parallel}, k_\perp, -k_\parallel\right)$